# A New Synthesis of Tribenzotriquinacene and the Rigidity of Carbon-Carbon Single Bonds

Von der Fakultät für Lebenswissenschaften

der Technischen Universität Carolo-Wilhelmina

zu Braunschweig

zur Erlangung des Grades eines

Doktors der Naturwissenschaften

(Dr. rer. nat.)

genehmigte

D i s s e r t a t i o n

von Georgios Markopoulos

aus Thessaloniki / Griechenland

1. Referent: Professor a. D. Dr. Henning Hopf

2. Referent: Professor Dr. Peter George Jones

3. Referent: Professor Dr. Matthias Tamm

eingereicht am: 07.01.2013

mündliche Prüfung (Disputation) am: 01.03.2013

Druckjahr 2013

## Vorveröffentlichungen der Dissertation

Teilergebnisse aus dieser Arbeit wurden mit Genehmigung der Fakultät für Lebenswissenschaften, vertreten durch den Mentor der Arbeit, in folgenden Beiträgen vorab veröffentlicht:

### Publikationen

G. Markopoulos, L. Henneicke, J. Shen, Y. Okamoto, P. G. Jones, H. Hopf
„Tribenzotriquinacene: a versatile synthesis and $C_3$-chiral platforms“
*Angew. Chem. Int. Ed.* **2012**, *51*, 12884–12887;
*Angew. Chem.* **2012**, *124*, 13057–13060.

### Tagungsbeiträge

G. Markopoulos, L. Henneicke, J. Shen, Y. Okamoto, H. Hopf
„Tribenzotriquinacene: a new synthesis and chiral derivatives” (Poster 31)
*14th International Symposium on Novel Aromatic Compounds,* Eugene (2011)

G. Markopoulos, L. Henneicke, J. Shen, Y. Okamoto, P. G. Jones, H. Hopf
„Tribenzotriquinacene: a new and versatile synthesis” (Poster P-0390)
*4th Congress of the European Association for Chemical and Molecular Sciences,* Prag (2012)

G. Markopoulos, L. Henneicke, J. Shen, Y. Okamoto, P. G. Jones, H. Hopf
„Tribenzotriquinacene: a new and versatile synthesis” (Poster P198)
*18. Vortragstagung der Liebig-Vereinigung für Organische Chemie,* Weimar (2012)

To my sisters

# Kurzfassung

Der erste Teil der vorliegenden Arbeit beschreibt eine neue Synthese des schalenförmigen Kohlenwasserstoffs Tribenzotriquinacen, die das Stammsystem erstmals im Gramm-Maßstab zugänglich macht. Die große Flexibilität des Syntheseschemas wurde weiterhin auf die regiospezifische Synthese von *ortho*-funktionalisierten Derivaten übertragen, die bisher nur schwer darstellbar waren. Dreifach substituierte Tribenzotriquinacene werden durch eine $C_3$-spezifische Cyclisierung erhalten, die ausschließliche zu $C_3$-chiralen Derivaten führt. Insgesamt 18 Kristallstrukturen von Haupt- und Zwischenprodukten werden besprochen. Die Kristallstrukturanalyse des Stammsystems belegt, dass die Tribenzotriquinacen-Einheiten in einer leicht gestaffelten Anordnung gestapelt sind. Die molekularen Dimensionen eines $C_3$-chiralen Trimethyltribenzotriquinacens versprechen interessante Anwendungen in der supramolekularen Chemie. Weiterhin wurde die Durchführbarkeit von intramolekularen Cyclisierungen in *ortho*-funktionalisierten Tribenzotriquinacenen durch computerchemische Methoden untersucht.

Der zweite Teil der vorliegenden Arbeit untersucht die Rigidität von Kohlenstoff-Kohlenstoff Einfachbindungen. Durch die Berechnung von Compliance-Konstanten werden die Bindungspotentiale einer Vielzahl von Einfachbindungen zwischen vierfach-koordinierten Kohlenstoffzentren charakterisiert. Ein empirischer Zusammenhang in Analogie zur Badger-Regel wird vorgestellt. Dieser kann zur Vorhersage der kinetischen Instabilität hypothetischer Moleküle herangezogen werden, was beispielhaft an fluktuierenden Molekülen und einer hochgespannten Verbindung gezeigt wird. Weiterhin wird nachgewiesen, dass Cyclobutan ein weicheres Bindungspotential als Cyclopropan aufweist, und dass Dichtefunktionalmethoden keine adäquate Beschreibung von dreigliedrigen Ringsystemen bieten. Ferner wird gezeigt, dass die Stauchung von Bindungen trotz der ungünstigeren Energie zu rigideren Bindungen führt.

# Abstract

The first part of the thesis describes a new synthesis of the bowl-shaped hydrocarbon tribenzotriquinacene. The synthetic scheme allows, for the first time, the gram-scale preparation of the parent hydrocarbon. The developed scheme is very versatile and has been extended to the regiospecific synthesis of derivatives that are functionalized in one or several of the hardly accessible *ortho*-positions. Notably, trisubstituted tribenzotriquinacenes are obtained in a $C_3$-specific manner leading exclusively to $C_3$-chiral derivatives. In total, 18 crystal structures of final and intermediate products are presented. The X-ray structural analysis of the parent tribenzotriquinacene demonstrates that its columnar stacks show a slightly staggered arrangement of the tribenzotriquinacene units. The dimensions of a $C_3$-chiral trimethyl tribenzotriquinacene show promising opportunities for supramolecular chemistry. As a guide for further experiments, the feasibility of intramolecular cyclizations in *ortho*-functionalized tribenzotriquinacenes is studied by computational means.

The second part of the thesis presents a computational investigation of the rigidity of carbon-carbon single bonds. Based on the calculation of compliance constants, the bond stretch potentials of a large series of carbon-carbon single bonds between tetracoordinate carbon centers are investigated. An empirical relationship in the form of Badger's rule is established and is shown to have predictive power about the viability of hypothetical molecules. Deviations from this relationship indicate fragile bonds and low-lying transition states. This is demonstrated for a highly strained compound and for fluxional molecules. The data also show that cyclobutane has a softer bond stretch potential than cyclopropane, and that density functional methods fail to describe three-membered rings adequately. It is furthermore established that compression of bonds, although being enthalpically unfavorable, leads to more rigid bonds.

# Acknowledgements

It is with the greatest appreciation that I would like to thank my supervisor Prof. Henning Hopf for continuous support and encouragement. His enthusiasm and optimism, paired with a strong belief in the value of experiments, provided the guiding principles in my daily work and have inspired me far beyond science. I also thank him for the freedom to follow my computational interests, which often proved very time consuming.

The computational aspects of this thesis were investigated under the supervision of PD Dr. Jörg Grunenberg and I would like to thank him for all the insightful discussions and his patience with my alternations between experiment and computation. I am also grateful to him for performing selected computationally expensive coupled cluster calculations.

I am very grateful to Prof. Dietmar Kuck from the University of Bielefeld. As the pioneer of tribenzotriquinacene chemistry he supported the ideas presented herein from the very beginning in open discussions and with kind encouragement. This scientific exchange in an atmosphere of mutual trust was a particularly valuable experience for me.

The thesis has benefited from numerous collaborations. First of all, I would like to thank Prof. Peter G. Jones for the numerous X-ray structures presented in this work and his continuous patience to study crystals that often proved to be disordered. The chiral resolutions by HPLC have been performed by Prof. Jun Shen and Prof. Yoshio Okamoto from the Harbin Engineering University in China and I am very grateful for their hard work. I am also very indebted to Dr. Ulrich Papke for the detailed ESI-MS investigations described in Chapter 1.5.4 and the insightful discussions on mass spectrometry. Furthermore, I thank Prof. Monika Mazik, now at the University of Freiberg, for discussions about halogen-halogen interactions.

I would also like to thank Dr. Kerstin Ibrom for providing me a hood and lab space in the first months of my thesis work. I am very grateful to Dr. Kai Brandhorst, who developed the computer program for the calculation of compliance constants during his PhD thesis and thereby made the work on bond rigidity possible. Furthermore, I would like to thank Prof. Sethuraman Sankararaman from the IIT Madras in India for many inspiring discussions during his stay as a Humboldt Visiting Professor.

I am very grateful to Prof. Ludger Ernst and Dr. Hans Martin Schiebel for numerous discussions of NMR spectra and mass spectra, respectively. I also thank Dr. Till Beuerle and Cornelia Mlynek for MS measurements, Petra Holba-Schulz and Gabrielle Krafft for high resolution NMR measurements, Karin Kadhim for IR and UV measurements and the Institut für Anorganische und Analytische Chemie and the Institut für Medizinische und Pharmazeutische Chemie for elemental analyses. Furthermore, I am grateful to Gabriele Salomon and Rose-Marie Weiss for help with all sorts of bureaucracy.

I am very grateful to my colleagues of the Hopf research group, in particular Anamaria Silaghi, Michael Szmatola, Dr. Vitaly Raev, Dr. Rajendran Saravanakumar, Dr. Jubi John and Eliza Tarcoveanu. Several students have worked under my supervision and I thank them for their contributions: Lars Henneicke, Mark D. Levin, Suryanarayana Birudukota, Pardha Peram, Oscar Arias I Burguera, Karin Gaida, Maren Schmidt and Florian Mann. I am furthermore grateful to Matthias Gehder for providing me with a layout template. Finally, I would like to thank my friends from the Mazik research group as well as Hilke Bruns, Ramona Riclea and Mona Al Batal.

I would also like to thank the mentors of my undergraduate years: Prof. Peter Hofmann from the University of Heidelberg and Prof. Roald Hoffmann from Cornell University in the USA. Both have shaped my thinking in chemistry in a decisive way and have also supported me in finding my way to Braunschweig.

The thesis would not have been possible without the generous financial support from the Fonds der chemischen Industrie and the Studienstiftung des deutschen Volkes. I am furthermore grateful for travel grants from the German Chemical Society and the Freunde des Institutes für Organische Chemie e.V.. The latter was made possible by the impressive commitment of Brigitte Brinkman and Dagmar Goedecke. I also thank Prof. Stefan Schulz for offering teaching positions in the last year of my thesis work.

The scientific endeavor would be without any meaning to me if I did not have my family and my wonderful friends here in Braunschweig and all over the world. I am deeply grateful to my parents who always lovingly supported my academic interests and personal development. I also extend these thanks to their partners, who have become a close part of my life in recent years. I am also very grateful to my godmother, who has inspired me ever since to keep a horizon beyond science. Finally, I wish to express my gratitude to my sisters for all their love and support. Both are absolutely wonderful and always make me smile. It is with these words that I wish to dedicate this thesis to them.

# Table of Contents

# Preface

The present thesis is concerned with two topics. Both fall into the realm of hydrocarbon chemistry but differ markedly in their methodology: Chapter 1 describes a new synthesis of the bowl-shaped hydrocarbon tribenzotriquinacene, while Chapter 2 uses the tools of computational chemistry to study the rigidity of carbon-carbon single bonds. Specific introductions and conclusions are presented individually in both chapters. Research in these two directions was motivated by a keen interest in strained organic molecules and the author hopes to transmit some of their fascination.

# 1 A new synthesis of tribenzotriquinacene

## 1.1 Bowl-shaped hydrocarbons

Bowl-shaped molecules are circular molecules with a curved surface. Prototypical examples are corannulene (**1**) and sumanene (**2**), both of which can be considered as molecular fragments of buckminsterfullerene $C_{60}$ [1–13] (Figure 1). These two representatives are conformationally labile and show bowl-to-bowl inversion, which has inspired a series of interesting studies in dynamic stereochemistry [14–20]. By contrast, a configurationally stable framework is found in the molecular bowl tribenzotriquinacene **3** (Figure 1). It consists of a triquinacene core [21] that is extended with three benzene units. Because of the all-*syn* arrangement of the four aliphatic hydrogen atoms in **3**, a convex-concave topology is generated as shown in the three-dimensional representation **4**.

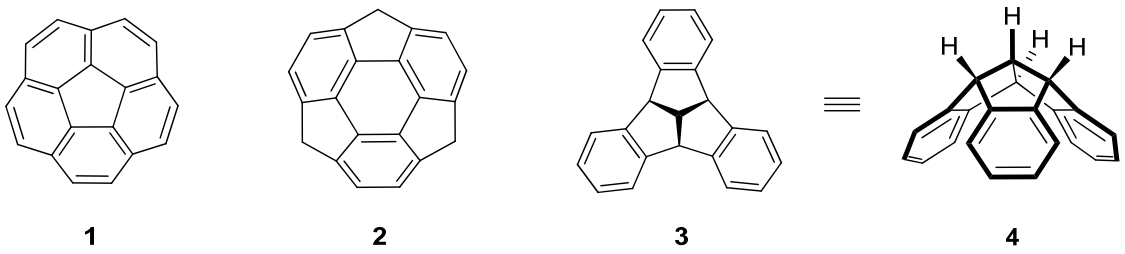


**Figure 1.** A selection of bowl-shaped hydrocarbons

The tribenzotriquinacene framework was first synthesized by Kuck in 1984 [22] and the same group also reported the first synthesis of the parent hydrocarbon **3** [23].[a] The most effective route is the three-step synthesis shown in Scheme 1 [25].[b] It starts from 1,3-indanedione **5a**, which is subjected to a condensation with benzhydrol. Subsequent reduction yields a set of diastereomeric diols **7a**. Ring closure to the desired tribenzotriquinacene **3** is achieved by twofold cyclodehydration in refluxing chlorobenzene under phosphoric acid catalysis. The yield in this final step is relatively low (11%). By using 2-methyl-1,3-indanedione **5b** as starting material in this sequence, the corresponding tribenzotriquinacene **8** with a methyl group in the central

[a] The tribenzotriquinacene framework itself was first mentioned by Baker et al. in 1957 [24].

[b] Kuck and coworkers have also reported a more elaborate synthesis that allows for stereocontrolled cyclizations [23,26].

12d-position can be obtained. All steps in the synthesis of this derivative feature higher yields, in particular the double cyclodehydration (33% vs. 11%).

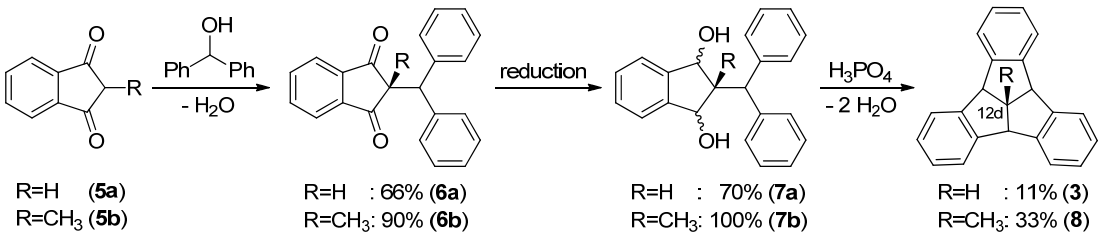


**Scheme 1.** Kuck's synthesis of tribenzotriquinacenes [25,26]

The rich chemistry of tribenzotriquinacenes was primarily explored by Kuck and coworkers. Examples and applications include transition metal carbonyl complexes [27,28], chiral derivatives [29,30], extended molecular bowls [31,32], supramolecular recognition [33–35] and functional chromophore assemblies [36] as well as the synthesis and exploration of the centropolyindane family [37]. Several reviews have been published in the field [38–41].

Tribenzotriquinacenes can in principle be functionalized at four different sites; the possibilities may be summarized briefly as follows:

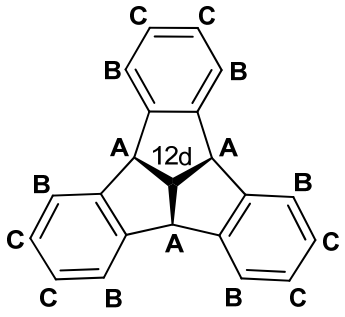


**Figure 2.** Different sites of functionalization in tribenzotriquinacenes

1) Tribenzotriquinacenes substituted at the central 12d-position (Figure 2) have been reported by Kuck and coworkers [25]. Their synthesis is based on the use of appropriately functionalized 1,3-indanedione precursors as demonstrated in Scheme 1. Derivatives are known with methyl, ethyl, allyl, isopropenyl, benzyl and diphenyl methyl groups [25,42]. As the parent hydrocarbon is more difficult to obtain than the 12d-methyl derivative, most of tribenzotriquinacene chemistry is based on the latter derivative. Functionalization at the 12d-position

after assembly of the tribenzotriquinacene framework is rare and very limited in scope [42].

2) The three benzhydrylic sites in tribenzotriquinacene (**A** in Figure 2) are highly reactive and can easily be functionalized. Extensive studies on this chemistry have been published by Kuck and coworkers [42–44]. The most common route to functionalization at these positions involves radical bromination followed by $S_N1$-type substitutions. The solubility of tribenzotriquinacenes can be increased by introduction of alkyl or ether chains at the benzhydrylic sites [44]. Strong bases transform the benzhydrylic sites into tribenzacepentalene dianions, which can react to a variety of tribenzodihydroacepentalene derivatives [23,45–47].

3) Reports of functionalization at the aromatic *ortho*-positions (**B** in Figure 2) are scarce, and the problem requires further investigation. These positions are not accessible via electrophilic aromatic substitution, even under forcing conditions. For a long time, only one example of an *ortho*-functionalized derivative was known and involved a manganese tricarbonyl complex of 12d-methyl tribenzotriquinacene [28].[c] Krüger and coworkers have recently reported the introduction of methyl groups at the *ortho*-positions of tribenzotriquinacenes by using Kuck's protocol in conjunction with suitably methylated precursors [49].[d] In a remarkable transformation Kuck and Mughal have achieved the formation of a cycloheptatriene unit between two opposing and unfunctionalized *ortho*-positions via Scholl reaction [51].

4) The aromatic positions at the outer rim (**C** in Figure 2) are easily accessible by electrophilic aromatic substitution and numerous transformations of this type have been reported by Kuck and his coworkers [29,31,43,44,52]. The derivatives thus obtained can be used for further elaboration of the tribenzotriquinacene core, thereby extending the size of the molecular bowl. Almost all applications of tribenzotriquinacene topology are based on this chemistry. Limitations in this area are selective mono- and difunctionalization, which has only been reported for titanium(IV)-mediated formylation [29,30], and the efficient synthesis of trifunctionalized derivatives with $C_3$ symmetry, which is hampered by the statistical preference for the unsymmetric regioisomer [36,53,54]. A second approach to rim-functionalized derivatives

[c] Kuck and coworkers have reported centrohexaindanes with *ortho*-methoxy substituents [48].

[d] Kuck and coworkers had used similar precursors for the synthesis of a tetra-*ortho*-methylated centrohexaindane [50].

involves the use of appropriately functionalized precursors, as demonstrated by the synthesis of hexamethoxy tribenzotriquinacenes [55,56].[e]

Despite these impressive advances in tribenzotriquinacene chemistry, some limitations remain, and these provide the motivation of the present investigation. By developing a new synthesis of tribenzotriquinacene the following challenges are to be addressed:

1) efficient access to parent hydrocarbon **3**
2) efficient access to derivatives functionalized in one or several *ortho*-positions
3) regiospecific synthesis of monofunctionalized derivatives
4) regiospecific synthesis of $C_3$-chiral derivatives
5) synthesis of chiral tribenzotriquinacenes and their resolution.

The respective target molecules are shown in Figure 3 and their syntheses and structural properties will be presented in the following chapters.

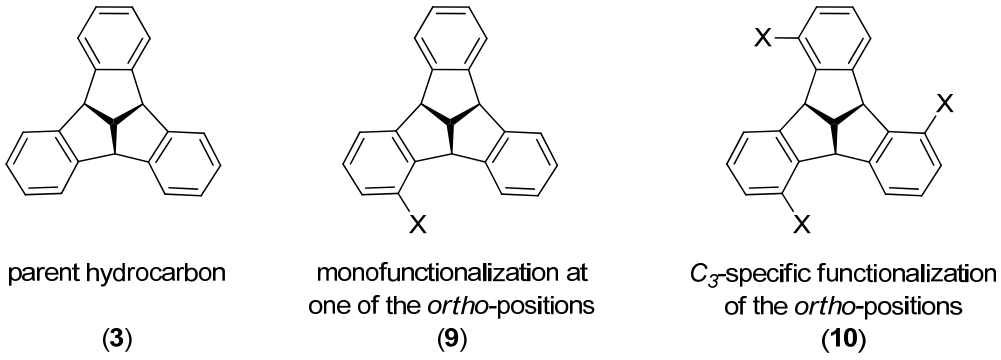


**Figure 3.** Target molecules of the present investigation

[e] The same approach has also been used for the successful synthesis of a dodecamethoxy centrohexaindane [57].

## 1.2 Synthesis of tribenzotriquinacene

The newly developed synthesis of tribenzotriquinacene is based on the retrosynthetic analysis shown in Scheme 2. It was assumed that **3** might arise from an acid-catalyzed cyclization of the dihydroindenoindene **11**. The intermediate **11** would be formed in a double cyclodehydration of the diastereomeric diols **12**.

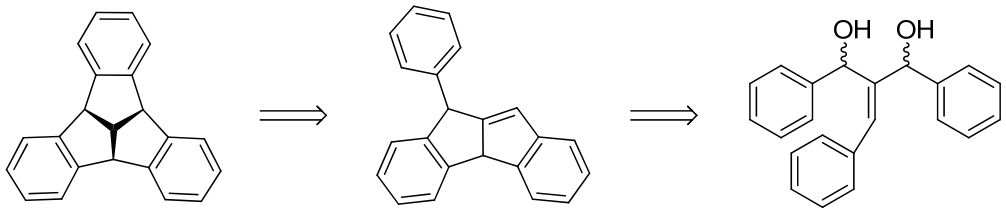


**Scheme 2.** Retrosynthetic analysis of tribenzotriquinacene (**3**)

The depicted scheme was conceived by careful study of the literature and a serendipitous observation in the laboratory. The diastereomeric diols **12** had already been reported by Olah and coworkers, who obtained them in a low-yield reduction of the easily available Knoevenagel adduct **14** (Scheme 3) [58]. Olah subjected diols **12** to superacidic conditions, under which he observed a cyclodehydrated cation, probably of the form **15**.

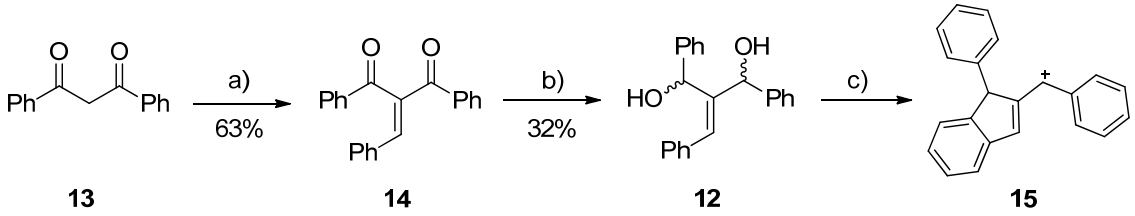


**Scheme 3.** Olah's synthesis of diols **12** and their reaction under superacidic conditions [58]; reaction conditions: a) benzaldehyde, piperidine (cat.), hexanoic acid (cat.), benzene (reflux), 20 h; b) $LiAlH_4$, $Et_2O$, 12 h; c) $FSO_3H$, $SO_2ClF$, -80 °C.

In the course of the present thesis it was observed that diols **12** were reactive even under mildly acidic conditions (catalytic amounts of *p*-toluenesulfonic acid in $CH_2Cl_2$ at room temperature). When subjecting a single diastereomer to these conditions, a mixture of both diastereomers was formed and the diastereomers equilibrated. Furthermore, additional less polar products were identified by TLC analysis, hinting at

the possibility of intramolecular cyclodehydrations. These findings inspired the following question: can reaction conditions be found under which the cation **15**, generated *in situ* from diols **12**, undergoes cyclization to **11** and subsequent cyclization to tribenzotriquinacene **3** (Scheme 4)?

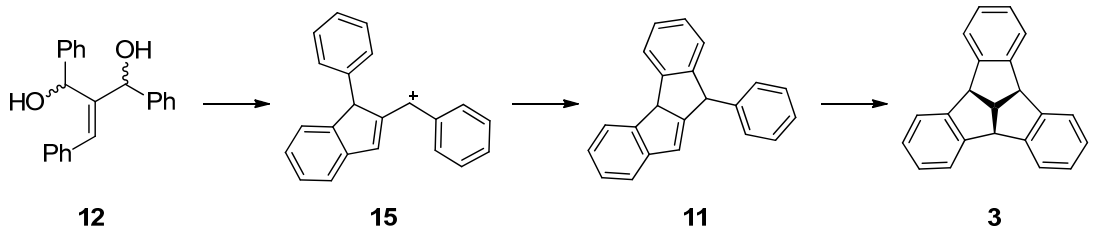


**Scheme 4.** Working hypothesis for the new synthesis of tribenzotriquinacene

To test this hypothesis, Olah's synthesis of the diastereomeric diols **12** was optimized. Whereas the Knoevenagel condensation of dibenzoylmethane (**13**, Scheme 5) with benzaldehyde necessitated only a change of solvent to the less toxic toluene, a more careful optimization was required for the subsequent reduction. In order to avoid conjugate 1,4-reduction of the *α,β*-unsaturated diketone **14**, the Luche protocol was chosen for this transformation.[f] To the best of the author's knowledge no double reduction of an *α,β*-unsaturated diketone under Luche conditions had been reported previously. Other methods were also tested but proved ineffective ($NaBH_4$/MeOH, $NaBH_4/H_2O$, DIBAL, $Mg/FeCl_3/DMF/H_2O$).

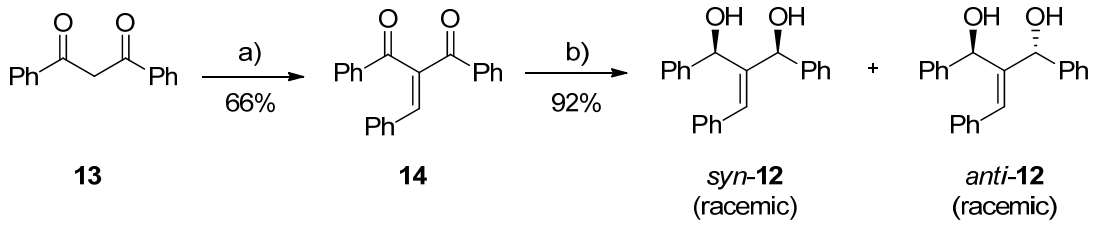


**Scheme 5.** Improved synthesis of **12**. Reaction conditions: a) benzaldehyde, piperidine (cat.), hexanoic acid (cat.), toluene (reflux), 20 h; b) $NaBH_4$, $CeCl_3 \bullet 7H_2O$, MeOH, $CH_2Cl_2$.

[f] A crystal structure was obtained for Knoevenagel adduct **14** and is discussed in Chapter 1.5.1.

| entry | $CeCl_3 \bullet 7H_2O$ (eq) | $NaBH_4$ (eq) | temperature and reaction time | yield (%) | *syn*/*anti* |
|---|---|---|---|---|---|
| 1 | 1.4 | 2.5 | -78 °C (1h) → r.t. (1h) | 92 | 1:1.4 |
| 2 | 1.1 | 2.5 | -78 °C (0.5h) → r.t. (1.5h) | 89 | 1:2.1 |
| 3 | 0.1 | 2.1 | -78 °C (1h) → r.t. (1.5h) | 84 | 1:1.6 |
| 4 | 1.1 | 2.1 | -78 °C (0.2h) → r.t. (0.3h) | 87 | 1:2.4 |
| 5 | 1.4 | 2.1 | -78 °C (0.5h) → r.t. (1h) | 92 | not determined |

**Table 1.** Reaction conditions for Luche reduction of diketone **14**

The reaction was performed at low temperatures to further suppress conjugate 1,4-reduction. As stated by Luche in his original publication, regioselective 1,2-reduction is achieved even with substoichiometric amounts of cerium(III). This is demonstrated by entry 1 in Table 1, which shows clean conversion in 92% yield with 1.4 eq cerium(III) chloride heptahydrate. Use of 1.1 eq of cerium(III) lowers the yield only marginally to 89% (entry 2); even as little as 0.1 eq are sufficient for a conversion with 84% yield (entry 4). The reaction is fast, as seen by comparison of entries 2 and 4. Furthermore, the shorter the reaction time at low temperature, the higher the yield of the *anti*-diastereomer (entries 2-4). Based on these findings the conditions of entry 5 were chosen as most convenient. The diastereomers can be separated by flash column chromatography and their relative stereochemistry was determined by single crystal X-ray analysis (see chapter 1.5.2).

With a high-yielding synthesis of diols **12** in hand, their cyclization to tribenzotriquinacene was studied. Indeed, application of Kuck's cyclodehydration conditions gave **3** in 28% yield (Scheme 6). The dihydroindenoindene derivative **16** was isolated in 9% yield, together with the fluorescent aceanthrylenone derivative **17** (1-2% yield). The yield of **3** was further increased to 32% by using polyphosphoric acid (PPA) as dehydrating agent. Other acids were also tested but proved ineffective (AcOH, MesOH, Eaton's reagent, TFA, TfOH, $Tf_2O$, $H_2SO_4$). The reaction presumably proceeds through a series of intramolecular Friedel-Crafts alkylations with

carbocation intermediates. This was demonstrated by the independence of the yield with respect to the diastereomer of **12** chosen as starting material.

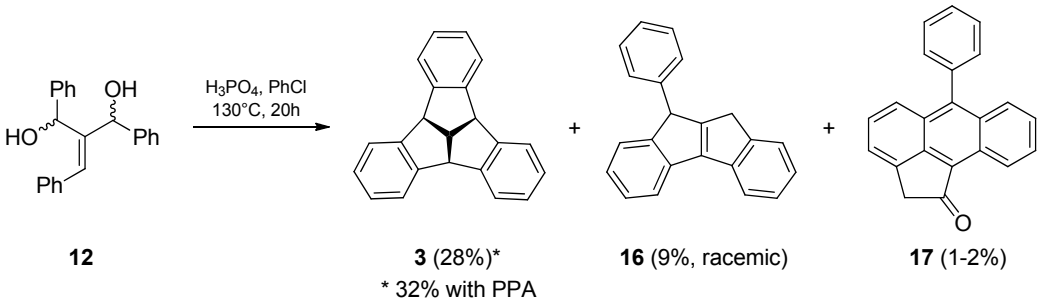


**Scheme 6.** Synthesis of tribenzotriquinacene and isolated byproducts

A possible reaction mechanism explaining the formation of **3** and **16** and the independence of stereochemical information is shown in Scheme 7. Two consecutive cyclodehydrations via cationic intermediates **18** and **15** lead to the five-membered rings in **11** (both the *syn*- and *anti*-diastereomer can be formed).[g,h,i] A $S_N1$-type mechanism for these cyclodehydrations is favored by the high resonance stabilization of the respective cations. It can therefore be assumed that all stereochemical information of the starting material is lost in **15** and does not influence the further course of the reaction. Of the two diastereomers of **11**, only *syn*-**11** shows the geometry required to react further in a Friedel-Crafts-type alkylation via *syn*-**20** to the desired tribenzotriquinacene **3**. For this sequence to take place, protonation at the convex side of the double bond in *syn*-**11** is required and should be favored on stereochemical grounds. Both diastereomers of **11** can also undergo an acid-catalyzed double bond shift via **21** leading to byproduct **16**. Kuck and coworkers also observed **16** as a byproduct in their synthesis of tribenzotriquinacene and also proposed **11** as an intermediate [25,26]. An X-ray structure of **16** is presented in Chapter 1.5.8.

[g] The structures of mesomeric cations and alternative cyclizations are not shown, but ultimately lead to the same intermediate (**11**).

[h] The descriptors *syn* and *anti* refer to the relative stereochemistry of the hydrogen atoms.

[i] Olefin **11** was mentioned by Baker et al., who also considered the possibility of tribenzotriquinacene formation [24].

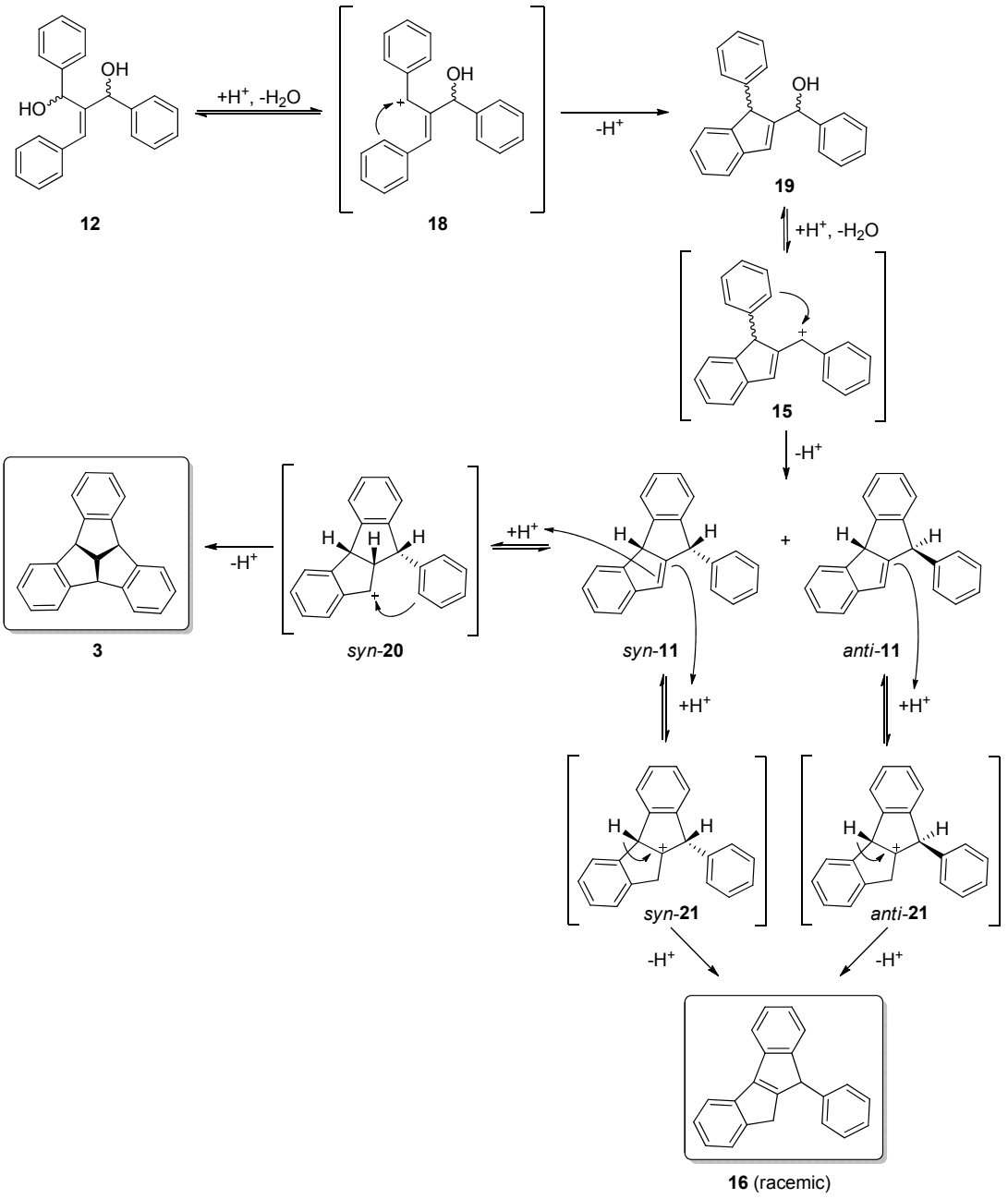


**Scheme 7.** Proposed mechanism for tribenzotriquinacene (**3**) and dihydroindenoindene (**16**) formation (*syn* and *anti* refer to hydrogen orientation)

It should be pointed out that the presented synthesis assembles the tricyclic core of **3** in one step starting from an acyclic precursor.[j] In analogy to Kuck's *double cyclodehydration* strategy (Scheme 1), the present approach might be called a *triple*

[j] The aromatic rings are not considered in this regard.

*cyclization* strategy.[k] In the light of this difference it is even more surprising that the yield of the triple cyclization strategy is almost three times as high as that of the double cyclodehydration strategy (32% vs. 11%). A possible explanation for this striking difference is that diols **12**, because of their unsaturated nature, might not suffer from the Grob fragmentation [60] that has been described for Kuck's benzhydryl indanediols [22,25,61].

An explanation for the formation of the aceanthrylenone derivative **17** is speculative but also possible. It starts with protonation of either diastereomer of **11** leading to cation **20** (Scheme 8). Instead of undergoing an intramolecular Friedel-Crafts-type reaction, this cation would have to undergo bond scission to the more stable benzhydrylic cation **22**. The latter could subsequently undergo an intramolecular Friedel-Crafts-type alkylation to **23**, thereby furnishing the carbocyclic core of **17**. Subsequent oxidations under the harsh reaction conditions would finally lead to **17**. To minimize such oxidative processes, cyclizations were performed under a nitrogen atmosphere.

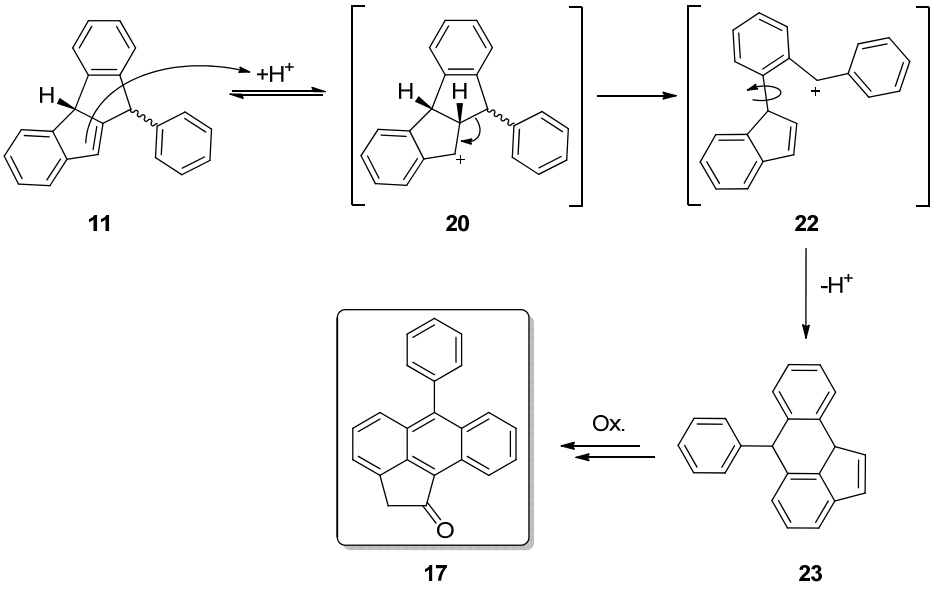


**Scheme 8.** Suggested mechanism for formation of **17**

In the light of the numerous $C_{22}H_{16}$ isomers that occur in the proposed mechanisms, it is instructive to compare their relative energies by computational methods. Density

[k] Kuck and coworkers employed a *triple cyclodehydration* strategy in the propellane route to centrohexaindanes [37,50,57,59].

functional theory calculations at the M06-2X/6-311G(d,p) level of theory were performed and the results are shown in Figure 4. The calculations indicate that tribenzotriquinacene **3** is the global minimum of the considered isomers and that byproduct **16** is the isomer with the second-lowest energy. Formation of the latter by acid-catalyzed double bond shift is likely, as it is 5.8-7.4 kcal/mol lower in energy than its precursors **11**. By contrast, the double bond isomer **24**, which could also arise from **11**, is only 3.5-5.1 kcal/mol lower in energy than **11** and was not observed in the reaction mixture. With respect to the *syn*- and *anti*-diastereomers of **11**, it is noteworthy that the *syn*-diastereomer, which is necessary for a productive cyclization leading to tribenzotriquinacene, is favored over the *anti*-diastereomer by 1.6 kcal/mol. Intermediates **23**, which are required for formation of the aceanthrylenone derivative **17**, are about 4.6-6.1 kcal/mol lower in energy than **11** and about 1 kcal/mol higher than **16**. Structures **25-27** constitute tribenzotriquinacene isomers that differ in the relative orientation of the aliphatic hydrogen atoms. These stereoisomers could in principle also form by appropriate protonation of **11** and subsequent cyclization, but their high energy (26-77 kcal/mol higher than **3**) seems to preclude their formation under the present conditions. It should be pointed out that the energies of transition structures are in fact required for accurate conclusions about product mixtures. However, because of the high temperature and long reaction time (130 °C, 20 h), a thermodynamic treatment seems to be an appropriate and reasonable approximation for the present case.

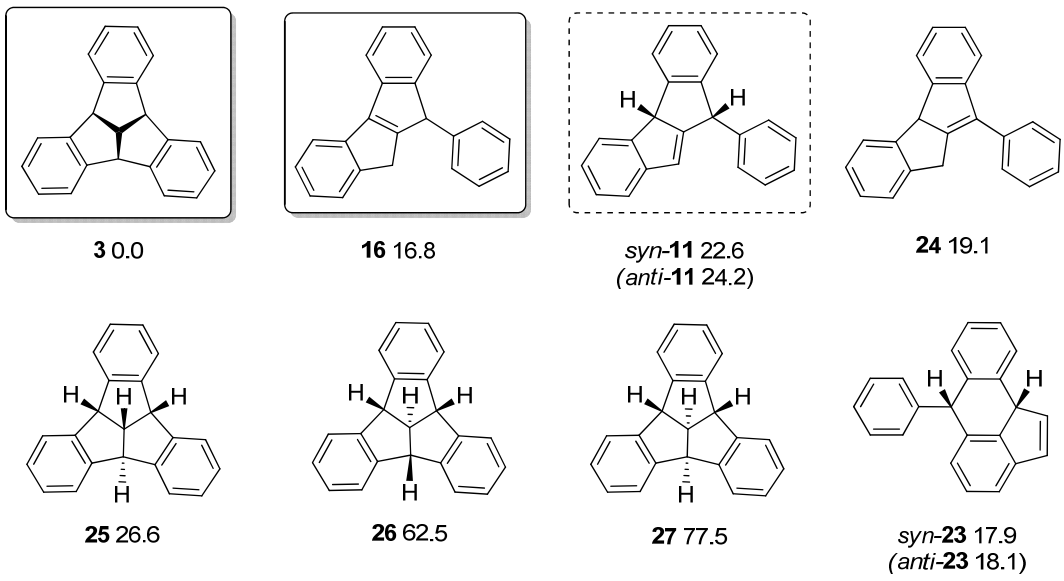


**Figure 4.** Relative energies of $C_{22}H_{16}$ isomers at the M06-2X/6-311G(d,p) level of theory; energies in kcal/mol at 0 K and without correction for zero-point energy.

Single crystals of **3** for X-ray analysis were obtained by recrystallization from refluxing toluene and the crystal structure is discussed in chapter 1.5.6. With gram amounts of **3** in hand, a small sample was also transformed into tribromide **28** as reported by Kuck and coworkers (Scheme 9) [42]. A crystal structure of **28** was obtained and is also discussed in chapter 1.5.6.

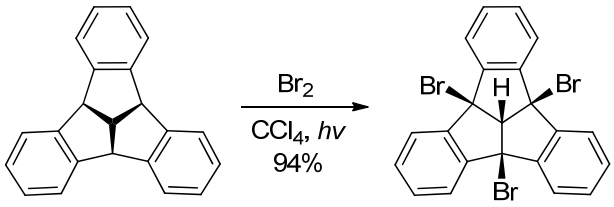


**3** **28**

**Scheme 9.** Bridgehead bromination of parent tribenzotriquinacene by Kuck et al. [42]

## 1.3 Synthesis of monosubstituted derivatives

The developed protocol can also be extended to the synthesis of monosubstituted tribenzotriquinacenes. By the use of appropriately functionalized benzaldehyde components it is possible to introduce substituents regiospecifically. For example, *ortho*-substituted benzaldehydes **29** lead exclusively to *ortho*-substituted tribenzotriquinacenes **9** (Scheme 10). As pointed out in Chapter 1.1, functionalization at the *ortho*-positions of tribenzotriquinacene is rare and therefore constitutes an appealing synthetic goal.

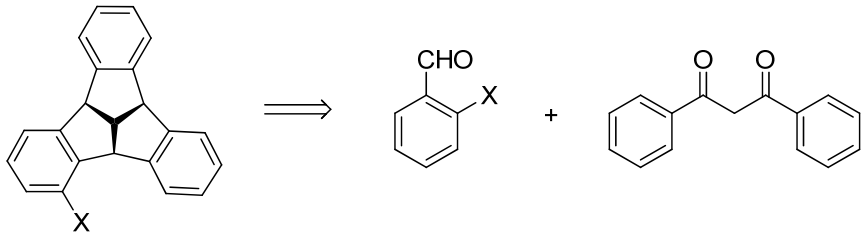


**9** **29** **13**

**Scheme 10.** Retrosynthetic analysis for *ortho*-substituted tribenzotriquinacenes

The developed reaction sequence was applied to 2-bromo- and 2-methoxybenzaldehyde as starting materials (Scheme 11). Knoevenagel adduct **30** had already been reported in the literature using acetonitrile and piperidine as solvent and catalyst [62,63]. For the preparation of methoxy derivative **31**, the reaction conditions used for the synthesis of the unsubstituted parent system were chosen. Both condensations proceeded with satisfactory yield (66%). Crystal structures were obtained for both Knoevenagel adducts and are discussed in Chapter 1.5.1. Subsequent Luche reduction proceeded smoothly in 89% yield for both **32** and **33**, underlining the robustness of the optimized protocol. The diastereomers of the diols can be separated by flash chromatography and crystal structures were obtained for *anti*-**32** and *syn*-**33** (see Chapter 1.5.2).

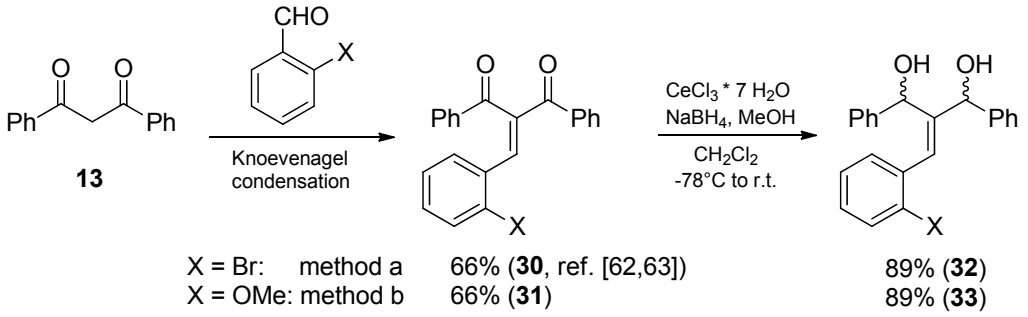


**Scheme 11.** Synthesis of monosubstituted diols **32** and **33**; reaction conditions: a) piperidine (cat.), acetonitrile (reflux), 12 h; b) piperidine (cat.), hexanoic acid (cat.), toluene (reflux), 20 h.

The diastereomeric diols **32** and **33** were subsequently subjected to cyclization conditions with polyphosphoric acid as dehydrating agent (Scheme 12). In the case of the brominated diol **32**, 1-bromotribenzotriquinacene **34** was isolated in 27% yield, which is only slightly less than the yield for the parent hydrocarbon (32%). Compound **34** is more soluble than parent hydrocarbon **3**. It can nevertheless be isolated by recrystallization, as the dihydroindenoindene byproducts **36** (13% yield) occur as a mixture of regioisomers. While one might expect that the bromine substituent should appear exclusively in the exocyclic phenyl ring at C9, because the bromine-substituted ring should be least reactive with respect to Friedel-Crafts-type alkylations, NMR analysis did not indicate a single regioisomer. Switching to the cyclization of methoxy diol **33**, it was surprising to find that the yield of 1-methoxytribenzotriquinacene **35** dropped to 13%. A control experiment demonstrated that the methoxy group is stable under the employed reaction conditions. The electron-donating property of the methoxy group seems to have a detrimental effect on the desired reaction sequence. It possibly renders the cations too stable for Friedel-Crafts alkylations. This is also reflected by the lower yield of the dihydroindenoindene byproducts **37** (7%), indicating a competing pathway before the reaction steps leading to **35** and its byproducts.

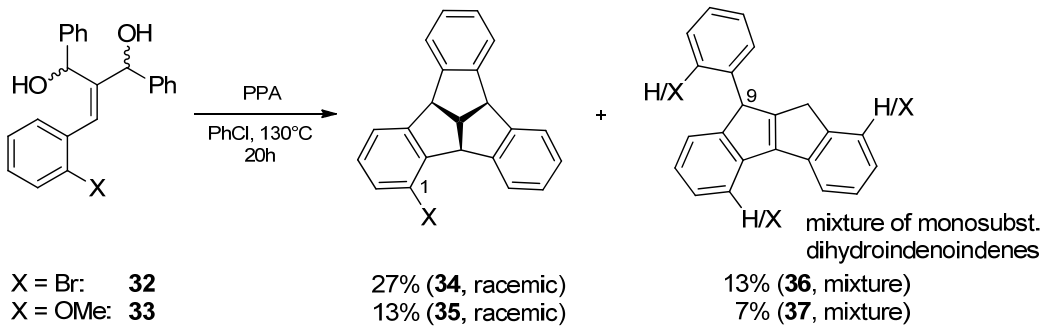


**Scheme 12.** Cyclization to monosubstituted tribenzotriquinacenes **34** and **35**

Monosubstituted tribenzotriquinacenes **34** and **35** are chiral, and resolution of their enantiomers by chiral phase HPLC is described in Chapter 1.5.7. Compound **35** was further transformed in very good yield to chiral phenol **38** by treatment with $BBr_3$ in dichloromethane (Scheme 13). The enantiomers of **38** were also resolved by chiral phase HPLC (Chapter 1.5.7).

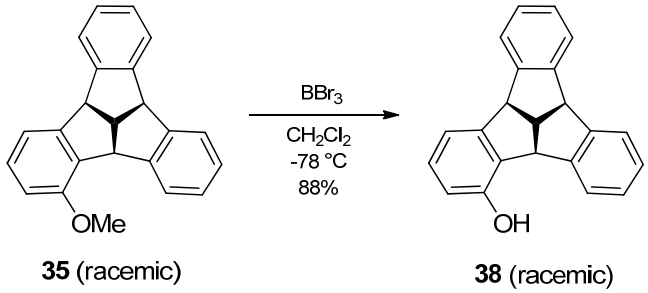


**Scheme 13.** Deprotection of methyl ether **35**

## 1.4 Synthesis of $C_3$-chiral derivatives

$C_3$-chiral molecules have recently attracted much interest because of their applications in asymmetric catalysis and molecular recognition [64–72]. New entries to families of $C_3$-chiral compounds are highly desirable, as the number of $C_3$-chiral molecules is still limited compared to the numerous $C_2$-chiral systems. The synthetic protocol developed in this thesis can contribute to this field by allowing the regiospecific synthesis of $C_3$-chiral tribenzotriquinacenes. By simultaneous use of appropriately functionalized benzaldehyde and dibenzoylmethane components, trisubstituted tribenzotriquinacenes can be obtained in a $C_3$-specific fashion. For example, *o,o'*-disubstituted dibenzoylmethanes **40** in conjunction with *ortho*-substituted benzaldehydes **29** give 1,5,9-substituted tribenzotriquinacenes **10** regiospecifically (Scheme 14). As pointed out in Chapter 1.1, a selective synthesis of $C_3$-chiral tribenzotriquinacenes is very attractive as their preparation by electrophilic substitution is usually hampered by lack of regioselectivity and separation problems [36,53,54]. *Ortho*-functionalized $C_3$-chiral tribenzotriquinacenes in particular were completely unknown until now.

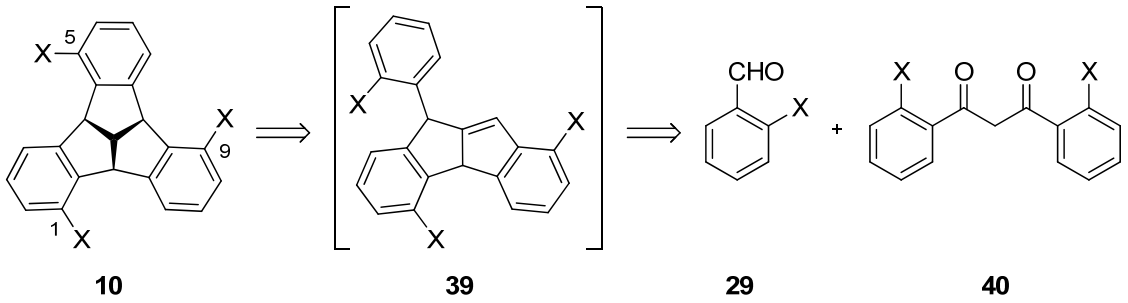


**10** **39** **29** **40**

**Scheme 14.** Retrosynthetic analysis of $C_3$-chiral tribenzotriquinacenes

The synthesis of the $C_3$-chiral tribenzotriquinacenes was pursued for the bromo, methoxy and methyl derivatives. The required *o,o*'-disubstituted dibenzoylmethanes can be synthesized by two alternative methods. Methoxy and methyl derivatives **44** and **45** were prepared by ester condensation as reported in the literature [73,74] (Scheme 15). Unfortunately, the analogous condensation for the bromo compound **43** proceeded only with 26% yield.

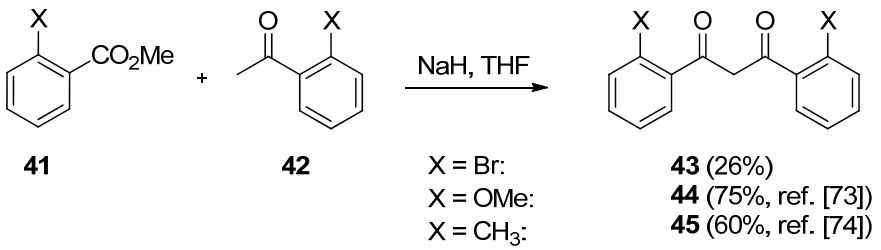


**Scheme 15.** Synthesis of **44** and **45** by Dubrovina et al. [73] and Hu et al. [74]

Because of the low yield in the ester condensation for bromo compound **43**, an easily scalable three-step synthesis as shown in Scheme 16 was adopted [75–78]. Aldol condensation of 2'-bromoacetophenone (**46**) with 2-bromobenzaldehyde gave the *α,β*-unsaturated ketone **47** in 95% yield, which was subsequently brominated in 78% yield to tetrabromide **48**. Reaction with methanol under basic conditions and subsequent acidification furnished the desired bromo compound **43** in 77% yield. The combined yield over three steps amounted to 57%. Single crystals of **43** for X-ray analysis were obtained by recrystallization from ethanol at 60 °C. The crystal structure revealed interesting bromine-bromine interactions and is discussed in detail in Chapter 1.5.5.

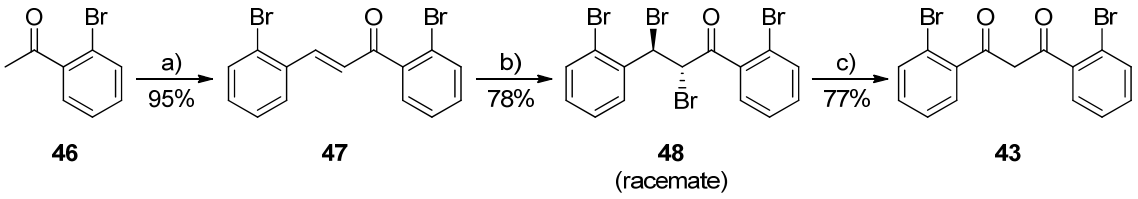


**Scheme 16.** Three-step synthesis of **43**; reagents: a) 2-bromobenzaldehyde, NaOH, $H_2O$, EtOH; b) $Br_2$, $CHCl_3$; c) KOH, MeOH, then HCl, $H_2O$.

With *o,o*'-disubstituted dibenzoylmethanes **43**, **44** and **45** in hand, the synthesis of the cyclization precursors was pursued. Knoevenagel condensation, performed in two different variants, proceeded reliably and gave the respective trisubstituted adducts **49**, **50** and **51** in 61-85% yield (Scheme 17).[1] Subsequent Luche reduction furnished the trisubstituted diols **52**, **53** and **54** in 74-82% yield despite increasing the reaction equivalents of cerium(III) to 2.1-3.0 and sodium borohydride to 2.1-3.0 respectively. It seems that the steric bulk of the three *ortho*-substituents has a negative influence on the double reduction as compared to the synthesis of the parent or monosubstituted diols (see Chapters 1.2 and 1.3). The diastereomers of the diols can be separated by

[1] A crystal structure was obtained for Knoevenagel adduct **50** and is discussed in Chapter 1.5.1.

flash chromatography and crystal structures were obtained for *anti*-**52** and *syn*-**54** (see Chapter 1.5.2).

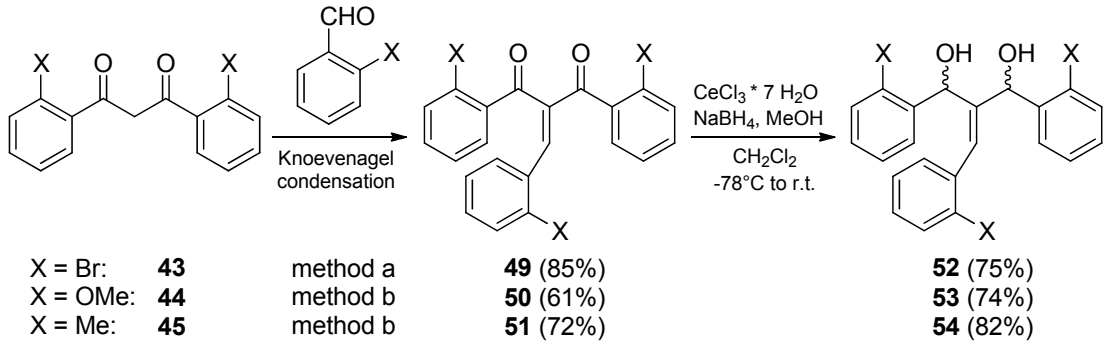


**Scheme 17.** Synthesis of trisubstituted diols **52-54**; reaction conditions: a) piperidine (cat.), acetonitrile (reflux), 12 h; b) piperidine (cat.), hexanoic acid (cat.), toluene (reflux), 20 h.

Triple cyclization to $C_3$-chiral tribenzotriquinacenes showed extreme differences in product yield. While the yield for the bromo and methoxy derivatives **55** and **56** dropped to less than 2% (Scheme 18), the methyl derivative **57** was obtained in 31% yield, which is only marginally less than the yield for parent tribenzotriquinacene **3** (32%, Chapter 1.2). Both bromo and methoxy substituents seem to have a detrimental effect on the desired reaction sequence, which is also reflected in the reduced yield of the dihydroindenoindene byproducts **58** and **59** (2-4%). Contrastingly, the methylated byproduct **60** was isolated in 12% yield. Crystal structures were obtained for the $C_3$-chiral tribenzotriquinacene **57** and the dihydroindenoindene byproducts **58**, **59** and **60** and are discussed in Chapters 1.5.6 and 1.5.8.

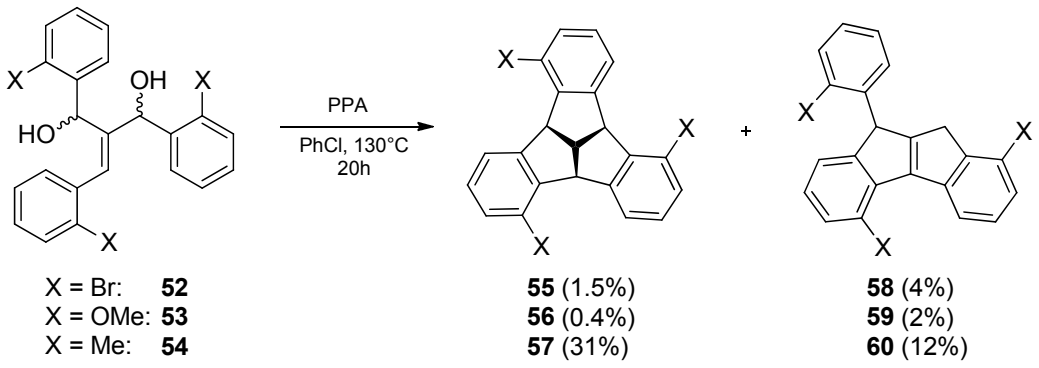


**Scheme 18.** Cyclization to $C_3$-chiral tribenzotriquinacenes **55-57**

It should be emphasized at this point that formation of an unsymmetric $C_1$-chiral tribenzotriquinacene is intrinsically precluded. The regiospecificity of the cyclization leading exclusively to the $C_3$-chiral tribenzotriquinacene can be explained by the reaction mechanism proposed in Chapter 1.2 and is demonstrated in Scheme 19. The exclusive regiochemistry of the dihydroindenoindene byproducts **63** is also portrayed.

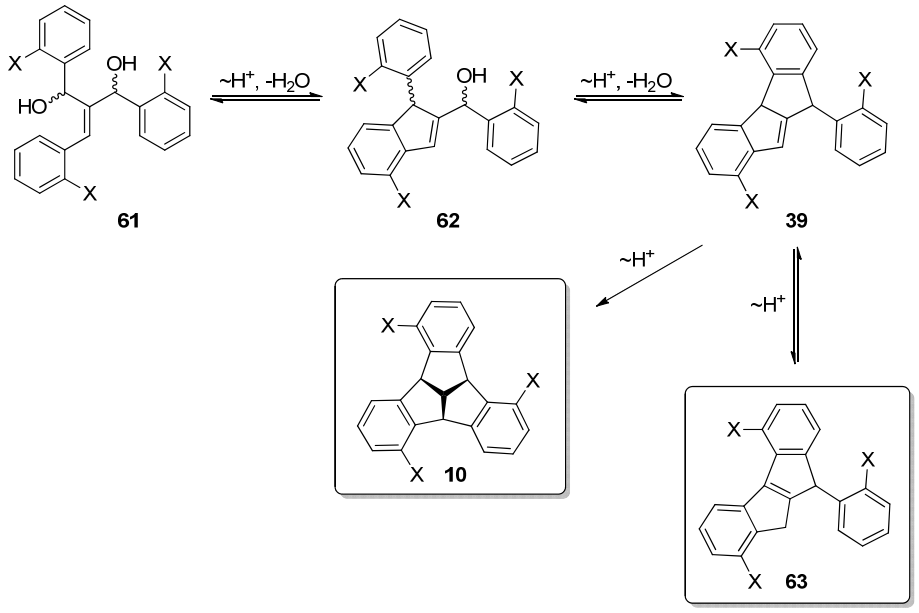


**Scheme 19.** Demonstration of regiospecificity in the cyclization of trisubstituted diols

Resolution of the enantiomers of tribenzotriquinacenes **55-57** by chiral phase HPLC is described in Chapter 1.5.7.

## 1.5 Comparison and discussion of structural data

As a series of analogous compounds was prepared in the course of this investigation, it is advantageous to discuss their structural characteristics in a joint context. Various styles will be used for the representation of crystal structures in order to optimize clarity for each individual compound.

### 1.5.1 Crystal structures of Knoevenagel adducts

Single crystals for X-ray crystallography were obtained for the following Knoevenagel adducts:

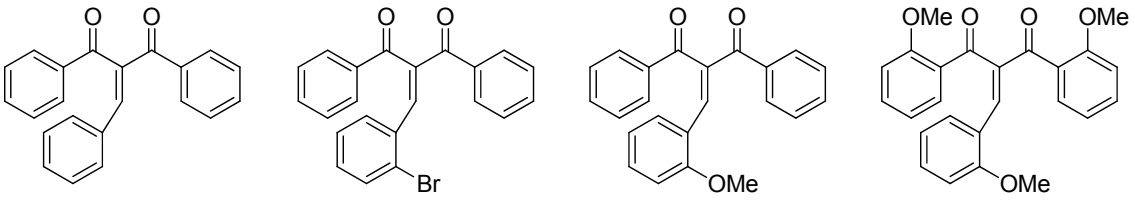


**14** orthorhombic $P2_12_12_1$ | **30** monoclinic $P2_1/c$ | **31** monoclinic $P2_1/c$ | **50** monoclinic $P2_1/c$

**Figure 5.** Knoevenagel adducts for which X-ray structures were obtained

Crystals of **30**, **31** and **50** were obtained by slow evaporation of an ethyl acetate / pentane solution; compound **14** was recrystallized from refluxing toluene. Parent compound **14** crystallized in the orthorhombic space group $P2_12_12_1$, the derivatives **30**, **31** and **50** in the monoclinic space group $P2_1$/c. **30** and **31** are almost perfectly isotypic. The molecular structures from the X-ray analyses are shown in Figure 6. To enhance comparability, the structures are shown perpendicular to the central olefin plane, and with the attached phenyl group pointing to the lower left corner. In this series of related compounds, the influence of the substituent on the solid state structure can be studied. The molecular conformation in the solid state is determined by intramolecular effects as well as by intermolecular crystal packing effects. Inspection of Figure 6 shows that the derivatives **30**, **31** and **50** adopt quite similar solid state conformations, while the conformation of parent compound **14** differs significantly.

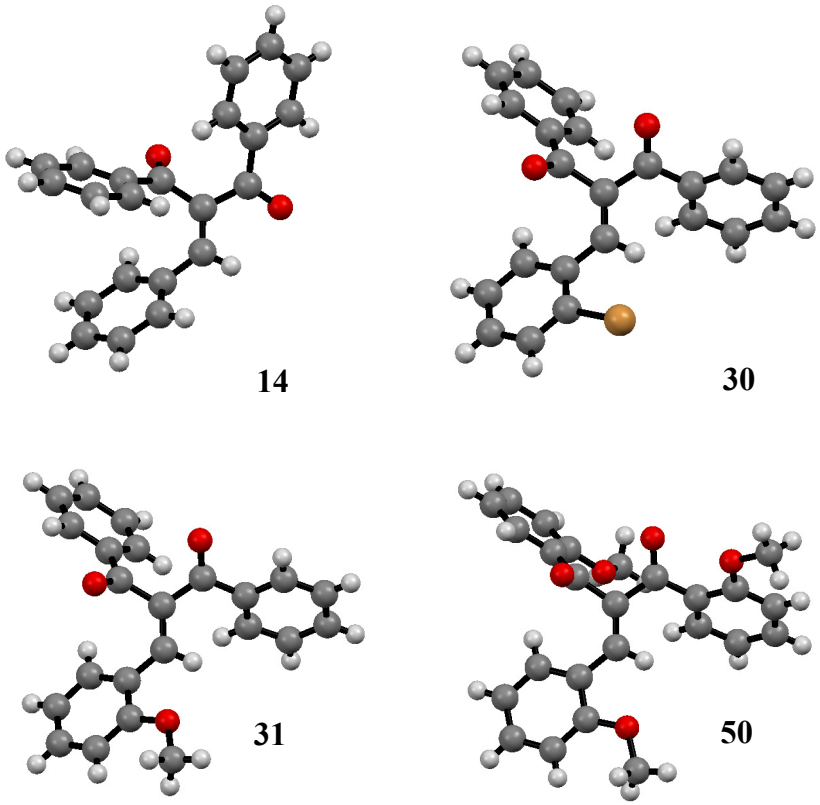


**Figure 6.** Molecular structures from X-ray analyses of Knoevenagel adducts **14**, **30**, **31** and **50**

In order to quantify these conformational differences, selected torsion angles were analyzed:

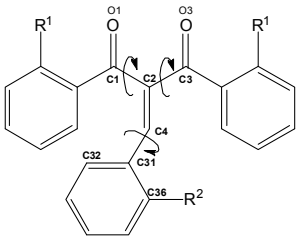


| | O1-C1⋯C3-O3 | O1-C1-C2-C4 | O3-C3-C2-C4 | C2-C4-C31-C32/C36 |
|---|---|---|---|---|
| **14** ($R^1 = R^2 = H$) | -88.8° | -129.3° | 29.3° | 40.0° |
| **30** ($R^1 = H$, $R^2 = Br$) | -74.9° | 52.9° | -147.5° | 37.7° |
| **31** ($R^1 = H$, $R^2 = OMe$) | -74.5° | 54.0° | -147.9° | 37.4° |
| **50** ($R^1 = R^2 = OMe$) | -76.2° | 69.6° | -163.8° | 27.2° |

**Table 2.** Selected torsion angles for Knoevenagel adducts **14**, **30**, **31** and **50**

The torsion angles support the similarity of conformations in **30**, **31** and **50** and their difference from that of **14**. In particular, the isotypy of **30** and **31** is supported by the data in Table 2. For all compounds, the carbonyl groups lie almost orthogonal to each other (see column “O1-C1⋯C3-O3”). The torsion angles between the carbonyl groups

and the olefinic double bond are in the range of 52 to 70° and -147 to -164° for **30**, **31** and **50**. These values are almost complementary to the respective torsion angles in **14** (-129° and 29°). The torsion angle between the phenyl group and the olefinic double bond lies between 27-40°. The phenyl groups of the ketone moieties are either coplanar with the carbonyl group with a torsion angle between -5 and 4° or slightly rotated with a torsion angle between 19-46° (not shown in Table 1). A closer look at the torsion angles in **14** reveals that its conformation does not differ so much from that of the other derivatives: If the labels C1 and C3 were exchanged (by 180° rotation of the molecule), the carbonyl arrangement would roughly correspond to the one found in **30**, **31** and **50** (Figure 7). However, the phenyl group would then point to the lower right corner.

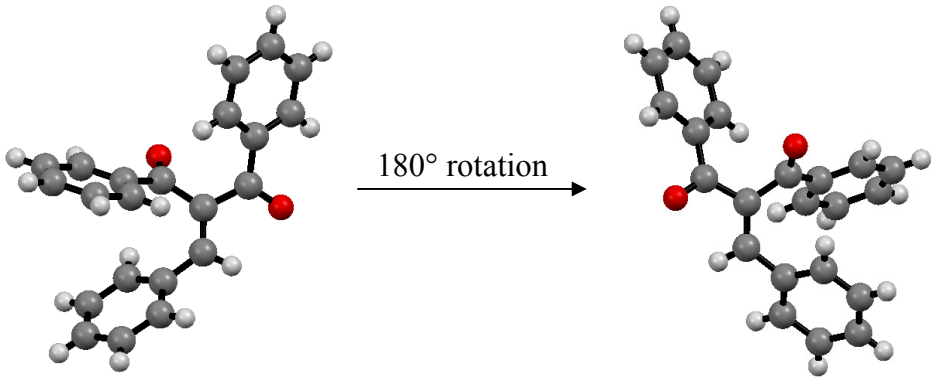


**Figure 7.** Alternative view of compound **14** to demonstrate its conformational similarity with **30**, **31** and **50** (oxygen atoms in dark grey)

To shed light on the conformational differences, the conformations observed in the solid state were used as input structures for gas phase calculations on the unsubstituted Knoevenagel adduct **14**.[m] The input structures were optimized at the M06-2X/6-311G(d,p) level of theory. The conformers of the unsubstituted compound were labeled according to the structure that they were derived from; their torsion angles and relative energies are shown in Table 3.

[m] A complete analysis of the conformational landscape was not undertaken, as it is not the focus of the present study.

| | O1-C1⋯ C3-O3 | O1-C1-C2-C4 | O3-C3-C2-C4 | C2-C4-C31-C32/C36 | rel. energy [kcal/mol] |
|---|---|---|---|---|---|
| **14**-type | -89.1° | -123.6° | 23.5° | 38.0° | 0.0 |
| **30/31/50**-type | -70.5° | 57.2° | -147.6° | 30.7° | 2.1 |

**Table 3.** Torsion angles and energies for calculated conformers of **14**

The calculations confirm the similarity of the conformation in **30**, **31** and **50**, as all three derivatives lead to the same minimum for an unsubstituted system in the gas phase (labeled **30/31/50**-type). This conformer is 2.1 kcal/mol higher in energy than the gas phase conformer derived from the solid state conformation of the parent diketone **14** (labeled **14**-type). It seems that the substituents impose a conformation in the solid state that is energetically slightly unfavorable. Although such assertions are difficult to prove, this conformational disadvantage is probably counterbalanced by more favorable crystal packing effects.

### 1.5.2 Crystal structures of diastereomeric diols

A series of analogous diastereomeric diols was prepared in the course of this investigation (Chapters 1.2-1.4). In order to assign their relative configuration, X-ray structures had to be obtained. Except for **53**, this was achieved for either one or both diastereomers of each diol (Table 4). Overall, crystal structures of three *syn*-diols and three *anti*-diols were obtained:

| | *syn*-diol | *anti*-diol | | *syn*-diol | *anti*-diol |
|---|---|---|---|---|---|
| 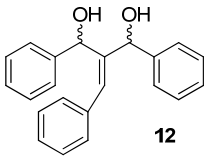 **12** | monoclinic $P2_1/n$ | monoclinic $C2/c$ | 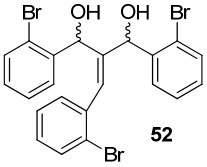 **52** | **X** | orthorhombic *Pbca* |
| 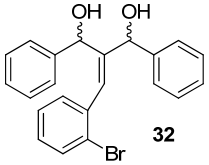 **32** | **X** | triclinic $P\bar{1}$ | 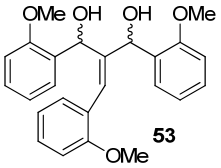 **53** | **X** | **X** |
| 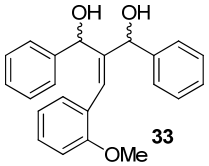 **33** | orthorhombic $P2_12_12_1$ | **X** | 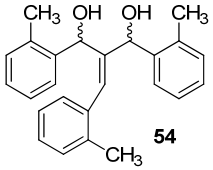 **54** | monoclinic $P2_1/n$ | **X** |

**Table 4.** Overview of obtained crystal structures for diastereomeric diols (**X** indicates that no crystal structure could be obtained)

Crystals were usually obtained by recrystallization from refluxing ethanol with the exception of *anti*-**12**, for which a diffusion method was applied (isopropanol/pentane). The remaining diols were either oils or disordered or did not give crystals of suitable size. The compounds crystallized in five different space groups. All diols analyzed by X-ray crystallography exhibited extended hydrogen-bonded networks in the solid state. The crystal structures and solid state packing of the *syn*-diols will be discussed first. Selected torsion angles were analyzed to describe the conformation of the allylic diol backbone (Table 5). Diols *syn*-**12** and *syn*-**33** adopt essentially the same conformation. However, the relative orientation of their hydroxy groups is inverted. One may conclude that introduction of a methoxy substituent as in *syn*-**33** has only a minor effect on the preferred solid state conformation. Changes are more profound when

three methyl groups are introduced, as in *syn*-**54**. Although the conformations are still comparable, the methyl groups give rise to a distinctly different hydrogen bond network.

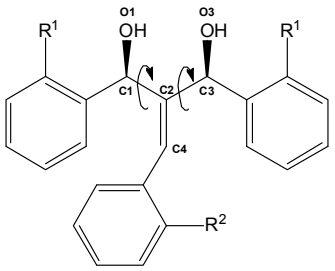


| | O1-C1⋯ C3-O3 | O1-C1-C2-C4 | O3-C3-C2-C4 |
|---|---|---|---|
| *syn*-**12** ($R^1 = R^2 = H$) | -96.6° | 127.0° | 129.4° |
| *syn*-**33** ($R^1 = H$, $R^2 = OMe$) | 96.0° | 128.5° | 128.0° |
| *syn*-**54** ($R^1 = R^2 = CH_3$) | -132.0° | 109.0° | 104.1° |

**Table 5.** Selected torsion angles for diols *syn*-**12**, *syn*-**33** and *syn*-**54**

All three *syn*-diols show polymeric hydrogen-bonded chains. However, only in *syn*-**12** and *syn*-**33** do both hydroxy groups engage in intermolecular hydrogen bonding, so that double stranded chains develop (Figure 8, next page). By contrast, only one hydroxy group in *syn*-**54** engages in intermolecular hydrogen bonding, the other one being involved in an intramolecular OH⋯π interaction. The consequence is a single stranded chain (Figure 9, next page).

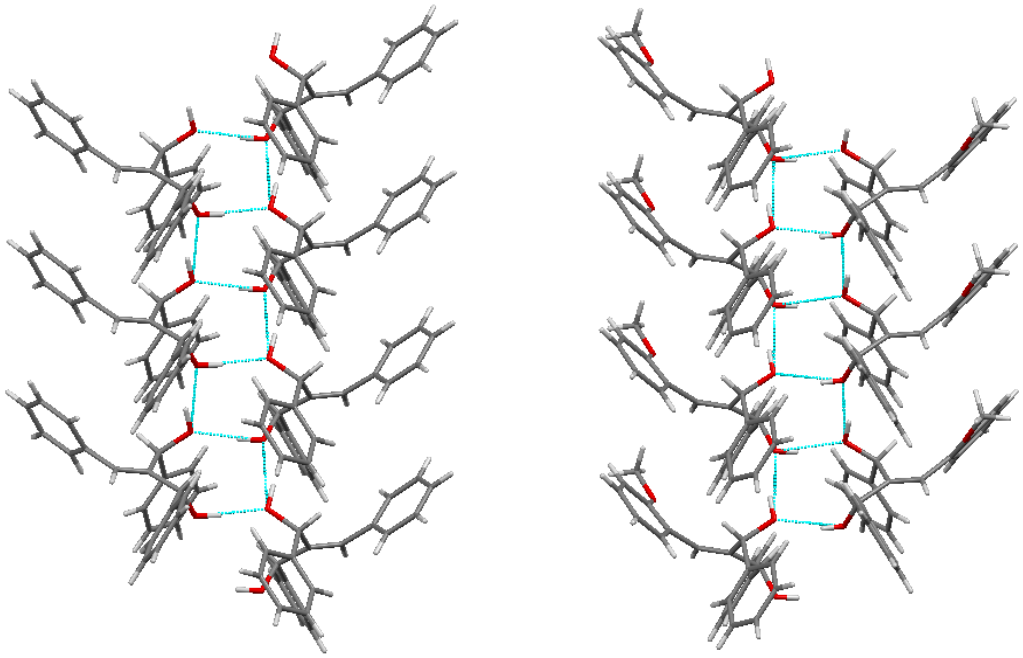

**Figure 8.** Projection of hydrogen-bonded double strands in *syn*-**12** and *syn*-**33**; view perpendicular to (103) and parallel to the *c* axis, respectively. Hydrogen bonds are indicated in light blue.

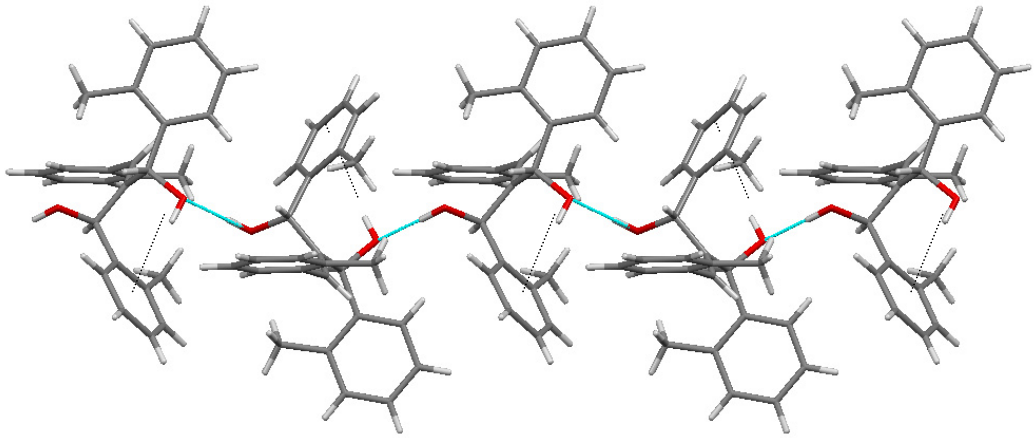

**Figure 9.** Projection of hydrogen-bonded single strand in *syn*-**54**; view parallel to the *c* axis. Hydrogen bonds are indicated in light blue, OH···π interaction by dotted lines.

Comparison of the crystal structures of the *anti*-diols is complicated by the fact that the unit cells contain two crystallographically independent molecules in all three cases. A discussion of the various conformers and solid state packing will nevertheless be attempted.

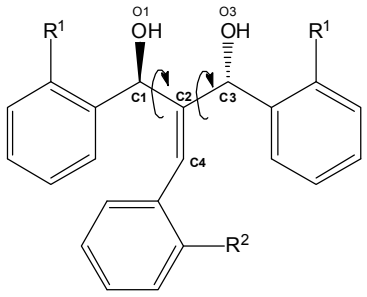


| | O1-C1⋯ C3-O3 | O1-C1-C2-C4 | O3-C3-C2-C4 |
|---|---|---|---|
| *anti*-**12** ($R^1 = R^2 = H$) | 38.3 | 148.4 | -102.1 |
| | -8.0 | 108.6 | -117.1 |
| *anti*-**32** ($R^1 = H$, $R^2 = Br$) | 34.7 | 143.6 | -100.8 |
| | 34.5 | 143.4 | -100.7 |
| *anti*-**52** ($R^1 = R^2 = Br$) | 85.2 | 103.9 | -15.5 |
| | 82.8 | 105.1 | -19.0 |

**Table 6.** Selected torsion angles for diols *anti*-**12**, *anti*-**32** and *anti*-**52** (all compounds contain two crystallographically independent molecules)

Diol *anti*-**12** exhibits two conformers in the solid state. They are related by rotation of the phenyl hydroxy methyl group of C1 (Table 6). The asymmetric unit of *anti*-**32** contains two crystallographically independent molecules that otherwise present the same conformation. Their conformation is very similar to one of the conformations observed in *anti*-**12**. This demonstrates again that the introduction of one substituent does not have a profound effect on the solid state conformation of the allylic diol backbone. The crystal structure of diol *anti*-**52** also exhibits two crystallographically independent molecules; they have very similar conformations, but differ markedly from those of the unsubstituted diol *anti*-**12**. Again, introduction of three substituents leads to a profound change in the solid state conformation.

As in the case of the *syn*-diols, all three *anti*-diols show polymeric hydrogen-bonded chains. Both conformers in the crystal structure of *anti*-**12** form intra- and intermolecular hydrogen bonds leading to polymeric strands. However, the strands of conformer 1 interact with each other via additional hydrogen bonding to form double strands, whereas the strands of conformer 2 remain isolated (Figure 10).

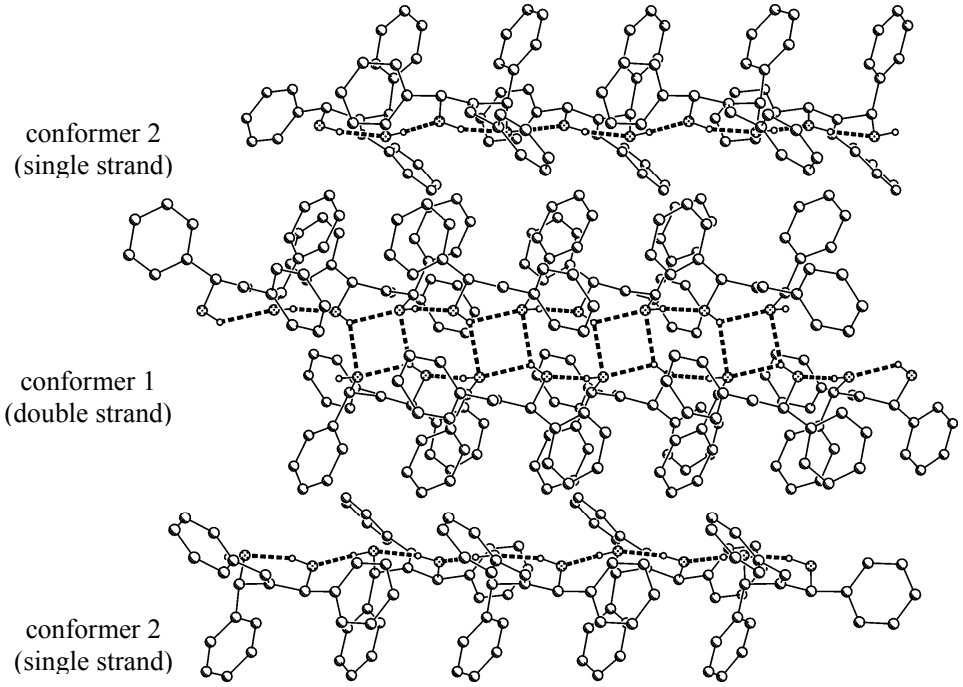


**Figure 10.** Projection of hydrogen-bonded strands in *anti*-**12**; view parallel to the *b* axis. Conformer 1 forms double strands, conformer 2 forms isolated single strands. Dashed lines indicate hydrogen bonds.[n]

The conformers in the crystal structure of *anti*-**32** form intra- and intermolecular hydrogen bonds, giving rise to one type of double strand. The conformers in crystal structure of *anti*-**52** engage only in intermolecular hydrogen bonds, also leading to one type of double strand (Figure 11).

[n] Figure courtesy of Prof. Peter G. Jones.

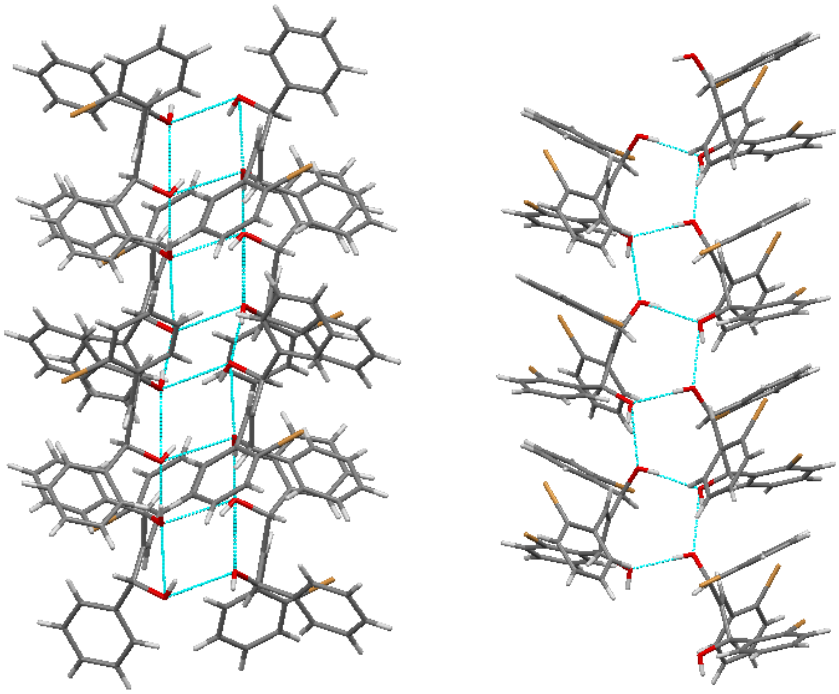

**Figure 11.** Projection of hydrogen-bonded double strands in *anti*-**32** and *anti*-**52**; view parallel to the *b* and *a* axis, respectively. Light blue lines indicate hydrogen bonds.

### 1.5.3 NMR spectra of diastereomeric diols

Based on the crystallographic assignment of the relative configuration of several diols (Chapter 1.5.2), it is possible to compare their NMR spectra for common features. NMR spectra depend on the conformation in solution and might therefore differ substantially because of the conformational flexibility of the diols. A comparison of their NMR spectra shall nevertheless be attempted.

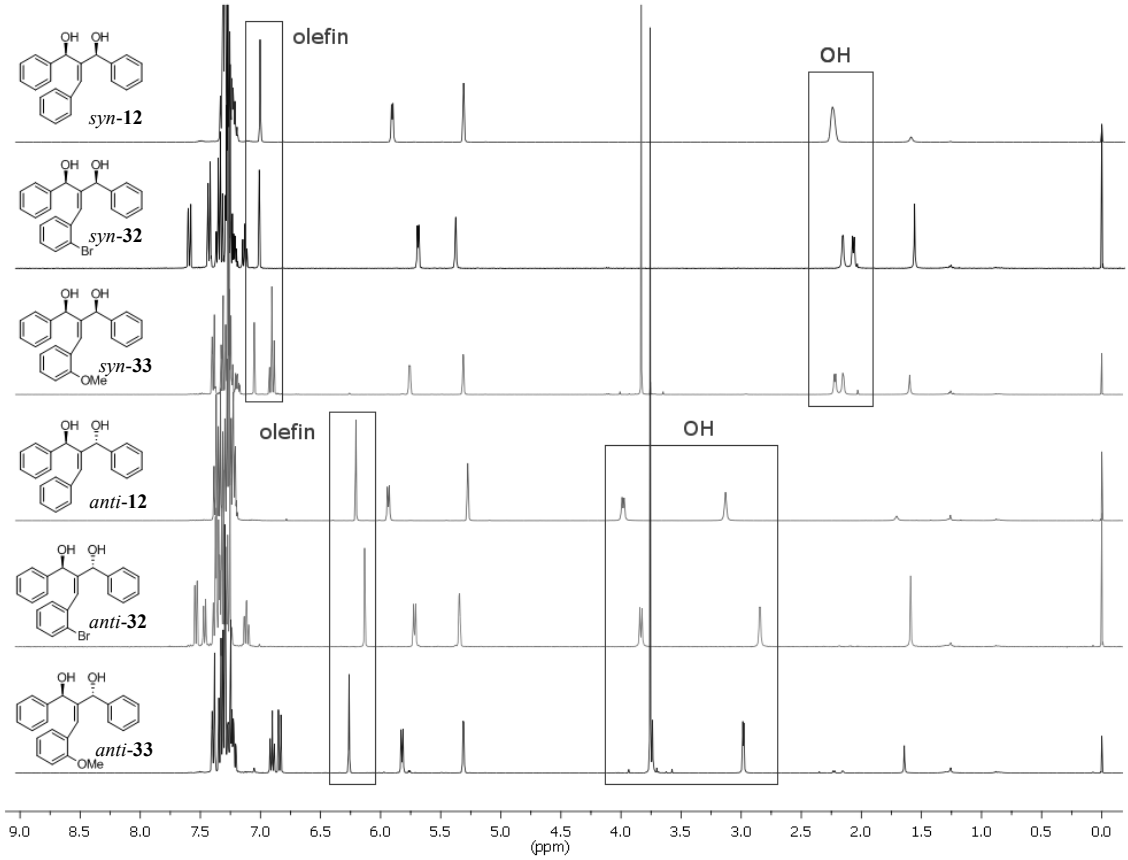


**Figure 12.** Comparison of $^{1}$H-NMR (400 MHz, $CDCl_3$) spectra of unsubstituted (**12**) and monosubstituted (**32**, **33**) diols

The NMR spectra of unsubstituted and monosubstituted diols **12**, **32** and **33** are shown in Figure 12. A clear pattern arises for this set of molecules: *syn*-diols show two close, sometimes even overlapping resonances for the hydroxy groups; the hydroxy resonances of the *anti*-diols are further apart and generally more downfield. Distinctive differences are also seen for the olefinic proton, which in the *syn*-diols is about 1 ppm downfield compared to the *anti*-diols. No clear pattern is visible for the C*H*OH resonance between 5.2-6.0 ppm. The overall similarity of the spectra suggests that the

respective *syn*- and *anti*-diastereomers prevail in the same conformation respectively, regardless of whether they are un- or monosubstituted.[o,p]

For the trisubstituted diols, the relative configuration of the bromine and methyl derivatives could be assigned by X-ray crystallography (see above). Their NMR spectra are shown in Figure 13 and suggest a recurrent pattern. The *syn*-diols show two close resonances for the hydroxy groups, while the respective signals in the *anti*-diols are further apart and more downfield. Furthermore, the olefinic signals of the *syn*-diols are more downfield than for the *anti*-diols.

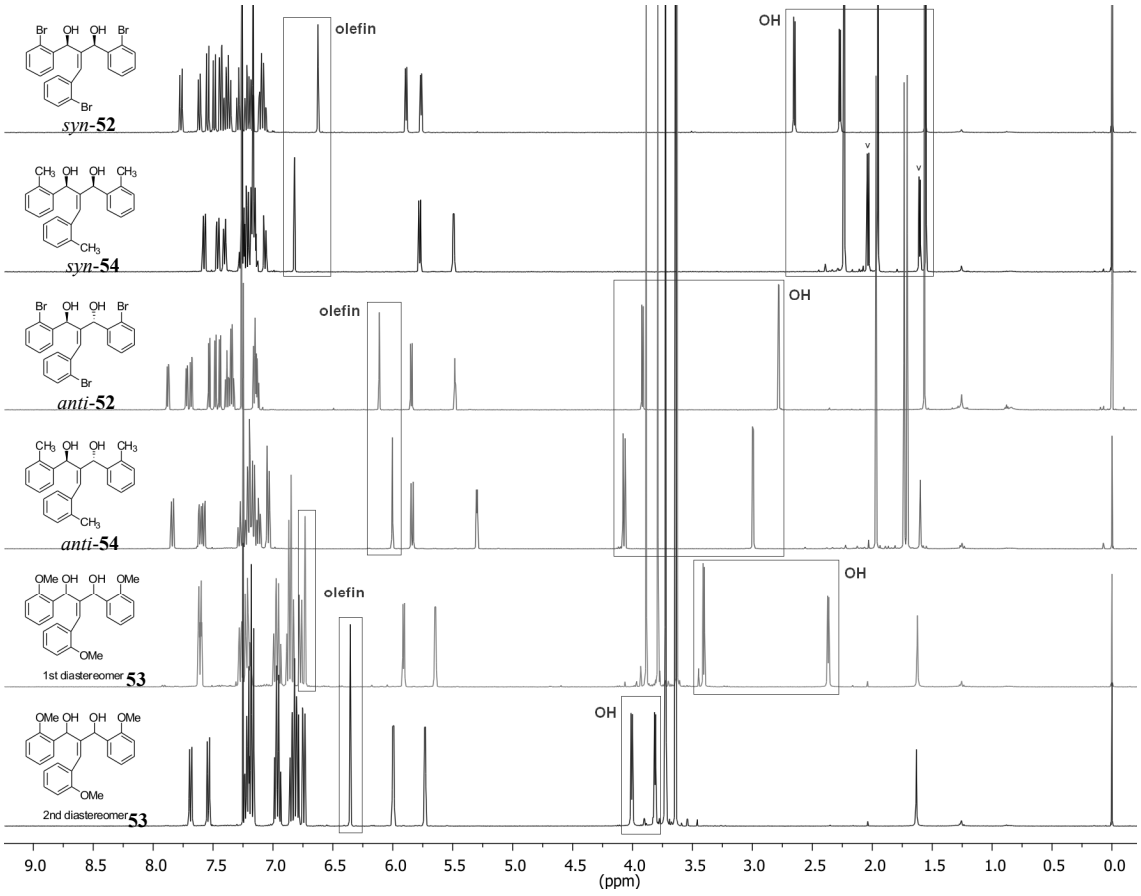


**Figure 13.** Comparison of $^{1}$H-NMR (400 MHz, $CDCl_3$) spectra of trisubstituted diols **52-54**

[o] The formation of dimers or higher aggregates in solution is not considered at this point.

[p] $^{1}$H-NMR spectra for diols *syn*-**12** and *anti*-**12** were also measured in DMSO-$d_6$ and H/D exchange of the alcoholic protons with $D_2O$ was demonstrated (see Experimental Section).

Based on this pattern it was hoped to assign the relative configuration of the trimethoxy diols by NMR analysis, as no crystal structures could be obtained for these compounds. However, inspection of their NMR spectra shows inconclusive evidence. The first trimethoxy isomer shows a wide separation of the hydroxy signals, as would be expected for an *anti*-diol. However, the olefinic proton is shifted more downfield compared to the second isomer, which would rather speak for a *syn*-diol. The second isomer shows two close hydroxy resonances, as would be expected for a *syn*-diol, but they appear far downfield and their chemical shift corresponds rather to that of an *anti*-diol. The chemical shift of the olefinic proton would also rather correspond to that of an *anti*-diol. Based on this NMR analysis, no clear assignment of the relative configuration of the trimethoxy diols can be made. Their conformations seem to differ substantially from those of the other derivatives.[q] This is not surprising as the X-ray studies already indicated that the introduction of three substituents has profound effects on the solid state conformation (Chapter 1.5.2). Similarly marked differences can therefore also be expected for the conformation in solution.

[q] The formation of dimers or higher aggregates in solution is not considered at this point.

### 1.5.4 ESI-MS of diols

All diols prepared in this study were analyzed by electrospray ionization mass spectrometry (ESI-MS). A recurrent pattern was observed that is worth discussing. Regardless of relative configuration, all diols showed a strong $[M + Na]^+$ signal along with a second signal corresponding to $[M - 35]^+$. Most of the diols also showed an additional signal corresponding to $[M - 17]^+$. As a representative example the ESI mass spectrum of *syn*-**12** is shown in Figure 14 and shall be discussed in full detail.[r]

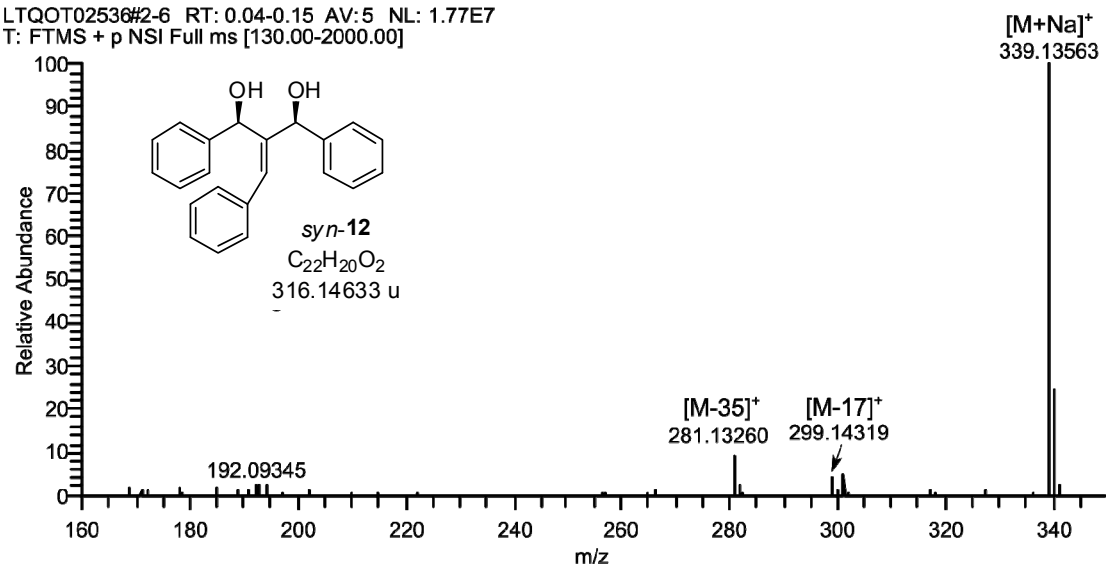


**Figure 14.** ESI-MS of diol *syn*-**12** (5 µg/mL in MeOH)

Accurate mass measurements confirmed that the $[M - 17]^+$ signal corresponds to the molecular formula $C_{22}H_{19}O^+$, which represents the formal loss of a hydroxide ion $OH^-$. The $[M - 35]^+$ signal corresponds to $C_{22}H_{17}^+$, which formally represents the loss of water in addition to the hydroxide loss. What are likely structures for these ions? Figure 15 on the next page shows two possible structures that reflect the observed mass differences. The structures correspond to the intermediates that have been postulated for the solution phase synthesis of tribenzotriquinacene (Scheme 7 in Chapter 1.2).

[r] Dimer formation $[2M + Na]^+$ was also observed, but is not included in the excerpt of the spectrum.

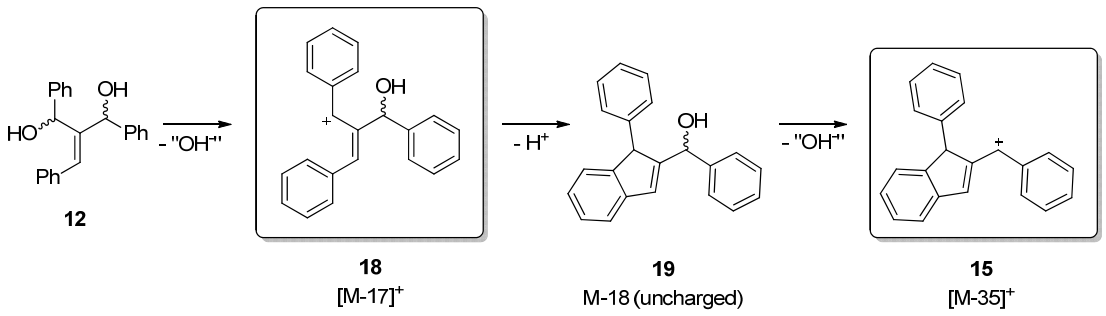


**Figure 15.** Possible structures corresponding to $[M - 17]^+$ and $[M - 35]^+$ signals in ESI-MS of **12**

Two possible sources have to be considered for these cations: First, the respective ions are already present in solution, probably because of proton-catalyzed cyclodehydration. Because of their cationic nature these species would give a strong ESI-MS signal, even if they were present in only trace amounts. The second possibility is that these ions arise from a spontaneous fragmentation in the course of the ionization process, although ESI is generally known as a "soft" ionization method [79]. In this context it should be noted that no proton adduct $[M + H]^+$ was observed for any of the studied diols.[s]

In order to shed light on these questions, MS/MS experiments were performed on the ions observed in the ESI-MS of *syn*-**12**. It was found that: a) collision-induced dissociation (CID) of $[M + Na]^+$ does not give rise to $[M - 17]^+$ and $[M - 35]^+$ (Figure 16). The sodium adduct primarily dissociates into the sodium ion and the neutral organic fragment; additionally, a minor fragment corresponding to water loss is observed; b) CID of $[M - 17]^+$ gives rise to $[M - 35]^+$, but only in minor amounts (Figure 17). Other fragments, which are not observed to the same extent in the full MS, are much more dominant. It is therefore concluded that $[M - 17]^+$ is a stable ion under standard ESI-MS conditions and that the strong $[M - 35]^+$ signal in the full spectrum has to be of different origin. This was further supported by a precursor ion scan that did not reveal any precursor ion for $[M - 35]^+$. No precursor ion was found for $[M - 17]^+$ either.

[s] The respective diketones usually showed a proton adduct $[M + H]^+$ next to the sodium adduct $[M + Na]^+$.

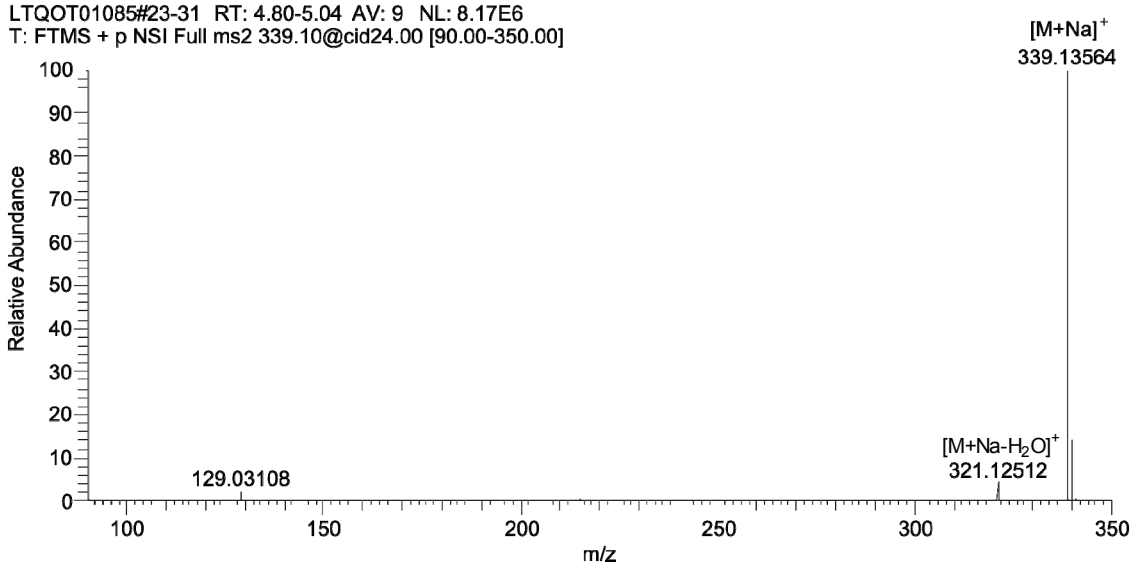


**Figure 16.** ESI-MS/MS on $[M + Na]^+$ adduct of *syn*-**12**

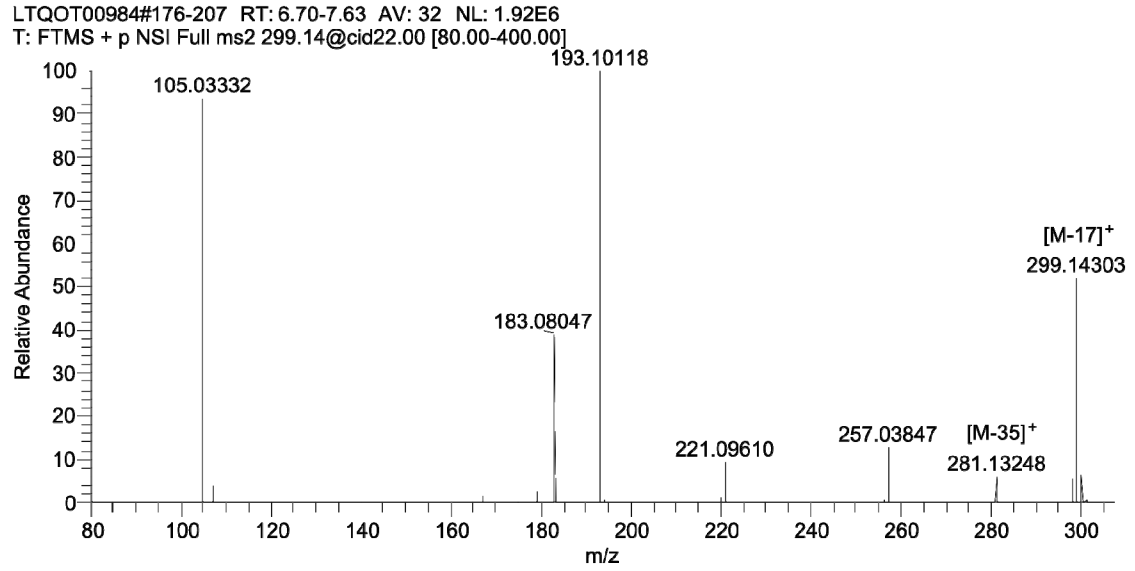


**Figure 17.** ESI-MS/MS on $[M - 17]^+$ signal of *syn*-**12**

The question of the missing proton adduct $[M + H]^+$ in the ESI-MS of *syn*-**12** was addressed by synthesizing reference compound **64** shown in Figure 18 [80,81]. It was assumed that the saturated diol **64** should have the same propensity to form a proton adduct $[M + H]^+$ as its unsaturated analogue **12**. However, the proton adduct of **64** should be more stable, as water elimination would lead to a less stabilized cation. The ESI-MS measurement exclusively revealed a strong $[M + Na]^+$ signal; no other signals were observed. It can therefore be assumed that the 1,3-diol arrangement in **12** has no

propensity to form proton adducts either. The lack of a $[M + H]^+$ signal in the ESI-MS of *syn*-**12** is therefore unlikely to result from a spontaneous fragmentation of the respective proton adduct.

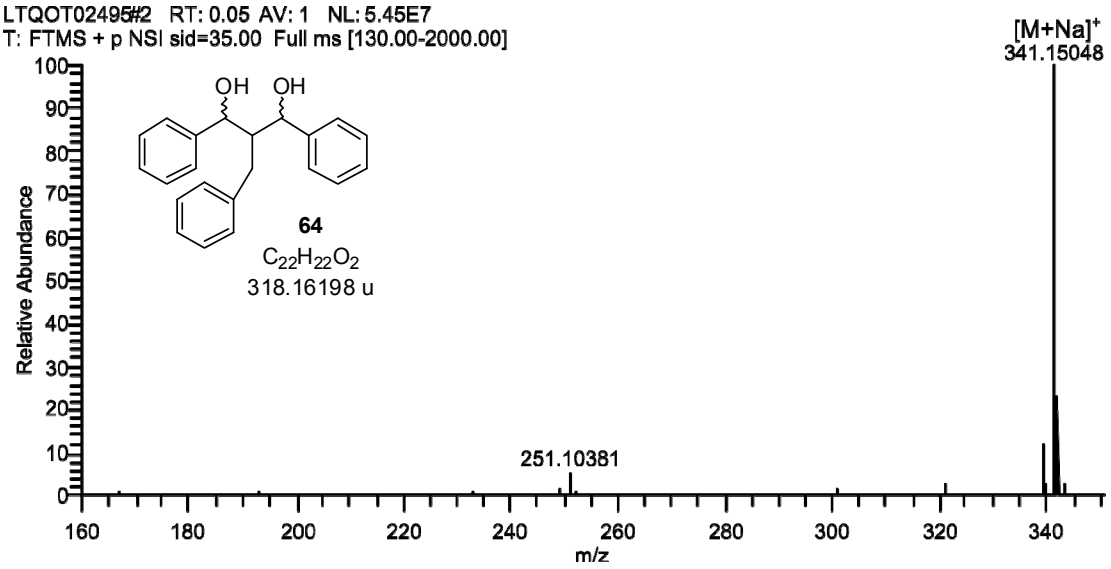


**Figure 18.** ESI-MS of saturated diol **64**

In order to test whether the cations **18** and **15** shown in Figure 15 are present in solution, an exchange experiment with $H_2{}^{18}O$ was performed. At least the cation corresponding to $[M - 17]^+$ should be in equilibrium with diol **12**, so that incorporation of $^{18}O$ into diol **12** should take place. However, no such process was observed under neutral or acidic conditions over a period of 40 days.

In a separate experiment it was shown that addition of formic acid led to an increase of the $[M - 35]^+$ signal in relation to the $[M + Na]^+$ signal. For example, the $[M - 35]^+$ signal in a methanol solution of *syn*-**12** (c = 5 µg/mL) had a relative intensity of ~10% in comparison to the $[M + Na]^+$ signal (Figure 14). Addition of 0.05 vol.-% formic acid increased this intensity to 30%; addition of 0.1 vol.-% to 55% intensity, respectively. Saturation (80% relative intensity) was achieved by addition of 1.0 vol.-% formic acid.

As pointed out earlier, the $[M - 35]^+$ signal corresponds to the molecular formula $C_{22}H_{17}{}^+$. This cation could in principle also arise from protonation of a hydrocarbon with molecular formula $C_{22}H_{16}$. This unlikely possibility was excluded by performing an ESI-MS experiment in deuterated methanol: no deuterium adduct $[C_{22}H_{16} + D]^+$ was observed under these conditions.

In summary, it can be concluded that the $[M - 17]^+$ and $[M - 35]^+$ signals most probably do not arise from the spontaneous fragmentation of a proton adduct during the ESI process. Rather, the corresponding cations seem to be present in solution. Their formation can be enforced by acidic conditions. However, as no incorporation of $^{18}O$ was observed in the exchange experiment, cation formation is either irreversible or exchange is slow because of very low cation concentration. In the latter case the cations would nevertheless give rise to a strong ESI-MS signal because of their already charged nature.

### 1.5.5 Halogen-halogen interactions in a dibenzoylmethane derivative

Halogen atoms in organic molecules are usually associated with a negative partial charge because of their high electronegativity. This partial charge can give rise to hydrogen bonds in which in the halogen atom acts as the Lewis base. However, halogen atoms can also act as Lewis-acidic sites and the respective halogen-halogen interactions have recently emerged as a paradigm in crystal engineering and supramolecular chemistry [82–85]. All halogens except fluorine exhibit an anisotropic electron distribution that leads to positive polarization in the polar region and negative polarization in the equatorial region (Figure 19a). This anisotropy gives rise to what has been termed an attractive "type-II halogen-halogen interaction" (Figure 19b): the positively polarized pole of a carbon-bound halogen ($\theta_1 \approx 180°$) interacts in an orthogonal fashion ($\theta_2 \approx 90°$) with the negatively polarized equator of a second carbon-bound halogen. A distorted type-II arrangement is also present in so called "$X_3$ synthons" (Figure 19c) [86,87]. An extensive computational study of such $X_3$ synthons has been performed by Zou and coworkers [88].

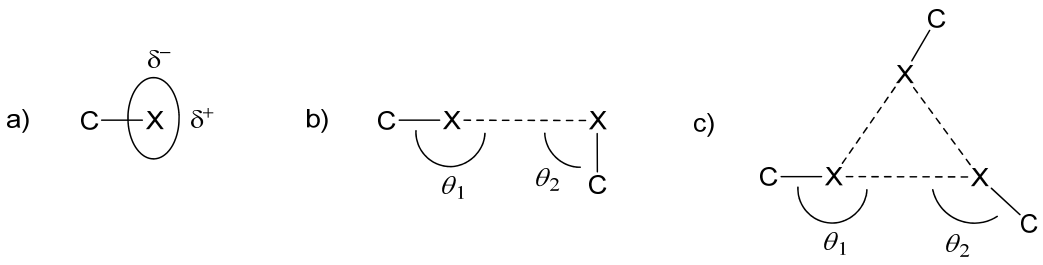


**Figure 19.** Origin and shape of halogen-halogen interactions. a) anisotropic electron distribution in carbon-bound halogens; b) type-II halogen-halogen interaction; c) supramolecular $X_3$ synthon. Figure adapted from reference [89].

The crystal structure of the dibrominated dibenzoylmethane **43** reveals the presence of bromine-mediated dimers that are related through a crystallographic inversion center (Figure 20). The diketone moiety crystallized in its enol form and both bromine substituents point "inwards", thereby allowing the interaction of four halogen centers.

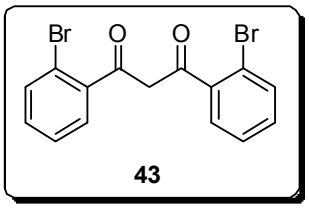


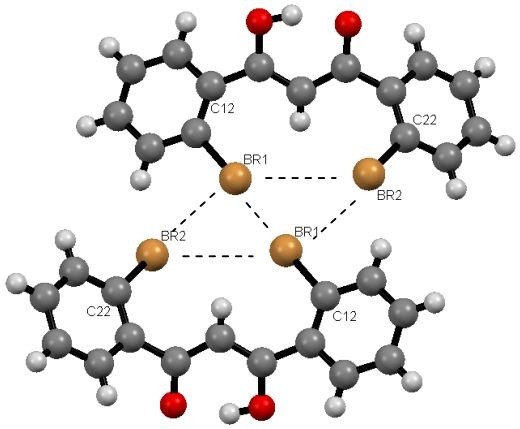


**Figure 20.** Bromine-mediated dimers in crystal structure of **43**

While one may recognize a double $X_3$ synthon motif, it is in fact only the intermolecular Br1···Br2 contact that exhibits the characteristic "head-to-side" arrangement of a type-II interaction ($\theta_1$ = 171.2°, $\theta_2$ = 105.6; see Table 7). The intramolecular Br1···Br2 contact has a "side-to-side" character (119° < θ < 127°). Both Br1···Br2 contacts exhibit a similar distance (3.75-3.77 Å) that corresponds to the van der Waals distance ($r_{vdW}$ (Br) = 1.85 Å). An intermolecular contact below the van der Waals distance is found between the Br1 atoms in the dimer (3.39 Å). The almost linear "head-to-head" arrangement, together with its occurrence around a crystallographic inversion center, is characteristic of a "type-I halogen-halogen interaction". The strength of the intermolecular Br···Br interactions was assessed through calculations at the M06-2X/6-311+G(d,p) level of theory. The interaction energy of the dimer at the frozen solid state geometries amounts to 3.2 kcal/mol.[t]

| distances | Å |
|---|---|
| Br1···Br1 | 3.39 |
| Br1···Br2 (intermol.) | 3.75 |
| Br1···Br2 (intermol.) | 3.77 |

| angles | ° |
|---|---|
| Br1···Br1-C12 | 163.4 |
| Br1···Br2-C22 (intermol.) | 171.2 |
| Br2···Br1-C12 (intermol.) | 105.6 |
| Br1···Br2-C22 (intramol.) | 119.3 |
| Br2···Br1-C21 (intramol.) | 126.6 |

**Table 7.** Representative distances and angles for the bromine-mediated dimer in **43**

[t] The basis set superposition error was estimated by applying the counterpoise technique [90,91]; it amounts to 0.4 kcal/mol for the dimer.

Further analysis of the solid state packing reveals another Br···Br contact: stacking of the dimers parallel to the *c* axis is mediated by a "side-to-side" interaction ($\theta_1 = 67.8°$, $\theta_1 = 110.1°$) with a distance of 3.96 Å (Figure 21). Overall, the structure shows a clean separation between bromine-mediated interactions and regions with hydrophilic character (Figure 22).

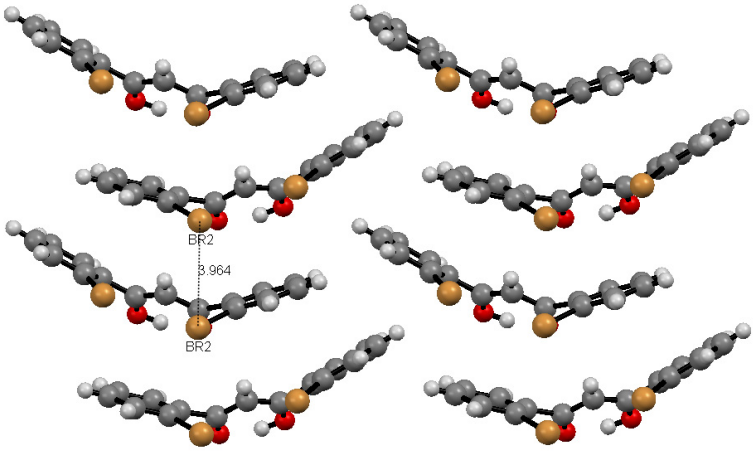


**Figure 21.** Stacking of dimers in crystal structure of **43**; stacks are parallel to the *c* axis (oxygen atoms in red, bromine atoms in brown)

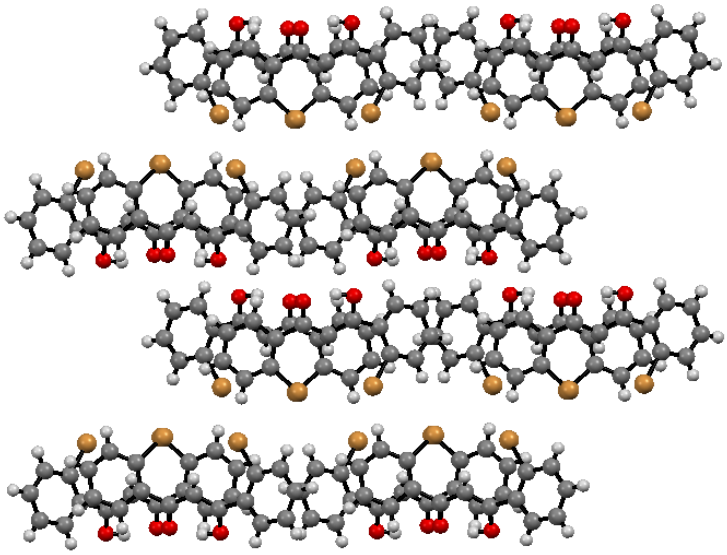

**Figure 22.** View parallel to the *c* axis of the crystal structure of **43** (oxygen atoms in red, bromine atoms in brown)

### 1.5.6 Crystal structures of tribenzotriquinacenes

Single crystals for X-ray analysis were obtained for three tribenzotriquinacenes[u,v] by recrystallization from refluxing toluene:

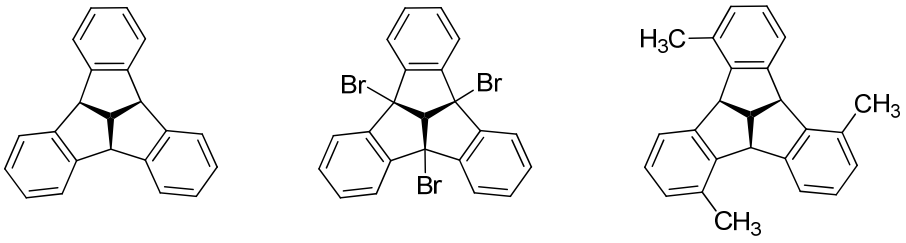


**3** **28** **57**

**Figure 23.** Tribenzotriquinacenes for which X-ray structures were obtained[u,v]

Before discussing their structural properties, the available crystallographic data for tribenzotriquinacenes will be summarized shortly. A structure search in the Cambridge Crystallographic Data files revealed that 24 tribenzotriquinacenes have presently been studied by X-ray crystallography.[w] Of these 24 entries, only one compound is not methylated at the central 12d-position: the hexa-*ortho*-methyl tribenzotriquinacene recently prepared by Krüger and coworkers [49]. The results of an X-ray structural analysis of parent tribenzotriquinacene **3** are mentioned in two reviews by Kuck [40,41], but no crystal structure has officially been published to date [92]. These unpublished results indicate that the crystal structure of **3** features unidirectional columnar stacks as known for the 12d-methyl derivative **8** [43]. However, the stacking distance in **3** is reduced to 4.75 Å as compared to 6.01 Å in **8**. Only one other tribenzotriquinacene derivative is known that exhibits columnar stacking similar to **3** and **8** [52].[x]

With a gram scale synthesis of parent tribenzotriquinacene in hand, it was possible to obtain high quality single crystals for X-ray analysis by recrystallization from refluxing toluene and slow cooling to room temperature. The X-ray analysis reproduced the columnar and unidirectional stacking reported by Kuck and Cyranski

[u] Structures **3** (CCDC 907602) and **57** (CCDC 904630) were deposited at The Cambridge Crystallographic Data Centre. The data can be obtained free of charge via www.ccdc.cam.ac.uk/data_request/cif.

[v] Crystals of the monosubstituted tribenzotriquinacenes **34** and **38** were disordered

[w] Database search performed on 31 October 2012.

[x] Reference [52] reports another derivative with columnar stacking. However, the tribenzotriquinacene units are strongly tilted away from the column axis.

with a stacking distance of 4.75 Å [92] (Figure 24). However, neighboring molecules are slightly rotated by 6° around the common molecular $C_{3v}$ axis (Figure 25) and are not perfectly eclipsed as reported by Kuck and Cyranski. This is also reflected in a different space group, i.e. *R*3*c* (as opposed to *R*3*m*), and a doubling of the *c* axis that describes the translation symmetry along the columnar stacks.

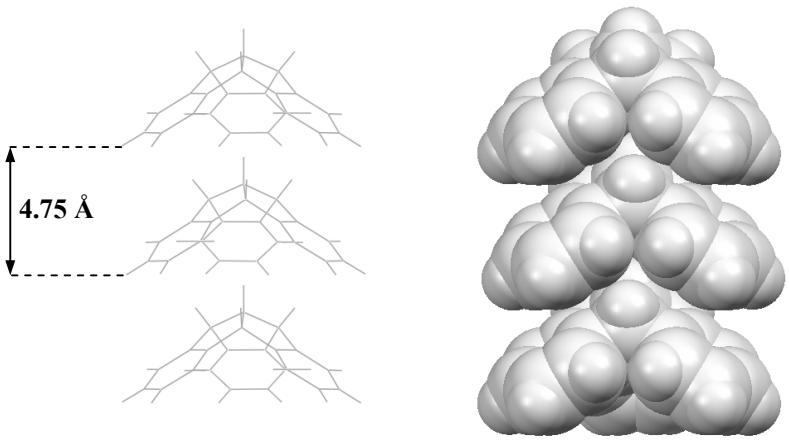


**Figure 24.** Wireframe and space-filling representations of columnar stacks in the crystal structure of parent tribenzotriquinacene **3**. Note the slight rotation around the common molecular $C_{3v}$ axis. Stacks are oriented parallel to the *c* axis.

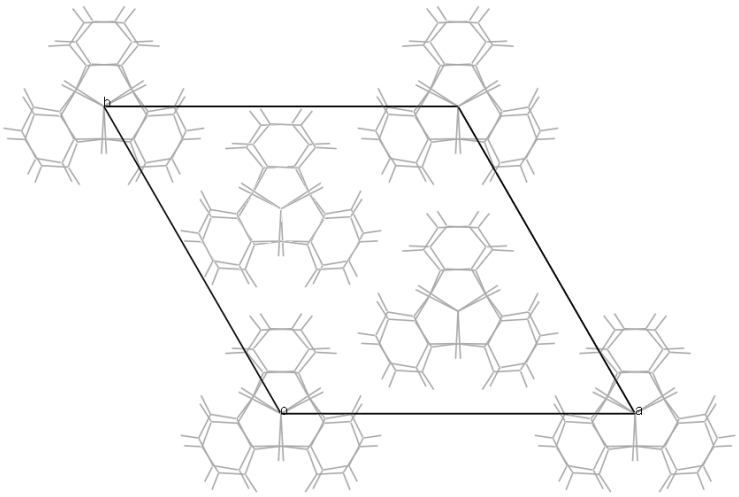

**Figure 25.** Wireframe representation parallel to the *c* axis in the crystal structure of parent tribenzotriquinacene **3**. Note the slight rotation around the common molecular $C_{3v}$ axes.

We next turn our attention to the $C_3$-chiral trimethyl derivative **57**. In which way, if at all, would the three methyl groups at the inner *ortho*-positions affect the crystal structure? Single crystals of **57** for X-ray analysis were obtained by recrystallization from refluxing toluene. The compound crystallized in the triclinic space group $P\bar{1}$, but $C_3$ symmetry of the tribenzotriquinacene unit was preserved to a good approximation (r.m.s. deviation from $C_3$ symmetry = 0.18 Å). The molecular structure as obtained from the X-ray analysis is shown in Figure 26.

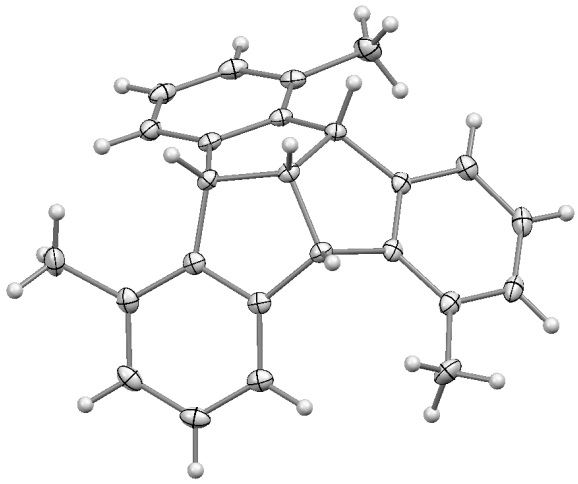

**Figure 26.** ORTEP of $C_3$-chiral tribenzotriquinacene **57** (ellipsoids set at 50% probability)

Interestingly, **57** did not exhibit the columnar stacking as known for **3** and **8** (see above). CH/π-mediated layers of bowls with opposite orientation were formed and the methyl substituents, even when "hidden" in the inner *ortho*-positions, seem to have a pronounced effect on the solid state structure. The respective layers have a repeat distance of 8.25 Å (Figure 27).

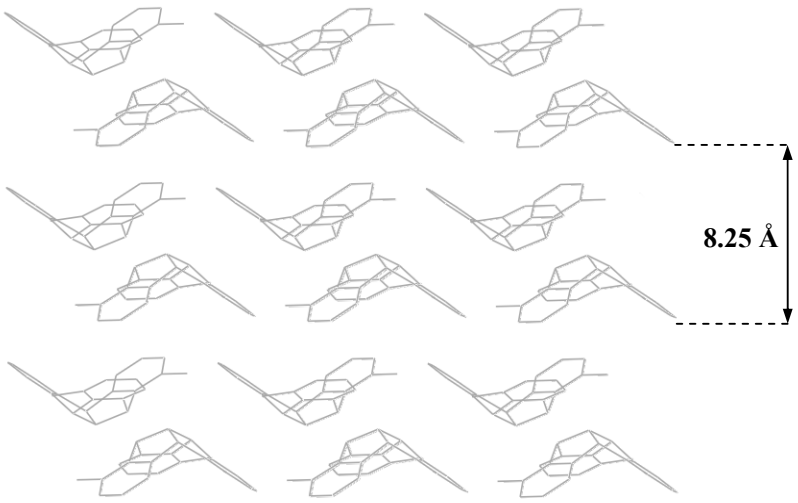


**Figure 27.** Packing diagram for **57** viewed approximately perpendicular to $(\bar{1}22)$; hydrogen atoms omitted for clarity.

As the trisubstituted tribenzotriquinacene **57** might be of interest as a $C_3$-chiral platform in supramolecular chemistry [64,66], it is instructive to compare its geometric parameters with that of other $C_3$-chiral platforms. This comparison is limited to aromatic platforms that have been functionalized with recognition units, and crystallographic data of relevant reference molecules are shown in Figure 28. The distances between the sites of functionalization in these tripodal molecules range between 5.0 and 10.0 Å.[y] $C_3$-Chiral tribenzotriquinacene **57** with a tripodal distance of 7.3 Å bridges the gap between the mesitylene derivatives and the other $C_3$-symmetric platforms. It therefore offers promising opportunities for the construction of chiral receptors.

[y] For $C_3$-symmetric platforms with tripodal distances above 10 Å, see references [93–102] and examples cited therein.

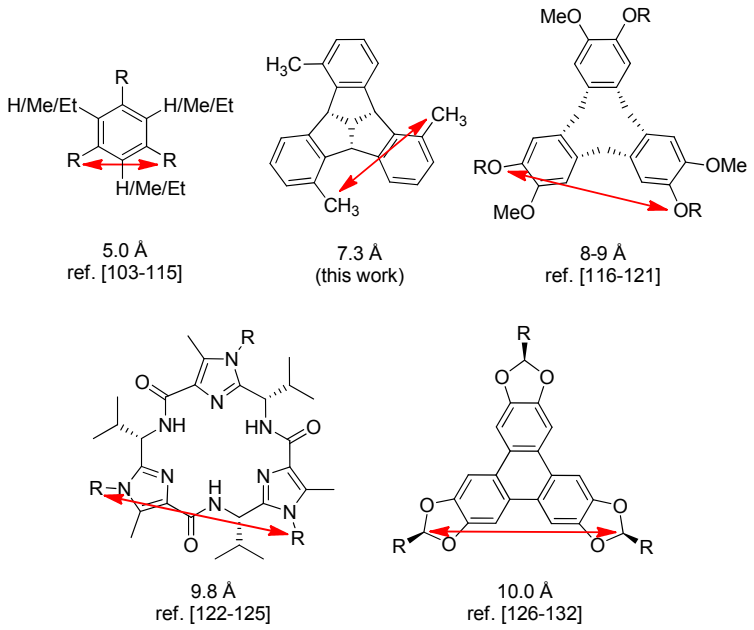


**Figure 28.** Structural parameters of selected platforms with threefold symmetry (X-ray data)

The bridgehead brominated tribenzotriquinacene **28** crystallized in the monoclinic space group $P2_1/c$, but $C_{3v}$ symmetry of the tribenzotriquinacene unit was preserved to a good approximation (r.m.s. deviation from $C_{3v}$ symmetry = 0.06 Å). The crystal structure shows dimers that are mediated by π/π stacking and CH/π interactions (Figure 29). Each bromine substituent exhibits Br···Br contacts to neighboring dimers ($d_{Br\cdots Br}$ = 3.76-3.81 Å, Figure 30); two of these contacts can be considered to be of type II (see Chapter 1.5.5). Extensive Br···Br interactions are also found in the only other reported crystal structure analysis of a bridgehead brominated tribenzotriquinacene [53].

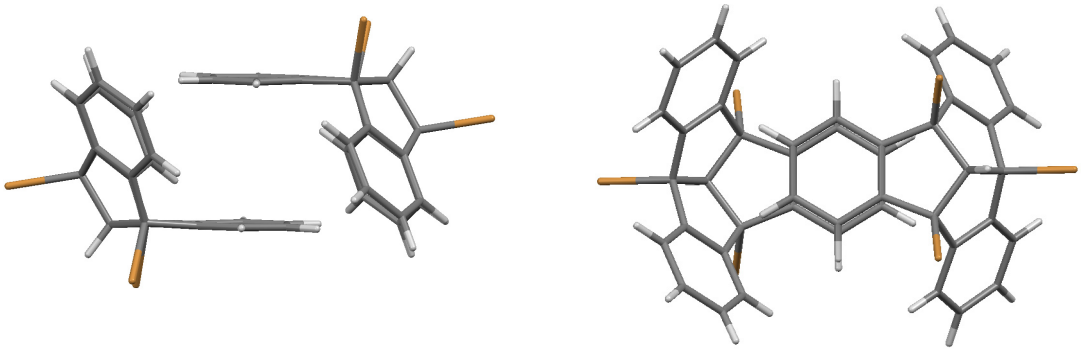

**Figure 29.** Two views of dimers in crystal structure of **28** (bromine atoms in brown)

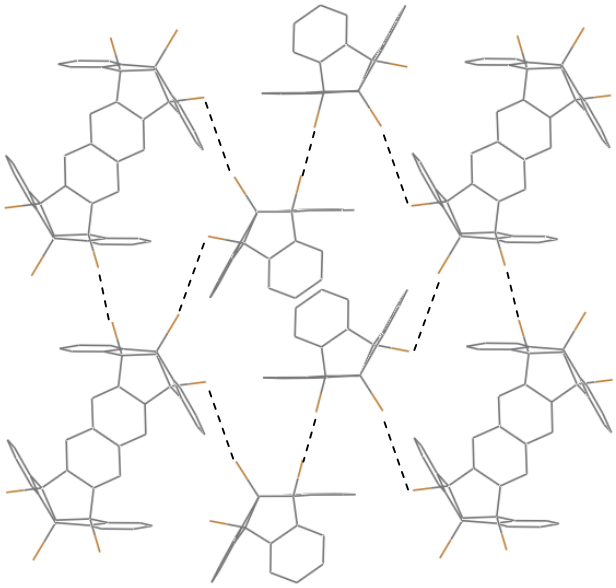

**Figure 30.** Bromine-bromine interactions in crystal structure of **28**. Projection parallel to the *a* axis; bromine atoms in brown, hydrogen atoms omitted for clarity.

### 1.5.7 Chiral resolution of tribenzotriquinacenes

Substitution at the aromatic periphery of the tribenzotriquinacene framework can lead to chiral systems. Several chiral tribenzotriquinacenes have been reported by Kuck and coworkers [29,30]. The tribenzotriquinacene derivatives presented in this thesis (Figure 31) are also chiral and their chiral resolution by HPLC was studied in collaboration with Prof. Yoshio Okamoto[z,aa] and Prof. Jun Shen[z].

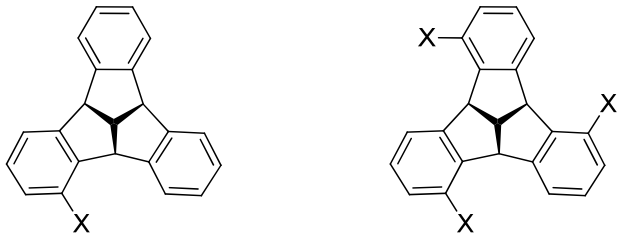


**34** (X = Br)
**35** (X = OMe)
**38** (X = OH)

**55** (X = Br)
**56** (X = OMe)
**57** (X = $CH_3$)

**Figure 31.** Chiral tribenzotriquinacenes in the present investigation

Resolution of the samples was investigated using four kinds of Daicel chiral columns. The results show that all samples can be efficiently separated on Chiralcel OD, Chiralcel OJ-H and Chiralpak AS. As a representative example the chromatogram of the resolution of racemic 1-bromotribenzotriquinacene **34** on Chiralcel OD is shown in Figure 32. A pair of enantiomers is clearly seen as two peaks in the UV chromatogram with opposite CD signals. The enantiomers were eluted at retention times $t_1$ = 12.6 min and $t_2$ = 14.9 min, respectively. Baseline separation of **34** was achieved. The complete chiral resolution results are summarized in Table 8.

[z] Harbin Engineering University, China

[aa] Nagoya University, Japan

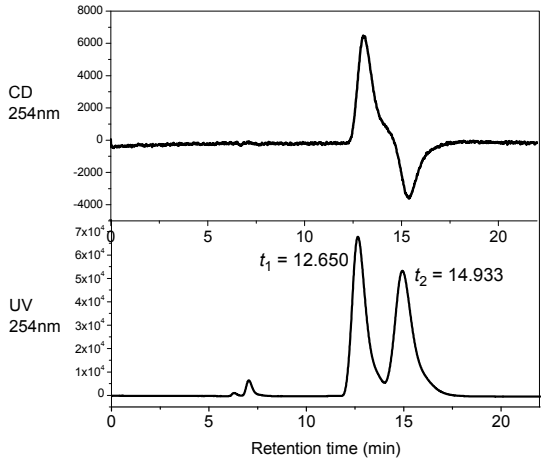


**Figure 32.** Chromatogram for the resolution of 1-bromotribenzotriquinacene **34** on Chiralcel OD[bb]

| | Chiralcel OD | | Chiralcel OJ-H | | Chiralpak AS | |
|---|---|---|---|---|---|---|
| **Racemate** | $t_1$ | $t_2$ | $t_1$ | $t_2$ | $t_1$ | $t_2$ |
| **34** | 12.65 | 14.93 | 16.97 | 19.20 | 8.84 | - |
| **35** | 11.33 | 12.40 | 21.91 | 22.71 | 9.54 | - |
| **38** | 23.36 | 24.21 | 6.92 | - | 23.78 | 25.20 |
| **55** | 8.97 | 9.58 | 12.93 | 13.28 | 9.16 | - |
| **56** | 8.48 | 10.49 | 20.83 | 26.79 | 9.49 | - |
| **57** | 9.41 | 11.18 | 11.23 | 18.93 | 7.37 | - |

Column: 25 × 0.46 cm (i.d.); Flow rate: 0.5 mL/min; Eluent: hexane/2-propanol (90/10, v/v) except for **55** (2-propanol). Concentration of racemate is less than 1 mg/mL.

**Table 8.** Resolution of chiral tribenzotriquinacenes by HPLC on Chiralcel OD, Chiralcel OJ-H and Chiralpak AS[bb]

[bb] Courtesy of Prof. Yoshio Okamoto and Prof. Jun Shen.

### 1.5.8 Crystal structures of dihydroindenoindene byproducts

Single crystals for X-ray analysis were obtained for four dihydroindenoindene byproducts[cc]:

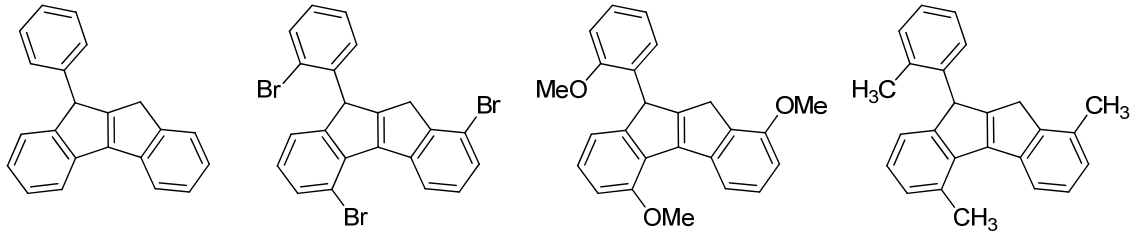


**16** monoclinic $P2_1/n$ | **58** orthorhombic *Pbca* | **59** monoclinic $P2_1/c$ | **60** monoclinic $P2_1/n$

**Figure 33.** Dihydroindenoindene byproducts for which crystal structures were obtained[cc]

Except for the bromine derivative, all compounds crystallized in a monoclinic space group. **16** and **60** are isotypic. The location of the double bond in **16** was initially misassigned by Kuck and coworkers, who also obtained **16** as a byproduct in their synthesis of tribenzotriquinacene [25]. A correction based on a COSY spectrum was published in 1994 [26] and is supported by the crystal structure obtained in the present investigation. The torsion angle of the phenyl group is similar in **16**, **58** and **60** (-11 to -26°), but differs substantially in **59** (42°, Table 9).

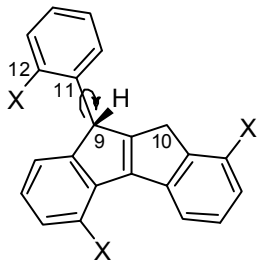


| torsion angle H9-C9-C11-C12 | |
|---|---|
| X = H (**16**): | -11.4° |
| X = Br (**58**): | -24.5° |
| X = $OCH_3$ (**59**): | 42.4° |
| X = $CH_3$ (**60**): | -26.0° |

**Table 9.** Phenyl torsion in dihydroindenoindene byproducts **16** and **58-60**

[cc] Structures **16** (CCDC 904629), **58** (CCDC 904631), **59** (CCDC 904632) and **60** (CCDC 904633) were deposited at The Cambridge Crystallographic Data Centre. The data can be obtained free of charge via www.ccdc.cam.ac.uk/data_request/cif.

The isotypy of hydrocarbons **16** and **60** is best demonstrated by projection parallel to the *b* axis (Figure 34). Introduction of methyl groups, as in **60**, has no significant effect on the crystal packing in this case.

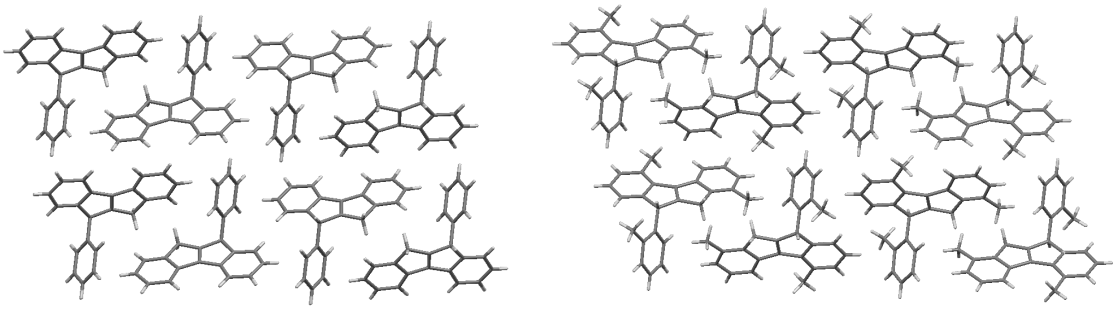

**Figure 34.** Crystal packing of dihydroindenoindene byproducts **16** and **60** (projection parallel to the *b* axis)

The crystal structure of the bromine derivative **58** features halogen-halogen interactions and CH/π-interactions. They are best seen in a wireframe depiction parallel to the *b* axis (Figure 35). The bromine-bromine interactions are of type II ($\theta_1$ = 176.3°, $\theta_2$ = 83.0) with a distance of 3.73 Å (see Chapter 1.5.5). They occur between the bromine of a "free" phenyl group and the bromine of an indene unit. The packing of the trimethoxy derivative **59** shows no striking features.

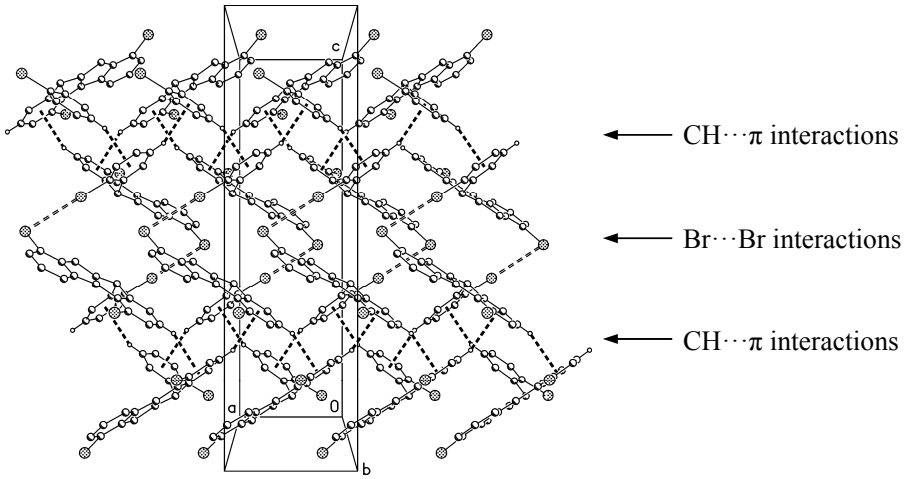


**Figure 35.** Crystal packing of the dihydroindenoindene byproduct **58** parallel to the *b* axis[dd]

[dd] Figure courtesy of Prof. Peter G. Jones.

### 1.5.9 Rotational isomerism in a dihydroindenoindene byproduct

The $^1$H-NMR spectrum of the dihydroindenoindene byproduct **60** showed a second signal set in an approximate 3:1 ratio (Figure 36). Most strikingly, the signal for H9 and for one methyl group was split into two peaks. An EXCY spectrum revealed cross peaks for the respective signals and demonstrated that an exchange process is at hand. It was assumed that the two signal sets might arise from hindered rotation around the C9-C11 bond. Consequently, the methyl group with the doubled signal would correspond to the one at C12.

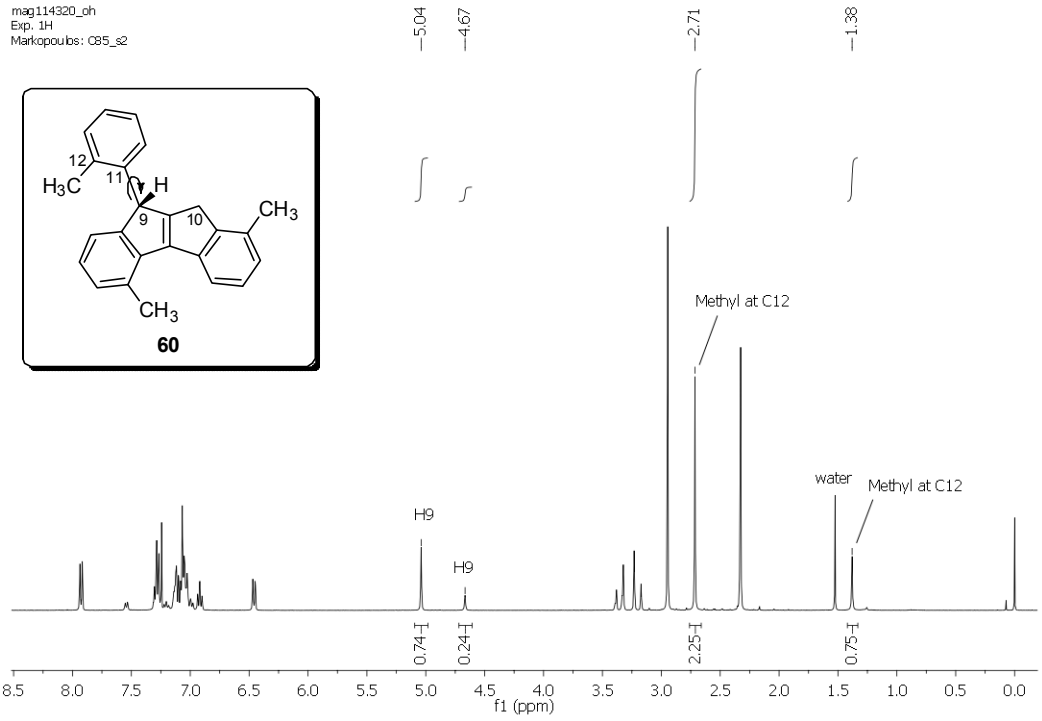


**Figure 36.** $^1$H-NMR spectrum of dihydroindenoindene **60** (400 MHz, $CDCl_3$)

Variable temperature NMR measurements were performed to determine the activation parameters for this process. The coalescence temperature for the H9 signal was found to be 75 ± 5 °C (see Experimental Section). Based on these values, a free enthalpy of activation $\Delta G^{\neq}$ (348 K) = 17.3 ± 0.3 kcal/mol was calculated for rotation around the C9-C11 bond.[ee] The determined value corresponds very well with the data for the

[ee] Calculation according to reference [133]. Data from NMR experiment (400 MHz, $CDCl_2CDCl_2$):
$T_c$ = 343 K; $\Delta\nu$ (extrapolated to $T_c$) = 147.2 Hz; K (extrapolated to $T_c$) = 0.32; $b_E$ = 3.0 Hz;
$T_c$ = 354 K; $\Delta\nu$ (extrapolated to $T_c$) = 146.9 Hz; K (extrapolated to $T_c$) = 0.33; $b_E$ = 3.0 Hz;
obtained $k_a$ (93.0 $s^{-1}$ at 343 K; 95.0 $s^{-1}$ at 354 K) was inserted into the Eyring equation to calculate $\Delta G^{\neq}$.

*ortho*-methylated phenyl fluorene **65** (Figure 37), for which a free energy of activation $\Delta F^{\neq}$ (333 K) = 16.3 kcal/mol was determined experimentally [134]. Hindered rotation was also observed by Kuck and Seifert in the tetrahydroindenoindenones **66** and **67** [135], which are closely related to the dihydroindenoindene **60**. However, we note that in these cases no *ortho*-substitution is necessary to induce hindered rotation. This is most probably because of the curvature of the tetrahydroindenoindenone backbone compared to the planar dihydroindenoindene unit[ff]. For example, no hindered rotation was observed for the dihydroindenoindene derivative **16**, which does not possess an *ortho*-methyl substituent (see Figure 33 on p. 51). An interesting study on the influence of a curved heterocyclic backbone on the rotation of phenyl rings without *ortho*-substitution has been published by Curran and coworkers [136].

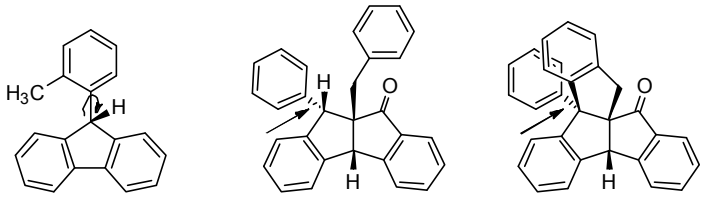


**65** ref. [134] **66** ref. [135] **67** ref. [135]

**Figure 37.** Literature examples for hindered rotation around $sp^2$-$sp^3$ bonds.

The observed rotational isomerism in **60** was also studied computationally by calculating the model system shown in Scheme 20 on the next page. Three rotamers were found and Table 10 gives the calculated relative energies at 0 K and the calculated relative free enthalpies at the coalescence temperature 348 K. Rotamer **70** has the lowest energy. It can interconvert via transition states **TS3** and **TS2** to rotamers **68** and **69**, respectively. Rotamers **68** and **69** are very close in energy and only ≤ 1.2 kcal/mol higher in energy than the low energy rotamer **70**. Their barrier of interconversion via transition state **TS1** is very low (≤ 1.9 kcal/mol). However, transition states **TS2** and **TS3** have a sizable energy of 16.2-18.9 kcal/mol with respect to **70**. The theoretical values, obtained under gas phase conditions, are in excellent agreement with the experimental result ($\Delta G^{\neq}$ = 17.3 ± 0.3 kcal/mol at 348 K).[gg]

[ff] For the planarity of the dihydroindenoindene backbone, see the X-ray analyses in Chapter 1.5.8.

[gg] The calculation of the experimental free enthalpy of activation $\Delta G^{\neq}$ according to reference [133] is based on the assumption of a two-state system. The DFT calculations revealed a three-state system. However, as **68** and **69** are very similar in energy and interconvert rapidly, the investigated system can be considered as a two-state system to a good approximation.

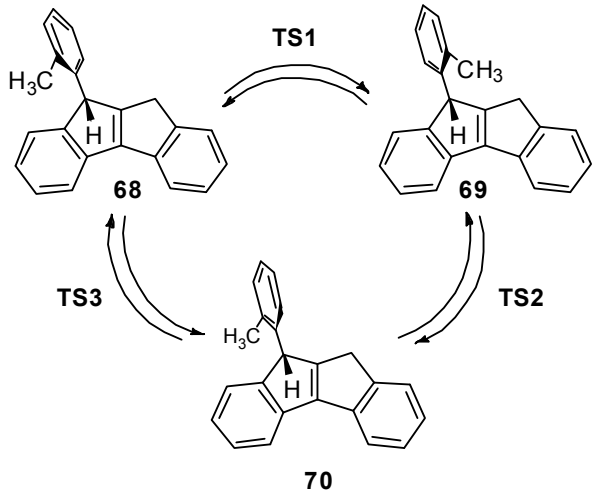


**Scheme 20.** Rotational isomerism in a simplified model of **60**
(DFT calculations at the M06-2X/6-311G(d,p) level of theory)

| | **68** | **TS1** | **69** | **TS2** | **70** | **TS3** |
|---|---|---|---|---|---|---|
| torsion angle H9-C9-C11-C12[hh] | -20.2 | 6.7 | 29.8 | 96.2 | 177.1 | -86.7 |
| rel. energy (0 K, no ZPE; kcal/mol) | 1.2 | 1.3 | 1.1 | 16.2 | 0.0 | 17.0 |
| rel. free enthalpy (348 K; kcal/mol) | 1.0 | 2.6 | 0.2 | 18.8 | 0.0 | 19.2 |

**Table 10.** DFT calculations on rotamers of simplified model of dihydroindenoindene **60** (M06-2X/6-311G(d,p)); rotamer **70** as reference for relative energies and relative free enthalpies.

[hh] For the definition of the torsion angle, see Figure 36.

## 1.6 Computational perspective on intramolecular cyclizations

As early as 1999 Kuck and coworkers envisioned that tribenzotriquinacene might serve as a building block for extended carbon networks [31,40]. An important step towards this aim has recently been reported by Mughal and Kuck: in a remarkable Scholl reaction the intramolecular cyclization between two opposing and unfunctionalized arene units in tribenzotriquinacene **71** was achieved (Scheme 21) [51]. This impressive result is even more important in light of the observation of pentagonal and heptagonal defects in graphene lattices [137].

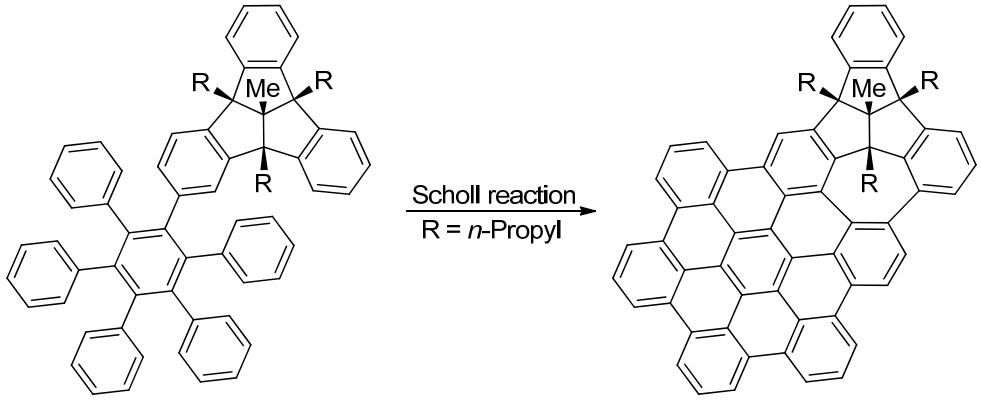


**Scheme 21.** Intramolecular cyclization via Scholl reaction by Mughal and Kuck [51]

The *ortho*-functionalized tribenzotriquinacenes **9**, prepared in the present investigation, open the door to a systematic study of intramolecular cyclizations between neighboring arene units (Scheme 22). The purpose of the present chapter is to provide a computational perspective on the feasibility of such cyclizations.

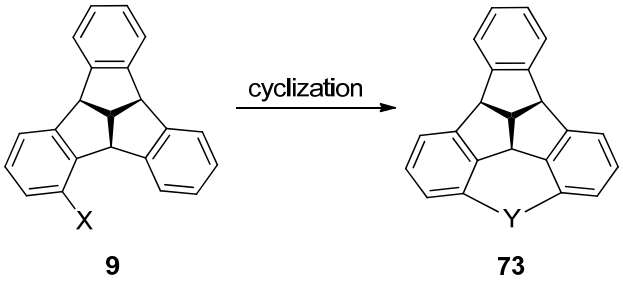


**Scheme 22.** Intramolecular cyclization of *ortho*-functionalized tribenzotriquinacenes

A thermodynamic approach was chosen to evaluate the strain associated with these cyclizations. DFT calculations at the M06-2X/6-311G(d,p) level of theory were performed on model systems with various ring sizes. The strain was assessed by comparison with a cyclization that is considered unstrained. As reference reactions the cyclization of the respective diphenylmethane derivative or biphenyl formation were chosen and their cyclization energy defined as 0 kcal/mol. Kinetic aspects, i.e. transition states, were not considered.

As can be seen from Table 11 (see next page), formation of a five-membered ring within the tribenzotriquinacene framework is associated with a remarkably high strain energy of 65.9 kcal/mol (entry 1). This value is even higher than that for biphenylene formation[ii], and the resulting fluorene derivative is highly deformed from planarity. Introduction of a six-membered ring is easier and formation of the respective dihydroanthracene within the tribenzotriquinacene framework is only 12.7 kcal/mol higher in energy than for the acyclic system (entry 2). Most surprisingly, a bridging ethylene unit can be introduced without any additional strain (entry 3). This model reaction is exothermic (calculated $\Delta E$ = -38.6 kcal/mol) and could proceed via acetylene-vinylidene rearrangement and subsequent CH insertion [2]. The resulting dibenzocycloheptatriene seems to fit perfectly into the bay of two flanking arene units. This is also reflected in the cyclization of a phenyl substituted tribenzotriquinacene: its cyclization energy is only 3.4 kcal/mol higher than that for biphenyl formation (entry 4). This computational result is supported by the experimental observation of Mughal and Kuck [51].

We next turned our attention to consecutive intramolecular cyclizations. Would the reaction energies increase in a series of intramolecular cyclizations or is the first cyclization the one with the highest strain? Table 12 on p. 59 indicates that consecutive cyclizations have similar reaction energies to within 3.5 kcal/mol. The last cyclization always has the highest reaction energy. Except for the unsubstituted case (R = H) the reaction energy of the second cyclization is usually halfway between the two others. One may conclude that the framework becomes stiffer with every cyclization.

[ii] Same computational model as above:

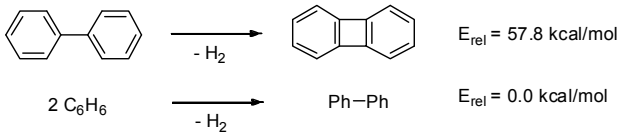

| entry | Tribenzotriquinacene cyclizations and reference reactions | rel. energy (kcal/mol) |
|---|---|---|
| 1 | 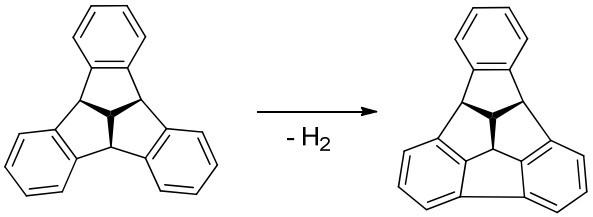 | 65.9 |
| | 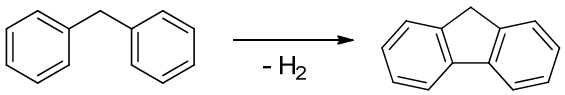 | 0.0 |
| 2 | 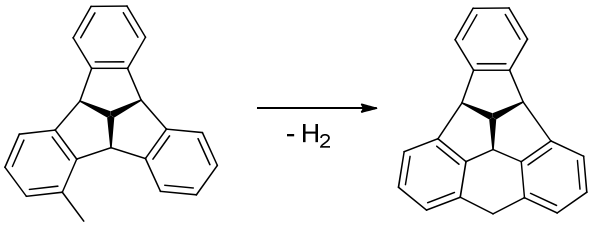 | 12.7 |
| | 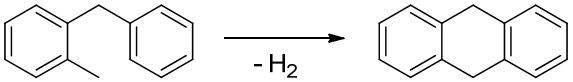 | 0.0 |
| 3 | 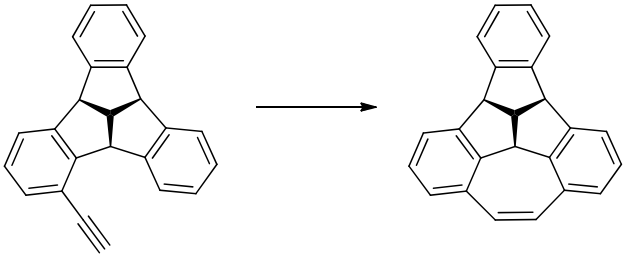 | 0.1 |
| | 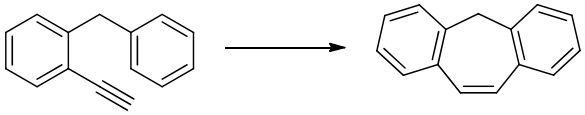 | 0.0 |
| 4 | 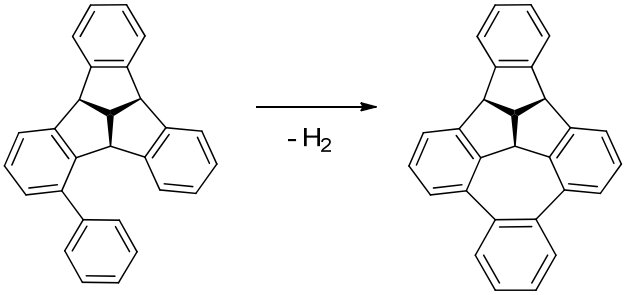 | 3.4 |
| | 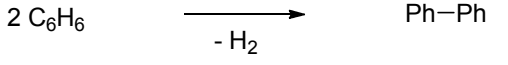 | 0.0 |

**Table 11.** Strain energies of intramolecular cyclizations in tribenzotriquinacenes (M06-2X/6-311G(d,p); energies at 0 K without correction for zero point energy)

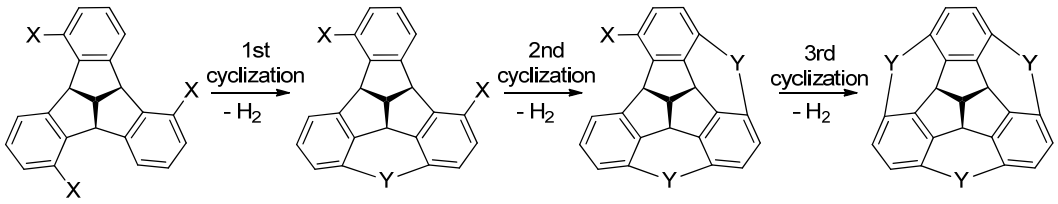


| X | Y | 1st cyclization (kcal/mol) | 2nd cyclization (kcal/mol) | 3rd cyclization (kcal/mol) |
|---|---|---|---|---|
| H | -- | 78.9 | 78.0 | 81.5 (**74**) |
| $CH_3$ | $CH_2$ | 26.3 | 28.2 | 28.3 (**75**) |
|  | 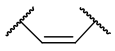 | 7.4 | 9.4 | 10.9 (**76**) |
| Ph | 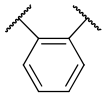 | 10.1 | 11.3 | 12.1 (**77**) |

**Table 12.** DFT calculations on consecutive intramolecular cyclizations (M06-2X/6-311G(d,p); relative energies at 0 K without correction for zero point energy)

The calculated geometries of **74**-**75** can be found in the Computational Section. The *ortho*-fused tribenzotriquinacene **74** (Table 12) has been used in computational studies as a building block for the construction of the fullerene derivatives $C_{26}H_8$ [138,139], $C_{26}Cl_8$ [140] and $C_{38}H_8$ [138].[jj] Structure **75** and its tetrachloro derivative have even been observed experimentally as substructures of the unconventional fullerene derivatives $C_{64}H_4$ [143] and $C_{64}Cl_4$ [144]. The tribenzotriquinacene units therein constitute a violation of the so-called "isolated pentagon rule" [145]. Fullerene derivatives with a **75**-substructure have also been described in a series of computational studies [142,146–148].

The intramolecular cyclizations of 1,5,9-trisethinyl tribenzotriquinacene **78** are exothermic in all steps and should be feasible via flash vacuum pyrolysis [2] (Scheme 23). It should be possible to prepare **78** from the tribromide **55** (see Scheme 18 on p. 20) by Sonogashira coupling.

[jj] For dehydro derivatives of **74** as building blocks for fullerenes, see additionally the computational studies in references [141,142].

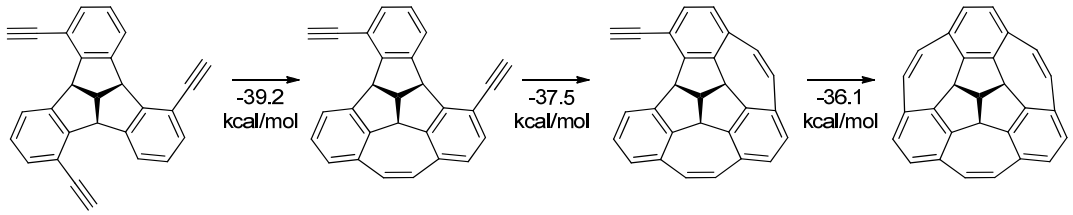


**78** **79** **80** **76**

**Scheme 23.** DFT calculations on the cyclization of 1,5,9-trisethinyl tribenzotriquinacene (M06-2X/6-311G(d,p); relative energies at 0 K without correction for zero point energy)

## 1.7 Summary and Outlook

A new and high yielding three-step synthesis of the bowl-shaped hydrocarbon tribenzotriquinacene (**3**) has been developed. The synthesis is based on simple and commercially available starting materials and its key step is the triple cyclization of an *α,β*-unsaturated diol of type **12**. A mechanism for this transformation has been proposed and is supported by the isolated byproducts and exploratory density functional theory calculations. Parent tribenzotriquinacene is now available on a gram scale for the first time (Chapter 1.2).

The protocol developed here also allows the regiospecific introduction of various substituents (R = Br, OMe, OH, $CH_3$) at the hitherto poorly accessible *ortho*-positions of tribenzotriquinacene. This has been demonstrated for both mono- and trisubstituted derivatives (**34**, **35**, **38** in Chapter 1.3 and **55**-**57** in Chapter 1.4, respectively). The latter are accessible in a $C_3$-specific fashion and constitute a novel class of $C_3$-chiral platforms. Although the yield of the tribromo and trimethoxy derivatives **55** and **56** was low, the trimethylated tribenzotriquinacene **57** was obtained in a yield comparable to that of parent tribenzotriquinacene **3**. The mono- and trisubstituted derivatives are chiral and resolution of their enantiomers was achieved by chiral phase HPLC (Chapter 1.5.7). *Ortho*-functionalized tribenzotriquinacenes open the door to intramolecular cyclizations and the feasibility of such cyclizations has been studied by density functional theory calculations. The computational results support the accessibility of seven-membered rings, while the intramolecular formation of five-membered rings seems unlikely. Intramolecular formation of six-membered rings constitutes an interesting border case that can lead to the rational chemical synthesis of unconventional fullerene fragments (Chapter 1.6).

A total of 18 crystal structures have been obtained, providing a broad basis for the comparison of analogous compounds: *α,β*-unsaturated diketones (4), *α,β*-unsaturated diols (6), tribenzotriquinacenes (3), dihydroindenoindenes (4) and a dibrominated dibenzoylmethane with halogen-halogen interactions (1). Based on the obtained X-ray data, the relative stereochemistry of 10 diastereomeric diols has been determined (Chapter 1.5.2). The dibenzoylmethane motif could provide an interesting starting point for a systematic study of intra- and intermolecular halogen-halogen interactions (Chapter 1.5.5). Most importantly, high quality X-ray structures for parent tribenzotriquinacene **3** and the $C_3$-chiral trimethyl derivative **57** have been obtained. Parent tribenzotriquinacene **3** is shown to possess a slightly staggered arrangement within the columnar stacks of its crystal structure. Based on its structural parameters,

the $C_3$-chiral tribenzotriquinacene **57** provides an interesting entry to novel supramolecular receptors.

Aside from the aforementioned intramolecular cyclizations, future work should focus on the selective oxidation of the methyl groups in the $C_3$-chiral tribenzotriquinacene **57**. This would allow the introduction of three recognition units, so that this $C_3$-chiral platform can be used for supramolecular chemistry. Analogously, the monobrominated tribenzotriquinacene **34** can serve as a supramolecular platform with a single recognition unit. However, **34** should also be considered as a chiral and bulky aryl unit for phosphine ligands. In order to realize the application of the described tribenzotriquinacenes in an asymmetric setting, a practicable large scale resolution of the racemates must be developed.

The great versatility of the presented synthesis has already been demonstrated and should be further explored by extending it to functionalization at the outer rim of tribenzotriquinacene. For example, the monofunctionalized derivatives **81** (Figure 38) could be obtained by using *para*-substituted aldehyde components. Establishing a $C_3$-chiral substitution pattern at the outer rim requires the use of "directing" *ortho*-substituents as demonstrated in **82**. This *hexa*-methylated compound could subsequently be functionalized by standard electrophilic aromatic substitution at the three remaining outer rim positions.

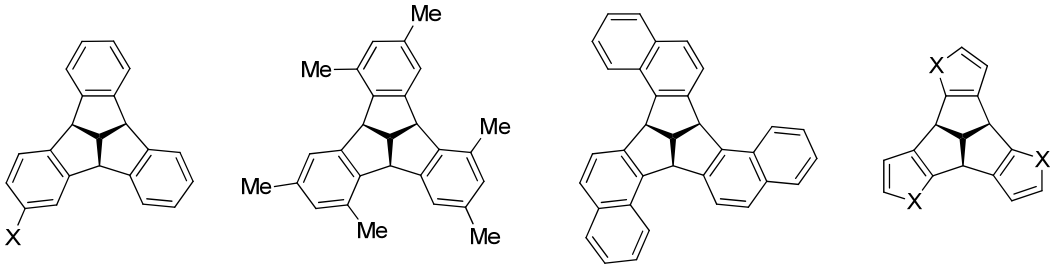


**81** (X = Br, OMe, OH) **82** **83** **84** (X = NH, S)

**Figure 38.** Future expansions of the developed synthesis

Polycyclic aldehyde and diketone components can also be envisioned. This approach is demonstrated in compound **83**, which features a $C_3$-chiral arrangement of naphthalene units. These novel extended tribenzotriquinacenes could be of interest for supramolecular recognition [33–35] and for the synthesis of extended carbon networks [31,49].

The synthetic scheme does not have to be limited to hydrocarbons, and indeed, the extension to heteroaromatics can provide unprecedented avenues. Of the many possible building blocks, the use of pyrrole and thiophene units is demonstrated in **84**. Such compounds represent a novel class of bowl-shaped molecules, in which heteroaromatics are condensed to the triquinacene core. While the tripyrrole **84** (X = NH) would be attractive as a $C_3$-chiral platform for supramolecular chemistry, the trithiophene **84** (X = S) would be of interest as a building block for organic semiconductors. Its close analogy to planar benzotrithiophene [149–152] offers promising opportunities in materials science.

# 2 The rigidity of carbon-carbon single bonds

## 2.1 Carbon-carbon single bonds

The carbon-carbon single bond lies at the heart of organic chemistry. Its bond length is usually associated with a value of 1.54 Å, and any undergraduate student in chemistry quickly becomes acquainted with this number. However, it should be kept in mind that this value refers to a single bond between two carbon atoms with ideal $sp^3$ hybridization as in diamond [153,154]. Bond lengths change dramatically if other hybrid orbitals are involved. Thus, the length of the single bond in the series ethane (**85**), propene (**86**), butadiene (**87**) and butadiyne (**88**) falls from 1.535 Å to 1.384 Å (Figure 39).

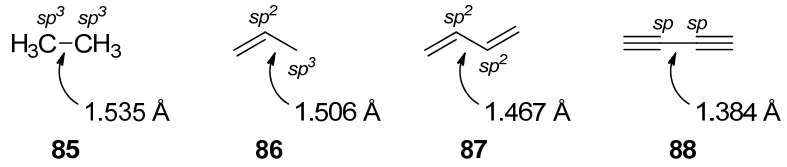


**Figure 39.** Bond lengths depend on hybridization (values from reference [155])

Strong variations can also be observed if steric constraints are imposed on a single bond between two tetracoordinate carbon centers (Figure 40). Experimentally, this has led to bond lengths ranging from 1.475/1.495 Å in **89** [156] to 1.771 Å in **90** [157–159].[a] An extraordinarily short bond length is achieved in **91** by interplay of geometric and electronic effects [161,162]. Computationally, even more extreme single bonds have been studied [163,164].

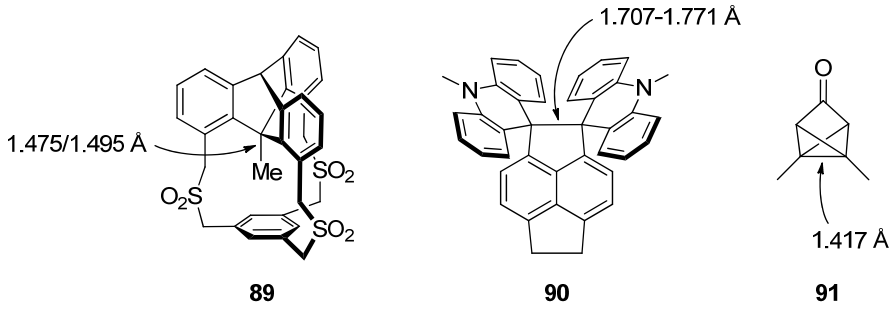


**Figure 40.** Unusual bond lengths because of steric and/or electronic effects[b]

[a] For a silicon-containing molecule, a carbon-carbon bond length of 1.781 Å has been reported [160].
[b] The unit cell of **89** and **90** contains two and four crystallographically independent molecules, respectively.

An empirical and widely used relationship in chemistry states that short bonds are stronger bonds, and vice versa [165,166]. Although exceptions to this correlation have been found [167–169], there is general agreement that an elongated bond as in **90** will be weakened. The picture, however, is less clear for bonds that are shortened because of steric constraints as in **89**. Are such carbon-carbon single bonds also stronger, because they are shorter?

## 2.2 Compliance constants as bond strength descriptors

Generally, the concept of bond strength is a difficult one and various descriptors have been used in the literature [170–172]. Bond energies, which can be obtained experimentally from atomization energies, are reasonable only for diatomic molecules or highly symmetric molecules with one type of bond. For more complex molecules one has to consider bond dissociation energies.[c] Although these are closely linked to the chemist's idea of thermodynamic stability, they depend critically on the stability of the obtained fragments and therefore do not constitute an intrinsic bond strength descriptor. For the carbon-carbon double bond, this effect may lead to a variation of the evaluated bond strength by more than 70 kcal/mol [174]. Sophisticated computational approaches have been developed to overcome these limitations [173,175,176]. Bond stretching frequencies or force constants obtained from vibrational spectroscopy are also limited to diatomic molecules. In polyatomic molecules, they usually refer to delocalized normal modes and cannot offer information about individual bonds. Theoretically obtained bond orders, which can also be used as a bond strength descriptor, suffer from the variability of the different population analyses [177].

Recent work by Grunenberg and coworkers has demonstrated the utility of compliance constants as bond strength descriptor [167,172,178–180]. Compliance constants were initially conceived by Decius in the 1950/60s in the context of vibrational spectroscopy [181,182] and provide localized information about the strength of individual bonds. A short introduction to their meaning and properties will be given.[d] Mathematically speaking, compliance constants are the diagonal matrix elements of

[c] Bond dissociation energies (BDE) can be considered as the sum of the intrinsic bond energy (BE) and the total reorganization energy (R) [173].

[d] For an in-depth discussion of compliance constants and the associated formalism, the interested reader is referred to the tutorial review by Brandhorst and Grunenberg [183].

the inverse Hessian matrix $\boldsymbol{C} = \boldsymbol{H}^{-1}$ ($\boldsymbol{C}$: compliance matrix, $\boldsymbol{H}$: Hessian matrix). The Hessian matrix $\boldsymbol{H}$ is of unique importance in computational chemistry.[e] It contains the second-order partial derivatives of the potential energy with respect to the defined coordinate system. The diagonal matrix elements are called *force constants*. They describe the force that is necessary to distort a molecular coordinate by a unit distance (or angle) while keeping all other nuclear positions fixed. Within the harmonic approximation, this corresponds to the curvature at the minimum of a rigid potential energy surface. This somewhat artificial setting is not the case for *compliance constants*: they describe the displacement that can be achieved by applying a unit force along a molecular coordinate while allowing all other nuclear coordinates to relax. The complete molecule adapts to the distortion: not only the strength of the distorted bond itself, but also the relaxation of its molecular environment will have an influence on the observed compliance constant. If the molecular environment around the distortion parameter is very rigid, a smaller compliance constant will be observed, and vice versa. Compliance constants are therefore an excellent tool to study the rigidity of molecular systems.[f]

Following the suggestion by Jones [185], the inverse of a compliance constant is called a *relaxed force constant*. Relaxed force constants are advantageous for the discussion of numerical values, as they are in direct relationship to the rigidity of the respective bond, i.e. the more rigid the bond, the larger the relaxed force constant.[g] They correspond to the curvature at the minimum of a relaxed potential energy surface. Cremer and coworkers have very recently shown that *adiabatic force constants*, developed by the same group in 1998 within the theory of adiabatic internal coordinate modes [186–189], are in fact equivalent to the relaxed force constants of Decius and Jones [190]. Adiabatic force constants have been used for the description of C-H [191], C-F [192] and various C-C bonds [191]. Carbon-carbon single bonds in highly strained and unusual bonding environments have not been studied so far.

[e] Important applications include geometry optimization and vibrational analysis [177].

[f] Another favorable property of compliance constants is their invariance to the coordinate system. This leads to excellent transferability [184].

[g] Relaxed force constants have the same unit as force constants, but a different meaning: they describe the remaining force along a distortion parameter after the molecule has relaxed under the imposed distortion. Because of this property, relaxed force constants are generally smaller than force constants.

## 2.3 Research objective

The present work calculates compliance constants and relaxed force constants of a variety of carbon-carbon single bonds in normal and unusual molecules. Conjugation and resonance effects are excluded as far as possible by constraining the study to single bonds between two tetracoordinate carbon centers. The discussed molecules, real and hypothetical, are taken from the literature. The work aims to provide a wide overview of the rigidity of carbon-carbon single bonds to further our understanding of bond length – bond strength relationships and the meaning of compliance constants and relaxed force constants.

## 2.4 Computational methodology

Quantum chemical calculations were performed with the Gaussian 09 software [193]. Stationary points were characterized by frequency calculations to assure that they are true minima (no imaginary frequencies) or transition states (one imaginary frequency). Compliance constants were calculated with the Compliance 3.0.0 software using the Cartesian force constants from frequency calculations [184,194]. The obtained (diagonal) compliance constants were subsequently inverted to relaxed force constants (unit: N $cm^{-1}$) [185]. Unscaled vibrational frequencies were used to calculate enthalpies at 298 K.

## 2.5 Evaluation of computational methods

In the following chapters the discussion of bond rigidity variations is dealing with differences around 5% and below. Therefore, the requirements concerning the robustness of the numerical results are unexceptionally high and an in-depth rating of the computational methods was a prerequisite. Ethane and three cycloalkanes served as a first test set for the evaluation of several computational methods with respect to their reliability of calculating compliance constants (Table 13).[h] Table 13 and all subsequent tables contain the calculated bond length and the relaxed force constant at various levels of theory; the relaxed force constant is additionally put into relation to the value of ethane at the respective level of theory (entry "% of ethane"). Coupled cluster

[h] Cyclopentane was excluded because of the low symmetry of the molecule and therefore high number of inequivalent carbon-carbon bonds.

calculations with excited singles and triples and an augmented correlation-consistent triple-zeta basis set were chosen as the "gold standard" [195] for the present investigation. However, the computational cost of this highly accurate method prohibited the calculation of ethane and cyclopropane. It was therefore decided to use the closely related QCISD method of Pople and Head-Gordon [196] in conjunction with a Pople-type triple-zeta basis set with additional polarization and diffuse functions to provide accurate data for a larger set of molecules. As can be seen in Table 13, QCISD reproduces the results of the coupled cluster calculations very accurately and can serve as a reliable reference for further comparisons.

| | bond length [Å] / relaxed force constant [N $cm^{-1}$] (% of ethane) | | | |
|---|---|---|---|---|
| | **CCSD(T)/ aug-cc-pVTZ** | **QCISD/ 6-311+G(2d,p)** | **MP2/ cc-pVTZ** | **MP2/ cc-pVDZ** |
| $H_3C-CH_3$ | 1.530 / 4.19 (100) | 1.531 / 4.20 (100) | 1.523 / 4.35 (100) | 1.530 / 4.50 (100) |
|  | -- | 1.533 / 4.08 (97) | 1.526 / 4.17 (96) | 1.535 / 4.28 (95) |
|  | 1.553 / 3.73 (89) | 1.553 / 3.76 (90) | 1.545 / 3.88 (89)[i] | 1.553 / 4.00 (89) |
|  | 1.511 / 4.03 (96) | 1.511 / 4.03 (96) | 1.503 / 4.22 (97) | 1.514 / 4.33 (96) |

**Table 13.** Comparison of highly correlated methods for cycloalkanes

We next turned our attention to 2nd order Møller-Plesset perturbation theory and evaluated the test set with a correlation-consistent triple-zeta basis set (Table 13). The MP2 calculations give bond lengths that are about 0.08 Å shorter than the QCISD results. The relaxed force constants are slightly increased; their relative ordering, however, is unaffected and nicely reproduced. As MP2 calculations with a triple-zeta basis are computationally expensive, a double-zeta basis was also tested. Geometries now compare better to the QCISD results, but the relaxed force constants deviate more. Relative ordering remains largely unaffected.

Density functional theory (DFT) methods have become the workhorse of computational chemistry and were also investigated. We used Becke's hybrid functional B3LYP [197] and two more recent functionals by Truhlar [198,199] and Grimme [200], which are extensively parameterized to include dispersion interactions

[i] For a calculation at the MP2/aug-cc-pVTZ level of theory, see reference [183].

(Table 14). Inclusion of the latter has been shown to be essential for the calculation of hydrocarbons [201] – the class of compounds that is also at the center of the present investigation. Geometries at the B3LYP level are in excellent agreement with the QCISD results (deviation < 0.004 Å); M06-2X tends to give bond lengths that are 0.002-0.009 Å shorter than the QCISD results, whereas B97-D gives bond lengths that 0.003-0.009 Å longer. The absolute value of the relaxed force constant for ethane is in the range of the QCISD result for B3LYP and M06-2X; a distinctly smaller value is observed for B97-D (3.73 vs. 4.20 N $cm^{-1}$).

Most importantly, while the relative ordering for cyclohexane and cyclobutane is reproduced well, all three DFT functionals overestimate the relaxed force constant for cyclopropane. This is particularly the case for M06-2X and B97-D; both functionals predict a more rigid bond for cyclopropane than for ethane in contrast to the CCSD(T) and QCISD results.

| | bond length [Å] / relaxed force constant [N $cm^{-1}$] (% of ethane) | | | |
|---|---|---|---|---|
| | **QCISD/ 6-311+G(2d,p)** | **B3LYP/ 6-311G(d,p)** | **M06-2X/ 6-311G(d,p)** | **B97-D/ 6-311G(d,p)** |
| $H_3C-CH_3$ | 1.531 / 4.20 (100) | 1.531 / 4.05 (100)[j] | 1.527 / 4.29 (100) | 1.538 / 3.73 (100) |
| ⬡ | 1.533 / 4.08 (97) | 1.536 / 3.85 (95)[k] | 1.531 / 4.11 (96) | 1.542 / 3.58 (96) |
| □ | 1.553 / 3.76 (90) | 1.554 / 3.68 (91) | 1.547 / 3.94 (92) | 1.560 / 3.40 (91) |
| △ | 1.511 / 4.03 (96) | 1.508 / 4.03 (100)[k] | 1.502 / 4.39 (102) | 1.514 / 3.83 (103) |

**Table 14.** Comparison of DFT methods for cycloalkanes

Cyclopropane has always been a challenge for theoretical chemistry [170,202] and it is well known that description of the energy of three-membered rings by DFT methods tends to be poor [203,204]. It was therefore decided to extend the methodological survey to a series of small-ring systems, as these form part of many compounds to be discussed in this work.

The extended test set is shown in Table 15. Computational resources allowed only the calculation of cyclobutene, [1.1.0]bicyclobutane and tetrahedrane at the CCSD(T)

[j] For a calculation at the B3LYP/6-311++G(d,p) level of theory, see reference [179].

[k] For adiabatic force constants by Cremer and coworkers at the B3LYP/6-31G(d,p) level of theory, see references [171,190,191].

level. QCISD reproduces the results nicely except for the interbridgehead bond in [1.1.0]bicyclobutane, for which a small deviation is observed. For other bonding situations, QCISD is a very reliable reference. MP2 calculations with a correlation-consistent triple-zeta basis set give slightly shorter bond lengths than QCISD, except for the interbridgehead bond in [1.1.0]bicyclobutane. The latter is also the only bond for which the relaxed force constant at the MP2 level shows a large deviation in the ethane relation. MP2 calculations with a correlation-consistent double-zeta basis set give slightly larger bond lengths than QCISD. The overall agreement of the relaxed force constants is poorer, but still acceptable except for the notorious interbridgehead bond in [1.1.0]bicyclobutane.

| | bond length [Å] / relaxed force constant [N cm$^{-1}$] (% of ethane) | | | |
|---|---|---|---|---|
| | **CCSD(T)/ aug-cc-pVTZ** | **QCISD/ 6-311+G(2d,p)** | **MP2/ cc-pVTZ** | **MP2/ cc-pVDZ** |
| $H_3C-CH_3$ | 1.530 / 4.19 (100) | 1.531 / 4.20 (100) | 1.523 / 4.35 (100) | 1.530 / 4.50 (100) |
| 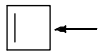 | 1.573 / 3.49 (83) | 1.573 / 3.51 (84) | 1.565 / 3.61 (83) | 1.574 / 3.70 (82) |
|  | -- | 1.572 / 3.56 (85) | 1.566 / 3.63 (83) | 1.577 / 3.67 (82) |
|  a) | -- | 1.559 / 3.82 (91) | 1.552 / 3.90 (90) | 1.562 / 3.96 (88) |
| b) | -- | 1.525 / 3.75 (89) | 1.522 / 3.81 (88) | 1.533 / 3.88 (86) |
|  a) | 1.501 / 4.10 (98) | 1.501 / 4.10 (98) | 1.495 / 4.25 (98) | 1.505 / 4.35 (97) |
| b) | 1.502 / 3.02 (72) | 1.497 / 3.20 (76) | 1.500 / 3.00 (69) | 1.520 / 2.85 (63) |
|  | 1.485 / 3.90 (93) | 1.485 / 3.91 (93) | 1.478 / 3.93 (90) | 1.494 / 4.01 (89) |

**Table 15.** Comparison of highly correlated methods for small-ring systems

The same set of molecules was also tested with DFT methods (Table 16). Again, overall agreement of geometries is good; only M06-2X shows a stronger deviation for tetrahedrane and the interbridgehead bond in [1.1.0]bicyclobutane (0.014-0.020 Å shorter compared to QCISD). However, marked differences are observed for the relaxed force constants. Most notably tetrahedrane, built up from four cyclopropane rings, has a 7% softer bond than ethane at the QCISD level, whereas the DFT methods

predict a more rigid bond than in ethane (2-12%).[l] It is also obvious that DFT methods overestimate the relaxed force constant in the three-membered rings of [1.1.0]bicyclobutane and prismane in comparison to ethane. It should be noted that the overestimation is more pronounced for the modern functionals M06-2X and B97-D; a hint that inclusion of dispersion interactions might render these small-ring compounds too "compact".

The relaxed force constants of the four-membered rings in prismane and cubane are also slightly overestimated in their relative order to ethane, but the deviation is substantially less compared to that of three-membered rings.

| | bond length [Å] / relaxed force constant [N cm$^{-1}$] (% of ethane) | | | |
|---|---|---|---|---|
| | **QCISD/ 6-311+G(2d,p)** | **B3LYP/ 6-311G(d,p)** | **M06-2X/ 6-311G(d,p)** | **B97-D/ 6-311G(d,p)** |
| $H_3C-CH_3$ | 1.531 / 4.20 (100) | 1.531 / 4.05 (100) | 1.527 / 4.29 (100) | 1.538 / 3.73 (100) |
| 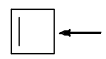 | 1.573 / 3.51 (84) | 1.572 / 3.44 (85)[m] | 1.563 / 3.72 (87) | 1.580 / 3.16 (85) |
|  | 1.572 / 3.56 (85) | 1.571 / 3.60 (89) | 1.562 / 3.92 (91) | 1.578 / 3.40 (91) |
| 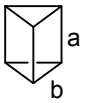 a) | 1.559 / 3.82 (91) | 1.559 / 3.78 (93) | 1.550 / 4.12 (96) | 1.564 / 3.64 (98) |
| b) | 1.525 / 3.75 (89) | 1.522 / 3.84 (95) | 1.514 / 4.27 (100) | 1.527 / 3.71 (99) |
|  a) | 1.501 / 4.10 (98) | 1.499 / 4.05 (100) | 1.493 / 4.44 (103) | 1.504 / 3.93 (105) |
| b) | 1.497 / 3.20 (76) | 1.490 / 3.45 (85) | 1.478 / 4.13 (96) | 1.495 / 3.44 (92) |
|  | 1.485 / 3.91 (93) | 1.479 / 4.12 (102) | 1.471 / 4.62 (108) | 1.481 / 4.16 (112) |

**Table 16.** Comparison of DFT methods for small-ring systems

The results of Table 13 - Table 16 are best summarized by graphic visualization. Chart 1 shows the absolute deviation from the QCISD relaxed force constant; Chart 2 depicts the absolute deviation from the QCISD ethane relationship. Except for [1.1.0]bicyclobutane, MP2 consistently overestimates the relaxed force constants; this consistency leads to a small deviation from the relative QCISD order. The picture is

[l] The Computational Section 4.3 contains an evaluation of five additional density functionals with respect to the calculation of relaxed force constants for ethane, cyclopropane and tetrahedrane. Similar trends are observed.

[m] For adiabatic force constants by Cremer and coworkers at the B3LYP/6-31G(d,p) level, see references [171,190].

more diverse with the DFT methods: M06-2X and B97-D show opposing trends in absolute error and equally poor deviations in the relative ethane ordering. The older B3LYP functional shows a better agreement.

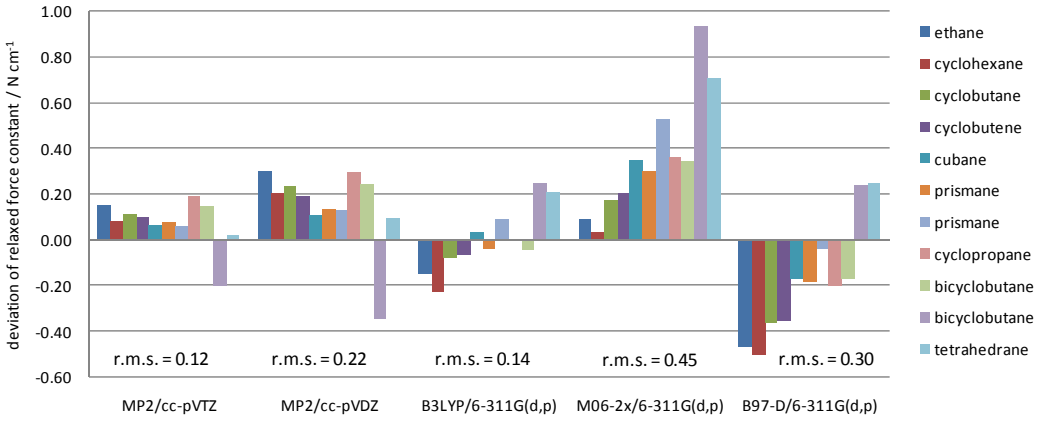


**Chart 1.** Deviation of relaxed force constants from QCISD result (method dependence)

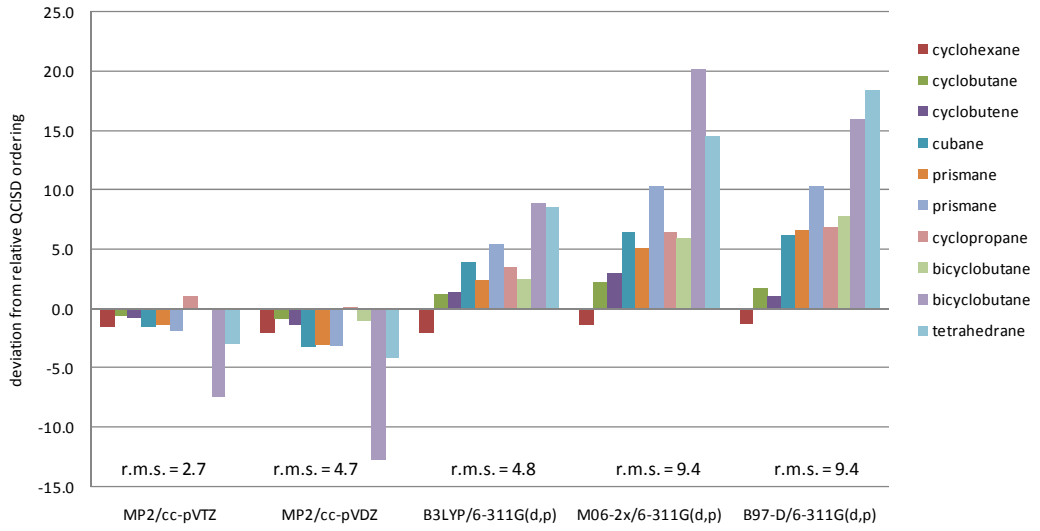


**Chart 2.** Deviation from relative QCISD ordering of relaxed force constants (method dependence)

In light of the surprisingly good B3LYP performance among the DFT methods, its basis set dependence was studied in detail. As shown in Chart 3, the smallest basis set, 6-31G(d), shows the best agreement with the QCISD results for ethane – an effect that might be due to fortuitous compensation of errors. Increasing the basis set to triple-

zeta and including additional polarization functions leads to a lower relaxed force constants, which deviate much further from the QCISD result. However, the r.m.s. deviation is similar for all three basis sets, as the absolute errors cancel out over the set of molecules. Relative ordering is, again, best for 6-31G(d) (Chart 4).

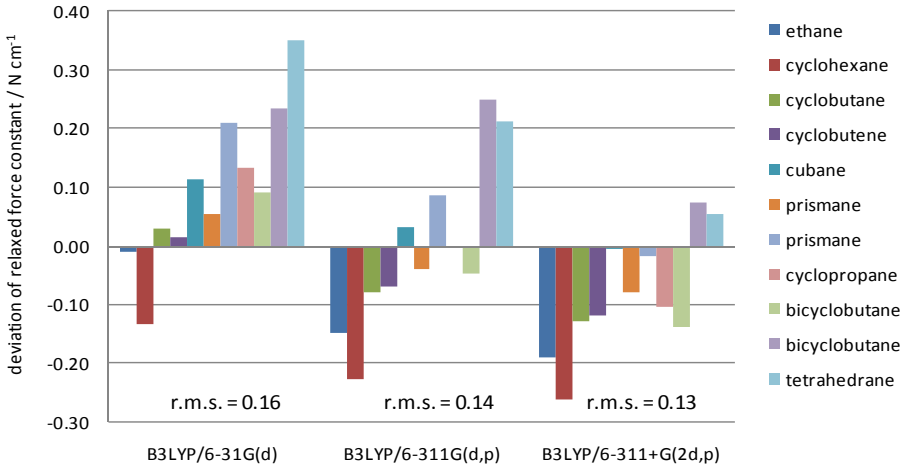


**Chart 3.** Deviation of relaxed force constants from QCISD result (basis set dependence with B3LYP)

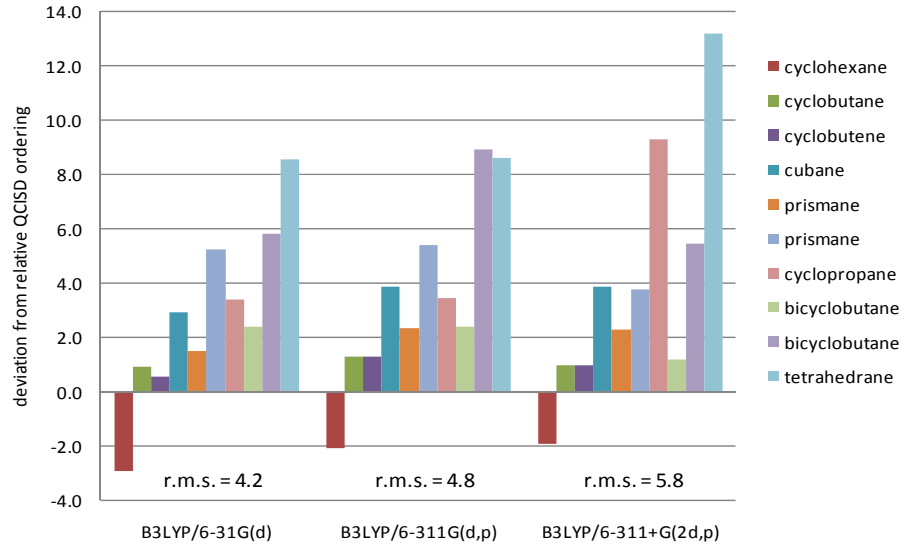


**Chart 4.** Deviation from relative QCISD ordering of relaxed force constants (basis set dependence with B3LYP)

Based on the results of this methodological survey, MP2/cc-pVTZ would be the best compromise for the description of bond rigidity. However, the size of some molecules

in this study precludes the use of MP2, even if the smaller double-zeta basis set were used. As the larger molecules necessitate the use of a DFT method, B3LYP/6-31G(d) was chosen as our standard method, because larger basis sets did not show significant improvement of the results. However, being carefully aware of B3LYP's failure with three-membered rings, it was decided to exclude these bonds from our study. Under this condition, the r.m.s. deviation from QCISD falls to 0.08 N $cm^{-1}$ for the relaxed force constants and 2.1 units for the ethane relationship.

## 2.6 Compliance constants of carbon-carbon single bonds

### 2.6.1 Acyclic hydrocarbons

Acyclic molecules will serve as the starting point of our study. Besides prototypical representatives like ethane and butane, Table 17 furthermore includes molecules for which the limitation to single bonds between tetracoordinate carbon centers has been lifted. Rather, an overview of the range of relaxed force constants that can be encountered in hydrocarbon chemistry shall be given. The molecules of Table 17 have already been studied by other authors at various levels of theory [171,179,183,190]; it is for ease of comparison that the results at the B3LYP/6-31G(d) level are repeated here.

Ethane in its staggered conformation features a relaxed force constant of 4.19 N $cm^{-1}$. The value for butane is 4 % smaller. By increasing the *s*-orbital contribution in the hybrids of a C-C single bond, the bond becomes increasingly shorter and more rigid: for example, the bond between the two formally $sp^2$ hybridized centers in butadiene has a relaxed force constant that is about one unit higher (5.18 N $cm^{-1}$) compared to ethane. Switching to *sp* hybridized carbons as in butadiyne almost doubles the relaxed force constant of the formal single bond to 7.58 N $cm^{-1}$. Clearly, these two molecules include conjugation effects. Values for ethylene and ethyne (9.92 and 17.67 N $cm^{-1}$ respectively) are also presented to gauge the range of common compliance constants. On the other end of the scale, we include the ethane radical cation in its $^2A_{1g}$ minimum [205]. It is interesting to note that a formally halved bond order leads to a 84 % reduction of the relaxed force constant.

| | bond length exp. / Å | bond length calc. / Å | rel. force const. / N cm$^{-1}$ | % of ethane |
|---|---|---|---|---|
| $H_3C-CH_3$ | 1.535 [155] | 1.531 | 4.19[n,o] | -- |
| 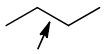 | 1.531 [155] | 1.534 | 4.00[p] | 95 |
| 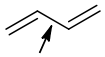 | 1.467 [155] | 1.457 | 5.17[o] | 123 |
| 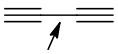 | 1.384 [155] | 1.369 | 7.69[o] | 184 |
| $H_2C=CH_2$ | 1.329 [155] | 1.331 | 9.92[n,o] | 237 |
| $HC\equiv CH$ | 1.203 [155] | 1.205 | 17.67[n,o] | 422 |
| $H_3C-CH_3]^{\bullet+}$ | -- | 1.964 | 0.68 | 16 |

**Table 17.** Relaxed force constants for carbon-carbon single bonds in acyclic molecules and for the multiple bonds in ethylene and ethyne (B3LYP/6-31G(d))

### 2.6.2 Cycloalkanes and hydrocarbon cages

Various representatives of this class of compounds have already been presented in the methodological survey. Cycloalkanes have been central to the development of strain theory [206]. As three-membered rings are known to possess the highest angle strain, it is counterintuitive that the QCISD results of Table 14 (see p. 70) give a less rigid bond for cyclobutane than for cyclopropane. However, it has been established that cyclobutane and cyclopropane have very similar strain energies (26.5 and 27.5 kcal/mol, respectively) [207–209]. This is commonly explained by the stabilizing effect of C-H bond strengthening and the lack of repulsive 1,3-interactions in cyclopropane [210]. Both effects compensate the intrinsically higher angle strain of the cyclopropane skeleton and might be the reason for its higher relaxed force constant compared to cyclobutane.[q,r] It is also noteworthy that cyclohexane, considered to be essentially unstrained, features a 3 % softer bond than ethane. Again, repulsive 1,3-interactions might be the reason for this observation [215]. Turning to cubane, we note

[n] For a calculation at the B3LYP/6-311++G(d,p) level of theory, see reference [179].

[o] For adiabatic force constants by Cremer and coworkers at the B3LYP/6-31G(d,p) level, see references [171,190].

[p] For a calculation at the MP2/aug-cc-pVTZ level of theory, see reference [183].

[q] We note the controversy about protobranching, which claims 1,3-interactions to be stabilizing [211,212].

[r] One might also put forward stabilizing σ-aromaticity for cyclopropane and destabilizing σ-antiaromaticity for cyclobutane as a possible explanation [213,214]; this concept, however, has recently been questioned [202].

that its angle strain leads to bond lengthening and considerable softening in comparison to the bond of cyclobutane (Table 14). In contrast, the bonds between two four-membered rings in prismane are slightly rigidified at the expense of the considerably softened bonds of the three-membered rings. Tetrahedrane, as yet not isolated although predicted to be kinetically stable [216], features a smaller relaxed force constant than cyclopropane; its bonds, however, are not as soft as those in cubane.

Table 18 contains the B3LYP/6-31G(d) results for these molecules in addition to the results for adamantane, dodecahedrane and [1.1.1]bicyclopentane. As discussed in the methodological survey, three-membered rings as in cyclopropane[t], tetrahedrane and prismane are omitted from the DFT data set. Our cyclohexane data compare well with Cremer's adiabatic force constant (3.923 N $cm^{-1}$) [190]. As observed for cubane, the C-C bonds are also softer in adamantane [215] and, even more so, in dodecahedrane and [1.1.1]bicyclopentane. Angle strain associated with the cage architecture and repulsive non-bonded interactions are the reasons; no rigidifying corset effect can be

| | bond length exp. / Å | bond length calc. / Å | rel. force const. / N $cm^{-1}$ | % of ethane |
|---|---|---|---|---|
|  | 1.536 [155] | 1.537 | 3.95 | 94 |
|  | 1.555 [155] | 1.554 | 3.79 | 90 |
|  | 1.529 [217] | 1.544 | 3.89 | 93 |
| 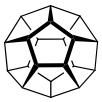 | 1.545 [218] | 1.556 | 3.70 | 88 |
|  | 1.551 [219] / 1.565 [220] | 1.571 | 3.68 | 88 |
|  | 1.545 [221] / 1.557 [222] | 1.556 | 3.50 | 84 |
|  | (1.551)[s] | 1.558 | 3.88 | 93 |

**Table 18.** Relaxed force constants for cycloalkanes and hydrocarbons cages (B3LYP/6-31G(d))

[s] Value refers to hexamethylprismane, see reference [223].

[t] For adiabatic force constants by Cremer and coworkers at the B3LYP/6-31G(d,p) level of theory, see references [171,190].

observed. [1.1.1]Bicyclopentane is also an example of violation of the bond length – bond strength relationship, i.e. its bond is only marginally longer but decisively softer than, for example, the bond of parent cyclobutane.

Returning to the QCISD results, it is instructive to demonstrate the unexpectedly low bond rigidity of cyclobutane by calculating the respective bond stretch potentials. Graph 1 compares the potentials of ethane, cyclobutane and cyclopropane at the QCISD/6-311+G(2d,p) level of theory for displacements of ± 0.10 Å around the equilibrium bond length. For further reference, the potentials of ethylene and the ethane radical cation ($^2A_{1g}$ state) are also included. Even though the effect is small, one can clearly see that cyclobutane has a less rigid bond than cyclopropane. Interestingly, no such comparison can be found in the literature. Early theoretical studies show bond stretch potentials for the bond breaking of cyclopropane (cyclobutane) to the trimethylene (tetramethylene) diradical independently [224–227].[u] Experimental studies on cyclobutane have usually focused on the ring puckering potential [230–234].

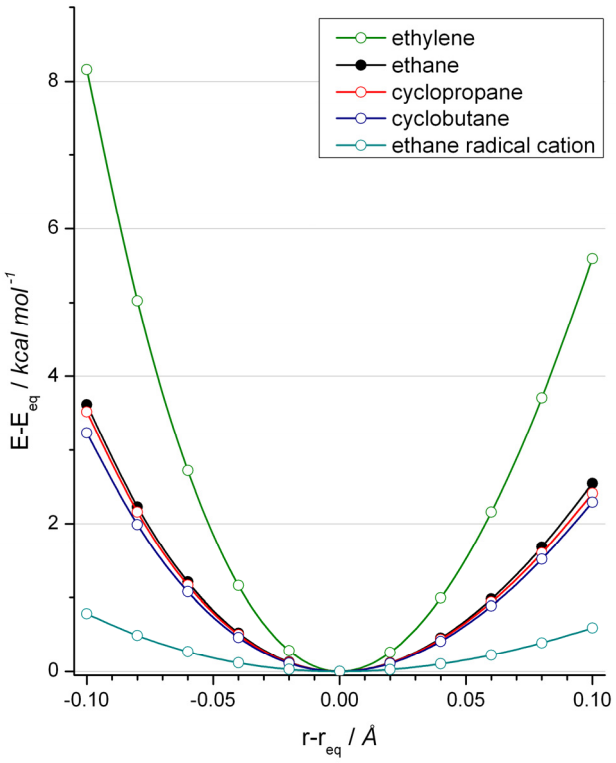


**Graph 1.** Comparison of bond stretch potentials (QCISD/6-311+G(2d,p))

[u] We note in this context the seminal spectroscopic studies by Zewail and coworkers, who studied the femtosecond dynamics of the trimethylene and tetramethylene diradical [228,229].

### 2.6.3 Exocyclic C-C bonds

Carbon-carbon bonds between tetracoordinate carbon centers can deviate strongly from the usual bond length of 1.54 Å if the carbon atoms form part of highly strained frameworks that modulate their hybridization. This bond shortening is usually explained by the increased *s*-orbital contribution to the involved hybrid orbitals. For example, the C-C bond between two bicyclo[1.1.1]pentane units is shortened to 1.492 Å (entry 1, Table 19); the relaxed force constant indicates an 8% more rigid bond compared to ethane. The bond shortening increases along the series cubylcubane (entry 2) [235], the bicyclo[1.1.0]butane dimers (entries 3 and 4) [236] and tetrahedryltetrahedrane (entry 5). The relaxed force constants follow this trend and rise up to 6.12 N cm$^{-1}$ for entry 5, which is 1.5 times the value of ethane.[v] We conclude that bond shortening by increased *s*-orbital contribution leads to more rigid bonds.

| entry | molecule | | bond length exp. / Å | bond length calc. / Å | rel. force const. / N cm$^{-1}$ | % of ethane |
|---|---|---|---|---|---|---|
| 1 | 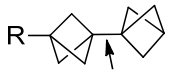 | R = H:<br>R = $CO_2Me$: | --<br>1.480 [237] | 1.492<br>-- | 4.52<br>-- | 108 |
| 2 | 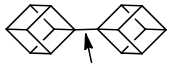 | | 1.475 [235] | 1.478 | 4.68 | 112 |
| 3 | 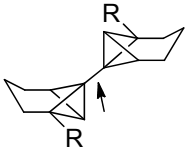 | R = H:<br>R = $CO_2Me$: | --<br>1.445 [236] | 1.463<br>-- | 5.15<br>-- | 123 |
| 4 | 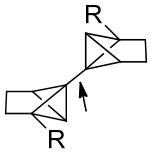 | R = H:<br>R = $CO_2Me$: | --<br>1.440 [236] | 1.458<br>-- | 5.32<br>-- | 127 |
| 5 | 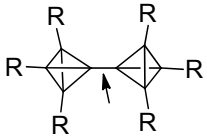 | R = H:<br>R = TMS: | --<br>1.436 [238] | 1.428<br>-- | 6.12[v]<br>-- | 146[v] |

**Table 19.** Relaxed force constants for exocyclic C-C bonds (B3LYP/6-31G(d))

[v] The reliability of the B3LYP calculation on the exocyclic carbon-carbon bond in tetrahedryltetrahedrane was established by a QCISD/6-311+G(2d,p) calculation: 1.429 Å, 6.09 N cm$^{-1}$, 145 %.

### 2.6.4 Elongated C-C bonds

Angle strain and steric crowding can lead to elongated C-C bonds. A large but by no means exhaustive number of examples are presented in Table 20 on the next page. Polyalkylated ethanes, which have been studied extensively by Rüchardt et al. [239], are not included, as B3LYP does not describe medium-range correlations correctly [201]. The same holds true for the diamondoid dimers recently described by Schreiner and coworkers [240,241]. Rather, we start our discussion with a group of angle-strained molecules, which are frequently used as building blocks for elongated bonds: acenaphthene (entry 1), cyclobutene (entry 2) and its benzene analog (entry 3) feature C-C single bonds that are 15 – 19 % softer than the ethane bond. Steric crowding of these "prestrained" bonds [242] by introduction of aryl units is demonstrated by entries 4 – 9. Their computed single bond lengths are in the range of 1.69 to 1.77 Å and the relaxed force constants fall to as little as one fifth of the ethane bond strength. We also note that B3LYP consistently overestimates the bond lengths. While the experimental bond lengths, despite being measured at low temperatures, might be artificially shortened because of thermal motion, the observed differences could also be a hint that dispersion corrections should be included in the calculation of these molecules.

However, another aspect should also be pointed out: the small relaxed force constants indicate that the respective bonds are extraordinarily soft, i.e. they can be very easily deformed. Elongated C-C bonds should therefore be particularly susceptible to crystal packing effects [242], which might also be an explanation for the observed differences between the experimental data and the gas phase calculations. For example, the crystal structure of entry 9 contains four crystallographically independent molecules with C-C bond lengths of 1.707, 1.712, 1.758 and 1.771 Å [157–159].

It is furthermore interesting to note that the largest elongations were achieved with the acenaphthene building block, which is less "prestrained" than, e.g., the benzocyclobutene building block (entry 3).

| entry | molecule | bond length exp. / Å | bond length calc. / Å | rel. force const. / N cm$^{-1}$ | % of ethane |
|---|---|---|---|---|---|
| 1 | 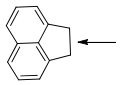 | 1.576 / 1.552 [243] | 1.569 | 3.58 | 85 |
| 2 |  | 1.566 [155] | 1.573 | 3.53 | 84 |
| 3 | 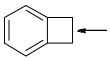 | 1.576 [244] | 1.581 | 3.40 | 81 |
| 4 | 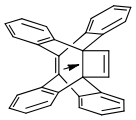 | 1.667 [245] | 1.698 | 1.65 | 39 |
| 5 | 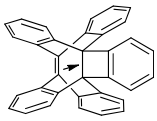 | 1.713 [245] | 1.723 | 1.42 | 34 |
| 6 | 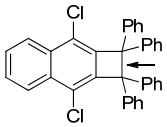 | 1.720 [246] | 1.732 | 1.28 | 31 |
| 7 | 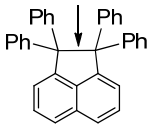 | 1.701 [247] | 1.722 | 1.40 | 33 |
| 8 | 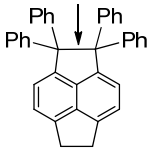 | 1.754 [159] | 1.760 | 1.05 | 25 |
| 9 | 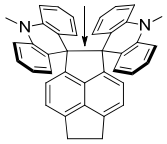 | 1.707-1.771[w] [157,158] | 1.768[x] | 0.84 | 20 |

**Table 20.** Relaxed force constants for elongated C-C bonds (B3LYP/6-31G(d))

[w] The X-ray structural analysis revealed four crystallographically independent molecules.

[x] Reference [159] reports a bond length of 1.776 Å at the UB3LYP/6-31G(d) level of theory.

### 2.6.5 Compressed C-C bonds

Short bonds can also be obtained by imposing steric constraints on a C-C bond [163,164]. It has been shown that such molecules exhibit a bond length that is shorter than the value that corresponds to their *s*-orbital contribution [163,164]. In contrast to the exocyclic bonds discussed earlier, the bond shortening in these molecules is attributable to compression, i.e. the short bonds would relax to a longer length if the steric constraint were relieved.

Apart from Pascal's *in*-cyclophane **89** [156], the molecules in Figure 41 have not yet been made and are taken from the computational studies of Huntley et al. (**92-97**) [163] and Martínez-Guajardo et al. (**98**) [164]. The shortest bonds in these molecules are in the range of 1.31 to 1.44 Å; the relaxed force constants rise as high as 11.37 N $cm^{-1}$ – which is almost three times as much as the value for ethane. Molecules **97** and **98** show bond lengths in the range of a double bond, and we note that the relaxed force constants of these formal single bonds reflect this too (see for comparison Table 17 on p. 76). The smaller relaxed force constant of **98** compared to **97** might be explained by the less extensive framework around the compressed bond. Compound **93**, which

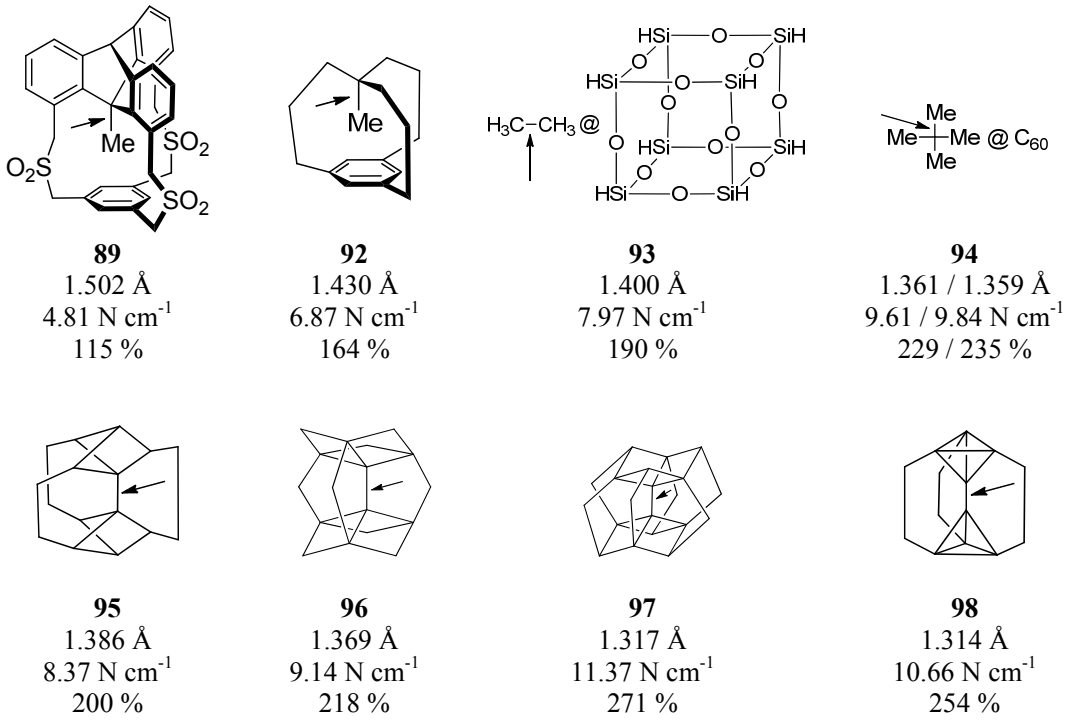


**89**
1.502 Å
4.81 N $cm^{-1}$
115 %

**92**
1.430 Å
6.87 N $cm^{-1}$
164 %

**93**
1.400 Å
7.97 N $cm^{-1}$
190 %

**94**
1.361 / 1.359 Å
9.61 / 9.84 N $cm^{-1}$
229 / 235 %

**95**
1.386 Å
8.37 N $cm^{-1}$
200 %

**96**
1.369 Å
9.14 N $cm^{-1}$
218 %

**97**
1.317 Å
11.37 N $cm^{-1}$
271 %

**98**
1.314 Å
10.66 N $cm^{-1}$
254 %

**Figure 41.** Bond lengths, relaxed force constants and ethane relationship for compressed C-C bonds (B3LYP/6-31G(d))

squeezes ethane into a silsesquioxane, and the endofullerene **94** are particularly good examples for a corset effect. The silsesquioxane cage compresses the ethane bond to 1.40 Å, thereby almost doubling the relaxed force constant compared to "free" ethane. Similarly, neopentane features a bond length of 1.54 Å and a relaxed force constant of 3.88 N $cm^{-1}$ at the B3LYP/6-31G(d) level of theory, but its encapsulation in $C_{60}$ compresses the bonds to ~ 1.36 Å and more than doubles the relaxed force constants.[y] One would hardly call this a "strong" bond – it is just a bond that is difficult to deform any further. The fullerene cage works against elongation, while nuclear repulsion between the bonded carbon atoms prohibits compression towards the other side.

As pointed out by Huntley et al., compression of a central bond as, for example, in **95-97** comes at the cost of elongated bonds in the periphery of the molecules [163]. We do not list these bonds and their relaxed force constants in this chapter, but have included them in the Computational Section (p. 159). The limiting case, however, is a bond length of 1.66 Å with a relaxed force constant of 1.60 N $cm^{-1}$ in **98**.

[y] Two different C-C bonds exist, as the $C_{60}$ cage lowers the $T_d$ symmetry of the neopentane unit to $C_3$.

## 2.7 Discussion

The B3LYP data set contains 30 molecules with 59 data points. The data for peripheral bonds, which have not been described in the tables, can be found in the Computational Section on p. 159. Graph 2 is a plot of the relaxed force constants versus bond length. The data span the range from 1.31 to 1.77 Å and 11.4 to 0.8 N cm$^{-1}$.[z] For comparison, the data points of the reference molecules ethylene, butadiyne and butadiene are also shown, although they have not been included in the fitting procedure. The same holds true for the red data points, which correspond to fluxional molecules that will be discussed below.

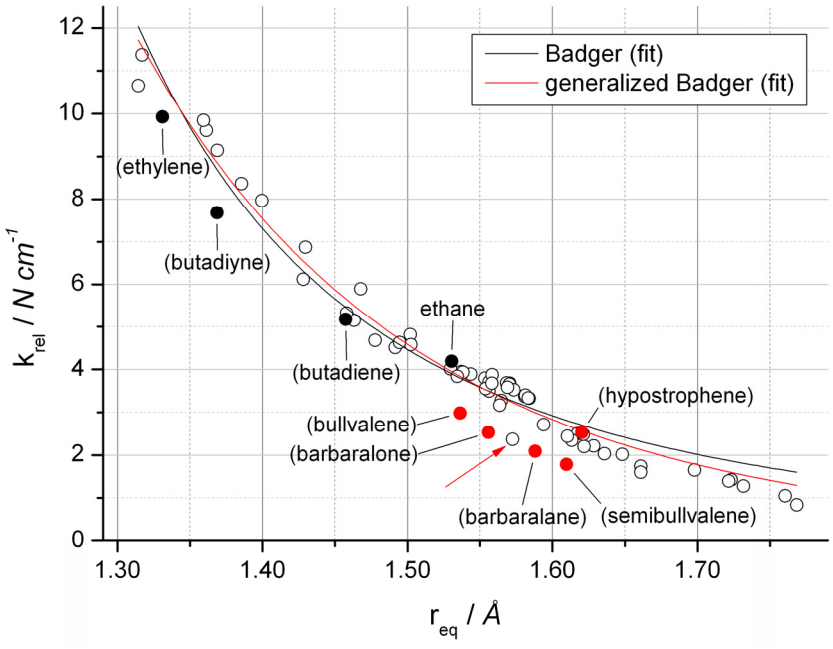


**Graph 2.** Plot of relaxed force constants vs. bond length (B3LYP/6-31G(d); reference molecules in brackets were not included in the fit; red arrow indicates outlier)

Numerous formulae have been derived to describe the relationship between force constants and equilibrium bond lengths [248]. The most popular relationship is Badger's rule (equation 1) [249–253], and a fit to this equation is included in Graph 2 (black curve):

[z] The QCISD/6-311+G(2d,p) data set contains 13 molecules with 19 data points. It spans a range from 1.429 to 1.584 Å, which is too small for a meaningful graphic analysis.

Badger's rule: $k = \frac{a}{(r-d)^3}$ (equation 1)

$R = 0.966$ with: $d = 0.841$ Å; $a = 1.279$ N Å$^3$ cm$^{-1}$

Badger's rule (generalized): $k = \frac{a}{(r-d)^p}$ (equation 2)

$R = 0.979$ with: $p = 15$; $d = -1.561$ Å ; $a = 8.878 \cdot 10^7$ N Å$^{15}$ cm$^{-1}$

We observe that Badger's rule generally underestimates the force constants of C-C bonds that are shorter than the ethane bond, while overestimating the force constants of longer bonds. A mathematically more accurate fit can be found if the exponent is used as a free parameter with integer values (equation 2). This leads to a significantly better description of the elongated bonds (Graph 2, red curve).[aa] However, it should be pointed out that Badger's original formula did not foresee negative values for the parameter $d$, which is supposed to describe an effective bond length $r - d$. Also, the presented data set is heavily biased towards unusual and highly strained molecules, so that a purely mathematical approach might not necessarily enhance chemical understanding. It was therefore decided to pursue a rather heuristic [254] approach for the analysis of Graph 2. Most data points cluster in groups slightly above or below the fitting line. A data point that obviously breaks this pattern is indicated by the red arrow. With a bond length of 1.573 Å, this bond falls into a range where many other data points are available. However, these other bonds generally feature relaxed force constants that are about one unit higher. The indicated bond seems to be unusually soft. Is this bond particularly prone to bond breaking?

The outlier is one of the peripheral bonds of molecule **98** (Scheme 24). The small relaxed force constant might reflect a generally flat potential energy surface, which seems unlikely for a structure as congested and strained as **98**, or might hint at a low-lying transition state. We therefore performed a scan along the respective bond stretch coordinate and were indeed able to find a transition state with a low activation enthalpy $\Delta H^{\neq} = 6.7$ kcal/mol (B3LYP/6-31G(d), corrected for 298 K). The calculated activation enthalpy is even lower at the SCS-MP2/cc-pVDZ level (4.3 kcal/mol). This transition state leads to a rearranged product **99**, in which two bonds have been broken to generate one new bond and (singlet) carbene. Product **99** is an impressive 105.7

[aa] Even better correlations are possible with exponential relationships, for example $k = a\, e^{b\, r}$ ($R = 0.981$ with $a = 8008$ N cm$^{-1}$; $b = -4.972$ Å$^{-1}$).

(110.0) kcal/mol lower in enthalpy than the starting material. That a low-valent carbene is energetically favored over a formally correct Lewis structure is a remarkable manifestation of the high strain in compound **98** [255]. To put the above numbers into context, we note that the barrier for rearrangement of **98** is, for example, significantly lower than the barrier for the chair-to-chair inversion of cyclohexane (11.2 kca1/mol at B3LYP/6-31G(d), 12.2 kcal/mol at SCS-MP2/cc-pVDZ respectively). Following the call of Hoffmann, Schleyer and Schaefer [256], **98** would have to be called a fleeting molecule: a stationary minimum that cannot be isolated under standard laboratory conditions.

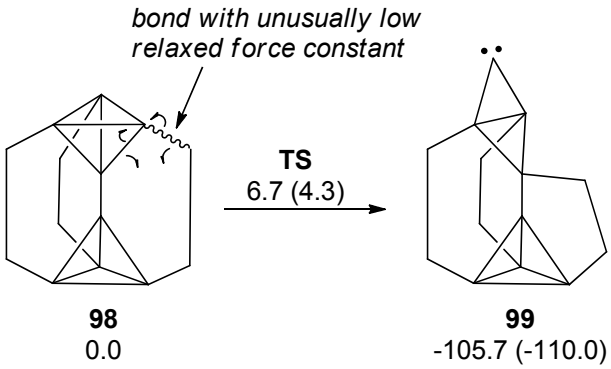


**Scheme 24.** Rearrangement of **98** along the bond with an unusually small relaxed force constant (relative enthalpies calculated for 298 K in kcal/mol at the B3LYP/6-31G(d) level of theory; values in brackets are at SCS-MP2/cc-pVDZ level, respectively)

The above example has demonstrated that Graph 2 might be used to identify fragile bonds in a molecule.[bb] Such a relationship would be highly desirable, as the proof of kinetic stability is an extensive endeavor with increasing molecule size.[cc] Identification of outliers in Graph 2 would allow a more directed search for reactive low-barrier modes. In order to test this hypothesis, we looked for further examples.

Unusually low barriers for the breaking of carbon-carbon bonds can be found in fluctuating molecules, which undergo degenerate Cope rearrangements. Typical representatives are shown in Table 21 on the next page.

[bb] We note in this context that the fragile bond is not the longest bond of the molecule, see p. 160 of the Computational Section.

[cc] For a recent example, see the comprehensive study on unusual benzene dimers [257].

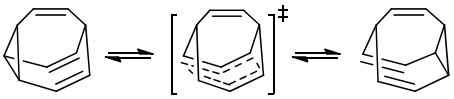

**100** **100**

| molecule | bond length calc. / Å | rel. force const. / N cm$^{-1}$ | % of ethane | $\Delta H^{\neq}$ (298 K) calc. / kcal mol$^{-1}$ |
|---|---|---|---|---|
| 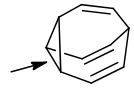 bullvalene (**100**) | 1.536 | 2.98 | 71 | 12.5 [258] |
| 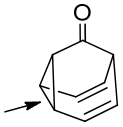 barbaralone (**101**) | 1.556 | 2.54 | 61 | 8.8[dd] |
| 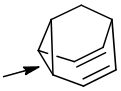 barbaralane (**102**) | 1.588 | 2.09 | 50 | 6.4 [258] |
| 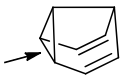 semibullvalene (**103**) | 1.610 (1.583) | 1.78 (2.34) | 42 (56) | 4.5 [258] |
| 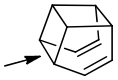 hypostrophene (**104**) | 1.620 | 2.53 | 60 | 21.9 [260] |

**Table 21.** Degenerate Cope rearrangement in bullvalene (**100**) and relaxed force constants for fluxional molecules (B3LYP/6-31G(d); data in brackets: QCISD/6-311+G(2d,p))

[dd] Schleyer and coworkers calculated an activation free enthalpy (at 298 K) of 9.1 kcal/mol at the B3P86/6-311+G(d,p) level [259].

We emphasize that in all of these molecules the bond of interest is part of a three-membered ring. As demonstrated in Chapter 2.5, DFT methods give unreliable relaxed force constants for three-membered rings, and therefore, this important structural unit was excluded from the B3LYP data set. The relaxed force constants of fluxional molecules at the B3LYP level should therefore be considered with a grain of salt and we will return to this point after discussion of the data.

Our analysis begins with bullvalene (**100**), which was first envisioned by Doering and Roth [261–263]. Its activation enthalpy for the Cope rearrangement was experimentally determined to 13.3 kcal/mol [264,265], and B3LYP/6-31G(d) calculations have reproduced this value accurately (12.5 kcal/mol) [258]. The calculated bond length is only marginally longer than in ethane, but the relaxed force constant is almost 30% smaller – a clear indication of an unusually soft bond stretch potential in conjunction with a low-lying transition state. The increasing strain along the series barbaralone (**101**) [263], barbaralane (**102**) [263] and semibullvalene (**103**) [266] leads to increasing bond elongation and decreasing activation enthalpies. This is consistently reflected by the relaxed force constants.

The sensitivity of relaxed force constants to low-lying transition states is demonstrated by hypostrophene (**104**). This compound, synthesized by Pettit in 1971, features all structural units necessary for a Cope rearrangement, but the rearrangement is slow at room temperature [267]. The respective activation enthalpy is calculated to be 21.9 kcal/mol and is considerably higher than for any other compound in Table 21. Most importantly, hypostrophene features almost the same bond length as semibullvalene, but its relaxed force constant is substantially higher than that of the latter. The almost fivefold increase in activation enthalpy is markedly reflected by the relaxed force constant.

The fleetingness of the bonds in fluxional molecules is also demonstrated by Graph 2. The red data points correspond to the molecules from Table 21. The molecules with a low activation enthalpy feature a substantially lower relaxed force constant than other molecules in the same bond length range. Contrastingly and as alluded to above, hypostrophene (**104**) does not show this deviation. We also note that the outlier **98**, which has been shown to possess a low activation enthalpy for bond breaking, falls perfectly into the line of fleeting molecules. Based on this analysis, we estimate that activation enthalpies < 15 – 20 kcal/mol lead to unusually low relaxed force constants that can be identified as outliers in Graph 2.

With respect to the reliability of the B3LYP relaxed force constants of fluxional molecules, we point out that our methodological study has shown that DFT methods generally overestimate the relaxed force constant of three-membered rings (Chapter 2.5). One might therefore expect that the actual relaxed force constant of fluxional molecules might be even lower. In order to support this hypothesis, we performed a QCISD/6-311+(2d,p) calculation on the smallest member of this group of molecules, semibullvalene (**103**). The data are given in Table 21; their interpretation, however, is difficult. Although activation enthalpies of fluxional molecules calculated at the B3LYP/6-31G(d) level of theory show excellent agreement with experimental data [258,268], we observe for the first time a significant bond length deviation from the QCISD result. Not surprisingly, the shorter QCISD bond also goes in hand with a higher relaxed force constant compared to B3LYP. For this class of molecules, a more extensive assessment of the reliability of DFT relaxed force constants would be desirable, but is currently limited by the high computational cost at the QCISD level.

## 2.8 Summary and Outlook

Compliance constants provide valuable information about chemical bonds. Based on compliance constants, the rigidities of 70 single bonds between tetracoordinate carbon atoms were investigated. A comprehensive study of both real and hypothetical molecules allows four different conclusions, which are of interest to various fields of research:

The methodological survey has demonstrated that commonly used density functionals overestimate the bond stretch potential of three-membered rings (Chapter 2.5). This finding is an example of the failures of DFT methods [201,203,204,269] and might help to improve the poor energy description of three-membered rings [203,204]. The analysis of bond stretch potentials during the optimization and parameterization of new density functionals could lead the way in this regard.

Calculations at the CCSD(T) and QCISD level have led to the counterintuitive conclusion that cyclobutane has a softer bond stretch potential than cyclopropane (Chapter 2.5 and Chapter 2.6.2). This seemingly simple analysis has not been performed up to now and might inspire further discussion about the strain of these two molecules [210]. It is a marked demonstration that pure emphasis on angle strain can be misleading and that the world of molecules is more complex. The presented results are also of interest to the rapidly growing field of mechanochemistry, where cyclobutane units are successfully employed as mechanophores [270,271].

Analysis of compressed carbon-carbon single bonds has established that despite their high energy [255], they are substantially more rigid than the ethane bond (Chapter 2.6.5). The analysis of inclusion compounds, for example endofullerene **94**, suggests that this is due to a rigidifying corset effect. In other words: only through the presence of a rigid environment, intermolecular or intramolecular, can such unusually short bond lengths be achieved. It is therefore interesting to note that compressed bonds exhibit a rigidity that is comparable to that of molecules where intrinsic effects of the bond, such as the presence of an additional π-bond in ethylene, are responsible for an increased rigidity.

Based on B3LYP/6-31G(d) calculations, a bond length – bond rigidity relationship in the form of Badger's rule has been established for the single bonds in the range of 1.31 to 1.77 Å (Chapter 2.7). Outliers of this relationship have been shown to possess particularly low activation enthalpies for bond breaking, which would classify them as fleeting molecules. While the traditional bond length – bond strength relationship fails

for these molecules from a kinetic point of view, the relaxed force constants give a reliable description of their chemical behavior. This procedure, which we estimate to be sensitive for activation enthalpies < 15 – 20 kcal/mol, provides an efficient way to identify labile bonds in a molecule. Put another way, the procedure may guide the chemist to the Achilles heel of real and hypothetical molecules and might serve as a valuable tool for more realism in the prediction of molecules [256]. Further efforts should focus on the compilation of a computationally expensive, but more reliable QCISD/6-311+G(2d,p) data set and on the transfer of this methodology to other bond types.

# 3 Experimental Section

## 3.1 General methods

Commercial chemicals were used without further purification. Thin layer chromatography plates (Macherey-Nagel Polygram Sil G/UV254) were stained with ceric ammonium molybdate solution. Flash chromatography was performed with silica gel (pore size 60 Å, 40- 63 mesh size). Melting points < 250 °C were determined with a Buechi 530 apparatus, all others with a Buechi M-560 respectively.

NMR spectra were obtained on Bruker DRX 400 and Avance II 600 spectrometers. Tetramethylsilane (TMS) was used as internal standard for all measurements. DEPT 13C NMR and standard two-dimensional techniques (COSY, HSQC, HMBC, NOESY) were used to assign the spectra.

Electron ionization (EI) mass spectra were measured with a Thermo Finnigan MAT95XL (double focusing sector field mass spectrometer). Accurate mass results were obtained by peak matching (resolution 10000 with 10% valley definition; mass calibrant: PFK).

Electrospray ionization (ESI) mass spectra were measured with a ThermoFisher Scientific LTQ-Orbitrap Velos (linear ion trap coupled with orbitrap mass analyzer; resolution: 100000 FWHM at m/z = 400 u). Typical spray voltage in positive ion mode was 2.3-2.8 kV. Measurements were performed in direct infusion mode using a custom made microspray device mounted on a Proxeon nanospray ion source. The microspray device allows for the sample infusion through a stainless steel capillary (90 µm I. D., flow approx. 1 µl/min). Unless otherwise noted, samples were measured in methanol spiked with 0.1 mg/mL tetradecyltrimethylammonium bromide. Sample concentrations were approx. 50 µg/mL. Accurate mass measurements in the orbitrap were performed using the lock mass option of the instrument control software using the cation of tetradecyltrimethylammonium bromide (256.29988 u) as internal mass reference.

Infrared spectra were measured on a Bruker Tensor 27 (ATR, 4000-520 cm-1), UV/Vis spectra on a Varian Carey 100 Bio (200-600 nm) respectively.

Elemental analyses were performed with a Elementar Vario Microcube or Thermo Quest Flash EA 1112.

## 3.2 List of compounds

Tribenzotriquinacenes:



Comment:

Dihydroindenoindene byproducts are described along with the respective tribenzotriquinacene.

## 3.3 Knoevenagel condensation of dibenzoylmethanes

### 3.3.1 General Procedure M1: 2-Benzylidene-1,3-diphenylpropane-1,3-dione (14)

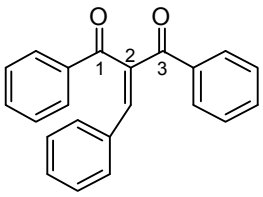


$C_{22}H_{16}O_2$
312.36 g/mol

A procedure from the literature [58] was modified as follows: To a solution of benzaldehyde (12.2 g, 115 mmol, 1.0 eq) and dibenzoylmethane (25.9 g, 115 mmol, 1.0 eq) in toluene (350 mL) were added piperidine (1.30 g, 15 mmol, 0.13 eq) and hexanoic acid (3.4 g, 29 mmol, 0.25 eq). The solution was heated under reflux for 20 h using a Dean-Stark trap. After cooling to room temperature the solution was washed with a 10% solution of $NaHCO_3$ (500 mL), 5% aqueous acetic acid (500 mL) and brine (500 mL). The organic phase was dried ($MgSO_4$) and the solvent was evaporated *in vacuo*. The desired diketone **14** was obtained after flash chromatography (silica, 10% ethyl acetate/pentane) as a viscous yellow oil (23.6 g, 76 mmol, 66% yield) that solidified upon standing to give a pale yellow solid (mp 87 °C, lit. [272]: 87-88 °C). NMR data corresponded to the data reported in the literature [273]. Single crystals for X-ray diffraction were obtained by recrystallization from refluxing diethyl ether.

**$^1$H NMR** (400 MHz, $CDCl_3$): δ [ppm] = 7.20-7.60 (m, 12H, Ph and C=C*H*), 7.85-7.89 (m, 2H, Ph), 7.95-7.99 (m, 2H, Ph)

**MS** (ESI): accurate mass calcd for $[C_{22}H_{16}O_2 + H]^+$ *m/z* 313.1223, found *m/z* 313.1224; accurate mass calcd for $[C_{22}H_{16}O_2 + Na]^+$ *m/z* 335.1043, found *m/z* 335.1041

**UV** ($CH_2Cl_2$): $\lambda_{max}$ [nm] (lg ε) = 223 (4.17), 259 (4.33), 295 (4.29)

**IR** (ATR): $\tilde{\nu}$ [$cm^{-1}$] = 3057 (w), 1644 (m), 1593 (m), 1267 (m), 1227 (m), 1209 (m), 980 (m), 733 (m), 693 (s)

### 3.3.2 General Procedure M2: 2-(2-Bromobenzylidene)-1,3-diphenylpropane-1,3-dione (30)

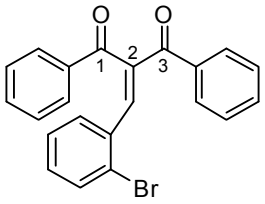


$C_{22}H_{15}BrO_2$
391.26 g/mol

The compound was prepared according to the reported literature procedure [63,62]: Dibenzoylmethane (10 mmol, 1.0 eq) and 2-bromobenzaldehyde (10 mmol, 1.0 eq) were dissolved in acetonitrile (50 mL) and piperidine (1.0 mmol, 0.1 eq) was added. The mixture was refluxed at 80 °C for 12 h. The solvent was removed *in vacuo* and the crude reaction mixture was purified by flash chromatography (silica, 5-10% ethyl acetate/pentane). The product was obtained as a yellow solid (mp 104 °C, lit. [63]: 103.7-104.3 °C) in 66% yield. Spectroscopic data corresponded to the reported in the literature data. Single crystals for X-ray diffraction were obtained by slow evaporation from an ethyl acetate/pentane solution.

**$^1$H NMR** (400 MHz, $CDCl_3$): δ [ppm] = 7.05-7.13 (m, 2H), 7.32-7.39 (m, 3H), 7.45-7.53 (m, 4H), 7.58-7.63 (m, 1H), 7.76 (s, 1H, C=C*H*), 7.90 (dd, 2H, *J* = 1.3, 8.5 Hz), 7.95 (dd, 2H, *J* = 1.4, 8.4 Hz)

**MS** (ESI): accurate mass calcd for $[C_{22}H_{15}BrO_2 + H]^+$ *m/z* 391.0328, found *m/z* 391.0329; accurate mass calcd for $[C_{22}H_{15}BrO_2 + Na]^+$ *m/z* 413.0148, found *m/z* 413.0149

**UV** ($CH_2Cl_2$): $\lambda_{max}$ [nm] (lg ε) = 222 (4.26), 258 (4.36), 279 (4.21, shoulder)

**IR** (ATR): $\tilde{\nu}$ [$cm^{-1}$] = 3272 (br), 2921 (w), 2852 (w), 1664 (m), 1642 (s), 1251 (m), 1229 (m), 750 (m), 713 (s), 687 (m), 588 (m)

### 3.3.3 2-(2-Methoxybenzylidene)-1,3-diphenylpropane-1,3-dione (31)

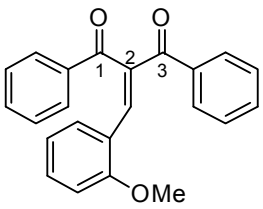


$C_{23}H_{18}O_3$
342.39 g/mol

The compound was prepared according to general procedure M1 by reacting dibenzoylmethane on a 6.00 g scale (26.7 mmol) with 2-methoxybenzaldehyde. The product was obtained after flash chromatography (silica, 15% ethyl acetate/pentane) in 66% yield as a yellow solid (mp 109-110 °C). Single crystals for X-ray diffraction were obtained by slow evaporation from an ethyl acetate/pentane mixture.

**$^1$H NMR** (400 MHz, $CDCl_3$): δ [ppm] = 3.65 (s, 3H, OC*H*$_3$), 6.74-6.80 (m, 2H), 7.22-7.27 (m, 2H), 7.34-7.40 (m, 2H), 7.45-7.50 (m, 3H), 7.54-7.60 (m, 1H), 7.82 (s, 1H, C=C*H*), 7.90 (dd, 2H, *J* = 1.2, 8.4 Hz), 7.94 (dd, 2H, *J* = 1.4, 8.5 Hz)

**$^{13}$C NMR** (100 MHz, $CDCl_3$): δ [ppm] = 196.4 (s, C1/C3), 195.1 (s, C1/C3), 157.5 (s, *C*OCH$_3$), 140.2 (d, C=*C*H), 139.1 (s, C2), 137.6 (s), 136.6 (s), 133.3 (d), 132.5 (d), 131.9 (d), 130.6 (d), 129.7 (d, 2C), 129.2 (d, 2C), 128.6 (d, 2C), 128.4 (d, 2C), 122.6 (s), 120.5 (d), 110.7 (d), 55.1 (q, O*C*H$_3$)

**MS** (ESI): accurate mass calcd for $[C_{23}H_{18}O_3 + H]^+$ *m/z* 343.1329, found *m/z* 343.1329; accurate mass calcd for $[C_{23}H_{18}O_3 + Na]^+$ *m/z* 365.1148, found *m/z* 365.1147

**UV** ($CH_2Cl_2$): $\lambda_{max}$ [nm] (lg ε) = 224 (4.20), 252 (4.33), 282 (4.12, shoulder), 338 (3.94)

**IR** (ATR): $\tilde{\nu}$ [$cm^{-1}$] = 3023 (w), 2945 (w), 1663 (m), 1639 (s), 1596 (s), 1259 (s), 1227 (s), 743 (s), 716 (s), 688 (m), 592 (m)

**EA**: calcd C 80.68%, H 5.30%; found C 80.67%, H 5.14%

### 3.3.4 (*E*)-1,3-Bis(2-bromophenyl)prop-2-en-1-one (47)

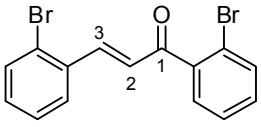


$C_{15}H_{10}Br_2O$
366.05 g/mol

A procedure from the literature [75,76] was modified as follows: In a 250 mL three-neck flask equipped with a thermometer and a mechanical stirrer, 4.14 g powdered sodium hydroxide (103.5 mmol, 1.25 eq) were dissolved in water (38 mL) and ethanol (24 mL). The solution was cooled to approx. 15 °C with an ice/water

bath. 2'-Bromoacetophenone (16.49 g, 82.8 mmol, 1.0 eq) was added in one portion; the solution turned slightly turbid. 2-Bromobenzaldehyde (15.33 g, 82.8 mmol, 1.0 eq) was added in one portion. The temperature rose to 25 °C and the solution was cooled to approx. 15 °C with an ice/water bath. The solution turned white and then yellow within a minute. Stirring was continued at room temperature for 22 h. Upon cooling in a salt/ice mixture, a viscous yellow paste formed at the bottom of the flask and stuck to the stirrer. The ethanol-water mixture was decanted from the yellow paste. Water (100 mL) was added to the yellow paste and decanted. The yellow paste was subsequently dissolved in dichloromethane (100 mL) and the organic phase was washed with water (3 x 100 mL) until the aqueous phase remained neutral. After drying ($MgSO_4$) the solvent was removed *in vacuo*, leaving **47** (28.78 g, 78.96 mmol, 95% yield) as a thick yellow liquid that turned into a pale yellow solid after prolonged standing. The product was used without further purification. Spectroscopic data corresponded to the data reported in the literature [75]. Crystals (mp 48-49 °C, lit. [75]: 43-45 °C) for X-ray diffraction were grown from ethanol or pentane but proved to be twins.

**$^1$H NMR** (400 MHz, $CDCl_3$): δ [ppm] = 7.03 (d, 1H, *J* = 16.0 Hz, H2), 7.22-7.47 (m, 5H), 7.61 (dd, 1H, *J* = 1.0, 8.0 Hz), 7.66 (dd, 1H, *J* = 0.9, 8.1 Hz), 7.69 (dd, 1H, *J* = 1.5, 7.8 Hz), 7.82 (d, 1H, *J* = 16.1 Hz, H3)

**$^{13}$C NMR** (100 MHz, $CDCl_3$): δ [ppm] = 194.4 (s, C1), 144.9 (d, C3), 140.8 (s), 134.5 (s), 133.5 (d), 133.4 (d), 131.7 (d), 131.5 (d), 129.3 (d), 128.5 (d, C2), 128.0 (d), 127.8 (d), 127.4 (d), 125.9 (s), 119.5 (s)

**MS** (ESI): accurate mass calcd for $[C_{15}H_{10}Br_2O + Na]^+$ *m/z* 386.8991, found *m/z* 386.8992

**UV** ($CH_2Cl_2$): $\lambda_{max}$ [nm] (lg ε) = 228 (4.08), 296 (4.27)

**IR** (ATR): $\tilde{\nu}$ [$cm^{-1}$] = 1643 (s), 1615 (m), 1289 (s), 1024 (m), 992 (m), 748 (s), 729 (s)

**EA**: calcd C 49.22%, H 2.75%; found C 49.34%, H 2.62%

### 3.3.5 2,3-Dibromo-1,3-bis(2-bromophenyl)propan-1-one (48)

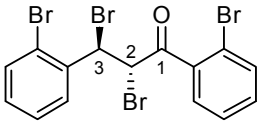


$C_{15}H_{10}Br_4O$
525.86 g/mol
(racemate)

A procedure from the literature [77] was modified as follows: In a 1L three-neck flask equipped with a reflux condenser and a 250 mL dropping funnel, **47** (28.76 g, 78.6 mmol, 1.0 eq) was dissolved in chloroform (600 mL) and heated to reflux. Bromine (12.56 g, 78.6 mmol, 1.0 eq) dissolved in chloroform (50 mL) was added dropwise over a period of 15 min. The mixture was refluxed for another 80 min. After cooling to room temperature the reaction was quenched by addition of sat. $Na_2SO_3$ solution (200 mL) and stirred for 10 min. The organic phase was separated, washed with water (3 x 250 mL) until neutrality and dried ($MgSO_4$). Removal of the solvent *in vacuo* gave a pale brown solid (40.14 g). Recrystallization from refluxing ethanol gave **48** (32.2 g, 61.3 mmol, 78% yield) as a colorless solid (mp 134 °C). The crystals were suitable for X-ray diffraction but proved disordered. The NMR signals of the aliphatic protons showed broadening because of hindered rotation. H2 and H3 were distinguished by HMBC correlation with aromatic carbon signals.

**$^1$H NMR** (400 MHz, $CDCl_3$): δ [ppm] = 5.82 (d broad, 1H, *J* = 11.2 Hz, H2), 6.22 (d broad, 1H, *J* = 11.2 Hz, H3), 7.22 (dt, 1H, *J* = 1.5, 8.0 Hz), 7.40 (m, 2H), 7.46 (dt, 1H, *J* = 1.3, 7.5 Hz), 7.62 (d, 2H, *J* = 7.5 Hz), 7.71 (dd, 1H, *J* = 1.2, 8.0 Hz), 7.78 (dd, 1H, *J* = 1.6, 7.6 Hz)

**$^{13}$C NMR** (100 MHz, $CDCl_3$): δ [ppm] = 192.0 (s, C1), 137.7 (s), 137.4 (s), 134.5 (d), 133.4 (d), 133.0 (d), 130.5 (d), 130.3 (d), 129.1 (d), 128.3 (d), 127.4 (d), 124.6 (s), 120.6 (s), 49.6 (d, C2), 47.0 (d, C3)

**MS** (EI, 70 eV): *m/z* (%) = 443 (1) $[M\text{-}Br]^+$, 368 (4), 367 (10), 366 (7), 365 (18), 364 (4), 363 (9), 287 (98), 285 (100), 185 (66), 183 (75), 157 (21), 155 (22), 102 (40), 101 (20), 76 (27), 75 (31)

**UV** ($CH_2Cl_2$): $\lambda_{max}$ [nm] (lg ε) = 228 (4.14), 255 (3.91)

**IR** (ATR): $\tilde{\nu}$ [$cm^{-1}$] = 1701 (m), 1213 (m), 976 (m), 745 (s), 578 (s), 547 (m)

**EA**: calcd C 34.26%, H 1.92%; found C 34.55%, H 1.76%

### 3.3.6 1,3-Bis-(2-bromophenyl)-propane-1,3-dione (43)

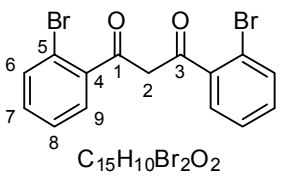


$C_{15}H_{10}Br_2O_2$
382.05 g/mol

A procedure from the literature [78] was modified as follows: In a 2L three-neck flask equipped with mechanical stirrer, reflux condenser and dropping funnel, **48** (22.87 g, 43.5 mmol, 1.0 eq) was suspended in methanol (650 mL) and stirred in an oil bath at 80 °C. A solution of KOH (10.95 g, 196.9 mmol, 4.5 eq) in methanol (200 mL) was added over 15 min in the course of which the suspension cleared up and turned into a yellow solution. After 4.5 h stirring conc. HCl (20 mL) diluted with water (180 mL) were added to the reaction mixture over 15 min; the solution turned colorless. After 8 h the heating bath was removed. Upon cooling to room temperature a colorless crystalline precipitate formed, as did brown chunks. TLC and NMR analysis indicated that both precipitates corresponded to the desired product. After cooling to 0 °C the precipitates were filtered off, washed with water und dried *in vacuo*, giving **43** as a pale yellow powder (12.78 g, 33.5 mmol, 77% yield) that was used without further purification. An analytically pure sample and single crystals (mp 76-77 °C) for X-ray diffraction were obtained by recrystallization from ethanol at 60 °C. The aqueous filtrate of the reaction mixture was extracted with dichloromethane, the organic phase separated, dried ($MgSO_4$) and the solvent removed *in vacuo*, giving a brown viscous liquid (2.83 g) that turned solid after prolonged standing. NMR analysis indicated that the mixture was composed of 65% product and 35% intermediate methyl enolether. The mixture was stored and used for a later run of the reaction.

**$^1$H NMR** (400 MHz, $CDCl_3$, enol tautomer): δ [ppm] = 6.49 (s, 1H, C=C*H*), 7.32 (m, 2H, H7), 7.41 (dt, 2H, *J* = 1.2, 7.6 Hz, H8), 7.62 (dd, 2H, *J* = 1.7, 7.7 Hz, H9), 7.66 (dd, 2H, *J* = 1.1, 8.0 Hz, H6), 15.8 (s, 1H, C=C-O*H*)

**$^{13}$C NMR** (100 MHz, $CDCl_3$, enol tautomer): δ [ppm] = 186.6 (s, 2C, C1/C3), 137.6 (s, 2C, C4), 134.0 (d, 2C, C6), 131.9 (d, 2C, C7), 130.1 (d, 2C, C9), 127.5 (d, 2C, C8), 120.4 (s, 2C, C5), 103.1 (d, 1C, C2)

**MS** (ESI): accurate mass calcd for $[C_{15}H_{10}Br_2O_2 + Na]^+$ *m/z* 402.8940, found *m/z* 402.8941

**UV** ($CH_2Cl_2$): $\lambda_{max}$ [nm] (lg ε) = 228 (4.03), 318 (4.20)

**IR** (ATR): $\tilde{\nu}$ [$cm^{-1}$] = 1590 (m), 1021 (m), 765 (s), 735 (s), 710 (m)

**EA**: calcd C 47.16%, H 2.64%; found C 47.14%, H 2.59%

### 3.3.7 2-(2-Bromobenzylidene)-1,3-bis(2-bromophenyl)propane-1,3-dione (49)

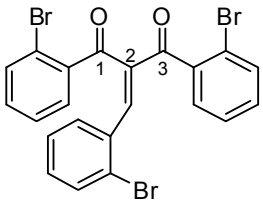


$C_{22}H_{13}Br_3O_2$
549.05 g/mol

The compound was prepared according to general procedure M2 by reacting 1,3-bis-(2-bromophenyl)-propane-1,3-dione (**43**) on a 1.11 g scale (2.90 mmol) with 2-bromobenzaldehyde (0.54 g, 2.90 mmol). The product was obtained after flash chromatography (silica, 15-20% ethyl acetate/pentane) as a yellow solid (mp 108 °C) in 85% yield (1.36 g, 2.47 mmol). Crystals grown by slow evaporation of $CDCl_3$ proved disordered.

**$^1$H NMR** (400 MHz, $CDCl_3$): δ [ppm] = 7.10 (dt, 1H, *J* = 1.7, 7.7 Hz), 7.17-7.22 (m, 2H), 7.26 (dt, 1H, *J* = 1.3, 7.6 Hz), 7.31-7.36 ("dt", 1H), 7.39-7.46 (m, 3H), 7.50 (dd, 1H, *J* = 7.6, 1.8 Hz), 7.53 (dd, 1H, *J* = 7.9, 1.3 Hz), 7.64 (dd, 1H, *J* = 8.0, 1.0 Hz), 7.69 (s, 1H, C=C*H*), 7.71 (dd, 1H, *J* = 1.8, 7.6 Hz)

**$^{13}$C NMR** (100 MHz, $CDCl_3$): δ [ppm] = 194.2 (s, C1/C3), 193.7 (s, C1/C3), 146.8 (d, C=*C*H), 141.3 (s), 139.6 (s), 137.3 (s), 134.6 (d), 133.5 (s), 133.3 (d), 133.1 (d), 132.7 (d), 131.9 (d), 131.5 (d), 131.4 (d), 130.8 (d), 128.9 (d), 127.4 (d), 127.3 (d), 127.1 (d), 124.1 (s), 121.5 (s), 119.5 (s)

**MS** (ESI, MeOH/$CHCl_3$ = 1:1): accurate mass calcd for $[C_{22}H_{13}Br_3O_2 + H]^+$ *m/z* 546.8538, found *m/z* 546.8540

**UV** ($CH_2Cl_2$): $\lambda_{max}$ [nm] (lg ε) = 228 (4.27), 296 (4.10)

**IR** (ATR): $\tilde{\nu}$ [$cm^{-1}$] = 1690 (m), 1658 (m), 1352 (m), 1027 (m), 759 (s), 723 (m)

**EA**: calcd C 48.13%, H 2.39%; found C 48.30%, H 2.36%

### 3.3.8 1,3-Bis(2-methoxyphenyl)propane-1,3-dione (44)

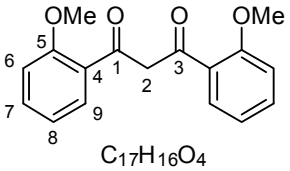


$C_{17}H_{16}O_4$
284.31 g/mol

The compound was prepared as described in the literature [73] and obtained as a pale brown solid (mp 64-65 °C) in 74% yield (Lit: 75%).

**$^1$H NMR** (400 MHz, $CDCl_3$, enol tautomer dominant): δ [ppm] = 3.93 (s, 6H, $OCH_3$), 6.99 (m, 2H, H6), 7.05 (m, 2H, H8), 7.31 (s, 1H, C=C*H*), 7.44 (ddd, 2H, *J* = 1.8, 7.3, 8.3 Hz, H7), 7.91 (dd, 2H, *J* = 1.8, 7.8 Hz, H9), 16.85 (s, 1H, C=C-O*H*)

**$^{13}$C NMR** (100 MHz, $CDCl_3$, enol tautomer dominant): δ [ppm] = 184.5 (s, 2C, C1/C3), 158.4 (s, 2C, C5), 132.8 (d, 2C, C7), 130.3 (d, 2C, C9), 125.5 (s, 2C, C4), 120.8 (d, 2C, C8), 111.7 (d, 2C, C6), 103.5 (d, C2), 55.7 (q, 2C, O*C*$H_3$)

**MS** (ESI): accurate mass calcd for $[C_{17}H_{16}O_4 + H]^+$ *m/z* 285.1121, found *m/z* 285.1121; accurate mass calcd for $[C_{17}H_{16}O_4 + Na]^+$ *m/z* 307.0941, found *m/z* 307.0940

**UV** ($CH_2Cl_2$): $\lambda_{max}$ [nm] (lg ε) = 227 (4.01), 316 (4.10, shoulder), 359 (4.30)

**IR** (ATR): $\tilde{\nu}$ [$cm^{-1}$] = 2937 (w), 2835 (w), 1599 (m), 1583 (m), 1486 (m), 1461 (m), 1241 (s), 1018 (s), 747 (s)

**EA**: calcd C 71.82%, H 5.67%; found C 71.86%, H 5.54%

### 3.3.9 2-(2-Methoxybenzylidene)-1,3-bis(2-methoxyphenyl)propane-1,3-dione (50)

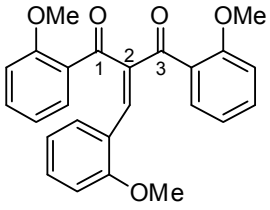


$C_{25}H_{22}O_5$
402.44 g/mol

The compound was prepared according to general procedure M1 by reacting 1,3-bis(2-methoxyphenyl)propane-1,3-dione (**44**) on a 4.45 g scale (15.7 mmol) with 2-methoxybenzaldehyde (2.14 g, 15.7 mmol). The product was obtained after flash chromatography (silica, 40% ethyl acetate/pentane) as a yellow solid (mp 162-163 °C) in 61% yield (3.84 g, 9.55 mmol). Single crystals for X-ray diffraction were obtained by slow evaporation from an ethyl acetate/pentane mixture.

**$^{1}$H NMR** (400 MHz, $CDCl_3$): δ [ppm] = 3.67 (s, 3H, OC$H_3$), 3.75 (s, 3H, OC$H_3$), 3.80 (s, 3H, OC$H_3$), 6.72-6.78 (m, 2H), 6.82-6.98 (m, 4H), 7.19-7.27 (m, 2H), 7.34-7.40 (m, 2H), 7.44 (dd, 1H, *J* = 1.7, 7.5 Hz), 7.74 (s, 1H, C=C*H*), 7.84 (dd, 1H, *J* = 1.8, 7.7 Hz)

**$^{13}$C NMR** (100 MHz, $CDCl_3$): δ [ppm] = 194.2 (s, C1/C3), 194.1 (s, C1/C3), 159.2 (s), 157.6 (s), 157.2 (s), 143.2 (s), 139.4 (d, C=*C*H), 134.1 (d), 131.8 (d), 131.5 (d), 131.2 (d), 130.8 (d), 129.9 (d), 128.6 (s), 127.2 (s), 123.4 (s), 120.3 (d), 120.2 (d), 120.1 (d), 111.6 (d), 111.2 (d), 110.6 (d), 55.5 (q, O*C*$H_3$), 55.4 (q, O*C*$H_3$), 55.1 (q, O*C*$H_3$)

**MS** (ESI): accurate mass calcd for $[C_{25}H_{22}O_5 + H]^+$ *m/z* 403.1540, found *m/z* 403.1542; accurate mass calcd for $[C_{25}H_{22}O_5 + Na]^+$ *m/z* 425.1359, found *m/z* 425.1359

**UV** ($CH_2Cl_2$): $\lambda_{max}$ [nm] (lg ε) = 228 (4.22), 251 (4.18), 292 (4.11), 324 (4.12)

**IR** (ATR): $\tilde{\nu}$ [$cm^{-1}$] = 2946 (w), 2925 (w), 2845 (w), 1658 (m), 1632 (m), 1592 (s), 1484 (m), 1465 (m), 1435 (m), 1248 (s), 1162 (m), 1017 (m), 983 (m), 749 (s)

### 3.3.10 1,3-Di-*o*-tolylpropane-1,3-dione (45)

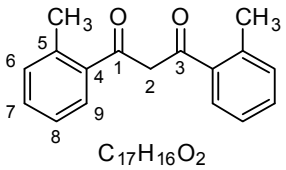

$C_{17}H_{16}O_2$
252.31 g/mol

A procedure from the literature [74] was modified as follows: methyl *o*-toluate (1.40 g, 9.31 mmol, 1.25 eq) and sodium hydride (50% dispersion in mineral oil, 0.90 g, 22.35 mmol, 3.0 eq) were dispersed in anhydrous THF (25 mL). 2'-Methylacetophenone (1.00 g, 7.45 mmol, 1.0 eq), dissolved in anhydrous THF (3 mL), was added dropwise. The mixture was refluxed for 14 h and turned increasingly brown. The solvent was removed *in vacuo*, leaving a dark red paste. The paste was dissolved in dichloromethane and poured onto ice-cooled 0.5 M HCl. The organic layer was separated and the acidic phase extracted twice with dichloromethane. The combined organic layers were washed with water and dried ($MgSO_4$). Removal of solvent *in vacuo* gave a yellow-orange oil (2.52 g) that was subjected to flash chromatography (silica, 30-40% toluene/pentane). The product eluted first and was obtained as an orange oil that solidified slowly upon standing (1.12 g, 4.44 mmol, 60% yield, lit. 50-60% yield). Washing with ethanol and drying *in vacuo* gave **45** as a colorless solid (mp 39-40 °C).

**$^1$H NMR** (400 MHz, $CDCl_3$, enol tautomer): δ [ppm] = 2.57 (s, 6H, $CH_3$), 6.22 (s, 1H, C=C*H*), 7.23-7.28 (m, 4H, H6 & H8), 7.37 ("dt", 2H, H7), 7.55 (dd, 2H, *J* = 1.2, 7.9 Hz, H9), 16.47 (s, 1H, C=C-O*H*)

**$^{13}$C NMR** (100 MHz, $CDCl_3$, enol tautomer): δ [ppm] = 189.5 (s, 2C, C1/C3), 137.1 (s, 2C, C4), 136.3 (s, 2C, C5), 131.4 (s, 2C, C6), 130.7 (s, 2C, C7), 128.4 (s, 2C, C9), 125.8 (s, 2C, C8), 101.2 (d, C2), 20.8 (q, 2C, *C*$H_3$)

**MS** (ESI): accurate mass calcd for $[C_{17}H_{16}O_2 + H]^+$ *m/z* 253.1223, found *m/z* 285.1224; accurate mass calcd for $[C_{17}H_{16}O_2 + Na]^+$ *m/z* 275.1043, found *m/z* 275.1043

**UV** ($CH_2Cl_2$): $\lambda_{max}$ [nm] (lg ε) = 228 (3.81), 258 (3.75), 320 (4.30)

**IR** (ATR): $\tilde{\nu}$ [$cm^{-1}$] = 2961 (w), 2864 (w), 1268 (m), 775 (s), 733 (s), 615 (m)

**EA**: calcd C 80.93%, H 6.39%; found C 80.88%, H 6.30%

### 3.3.11 2-(2-Methylbenzylidene)-1,3-di-*o*-tolylpropane-1,3-dione (51)

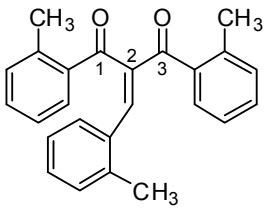


$C_{25}H_{22}O_2$
354.44 g/mol

The compound was prepared according to general procedure M1 by reacting 1,3-di-*o*-tolylpropane-1,3-dione (**45**) on a 1.12 g scale (4.44 mmol) with 2-methylbenzaldehyde (0.53 g, 4.44 mmol). The product was obtained after flash chromatography (silica, 5% ethyl acetate/pentane) as an orange oil (1.13 g, 3.19 mmol, 72% yield). Upon standing the oil turned into a pale orange solid (mp 86-87 °C). Crystals for X-ray analysis were grown by slow evaporation of $CDCl_3$ but proved to be twinned. **45** was recovered in 11% yield (0.12 g, 0.47 mmol) and kept for a later run of the reaction.

**$^1$H NMR** (400 MHz, $CDCl_3$): δ [ppm] = 7.66 (m, 1H), 7.63 (s, 1H, C=C*H*), 7.47 (m, 1H), 7.38 – 7.21 (m, 5H), 7.18 – 7.12 (m, 3H), 7.09 (d, *J* = 7.4 Hz, 1H), 7.01 (t, *J* = 7.5 Hz, 1H), 2.52 (s, 3H, C$H_3$), 2.40 (s, 3H, C$H_3$), 2.24 (s, 3H, C$H_3$)

**$^{13}$C NMR** (100 MHz, $CDCl_3$): δ [ppm] = 198.2 (s, C1/C3), 197.5 (s, C1/C3), 143.5 (d, C=*C*H), 143.3 (s), 140.1 (s), 138.2 (s), 137.3 (s), 136.8 (s), 136.4 (s), 132.7 (s), 132.2 (d), 132.1 (d), 131.1 (d), 130.8 (d), 130.5 (d), 130.4 (d), 130.1 (d), 128.8 (d), 128.0 (d), 126.0 (d), 125.6 (d), 125.3 (d), 21.3 (q, *C*$H_3$), 19.9 (q, *C*$H_3$), 19.8 (q, *C*$H_3$)

**MS** (ESI): accurate mass calcd for $[C_{25}H_{22}O_2 + H]^+$ *m/z* 355.1693, found *m/z* 355.1693; accurate mass calcd for $[C_{25}H_{22}O_2 + Na]^+$ *m/z* 377.1512, found *m/z* 377.1512

**UV** ($CH_2Cl_2$): $\lambda_{max}$ [nm] (lg ε) = 225 (4.13), 254 (4.21), 297 (4.18)

**IR** (ATR): $\tilde{\nu}$ [$cm^{-1}$] = 2960 (w), 2924 (w), 1657 (s), 1585 (m), 1251 (m), 1213 (s), 980 (m), 761 (m), 737 (s)

**EA**: calcd C 84.72%, H 6.26%; found C 84.75%, H 6.15%

## 3.4 Luche reduction of unsaturated diketones

### 3.4.1 General Procedure M3: 2-Benzylidene-1,3-diphenylpropane-1,3-diol (12)

A 100 mL Schlenk flask was charged with diketone **14** (2.02 g, 6.47 mmol), a magnetic stirring bar and $CH_2Cl_2$ (30 mL). The mixture was cooled to -78 °C in a dry ice/acetone bath under nitrogen. To this solution was added a 0.4 M solution of cerium trichloride heptahydrate in methanol (3.4 g $CeCl_3 \cdot 7\ H_2O$ in 23 mL MeOH, 9.12 mmol, 1.4 eq). After additional stirring and continued cooling, $NaBH_4$ (0.51 g, 13.6 mmol, 2.1 eq) was added; the reaction mixture started foaming. After 30 min stirring at -78 °C, the cooling bath was removed and the reaction mixture was allowed to warm up to room temperature over a 1 h period. TLC monitoring indicated complete conversion; the diols can be easily recognized by TLC analysis because of their bright red color upon staining in ceric ammonium molybdate solution. The reaction was diluted with ether (50 mL) and quenched by the addition of 0.5 M HCl (30 mL). The mixture was allowed to stir for 20 min and the phases were separated. The aqueous layer was extracted with ether (3 × 30 mL) and the combined organic layers were washed with brine, dried ($MgSO_4$) and concentrated under reduced pressure. The diastereomers were separated by flash chromatography (silica, 2-3% ethyl acetate/chloroform) with 92% combined yield (1.89 g, 5.97 mmol). Occasionally a faint green color was observed in the product despite purity by NMR analysis. The color was removed through a second process of column chromatography with an appropriate mixture of ethyl acetate/pentane ($R_f \approx 0.3$). In our experience removal of this colored impurity was essential for an optimal yield in the subsequent cyclodehydration.

2-Benzylidene-1,3-diphenylpropane-*cis*-1,3-diol (*syn*-**12**, racemic)[a]

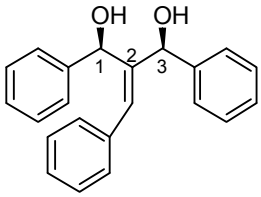


$C_{22}H_{20}O_2$
316.39 g/mol
(racemate)

Flash chromatography gave *syn*-**12** (0.77 g, 2.43 mmol, 37% yield) as a colorless solid (mp 108-109 °C). Single crystals for X-ray diffraction were obtained by recrystallization from refluxing ethanol. The NMR signals of H1 and H3 were assigned via NOE with C=C-*H*. Exchange of the alcoholic protons with $D_2O$ was demonstrated for a $^1$H NMR measurement in deuterated DMSO.

**$^1$H NMR** (400 MHz, $CDCl_3$): δ [ppm] = 2.24 (s, broad, 2H, O*H*), 5.31 (s, 1H, H3), 5.90 (d, 1H, *J* = 5.2 Hz, H1), 7.00 (s, 1H, C=C*H*), 7.19-7.34 (m, 15H)

**$^{13}$C NMR** (100 MHz, $CDCl_3$): δ [ppm] = 143.6 (s), 142.9 (s), 142.1 (s), 136.3 (s), 130.3 (d, C=*C*H), 128.7 (d, 2C), 128.6 (d, 2C), 128.4 (d, 2C), 128.3 (d, 2C), 127.8 (d), 127.3 (d), 127.1 (d), 127.0 (d, 2C), 125.8 (d, 2C), 74.1 (d, C3), 71.1 (d, C1)

**$^1$H NMR** (400 MHz, DMSO-$d_6$) δ [ppm] = 5.10 (d, *J* = 4.7 Hz, 1H, H1/H3), 5.26 (d, *J* = 4.7 Hz, 1H, OH; exchange with $D_2O$), 5.43 (d, *J* = 4.8 Hz, 1H, OH; exchange with $D_2O$), 5.72 (d, *J* = 4.8 Hz, 1H, H1/H3), 6.91 (s, 1H, C=C*H*), 7.15-7.26 (m, 3H), 7.26-7.33 (m, 8H), 7.33-7.39 (m, 2H), 7.41-7.48 (m, 2H)

**MS** (ESI): accurate mass calcd for $[C_{22}H_{20}O_2 + Na]^+$ *m/z* 339.1356, found *m/z* 339.1354

**UV** ($CH_2Cl_2$): $\lambda_{max}$ [nm] (lg ε) = 230 (4.07), 249 (4.17)

**IR** (ATR): $\tilde{\nu}$ [$cm^{-1}$] = 3299 (br), 3024 (w), 1007 (s), 767 (m), 743 (m), 695 (s), 541 (m)

**EA**: calcd C 83.51%, H 6.37%; found C 83.67%, H 6.38%

**$R_f$** (10% ethyl acetate/chloroform): 0.54

[a] The ratio of the diastereomeric diols refers to a run that was performed with 60 min at -78 °C and 2.5 eq $NaBH_4$.

2-Benzylidene-1,3-diphenylpropane-*anti*-1,3-diol (*anti*-**12**, racemic)[b]

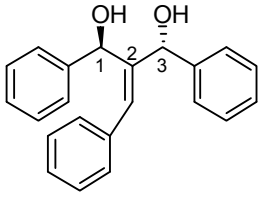


$C_{22}H_{20}O_2$
316.39 g/mol
(racemate)

Flash chromatography gave *anti*-**12** (1.12 g, 3.53 mmol, 55% yield) as a pale yellow oil that turned into a colorless solid after prolonged standing (mp 98-99 °C). Single crystals for X-ray diffraction were obtained by slow diffusion of an isopropanol/pentane mixture. The NMR signals of H1 and H3 were assigned via NOE with C=C-*H*. Exchange of the alcoholic protons with $D_2O$ was demonstrated for a $^1$H NMR measurement in deuterated DMSO.

**$^1$H NMR** (400 MHz, $CDCl_3$): δ [ppm] = 3.13 (s, 1H, C3-O*H*), 3.98 (d, 1H, *J* = 6.9 Hz, C1-O*H*), 5.28 (s, 1H, H3), 5.94 (d, 1H, *J* = 6.5 Hz, H1), 6.21 (s, 1H, C=C*H*), 7.20-7.39 (m, 15H, Ph)

**$^{13}$C NMR** (100 MHz, $CDCl_3$): δ [ppm] = 143.5 (s), 142.5 (s), 141.3 (s), 136.1 (s), 132.8 (d, C=*C*H), 128.6 (d, 2C), 128.3 (d, 4C), 128.1 (d, 2C), 127.6 (d), 127.3 (d), 127.0 (d, 3C), 125.5 (d, 2C), 74.5 (d, C3), 72.0 (d, C1)

**$^1$H NMR** (400 MHz, DMSO-$d_6$) δ [ppm] = 5.24 (d, *J* = 3.8 Hz, 1H, H1/H3), 5.42 (d, *J* = 3.8 Hz, 1H, OH; exchange with $D_2O$), 5.78 ("s", 2H, H1/H3 and OH, exchange with $D_2O$), 6.63 (s, 1H, C=C*H*), 7.02 (dt, *J* = 4.0, 2.2 Hz, 2H), 7.06-7.19 (m, 8H), 7.22-7.28 (m, 1H), 7.31-7.38 (m, 4H)

**MS** (ESI): accurate mass calcd for $[C_{22}H_{20}O_2 + Na]^+$ *m/z* 339.1356, found *m/z* 339.1355

**UV** ($CH_2Cl_2$): $\lambda_{max}$ [nm] (lg ε) = 230 (4.07, shoulder), 247 (4.13)

**IR** (ATR): $\tilde{\nu}$ [$cm^{-1}$] = 3303 (br), 3027 (w), 1006 (m), 754 (m), 696 (s), 543 (m)

**EA**: calcd C 83.51%, H 6.37%; found C 83.32%, H 6.36%

**$R_f$** (10% ethyl acetate/chloroform): 0.39

[b] The ratio of the diastereomeric diols refers to a run that was performed in 60 min at -78 °C and with 2.5 eq $NaBH_4$.

### 3.4.2 2-(2-Bromobenzylidene)-1,3-diphenylpropane-1,3-diol (32)

Diketone **30** was reduced according to general procedure M3. The reduction was performed on a 1.17 g (3.00 mmol) scale and the diastereomers were separated by flash chromatography (silica, 5% ethyl acetate/chloroform) in 89% combined yield (1.06g, 2.68 mmol). An occasional faint green color was removed through a second process of column chromatography (silica, 20% ethyl acetate/pentane).

2-(2-Bromobenzylidene)-1,3-diphenylpropane-*syn*-1,3-diol (*syn*-**32**, racemic)

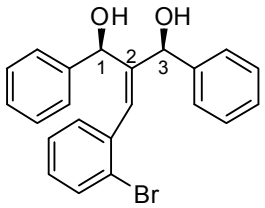


$C_{22}H_{19}BrO_2$
395.29 g/mol
(racemate)

Flash chromatography gave *syn*-**32** (0.63 g, 1.59 mmol, 53% yield) as a pale yellow oil that turned into a colorless solid after prolonged standing (mp 73 °C). The NMR signals of H1 and H3 were assigned via NOE with C=C-*H*.

**$^1$H NMR** (400 MHz, $CDCl_3$): δ [ppm] = 2.07 (d, 1H, *J* = 5.6 Hz, C1-O*H*), 2.15 (d, 1H, *J* = 3.1 Hz, C3-O*H*), 5.38 (d, 1H, *J* = 0.8 Hz, H3), 5.69 (d, 1H, *J* = 5.1 Hz, H1), 7.01 (s, 1H, C=C*H*), 7.13 (dt, 1H, *J* = 1.7, 7.7 Hz), 7.19-7.38 (m, 10H), 7.42 (m, 2H), 7.59 (dd, 1H, *J* = 1.2, 8.0 Hz)

**$^{13}$C NMR** (100 MHz, $CDCl_3$): δ [ppm] = 144.9 (s), 142.6 (s), 141.7 (s), 136.9 (s), 132.5 (d), 130.4 (d), 129.7 (d, C=*C*H), 128.9 (d), 128.6 (d, 2C), 128.2 (d, 2C), 127.9 (d), 127.2 (d), 127.15 (d), 127.11 (d, 2C), 125.6 (d, 2C), 124.1 (s, *C*-Br), 73.9 (d, C3), 71.3 (d, C1)

**MS** (ESI): accurate mass calcd for $[C_{22}H_{19}BrO_2 + Na]^+$ *m/z* 417.0461, found *m/z* 417.0461

**UV** ($CH_2Cl_2$): $\lambda_{max}$ [nm] (lg ε) = 228 (4.18), 240 (4.05, shoulder)

**IR** (ATR): $\tilde{\nu}$ [$cm^{-1}$] = 3213 (br), 1451 (m), 1022 (s), 743 (s), 725 (m), 690 (s)

**EA**: calcd C 66.85%, H 4.84%; found C 66.82%, H 4.88%

**$R_f$** (10% ethyl acetate/chloroform): 0.54

2-(2-Bromobenzylidene)-1,3-diphenylpropane-*anti*-1,3-diol (*anti*-**32**, racemic)

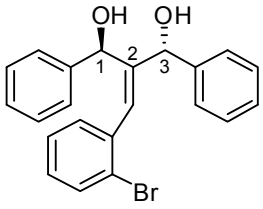


$C_{22}H_{19}BrO_2$
395.29 g/mol
(racemate)

Flash chromatography gave *anti*-**32** (0.43 g, 1.09 mmol, 36% yield) as a colorless solid (mp 124-126 °C). Single crystals for X-ray diffraction were obtained by recrystallization from refluxing ethanol. The NMR signals of H1 and H3 were assigned via NOE with C=C-*H*.

**$^1$H NMR** (400 MHz, $CDCl_3$): δ [ppm] = 2.84 (d, 1H, *J* = 3.3 Hz, C3-O*H*), 3.83 (d, 1H, *J* = 7.3 Hz, C1-O*H*), 5.34 (d, 1H, *J* = 0.9 Hz, H3), 5.72 (d, 1H, *J* = 7.0 Hz, H1), 6.13 (s, 1H, C=C*H*), 7.12 (dt, 1H, *J* = 1.6, 7.7 Hz), 7.23-7.40 (m, 11H), 7.46 (dd, 1H, *J* = 1.2, 7.6 Hz), 7.54 (dd, 1H, *J* = 1.1, 8.0 Hz)

**$^{13}$C NMR** (100 MHz, $CDCl_3$): δ [ppm] = 144.1 (s), 142.2 (s), 141.1 (s), 136.8 (s), 132.6 (d, C=*C*H), 132.4 (d), 130.5 (d), 129.0 (d), 128.3 (d, 2C), 128.2 (d, 2C), 127.7 (d), 127.2 (d), 127.0 (d), 126.9 (d, 2C), 125.4 (d, 2C), 124.1 (s, *C*-Br), 74.5 (d, C3), 72.3 (d, C1)

**MS** (ESI): accurate mass calcd for $[C_{22}H_{19}BrO_2 + Na]^+$ *m/z* 417.0461, found *m/z* 417.0462

**UV** ($CH_2Cl_2$): $\lambda_{max}$ [nm] (lg ε) = 228 (4.16), 240 (4.02, shoulder)

**IR** (ATR): $\tilde{\nu}$ [$cm^{-1}$] = 3456 (w), 3307 (br), 1043 (m), 1009 (m), 753 (s), 723 (m), 699 (s)

**$R_f$** (10% ethyl acetate/chloroform): 0.38

### 3.4.3 2-(2-Methoxybenzylidene)-1,3-diphenylpropane-1,3-diol (33)

Diketone **31** was reduced according to general procedure M3. The reduction was performed on a 3.2 g scale (9.46 mmol) and the diastereomers were separated by flash chromatography (silica, 10-15% ethyl acetate/chloroform) in 89% combined yield (2.92 g, 8.43 mmol).

2-(2-Methoxybenzylidene)-1,3-diphenylpropane-*syn*-1,3-diol (*syn*-**33**, racemic)

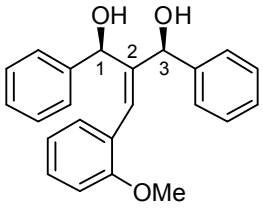


$C_{23}H_{22}O_3$
346.42 g/mol
(racemate)

Flash chromatography gave *syn*-**33** as a colorless solid (mp 79-80 °C) in 16% yield (0.54 g, 1.56 mmol). Single crystals for X-ray diffraction were obtained by recrystallization from refluxing ethanol. The NMR signals of H1 and H3 were assigned via NOE with C=C-*H*.

**$^1$H NMR** (400 MHz, $CDCl_3$): δ [ppm] = 2.15 (s, 1H, C3-O*H*), 2.22 (d, 1H, *J* = 5.0 Hz, C1-O*H*), 3.83 (s, 3H, O$CH_3$), 5.31 (s, 1H, H3), 5.76 (d, 1H, *J* = 4.3 Hz, H1), 6.88-6.93 (m, 2H), 7.05 (s, 1H, C=C*H*), 7.16-7.34 (m, 10H), 7.37-7.41 (m, 2H)

**$^{13}$C NMR** (100 MHz, $CDCl_3$): δ [ppm] = 157.0 (s), 144.2 (s), 143.1 (s), 141.9 (s), 129.9 (d), 128.8 (d), 128.4 (d, 2C), 128.1 (d, 2C), 127.6 (d), 127.0 (d, 2C), 126.8 (d), 126.1 (d, C=*C*H), 125.7 (d, 2C), 125.5 (s, *C*-$OCH_3$), 120.5 (d), 110.8 (d), 73.9 (d, C3), 71.5 (d, C1), 55.6 (q, O*C*$H_3$)

**MS** (ESI): accurate mass calcd for $[C_{23}H_{22}O_3 + Na]^+$ *m/z* 369.1461, found *m/z* 369.1460

**UV** ($CH_2Cl_2$): $\lambda_{max}$ [nm] (lg ε) = 228 (4.14), 249 (4.01), 286 (3.63)

**IR** (ATR): $\tilde{\nu}$ [$cm^{-1}$] = 3282 (br), 1488 (m), 1458 (m), 1249 (s), 1047 (m), 1024 (s), 1009 (s), 753 (s), 696 (s)

**EA**: calcd C 79.74%, H 6.40%; found C 79.82%, H 6.37%

**$R_f$** (30% ethyl acetate/chloroform): 0.65

2-(2-Methoxybenzylidene)-1,3-diphenylpropane-*anti*-1,3-diol (*anti*-**33**, racemic)

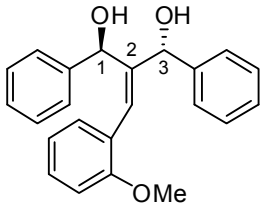


$C_{23}H_{22}O_3$
346.42 g/mol
(racemate)

Flash chromatography gave *anti*-**33** in 73% yield (2.38 g, 6.87 mmol) as a sticky, partially solid oil (mp < 45 °C). The NMR signals of H1 and H3 were assigned via NOE with C=C-*H*.

**$^1$H NMR** (400 MHz, $CDCl_3$): δ [ppm] = 2.98 (d, 1H, *J* = 3.3 Hz, C3-O*H*), 3.74-3.76 ("d", 1H, C1-O*H*), 3.76 (s, 3H, O$CH_3$), 5.31 (d, 1H, *J* = 2.3 Hz, H3), 5.82 (d, 1H, *J* = 6.3 Hz, H1), 6.26 (s, 1H, C=C*H*), 6.84 (d, 1H, *J* = 8.3 Hz), 6.90 (dt, 1H, *J* = 0.9, 7.5 Hz), 7.20-7.35 (m, 10H), 7.37-7.41 (m, 2H)

**$^{13}$C NMR** (100 MHz, $CDCl_3$): δ [ppm] = 157.0 (s), 143.8 (s), 142.3 (s), 141.6 (s), 130.1 (d), 129.0 (d, C=*C*H), 128.9 (d), 128.2 (d, 2C), 128.1 (d, 2C), 127.4 (d), 127.0 (d, 2C), 126.8 (d), 125.6 (d, 2C), 125.4 (s, *C*-$OCH_3$), 120.5 (d), 110.7 (d), 74.6 (d, C3), 72.5 (d, C1), 55.5 (q, O*C*$H_3$)

**MS** (ESI): accurate mass calcd for $[C_{23}H_{22}O_3 + Na]^+$ *m/z* 369.1461, found *m/z* 369.1460

**UV** ($CH_2Cl_2$): $\lambda_{max}$ [nm] (lg ε) = 228 (4.11), 248 (3.99), 287 (3.62)

**IR** (ATR): $\tilde{\nu}$ [$cm^{-1}$] = 3332 (br), 1489 (m), 1452 (m), 1244 (s), 1019 (s), 751 (s), 697 (s)

**$R_f$** (30% ethyl acetate/chloroform): 0.54

### 3.4.4 2-(2-Bromobenzylidene)-1,3-bis(2-bromophenyl)propane-1,3-diol (52)

Diketone **49** was reduced according to general procedure M3 *with 3.0 eq $CeCl_3$ and 3.0 eq $NaBH_4$*. The reduction was performed on a 2.0 g scale (20.3 mmol) and the diastereomers were separated by flash chromatography (silica, 0-10% ethyl acetate/chloroform) in 88% combined yield (9.87 g, 17.8 mmol). An occasional faint rose color was removed through a second process of column chromatography (silica, 10% ethyl acetate/pentane).

2-(2-Bromobenzylidene)-1,3-bis(2-bromophenyl)propane-*syn*-1,3-diol (*syn*-**52**, racemic)

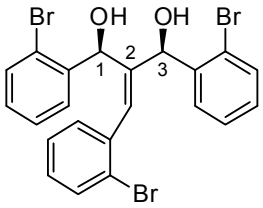


$C_{22}H_{17}Br_3O_2$
553.08 g/mol
(racemate)

Flash chromatography gave *syn*-**52** in 29% yield (3.25 g, 5.88 mmol) as a pale yellow oil that turned solid after prolonged standing (mp 111-112 °C). The NMR signals of H1 and H3 were assigned via NOE with C=C-*H*.

**$^1$H NMR** (400 MHz, $CDCl_3$): δ [ppm] = 2.27 (d, 1H, *J* = 4.2 Hz, C3-O*H*), 2.65 (d, 1H, *J* = 4.7 Hz, C1-O*H*), 5.76 (d, 1H, *J* = 4.0 Hz, H3), 5.89 (d, 1H, *J* = 4.6 Hz, H1), 6.63 (s, 1H, C=C*H*), 7.05-7.12 (m, 2H), 7.16-7.24 (m, 2H), 7.28 (dt, 1H, *J* = 1.2, 7.6 Hz), 7.35-7.41 (m, 2H), 7.44 (dd, 1H, *J* = 1.2, 7.9 Hz), 7.49 (dd, 1H, *J* = 1.2, 8.0 Hz), 7.55 (dd, 1H, *J* = 1.2, 8.0 Hz), 7.61 (dd, 1H, *J* = 1.7, 7.8 Hz), 7.77 (dd, 1H, *J* = 1.7, 7.8 Hz)

**$^{13}$C NMR** (100 MHz, $CDCl_3$): δ [ppm] = 141.6 (s), 140.7 (s), 140.6 (s), 136.6 (s), 132.9 (d, C=*C*H), 132.8 (d), 132.6 (d), 132.4 (d), 130.2 (d), 129.4 (d), 129.3 (d), 129.1 (d), 128.9 (d), 128.7 (d), 127.7 (d), 127.6 (d), 127.0 (d), 123.7 (s, *C*-Br), 123.3 (s, *C*-Br), 122.8 (s, *C*-Br), 72.6 (d, C3), 71.7 (d, C1)

**MS** (ESI): accurate mass calcd for $[C_{22}H_{17}Br_3O_2 + Na]^+$ *m/z* 572.8671, found *m/z* 572.8674

**UV** ($CH_2Cl_2$): $\lambda_{max}$ [nm] (lg ε) = 228 (4.27), 244 (4.02, shoulder)

**IR** (ATR): $\tilde{\nu}$ [$cm^{-1}$] = 3465 (w), 3370 (broad), 1431 (m), 1038 (s), 1005 (s), 752 (s), 588 (m)

**$R_f$** (10% ethyl acetate/chloroform): 0.67

2-(2-Bromobenzylidene)-1,3-bis(2-bromophenyl)propane-*anti*-1,3-diol (*anti*-**52**, racemic)

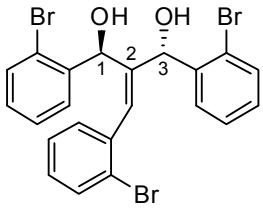


$C_{22}H_{17}Br_3O_2$
553.08 g/mol
(racemate)

Flash chromatography gave *anti*-**52** as a colorless solid (mp 166-167 °C) in 59% yield (6.62 g, 12.0 mmol). Single crystals for X-ray diffraction were obtained by recrystallization from refluxing ethanol. The NMR signals of H1 and H3 were assigned via NOE with C=C-*H*.

**$^1$H NMR** (400 MHz, $CDCl_3$): δ [ppm] = 2.78 (d, 1H, *J* = 3.4 Hz, C3-O*H*), 3.92 (d, 1H, *J* = 7.4 Hz, C1-O*H*), 5.48 (d, 1H, *J* = 2.8 Hz, H3), 5.85 (d, 1H, *J* = 7.4 Hz, H1), 6.11 (s, 1H, C=C*H*), 7.11-7.17 (m, 3H), 7.32-7.36 (m, 2H), 7.38 (dt, 1H, *J* = 1.1, 7.5 Hz), 7.44 (dd, 1H, *J* = 1.2, 7.9 Hz), 7.48 (dd, 1H, *J* = 1.2, 8.0 Hz), 7.53 (dd, 1H, *J* = 1.2, 8.0 Hz), 7.68 (dd, 1H, *J* = 1.7, 7.8 Hz), 7.72 (dd, 1H, *J* = 1.5, 7.6 Hz), 7.88 (dd, 1H, *J* = 1.4, 7.7 Hz)

**$^{13}$C NMR** (100 MHz, $CDCl_3$): δ [ppm] = 140.7 (s), 139.9 (s), 138.4 (s), 136.4 (s), 133.9 (d, C=*C*H), 132.7 (d), 132.6 (d), 132.5 (d), 130.7 (d), 129.3 (d), 129.1 (d), 129.0 (d), 128.9 (d), 127.5 (d), 127.4 (d), 127.1 (d), 127.0 (d), 124.6 (s, *C*-Br), 122.9 (s, *C*-Br), 122.8 (s, *C*-Br), 73.8 (d, C3), 72.7 (d, C1)

**MS** (ESI): accurate mass calcd for $[C_{22}H_{17}Br_3O_2 + Na]^+$ *m/z* 572.8671, found *m/z* 572.8671

**UV** ($CH_2Cl_2$): $\lambda_{max}$ [nm] (lg ε) = 229 (4.29), 248 (4.10)

**IR** (ATR): $\tilde{\nu}$ [$cm^{-1}$] = 3286 (br), 1433 (m), 1012 (s), 749 (s), 723 (m), 669 (m)

**EA**: calcd C 47.78%, H 3.10%; found C 47.73%, H 2.96%

**$R_f$** (10% ethyl acetate/chloroform): 0.51

### 3.4.5 2-(2-Methoxybenzylidene)-1,3-bis(2-methoxyphenyl)propane-1,3-diol (53)

Diketone **50** was reduced according to general procedure M3 *with 2.1 eq $CeCl_3$*. The reduction was performed on a 2.0 g scale (4.97 mmol) and the diastereomers were separated by flash chromatography (silica, 10-15% ethyl acetate/chloroform) in 74% combined yield (1.50 g, 3.68 mmol). An occasional faint green color was removed through a second process of column chromatography (silica, 25% ethyl acetate/pentane).

2-(2-Methoxybenzylidene)-1,3-bis(2-methoxyphenyl)propane-1,3-diol (**53**, 1st diastereomer, racemic)

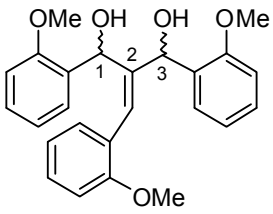


$C_{25}H_{26}O_5$
406.47 g/mol
(1st diastereomer)

Flash chromatography gave the first diastereomer of **53** as a colorless solid (mp 41-43 °C) in 30% yield (0.60 g, 1.49 mmol). The NMR signals of H1 and H3 were assigned via NOE with C=C-*H*.

**$^1$H NMR** (400 MHz, $CDCl_3$): δ [ppm] = 2.37 (d, 1H, *J* = 4.1 Hz, C3-O*H*), 3.41 (d, 1H, *J* = 4.7 Hz, C1-O*H*), 3.63 (s, 3H, OC$H_3$), 3.79 (s, 3H, OC$H_3$), 3.89 (s, 3H, OC$H_3$), 5.65 (d, 1H, *J* = 3.9 Hz, H3), 5.91 (d, 1H, *J* = 4.6 Hz, H1), 6.73 (s, 1H, C=C*H*), 6.77 (dd, 1H, *J* = 0.8, 8.2 Hz), 6.82-6.89 (m, 3H), 6.93-7.00 (m, 2H), 7.17-7.24 (m, 3H), 7.27 (dd, 1H, *J* = 1.0, 7.5 Hz), 7.59-7.63 (m, 2H)

**$^{13}$C NMR** (100 MHz, $CDCl_3$): δ [ppm] = 156.9 (s), 156.4 (s), 155.7 (s), 143.2 (s), 131.7 (s), 130.6 (s), 129.9 (d), 128.3 (d), 128.2 (d), 128.1 (d), 127.4 (d, C=*C*H), 127.3 (d), 127.2 (d), 126.2 (s), 120.8 (d), 120.5 (d), 120.1 (d), 110.4 (d), 110.3 (d), 110.1 (d), 68.3 (d, C3), 68.2 (d, C1), 55.4 (q, O*C*$H_3$), 55.4 (q, O*C*$H_3$), 55.0 (q, O*C*$H_3$)

**MS** (ESI): accurate mass calcd for $[C_{25}H_{26}O_5 + Na]^+$ *m/z* 429.1672, found *m/z* 429.1673

**UV** ($CH_2Cl_2$): $\lambda_{max}$ [nm] (lg ε) = 229 (4.22), 251 (3.99), 277 (3.89)

**IR** (ATR): $\tilde{\nu}$ [$cm^{-1}$] = 3482 (br), 2938 (w), 2835 (w), 1487 (m), 1460 (m), 1237 (s), 1021 (s), 749 (s)

**$R_f$** (30% ethyl acetate/chloroform): 0.62

2-(2-Methoxybenzylidene)-1,3-bis(2-methoxyphenyl)propane-1,3-diol (**53**, 2nd diastereomer, racemic)

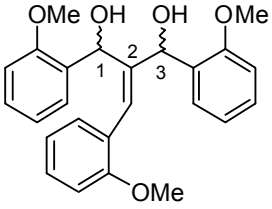


$C_{25}H_{26}O_5$
406.47 g/mol
(2nd diastereomer)

Flash chromatography gave the second diastereomer of **53** as a colorless solid (mp 46-47 °C) in 44% yield (0.90 g, 2.19 mmol). The NMR signals of H1 and H3 were assigned via NOE with C=C-*H*.

**$^1$H NMR** (400 MHz, $CDCl_3$): δ [ppm] = 3.64 (s, 3H, OC*H*$_3$), 3.72 (s, 3H, OC*H*$_3$), 3.73 (s, 3H, OC*H*$_3$), 3.81 (d, 1H, *J* = 3.6 Hz, C3-O*H*), 4.01 (d, 1H, *J* = 4.5 Hz, C1-O*H*), 5.73 (d, 1H, *J* = 3.1 Hz, H3), 6.00 (d, 1H, *J* = 4.3 Hz, H1), 6.36 (s, 1H, C=C*H*), 6.74 (dd, 1H, *J* = 0.8, 8.2 Hz), 6.78-6.86 (m, 3H), 6.93-6.99 (m, 2H), 7.15-7.24 (m, 4H), 7.54 (dd, 1H, *J* = 1.7, 7.6 Hz), 7.69 (dd, 1H, *J* = 1.1, 7.6 Hz)

**$^{13}$C NMR** (100 MHz, $CDCl_3$): δ [ppm] = 157.0 (s), 156.7 (s), 156.4 (s), 141.5 (s), 130.2 (s), 130.0 (s), 129.9 (d), 128.4 (d), 128.3 (d), 128.2 (d), 128.2 (d), 127.4 (d), 126.5 (d, C=*C*H), 126.3 (s), 120.5 (d), 120.3 (d), 120.2 (d), 110.5 (d), 110.2 (d), 109.8 (d), 69.8 (d, C1), 69.7 (d, C3), 55.4 (q, O*C*H$_3$), 55.1 (q, O*C*H$_3$), 54.9 (q, O*C*H$_3$)

**MS** (ESI): accurate mass calcd for $[C_{25}H_{26}O_5 + Na]^+$ *m/z* 429.1672, found *m/z* 429.1673

**UV** ($CH_2Cl_2$): $\lambda_{max}$ [nm] (lg ε) = 228 (4.21), 249 (4.01), 279 (3.89)

**IR** (ATR): $\tilde{\nu}$ [$cm^{-1}$] = 3384 (br), 2935 (w), 2834 (w), 1488 (m), 1459 (m), 1239 (s), 1023 (s), 749 (s)

**$R_f$** (30% ethyl acetate/chloroform): 0.51

### 3.4.6 2-(2-Methylbenzylidene)-1,3-di-*o*-tolylpropane-1,3-diol (54)

Diketone **51** was reduced according to general procedure M3 *with 2.1 eq $CeCl_3$ and 3.0 eq $NaBH_4$*. The reduction was performed on a 2.76 g scale (7.79 mmol) and the diastereomers were separated by flash chromatography (silica, 1-2% ethyl acetate/chloroform) in 82% combined yield (2.27 g, 6.34 mmol). An occasional faint green color in the products was removed through a second process of column chromatography (silica, 10% ethyl acetate/pentane).

2-(2-Methylbenzylidene)-1,3-di-o-tolylpropane-*syn*-1,3-diol (*syn*-**54**, racemic)

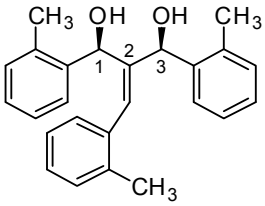


$C_{25}H_{26}O_2$
358.47 g/mol
(racemate)

Flash chromatography gave *syn*-**54** (1.16 g, 3.24 mmol, 42% yield) as a colorless solid (mp 135 °C). Crystals for X-ray diffraction were obtained by recrystallization from refluxing ethanol. The NMR signals of H1 and H3 were assigned via NOE with C=C-*H*.

**$^1$H NMR** (400 MHz, $CDCl_3$): δ [ppm] = 7.57 (dd, *J* = 7.5, 1.6 Hz, 1H), 7.46 (dd, *J* = 7.4, 1.5 Hz, 1H), 7.40 (d, *J* = 6.7 Hz, 1H), 7.30 – 7.12 (m, 8H), 7.07 (dd, *J* = 4.2, 3.2 Hz, 1H), 6.82 (s, 1H, C=C*H*), 5.78 (d, *J* = 5.7 Hz, 1H, H1), 5.49 (d, *J* = 3.3 Hz, 1H, H3), 2.23 (s, 6H, C$H_3$), 2.04 (d, *J* = 5.7 Hz, 1H, C1-O*H*), 1.95 (s, 3H, C$H_3$), 1.60 (d, *J* = 4.2 Hz, 1H, C3-O*H*)

**$^{13}$C NMR** (100 MHz, $CDCl_3$): δ [ppm] = 141.4 (s), 140.6 (s), 140.1 (s), 136.3 (s), 136.2 (s), 135.6 (s), 135.4 (s), 130.8 (d), 130.7 (d, C=*C*H), 130.3 (d), 129.9 (d), 128.9 (d), 127.9 (d), 127.6 (d), 127.4 (d), 126.9 (d), 126.2 (d), 126.2 (d), 125.6 (d), 125.5 (d), 69.7 (d, C3), 69.5 (d, C1), 19.8 (q, *C*$H_3$), 19.0 (q, *C*$H_3$), 18.7 (q, *C*$H_3$)

**MS** (ESI): accurate mass calcd for $[C_{25}H_{26}O_2 + Na]^+$ *m/z* 381.1825, found *m/z* 381.1825

**UV** ($CH_2Cl_2$): $\lambda_{max}$ [nm] (lg ε) = 227 (4.14), 245 (4.10)

**IR** (ATR): $\tilde{\nu}$ [$cm^{-1}$] = 3566 (w), 3412 (br), 1483 (w), 1456 (w), 1030 (m), 999 (m), 746 (s), 724 (m)

**EA**: calcd C 83.76%, H 7.31%; found C 83.61%, H 7.40%

**$R_f$** (10% ethyl acetate/chloroform): 0.71

2-(2-Methylbenzylidene)-1,3-di-o-tolylpropane-*anti*-1,3-diol (*anti*-**54**, racemic)

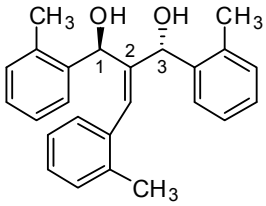


$C_{25}H_{26}O_2$
358.47 g/mol
(racemate)

Flash chromatography gave *anti*-**54** (1.11 g, 3.10 mmol, 40% yield) as a pale yellow solid (mp 158-159 °C). The NMR signals of H1 and H3 were assigned via NOE with C=C-*H*.

**$^1$H NMR** (400 MHz, $CDCl_3$): δ [ppm] = 7.84 (d, *J* = 7.6 Hz, 1H), 7.65 – 7.54 (m, 2H), 7.31 – 7.09 (m, 7H), 7.04 (d, *J* = 7.5 Hz, 2H), 6.00 (s, 1H, C=C*H*), 5.84 (d, *J* = 7.1 Hz, 1H, H1), 5.30 (d, *J* = 3.0 Hz, 1H, H3), 4.07 (d, *J* = 7.1 Hz, 1H, C1-O*H*), 2.99 (d, *J* = 3.2 Hz, 1H, C3-O*H*), 1.97 (s, 3H, C$H_3$), 1.73 (s, 3H, C$H_3$), 1.71 (s, 3H, C$H_3$).

**$^{13}$C NMR** (100 MHz, $CDCl_3$): δ [ppm] = 140.4 (s), 139.3 (s), 139.2 (s), 136.4 (s), 135.0 (s), 134.8 (s, 2C), 131.7 (d, C=*C*H), 130.2 (d), 129.9 (d), 129.8 (d), 129.3 (d), 127.9 (d), 127.4 (d), 127.2 (d), 126.7 (d), 126.0 (d), 125.8 (d), 125.8 (d), 125.3 (d), 71.5 (d, C3), 70.9 (d, C1), 19.5 (q, *C*$H_3$), 18.3 (q, *C*$H_3$), 17.9 (q, *C*$H_3$)

**MS** (ESI): accurate mass calcd for $[C_{25}H_{26}O_2 + Na]^+$ *m/z* 381.1825, found *m/z* 381.1825

**UV** ($CH_2Cl_2$): $\lambda_{max}$ [nm] (lg ε) = 228 (4.13), 244 (4.15)

**IR** (ATR): $\tilde{\nu}$ [$cm^{-1}$] = 3175 (br), 1484 (w), 1456 (w), 1016 (s), 750 (s), 725 (m)

**EA**: calcd C 83.76%, H 7.31%; found C 83.73%, H 7.46%

**$R_f$** (10% ethyl acetate/chloroform): 0.57

## 3.5 Cyclization of unsaturated diols

### 3.5.1 Tribenzotriquinacene (3)

IUPAC: 4b,8b,12b,12d-Tetrahydrodibenzo[2,3:4,5]pentaleno[1,6-*ab*]indene

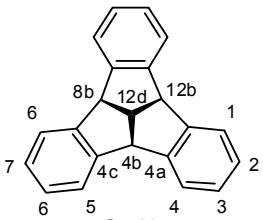


$C_{22}H_{16}$
280.36 g/mol

A procedure from the literature [26] was adapted as follows: a mixture of *syn*-**12** and *anti*-**12** (1.00 g, 3.2 mmol) was suspended in chlorobenzene (7 mL), and polyphosphoric acid (0.48 g) was added under nitrogen. The mixture was heated to 130 °C for 20 h with vigorous stirring (rpm > 1000). The mixture turned brown in the course of the reaction. Upon cooling to room temperature

**3** crystallized quantitatively as thin colorless needles (0.29 g, 32% yield). The product was filtered off, washed with acetone and dried *in vacuo*. Spectroscopic data corresponded to the data reported in the literature. Single crystals for X-ray analysis were obtained by recrystallization from refluxing toluene. Differential scanning calorimetry indicated an endothermal transition at 338-340 °C; a subsequent exothermal transition was observed at 400 °C.[c] Visual determination of the melting point indicated slow decomposition at temperatures above 322 °C and melting at 362 °C (lit. [23]: 390 °C).

**$^1$H NMR** (400 MHz, $CDCl_3$): δ [ppm] = 4.50 (q, $J$ = 9.7 Hz, 1H, H12d), 4.98 (d, $J$ = 9.7 Hz, 3H, H4b), 7.18 (AA'XX', $\underline{N} = |J_{AX}+J_{AX'}| = |J_{ortho}+J_{meta}|$ = 8.8 Hz, 6H, H2), 7.46 (AA'XX', $\underline{N} = |J_{XA}+J_{XA'}| = |J_{ortho}+J_{meta}|$ = 8.8 Hz, 6H, H1)

**$^{13}$C NMR** (100 MHz, $CDCl_3$): δ [ppm] = 145.8 (s, 6C, C4a), 127.3 (d, 6C, C2), 124.2 (d, 6C, C1), 55.5 (d, 3C, C4b), 51.0 (d, C12d)

**MS** (EI, 70 eV): accurate mass calcd for $[C_{22}H_{16}]^{+\bullet}$ *m/z* 280.1247, found *m/z* 280.1249

**UV** ($CH_2Cl_2$): $\lambda_{max}$ [nm] (lg ε) = 229 (3.89), 269 (3.55), 276 (3.59)

**IR** (ATR): $\tilde{\nu}$ [$cm^{-1}$] = 3068 (w), 3020 (w), 2900 (w), 1477 (m), 742 (s), 711 (m), 573 (m)

Determination of byproducts:

In one of the early runs a mixture of *syn*-**12** and *anti*-**12** (2.00 g, 6.3 mmol) was suspended in chlorobenzene (15 mL) and 85% orthophosphoric acid (0.95 g) was added. The mixture was heated to 130 °C for 20 h with vigorous stirring (rpm > 1000). The reflux condenser was equipped with a drying tube ($CaCl_2$). The mixture turned brown in the course of the reaction. Upon cooling to room temperature **3** crystallized quantitatively as thin colorless needles. The organic phase was carefully decanted and the precipitate was filtered off, giving **3** in 24% yield (0.42 g, 1.50 mmol). The filtrate was stripped of solvent and subjected to flash chromatography (silica, 5-10% toluene/pentane until elution of **16**, then pure chloroform to elute **17**). The first fractions were mainly composed of **16**, which was obtained in pure form by recrystallization from refluxing toluene (0.16 g, 0.57 mmol, 9% yield). The spectroscopic data corresponded to the data reported in the literature [26] and the

[c] The author thanks Martin Butschies and Prof. Sabine Laschat from the University of Stuttgart for the measurement.

structure was unambiguously confirmed by single crystal X-ray diffraction. After switching to chloroform for elution, the separation focused on the isolation of a bright yellow band that showed blue fluorescence under near-UV irradiation (366 nm). After removal of solvent a bright yellow oil was obtained (0.03 g, 0.10 mmol, 1-2% yield) that was recrystallized from refluxing toluene. The yellow crystals (mp 228-229 °C) proved disordered, but hinted at structure **17**. The analytical data supported the structural assignment and compared well with the data of parent hydrocarbon 1(*2H*)-aceanthrylenone [274] and its regioisomer 2(*1H*)-aceanthrylenone [275]. As the formation of **17** could only be explained by an oxidation processes, it was decided to run future cyclodehydrations under nitrogen.

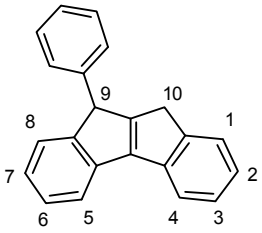


$C_{22}H_{16}$
280.36 g/mol

9-Phenyl-9,10-dihydroindeno[1,2-*a*]indene (**16**, racemic):

**$^1$H NMR** (400 MHz, $CDCl_3$): δ [ppm] = 3.43 (d, 1H, *J* = 23.2 Hz, H10), 3.53 (d, 1H, *J* = 23.2 Hz, H10'), 4.79 (s, 1H, H9), 7.11 (m, 2H), 7.18 (dt, 1H, *J* = 1.1, 7.5 Hz), 7.20-7.30 (m, 5H), 7.37 (ddt, 1H, *J* = 0.5, 1.1, 7.4 Hz), 7.40 (m, 1H), 7.48 ("d", 1H, *J* = 7.4 Hz), 7.75 ("d", 1H, *J* = 7.5 Hz), 7.79 ("d", 1H, *J* = 7.5 Hz)

**$^{13}$C NMR** (150 MHz, $CDCl_3$): δ [ppm] = 157.8 (s), 152.8 (s), 148.0 (s), 147.5 (s), 140.0 (s), 139.3 (s), 138.7 (s), 128.7 (d, 2C), 127.9 (d, 2C), 126.9 (d), 126.8 (d), 126.5 (d), 125.0 (d), 124.8 (d), 124.7 (d), 124.6 (d), 119.9 (d), 119.6 (d), 53.1 (d, C9), 34.5 (t, C10)

**MS** (EI, 70 eV): accurate mass calcd for $[C_{22}H_{16}]^{+\bullet}$ *m/z* 280.1247, found *m/z* 280.1245

**UV** ($CH_2Cl_2$): $\lambda_{max}$ [nm] (lg ε) = 235 (4.47), 265 (4.03), 284 (3.90, shoulder), 312 (3.14)

**IR** (ATR): $\tilde{\nu}$ [$cm^{-1}$] = 3024 (w), 1451 (m), 1391 (m), 771 (m), 757 (m), 724 (s), 698 (s), 642 (m), 608 (m)

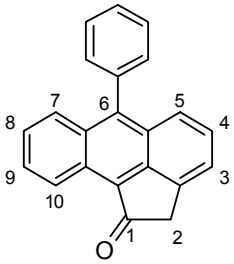


$C_{22}H_{14}O$
294.35 g/mol

6-Phenyl-1(*2*H)-aceanthrylenone (**17**):

**$^1$H NMR** (400 MHz, $CDCl_3$): δ [ppm] = 3.92 (s, 2H, H2), 7.39-7.47 (m, 4H), 7.49 (ddd, 1H, *J* = 1.3, 6.6, 8.8 Hz, H8), 7.52-7.63 (m, 4H), 7.72 (ddd, 1H, *J* = 1.2, 6.6, 8.5 Hz, H9), 7.87 ("d", 1H, *J* = 8.8 Hz, H7), 9.28 ("d", 1H, *J* = 8.6 Hz, H10)

**$^{13}$C NMR** (100 MHz, $CDCl_3$): δ [ppm] = 202.8 (s), 144.5 (s), 144.2 (s), 137.1 (s), 134.9 (s), 131.6 (s), 130.6 (d, 2C), 128.7 (d, C9), 128.5 (s), 128.4 (d, 2C), 128.1 (d), 127.7 (d, C7), 127.4 (s), 127.3 (d), 127.2 (s), 126.2 (d, C8), 124.5 (d, C10), 123.5 (d), 120.2 (d, C3), 42.3 (t, C2)

**MS** (EI, 70 eV): *m/z* (%) = 294 (100) $[M]^{\bullet+}$, 293 (8), 277 (3), 266 (20), 265 (54), 263 (27), 261 (7), 250 (2), 239 (8), 237 (5), 235 (2); accurate mass calcd for $[C_{22}H_{14}O]^{\bullet+}$ *m/z* 294.1039, found *m/z* 294.1038

**UV** ($CH_2Cl_2$): $\lambda_{max}$ [nm] (lg ε) = 234 (4.44), 268 (4.91), 407 (4.05), 429 (4.02)

**IR** (ATR): $\tilde{\nu}$ [$cm^{-1}$] = 1683 (s), 758 (s), 702 (s), 672 (m), 582 (m)

## 3.5.2 General Procedure M4: 1-Bromotribenzotriquinacene (34, racemic)

IUPAC: 1-Bromo-4b,8b,12b,12d-tetrahydro-dibenzo[2,3:4,5]pentaleno[1,6-*ab*]indene

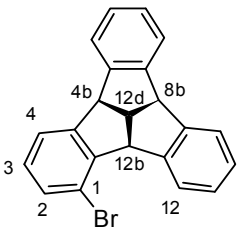


$C_{22}H_{15}Br$
359.26 g/mol
(racemate)

A mixture of *syn*-**32** and *anti*-**32** (1.00 g, 2.53 mmol) was suspended in chlorobenzene (6 mL) and polyphosphoric acid (0.48 g) was added under nitrogen. The mixture was heated to 130 °C for 20 h with vigorous stirring (rpm > 1000). The mixture turned brown in the course of the reaction. After cooling, the reaction mixture was washed twice with water, the organic layer was separated and the aqueous layer extracted twice with dichloromethane. The combined organic layers were dried ($MgSO_4$) and the solvent was evaporated under reduced pressure, leaving a brown foam (0.88 g). The complex reaction mixture was subjected to dry-column flash chromatography (short column, 5-20% toluene/pentane) to separate the nonpolar products from the brown colored components. A colorless solid was obtained (0.38 g) which was recrystallized twice from boiling toluene. The combined yield of **34**

amounted to 0.25 g (0.70 mmol, 27% yield) as colorless needles (decomp 217 °C, melting 224 °C).

**$^{1}$H NMR** (400 MHz, $CDCl_3$): δ [ppm] = 4.48 (q, 1H, *J* = 9.8 Hz, H12d), 4.93 (d, 1H, *J* = 9.5 Hz, H8b), 4.94 (d, 1H, *J* = 10.2 Hz, H4b), 5.20 (d, 1H, *J* = 9.6 Hz, H12b), 7.05 (t, 1H, *J* = 7.7 Hz, H3), 7.15 (dt, 1H, *J* = 1.4, 7.5 Hz, H11), 7.17-7.23 (m, 3H), 7.37 (d, 1H, *J* = 7.9 Hz, H2), 7.40 (d, 1H, *J* = 7.5 Hz, H4), 7.42-7.51 (m, 3H), 8.25 (d, 1H, *J* = 7.8 Hz, H12)

**$^{13}$C NMR** (100 MHz, $CDCl_3$): δ [ppm] = 148.2 (s), 146.5 (s), 146.4 (s), 145.9 (s), 145.0 (s), 144.2 (s), 131.3 (d, C2), 129.1 (d, C3), 127.8 (d), 127.7 (d), 127.4 (d), 127.1 (d, C11), 126.6 (d, C12), 124.3 (d), 124.2 (d), 124.1 (d), 123.5 (d, C4), 119.5 (s), 56.8 (d, C12b), 56.6 (d, C4b), 55.4 (d, C8b), 50.6 (d, C12d)

**MS** (EI, 70 eV): *m/z* (%) = 358 (59) $[M]^{\bullet+}$, 357 (7), 283 (5), 282 (5), 281 (8), 279 (100), 280 (23), 279 (100), 278 (30), 277 (32), 276 (40), 275 (5), 274 (11), 129 (18), 138 (32); accurate mass calcd for $[C_{22}H_{15}Br]^{+\bullet}$ *m/z* 358.0352, found *m/z* 358.0348

**UV** ($CH_2Cl_2$): $\lambda_{max}$ [nm] (lg ε) = 229 (4.17), 269 (3.43), 276 (344)

**IR** (ATR): $\tilde{\nu}$ [$cm^{-1}$] = 3064 (w), 3021 (w), 2900 (w), 1477 (m), 1442 (m), 1114 (m), 905 (m), 742 (s), 593 (m), 577 (m)

**EA**: calcd C 73.55%, H 4.21%; found C 73.35%, H 4.32%

Determination of byproducts

The mother liquor contains a mixture of regioisomeric monobrominated 9-phenyl-9,10-dihydroindeno[1,2-a]indenes (0.12 g, 0.33 mmol, 13% yield) that could not be separated.

### 3.5.3 1-Methoxytribenzotriquinacene (35, racemic)

IUPAC: 1-Methoxy-4b,8b,12b,12d-tetrahydrodibenzo-[2,3:4,5]pentaleno-[1,6-*ab*]-indene

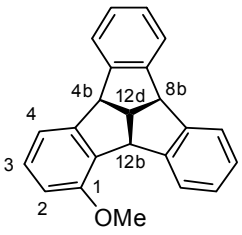


$C_{23}H_{18}O$
310.39 g/mol
(racemate)

The compound was prepared according to general procedure M4 by reacting a mixture of *syn*-**33** and *anti*-**33** (0.96 g, 2.74 mmol). Dry-column flash chromatography was performed with 20-30% toluene/pentane. A colorless solid was obtained (0.17 g) which was recrystallized twice from boiling toluene. The combined yield of **35** amounted to 0.11 g (0.35 mmol, 13% yield) as a colorless solid (decomp 219-222 °C, melting 232 °C).

**$^1$H NMR** (400 MHz, $CDCl_3$): δ [ppm] = 3.90 (s, 3H, OC*H*$_3$), 4.45 (q, 1H, *J* = 9.7 Hz, H12d), 4.91 (“t”, 2H, *J* = 10.1 Hz, H4b/H8b), 5.14 (d, 1H, *J* = 9.7 Hz, H12b), 6.68 (d, 1H, *J* = 8.0 Hz, H2), 7.08 (d, 1H, *J* = 7.4 Hz), 7.11-7.19 (m, 5H), 7.42-7.47 (m, 3H), 7.80 (d, 1H, *J* = 7.1 Hz, H12)

**$^{13}$C NMR** (100 MHz, $CDCl_3$): δ [ppm] = 156.2 (s), 147.8 (s), 146.1 (s), 145.9 (s), 145.7 (s), 145.4 (s), 133.2 (s), 128.9 (d), 127.3 (d), 127.2 (d), 127.2 (d), 127.0 (d), 126.6 (d), 124.2 (d, 2C), 123.9 (d), 116.5 (d), 108.6 (d), 56.1 (d, C4b/8b), 55.6 (d, C4b/8b), 55.0 (q, O*C*H$_3$), 54.1 (d, C12b), 51.3 (d, C12d)

**MS** (EI, 70 eV): *m/z* (%) = 310 (100) $[M]^{\bullet+}$, 309 (17), 295 (14), 279 (29), 278 (9), 277 (10), 276 (10), 265 (17), 263 (10), 252 (7), 233 (13); accurate mass calcd for $[C_{23}H_{18}O]^{\bullet+}$ *m/z* 310.1352, found *m/z* 310.1346

**UV** ($CH_2Cl_2$): $\lambda_{max}$ [nm] (lg ε) = 229 (4.08), 268 (3.51), 275 (3.50)

**IR** (ATR): $\tilde{\nu}$ [$cm^{-1}$] = 2899 (w), 2834 (w), 1470 (m), 1254 (m), 1065 (m), 739 (s)

**EA**: calcd C 89.00%, H 5.82%; found C 88.79%, H 5.82%

Determination of byproducts

The mother liquor contains a mixture of regioisomeric methoxy-substituted 9-phenyl-9,10-dihydroindeno[1,2-a]indenes (0.06 g, 0.19 mmol, 7% yield) that could not be separated.

### 3.5.4 1,5,9-Tribromotribenzotriquinacene (55, racemic)

IUPAC: 1,5,9-Tribromo-4b,8b,12b,12d-tetrahydrodibenzo[2,3:4,5]-pentaleno[1,6-*ab*]-indene

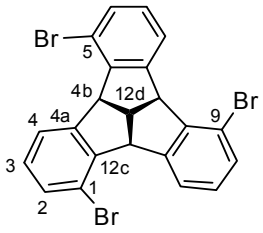


$C_{22}H_{13}Br_3$
517.05 g/mol
(racemate)

The compound was prepared according to general procedure M4 by reacting a mixture of *syn*-**52** and *anti*-**52** (2.92 g, 5.28 mmol). Dry-column flash chromatography was performed with pentane. A colorless solid was obtained (0.31 g) which was recrystallized from refluxing toluene. The yield of **55** amounted to 0.04 g (0.08 mmol, 1.5% yield) as colorless needles (decomp ~ 314 °C, mp 327 °C).

**$^1$H NMR** (400 MHz, $CDCl_3$): δ [ppm] = 4.49 (q, 1H, *J* = 10.0 Hz, H12d), 5.15 (d, 3H, *J* = 10.0 Hz, H4b), 7.07 (t, 3H, *J* = 7.9 Hz, H3), 7.43 (dd, 3H, *J* = 7.8, 0.7 Hz, H2), 8.32 („d“, 3H, *J* = 7.8 Hz, H4)

**$^{13}$C NMR** (100 MHz, $CDCl_3$): δ [ppm] = 148.2 (s, 3C, C4a), 144.8 (s, 3C, C12c), 131.9 (d, 3C, C2), 129.2 (d, 3C, C3), 126.1 (d, 3C, C4), 119.1 (s, 3C, C1), 57.0 (d, 3C, C4b), 49.6 (d, 1C, C12d)

**MS** (EI, 70 eV): *m/z* (%) = 514 (17) $[M]^{\bullet+}$, 440 (11), 439 (45), 438 (22), 437 (94), 436 (13), 435 (46), 359 (7), 358 (20), 357 (10), 356 (25), 277 (52), 276 (100), 274 (37), 138.5 (34), 138 (85), 137 (48); accurate mass calcd for $[C_{22}H_{13}Br_3]^{\bullet+}$ *m/z* 513.8562, found *m/z* 513.8562

**UV** ($CH_2Cl_2$): $\lambda_{max}$ [nm] (lg ε) = 228 (4.36), 271 (3.19), 279 (3.12)

**IR** (ATR): $\tilde{\nu}$ [$cm^{-1}$] = 3200-2600 (br), 1440 (m), 1099 (m), 1062 (m), 770 (s), 691 (m)

Determination of byproducts

The mother liquor was stripped of solvent and recrystallized from refluxing toluene. **58** (0.12 g, 0.23 mmol, 4% yield) was obtained as colorless crystals (mp 164-165). The crystals were suitable for X-ray diffraction. The remaining mother liquor (0.11 g) is mainly composed of **58**, but was not further purified.

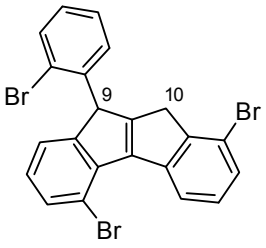


$C_{22}H_{13}Br_3$
517.05 g/mol

1,5-Dibromo-9-(2-bromophenyl)-9,10-dihydroindeno[1,2-*a*]indene (**58**, racemic):

**$^1$H NMR** (400 MHz, $CDCl_3$): δ [ppm] = 3.31 (d, 1H, *J* = 24.2 Hz, H10), 3.54 (d, 1H, *J* = 24.2 Hz, H10'), 5.46 (s, 1H, H9), 6.53 (dd, 1H, *J* = 1.9, 7.6 Hz), 7.01-7.13 (m, 3H), 7.25 (t, 1H, *J* = 7.9 Hz), 7.30 (td, 1H, *J* = 0.9, 7.5 Hz), 7.37 (dd, 1H, *J* = 0.8, 7.9 Hz), 7.53 (d, 1H, *J* = 8.0 Hz), 7.68 (dd, 1H, *J* = 1.5, 7.8 Hz), 8.73 (dd, 1H, *J* = 0.6, 7.8 Hz)

**$^{13}$C NMR** (100 MHz, $CDCl_3$): δ [ppm] = 159.8 (s), 154.2 (s), 147.2 (s), 146.9 (s), 140.1 (s), 139.9 (s), 138.8 (s), 133.1 (d), 132.2 (d), 128.8 (d), 128.4 (d), 128.3 (d), 128.0 (d, 2C), 126.9 (d), 125.2 (s), 123.9 (d), 122.9 (d), 119.2 (s), 113.6 (s), 51.8 (d, C9), 36.3 (t, C10)

**MS** (EI, 70 eV): *m/z* (%) = 514 (10) $[M]^{\bullet+}$, 440 (10), 439 (79), 438 (22), 437 (100), 436 (22), 435 (47), 359 (8), 358 (30), 357 (11), 356 (32), 277 (54), 276 (93), 274 (34), 138.5 (28), 138 (85), 137 (41); accurate mass calcd for $[C_{22}H_{13}Br_3]^{\bullet+}$ *m/z* 513.8562, found *m/z* 513.8566

**UV** ($CH_2Cl_2$): $\lambda_{max}$ [nm] (lg ε) = 229 (4.39), 239 (4.39), 268 (4.07, shoulder), 287 (3.78, shoulder), 316 (3.26, shoulder)

**IR** (ATR): $\tilde{\nu}$ [$cm^{-1}$] = 2923 (w), 1457 (m), 1438 (m), 1101 (m), 1020 (m), 763 (s), 745 (s), 726 (m), 703 (m), 676 (m)

**EA**: calcd C 51.10%, H 2.53%; found C 51.09%, H 2.61%

### 3.5.5 1,5,9-Trimethoxytribenzotriquinacene (56, racemic)

IUPAC: 1,5,9-Trimethoxy-4b,8b,12b,12d-tetrahydro-dibenzo[2,3:4,5]-pentaleno[1,6-*ab*]indene

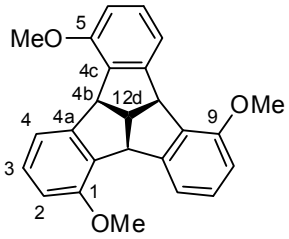


$C_{25}H_{22}O_3$
370.44 g/mol
(racemate)

The compound was prepared according to general procedure M4 by reacting a mixture of both **53**-diastereomers (3.33 g, 8.19 mmol). Dry-column flash chromatography was performed with 60% toluene/pentane. A brown foam was obtained (126 mg), which was subjected to flash chromatography (silica, 50% toluene/pentane). The product elutes first, closely followed by the byproduct fraction. **56** (12 mg, 0.03 mmol, 0.4% yield) was obtained as a pale brown solid (decomp ~ 212 °C, melting 218-229 °C). The byproduct fraction was stripped of solvent and recrystallized from refluxing toluene. **59** (57 mg, 0.153 mmol, 1.8% yield) was obtained as a colorless solid (mp 197 °C).

**$^1$H NMR** (400 MHz, $CDCl_3$): δ [ppm] = 7.45 (d, *J* = 7.8 Hz, 3H, H4), 7.11 (t, *J* = 7.9 Hz, 3H, H3), 6.67 (d, *J* = 8.1 Hz, 3H, H2), 5.06 (d, *J* = 9.8 Hz, 3H, H4b), 4.41 (q, *J* = 9.8 Hz, 1H, H12d), 3.90 (s, 9H, OC*H*$_3$)

**$^{13}$C NMR** (100 MHz, $CDCl_3$): δ [ppm] = 156.0 (s, 3C, C1), 148.3 (s, 3C, C4a), 133.2 (s, 3C, C4c), 128.5 (d, 3C, C3), 119.1 (d, 3C, C4), 108.5 (d, 3C, C2), 55.0 (d, 3C, O*C*H$_3$), 54.1 (d, 3C, C4b), 52.0 (d, C12d)

**MS** (EI, 70 eV): *m/z* (%) = 370 (100) $[M]^{\bullet+}$, 369 (11), 355 (16), 340 (9), 339 (32); accurate mass calcd for $[C_{25}H_{22}O_3]^{\bullet+}$ *m/z* 370.1564, found *m/z* 370.1563

**UV** ($CH_2Cl_2$): $\lambda_{max}$ [nm] (lg ε) = 228 (4.27), 272 (3.56), 279 (3.61)

**IR** (ATR): $\tilde{\nu}$ [$cm^{-1}$] = 2924 (w), 2900 (w), 2837 (w), 1582 (m), 1472 (s), 1253 (s), 1224 (m), 1073 (s), 1058 (s), 756 (s), 718 (s)

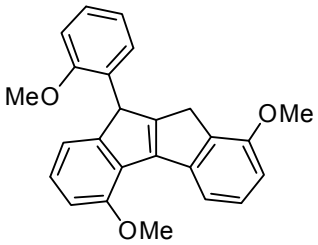


$C_{25}H_{22}O_3$
370.44 g/mol
(racemate)

1,5-Dimethoxy-9-(2-methoxyphenyl)-9,10-dihydroindeno[1,2-*a*]indene (**59**, racemic):

Single crystals for X-ray diffraction were obtained by slow evaporation of a $CDCl_3$ solution.

**$^1$H NMR** (400 MHz, $CDCl_3$): δ [ppm] = 7.81 (d, *J* = 7.5 Hz, 1H), 7.34 (t, *J* = 7.9 Hz, 1H), 7.21 – 7.08 (m, 2H), 7.03 – 6.93 (m, 2H), 6.88 (d, *J* = 8.2 Hz, 1H), 6.77 (d, *J* = 8.1 Hz, 1H), 6.70 (td, *J* = 7.4, 1.0 Hz, 1H), 6.67 – 6.58 (m, 1H), 5.35 (s, 1H, H9), 4.03 (s, 3H, OC$H_3$), 3.98 (s, 3H, OC$H_3$), 3.88 (s, 3H, OC$H_3$), 3.47 (d, *J* = 24.0 Hz, 1H, H10), 3.32 (d, *J* = 23.9 Hz, 1H, H10')

**$^{13}$C NMR** (100 MHz, $CDCl_3$): δ [ppm] = 157.7 (s), 156.7 (s), 155.3 (s), 154.5 (s), 152.8 (s), 146.4 (s), 141.4 (s), 134.4 (s), 128.5 (s), 128.2 (s), 127.9 (d), 127.7 (d), 127.6 (d), 126.1 (d), 120.8 (d), 118.0 (d), 115.8 (d), 110.5 (d), 109.4 (d), 107.1 (d), 55.6 (q, O*C*H$_3$), 55.4 (q, O*C*H$_3$), 55.2 (q, O*C*H$_3$), 46.3 (d, C9), 32.0 (t, C10)

**MS** (EI, 70 eV): *m/z* (%) = 370 (100) $[M]^{\bullet+}$, 356 (10), 355 (37), 340 (20), 339 (66), 324 (7), 323 (6), 309 (5), 281 (5), 279 (6), 263 (31); accurate mass calcd for $[C_{25}H_{22}O_3]^{\bullet+}$ *m/z* 370.1564, found *m/z* 370.1562

**UV** ($CH_2Cl_2$): $\lambda_{max}$ [nm] (lg ε) = 228 (4.49), 243 (4.39), 271 (4.12), 314 (3.64), 325 (3.48, shoulder)

**IR** (ATR): $\tilde{\nu}$ [$cm^{-1}$] = 2832 (w), 1476 (m), 1255 (s), 777 (m), 756 (s), 712 (m)

### 3.5.6 1,5,9-Trimethyltribenzotriquinacene (57, racemic)

IUPAC: 1,5,9-Trimethyl-4b,8b,12b,12d-tetrahydrodibenzo[2,3:4,5]-pentaleno[1,6-*ab*]-indene

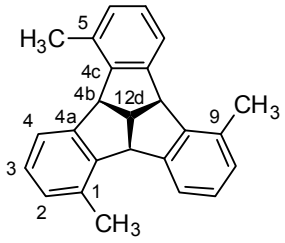


$C_{25}H_{22}$
322.44 g/mol
(racemate)

The compound was prepared according to general procedure M4 by reacting a mixture of *syn*-**54** and *anti*-**54** on a 0.91 g scale (2.54 mmol). Dry-column flash chromatography was performed with 20% toluene/pentane. A red solid was obtained (0.57 g). Recrystallization from refluxing toluene gave **57** (195 mg, 0.60 mmol, 24% yield). The colorless crystals were suitable for X-ray diffraction (decomp ~250 °C, melting 264 °C). Flash chromatography of the mother liquor (silica, 5% toluene/pentane) gave byproduct **60** (98 mg, 0.30 mmol, 12% yield) and another batch of **57** (59 mg, 0.18 mmol, 7% yield).

**$^1$H NMR** (400 MHz, $CDCl_3$): δ [ppm] = 7.46 (d, *J* = 7.5 Hz, 3H, H4), 7.07 (t, *J* = 7.5 Hz, 3H, H3), 7.02 (d, *J* = 7.0 Hz, 3H, H2), 5.03 (d, *J* = 10.0 Hz, 3H, H4b), 4.46 (q, *J* = 10.0 Hz, 1H, H12d), 2.67 (s, 9H, C*H*$_3$).

**$^{13}$C NMR** (100 MHz, $CDCl_3$): δ [ppm] = 146.8 (s, 3C, C4a), 144.9 (s, 3C, C4c), 134.2 (s, 3C, C1), 129.0 (d, 3C, C2), 127.2 (d, 3C, C3), 123.2 (d, 3C, C4), 55.2 (d, 3C, C4b), 51.4 (d, C12d), 21.9 (q, 3C, *C*H$_3$)

**MS** (EI, 70 eV): *m/z* (%) = 322 (100) $[M]^{\bullet+}$, 312 (10), 308 (21), 307 (91), 306 (7), 305 (5), 292 (13), 291 (12), 290 (9), 289 (12), 277 (7), 276 (10); accurate mass calcd for $[C_{25}H_{22}]^{\bullet+}$ *m/z* 322.1716, found *m/z* 322.1716

**UV** ($CH_2Cl_2$): $\lambda_{max}$ [nm] (lg ε) = 230 (4.16), 269 (3.08), 276 (3.00)

**IR** (ATR): $\tilde{\nu}$ [$cm^{-1}$] = 2975 (w), 2953 (w), 2873 (w), 1460 (m), 773 (s), 758 (s), 722 (m), 639 (m)

**EA**: calcd C 93.12%, H 6.88%; found C 93.32%, H 6.95%

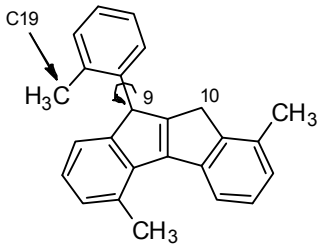


$C_{25}H_{22}$
322.44 g/mol
(racemate)

1,5-Dimethyl-9-(*o*-tolyl)-9,10-dihydroindeno[1,2-*a*]indene (**60**, racemic):

Crystals for X-ray diffraction were obtained by recrystallization from refluxing toluene. Two rotational isomers in an approximate 1:3 ratio were observed in the NMR spectrum, arising from hindered rotation of the ortho-tolyl group at C9. This analysis was supported by observation of the respective cross peaks in the EXSY spectrum. VT-NMR experiments were performed to determine the activation parameters for bond rotation (see next page).

**$^1$H NMR** (400 MHz, $CDCl_3$): δ [ppm] = 7.93 (d, *J* = 7.7 Hz, 1H), 7.34 – 7.25 (m, 2H), 7.17 – 7.01 (m, 5H), 6.92 (t, *J* = 7.5 Hz, 1H), 6.46 (d, *J* = 7.7 Hz, 1H), 5.04 (s, 1H, H9), 3.35 (d, *J* = 23.4 Hz, 1H, H10), 3.20 (d, *J* = 23.4 Hz, 1H, H10'), 2.95 (s, 3H, C*H*$_3$), 2.71 (s, 3H, C*H*$_3$), 2.33 (s, 3H, C*H*$_3$); unknown signal set (ratio 1:1:1:1): 7.54 (d, *J* = 7.2 Hz), 7.20 (t, *J* = 7.5 Hz), 6.99 (d, *J* = 7.7 Hz), 4.67 (s)

**$^{13}$C NMR** (100 MHz, $CDCl_3$): δ [ppm] = 158.8 (s), 153.5 (s), 148.3 (s), 146.7 (s), 139.3 (s), 139.3 (s), 138.9 (s), 136.0 (s), 133.8 (s), 130.4 (d), 130.0 (s), 129.2 (d), 126.9 (d), 126.7 (d), 126.6 (d), 126.5 (d), 125.7 (d), 125.1 (d), 122.4 (d), 119.3 (d), 48.5 (d, C9), 33.2 (t, C10), 23.6 (q, *C*H$_3$), 20.4 (q, *C*H$_3$), 18.7 (q, *C*H$_3$)

**MS** (EI, 70 eV): *m/z* (%) = 322 (85) $[M]^{\bullet+}$, 308 (21), 307 (100), 292 (12), 291 (12), 290 (9), 289 (12), 277 (5), 276 (7); accurate mass calcd for $[C_{25}H_{22}]^{\bullet+}$ *m/z* 322.1716, found *m/z* 322.1719

**IR** (ATR): $\tilde{\nu}$ [$cm^{-1}$] = 3013 (w), 2958 (w), 1459 (m), 784 (m), 746 (s), 720 (m)

**VT-NMR** (400 MHz, 1,1,2,2-Tetrachloroethane-$d_2$):

*The author thanks Petra Holba-Schulz for the measurement.*

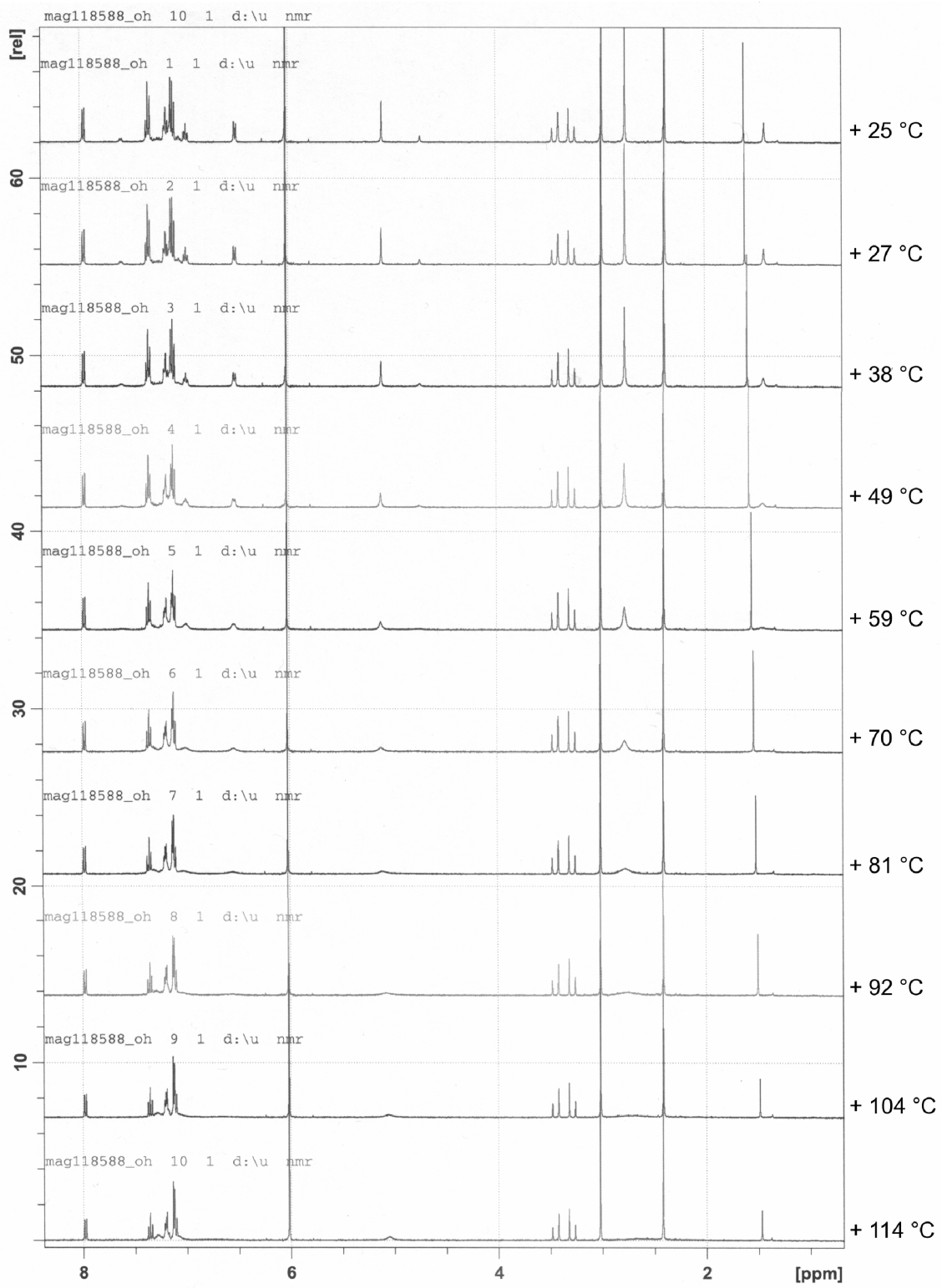


Temperature measurement with 80% Glycol in DMSO-$d_6$.

## 3.6 Various derivatives

### 3.6.1 4b,8b,12b-Tribromotribenzotriquinacene (28)

IUPAC: 4b,8b,12b-Tribromo-4b,8b,12b,12d-Tetrahydrodibenzo[2,3:4,5]pentaleno-[1,6-*ab*]indene

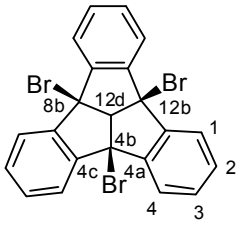


$C_{22}H_{13}Br_3$
517.05 g/mol

The compound was prepared according to the reported literature procedure [42]. Very small single crystals for X-ray diffraction were obtained by recrystallization from refluxing toluene (decomp ~ 302 °C, melting 325 °C; lit. [42]: decomp 320-325 °C). Spectroscopic data corresponded to the data reported in the literature.

**$^{1}$H NMR** (400 MHz, $CDCl_3$): δ [ppm] = 7.67 (AA'XX', $\underline{N} = |J_{AX}+J_{AX'}| = |J_{ortho}+J_{meta}|$ = 9.1 Hz, 6H, H1), 7.37 (AA'XX', $\underline{N} = |J_{AX}+J_{AX'}| = |J_{ortho}+J_{meta}|$ = 9.1 Hz, 6H, H2), 5.58 (s, 1H, H12d)

**$^{13}$C NMR** (100 MHz, $CDCl_3$): δ [ppm] = 143.6 (s, 6C, C4a), 130.6 (d, 6C, C2), 125.1 (d, 6C, C1), 89.2 (d, C12d), 67.1 (s, 3C, C4b)

**MS** (EI, 70 eV): *m/z* (%) = 439 (46) $[M\text{-}Br]^+$, 437 (100) $[M\text{-}Br]^+$, 435 (47) $[M\text{-}Br]^+$, 375 (8), 373 (8), 357 (12), 355 (8), 278 (23), 277 (74), 276 (76), 274 (21), 138 (24)

**UV** ($CH_2Cl_2$): $\lambda_{max}$ [nm] (lg ε) = 230 (4.65), 290 (3.66, shoulder)

**IR** (ATR): $\tilde{\nu}$ [$cm^{-1}$] = 884 (m), 820 (m), 757 (s), 622 (m), 574 (s)

### 3.6.2 1-Hydroxytribenzotriquinacene (38, racemic)

IUPAC: 4b,8b,12b,12d-tetrahydrodibenzo[2,3:4,5]pentaleno[1,6-*ab*]inden-1-ol

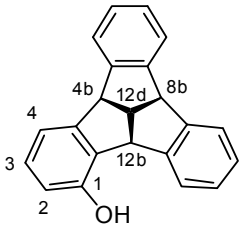


$C_{22}H_{16}O$
296.36 g/mol
(racemate)

Under nitrogen 1-methoxytribenzotriquinacene **35** (65 mg, 0.21 mmol, 1.0 eq) was dissolved in dichloromethane (5 mL). The solution was cooled to -78 °C and 270 mg boron tribromide (1.08 mmol, 5.1 eq) were added dropwise. The solution turned brown and after 45 min the cooling bath was removed. The solution was stirred for another 20 h after which the reaction was quenched by addition of water under ice cooling. The organic layer was separated and the aqueous phase was extracted twice with dichloromethane. The combined organic layers were dried ($MgSO_4$) and the solvent was removed *in vacuo*. The pale brown solid (61 mg) was subjected to flash chromatography (silica, 15-20% ethyl acetate/pentane), giving **38** (55 mg, 0.19 mmol, 88% yield) as a pale yellow solid. No melting was observed for temperatures between 280-400 °C, but the sample turned increasingly brown in this temperature range (heating rate 5 °C/min) and eventually turned into a black residue.

**$^1$H NMR** (400 MHz, $CDCl_3$): δ [ppm] = 4.48 (q, 1H, *J* = 9.7 Hz, H12d), 4.92 (m, 3H, H4b/8b and O*H*), 5.18 (d, 1H, *J* = 9.7 Hz, H12b), 6.55 (dd, 1H, *J* = 2.3, 6.5 Hz), 7.02-7.08 (m, 2H), 7.11-7.21 (m, 4H), 7.42-7.49 (m, 3H), 7.89 (m, 1H)

**$^{13}$C NMR** (100 MHz, $CDCl_3$): δ [ppm] = 152.0 (s), 148.7 (s), 146.1 (s), 145.9 (s), 145.5 (s), 145.3 (s), 131.7 (s), 128.8 (d), 127.4 (d), 127.3 (d), 127.2 (d), 127.1 (d), 126.6 (d), 124.3 (d), 124.2 (d), 124.0 (d), 116.9 (d), 113.6 (d), 56.1 (d, C4b/8b), 55.6 (d, C4b/8b), 53.9 (d, C12b), 51.4 (d, C12d)

**MS** (ESI, MeOH/$CHCl_3$ = 1:1, weak signal): accurate mass calcd for $[C_{22}H_{16}O + H]^+$ *m/z* 297.1274, found *m/z* 297.1273, accurate mass calcd for $[C_{22}H_{16}O + Na]^+$ *m/z* 319.1093, found *m/z* 319.1091

**UV** ($CH_2Cl_2$): $\lambda_{max}$ [nm] (lg ε) = 229 (4.05), 268 (3.46), 275 (3.45)

**IR** (ATR): $\tilde{\nu}$ [$cm^{-1}$] = 3496 (br), 3020 (w), 2899 (w), 1462 (m), 1274 (m), 1148 (m), 987 (m), 745 (s)

# 4 Computational Section

## 4.1 Computational methods

Quantum chemical calculations were performed with the Gaussian 09 software [193]. Stationary points were characterized by frequency calculations to assure that they are local minima (i.e. that they do not possess imaginary frequencies) or transition states (i.e. that they possess one imaginary frequency). For the calculations in Chapter 1, the hybrid meta functional M06-2X by Zhao and Truhlar [198,199] was used throughout, usually in conjunction with a Pople-type 6-311G(d,p) basis set. For the description of the halogen-halogen interactions in Chapter 1.5.5, the basis set was augmented with diffuse functions on all atoms except hydrogen. Unless otherwise noted, energies given in Chapter 1 do not include zero-point energy corrections. The interested reader can find these in Section 4.2. The theoretical approach used for the analysis of bond rigidities is discussed in detail in Chapter 2. Of the molecules described in Chapter 2, only the calculated geometries of hydrocarbon **99** and of the transition state leading to **99** are given here. All other geometries, if not already available in the literature, can be easily reproduced at the B3LYP/6-31G(d) level.

## 4.2 Calculated energies and selected geometries

### 4.2.1 Tribenzotriquinacene isomers

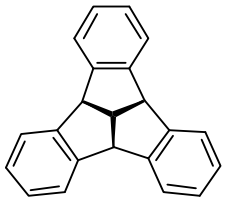

**3**

M06-2X/6-311G(d,p)
point group: $C_{3v}$
total energy: -847.84840 a.u.
ZPE correction: 0.31416 a.u.

| | x | y | c | | x | y | c |
|---|---|---|---|---|---|---|---|
| C | -3.652753 | 1.304570 | -0.989508 | C | 1.966603 | 0.331920 | 0.412854 |
| C | -3.161912 | 0.209364 | -0.286018 | C | 3.161912 | 0.209364 | -0.286018 |
| C | -1.966603 | 0.331920 | 0.412854 | C | 3.652753 | 1.304570 | -0.989508 |
| C | -1.270753 | 1.537168 | 0.412854 | C | 2.956167 | 2.511093 | -0.989508 |
| C | -1.762270 | 2.633614 | -0.286018 | C | 1.762270 | 2.633614 | -0.286018 |
| C | -2.956167 | 2.511093 | -0.989508 | C | 1.270753 | 1.537168 | 0.412854 |
| H | -4.585221 | 1.221536 | -1.535170 | H | 4.585221 | 1.221536 | -1.535170 |
| H | -3.350492 | 3.360150 | -1.535170 | H | 3.350492 | 3.360150 | -1.535170 |

| | | | | | | | |
|---|---|---|---|---|---|---|---|
| C | -1.399642 | -2.842978 | -0.286018 | H | 0.000000 | 2.210719 | 2.019139 |
| C | -0.696586 | -3.815662 | -0.989508 | C | 1.256422 | -0.725396 | 1.231802 |
| C | 0.696586 | -3.815662 | -0.989508 | H | 1.914539 | -1.105360 | 2.019139 |
| C | 1.399642 | -2.842978 | -0.286018 | H | -1.914539 | -1.105360 | 2.019139 |
| C | 0.695850 | -1.869088 | 0.412854 | H | 1.228236 | 3.577422 | -0.281151 |
| C | -0.695850 | -1.869088 | 0.412854 | H | -1.228236 | 3.577422 | -0.281151 |
| H | -1.234729 | -4.581686 | -1.535170 | H | -3.712256 | -0.725027 | -0.281151 |
| H | 1.234729 | -4.581686 | -1.535170 | H | -2.484020 | -2.852394 | -0.281151 |
| C | -1.256422 | -0.725396 | 1.231802 | H | 2.484020 | -2.852394 | -0.281151 |
| C | 0.000000 | 0.000000 | 1.805128 | H | 3.712256 | -0.725027 | -0.281151 |
| H | 0.000000 | 0.000000 | 2.893523 | | | | |
| C | 0.000000 | 1.450792 | 1.231802 | | | | |

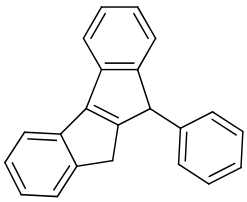

**16**

M06-2X/6-311G(d,p)
point group: $C_1$
total energy: -847.82158 a.u.
ZPE correction: 0.31055 a.u.

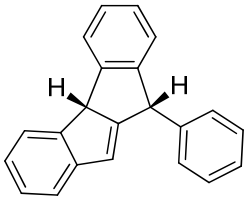


*syn*-**11**

M06-2X/6-311G(d,p)
point group: $C_1$
total energy: -847.81241 a.u.
ZPE correction: 0.31135 a.u.

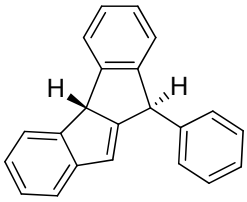


*anti*-**11**

M06-2X/6-311G(d,p)
point group: $C_1$
total energy: -847.80978 a.u.
ZPE correction: 0.31111 a.u.

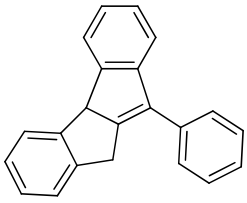

**24**

M06-2X/6-311G(d,p)
point group: $C_1$
total energy: -847.81791 a.u.
ZPE correction: 0.31139 a.u.

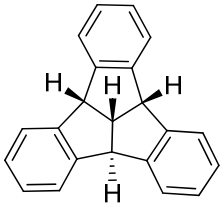

**25**

M06-2X/6-311G(d,p)
point group: $C_s$
total energy: -847.80606 a.u.
ZPE correction: 0.31382 a.u.

| | x | y | z | | x | y | z |
|---|---|---|---|---|---|---|---|
| C | -3.806154 | -1.039597 | 0.695318 | C | 2.474911 | -0.685361 | 2.053919 |
| C | -2.819260 | -0.352570 | 1.402449 | C | 1.397185 | -0.091190 | 1.427048 |
| C | -1.843689 | 0.340290 | 0.704258 | C | 0.349977 | 0.487307 | 2.185230 |
| C | -1.843689 | 0.340290 | -0.704258 | H | 1.547340 | -0.147547 | 5.281358 |
| C | -2.819260 | -0.352570 | -1.402449 | H | 3.365757 | -1.147316 | 3.956434 |
| C | -3.806154 | -1.039597 | -0.695318 | C | -0.681085 | 1.161517 | 1.271761 |
| H | -4.574900 | -1.582076 | 1.232908 | C | 0.146714 | 1.320137 | 0.000000 |
| H | -4.574900 | -1.582076 | -1.232908 | H | 0.841138 | 2.162495 | 0.000000 |
| C | 1.397185 | -0.091190 | -1.427048 | C | -0.681085 | 1.161517 | -1.271761 |
| C | 2.474911 | -0.685361 | -2.053919 | H | -1.050181 | 2.093947 | -1.707225 |
| C | 2.520148 | -0.694520 | -3.452231 | C | 0.926627 | -0.009875 | 0.000000 |
| C | 1.494668 | -0.132837 | -4.199320 | H | 0.153501 | -0.793784 | 0.000000 |
| C | 0.399797 | 0.465556 | -3.566200 | H | -1.050181 | 2.093947 | 1.707225 |
| C | 0.349977 | 0.487307 | -2.185230 | H | -0.389859 | 0.922431 | -4.153558 |
| H | 3.365757 | -1.147316 | -3.956434 | H | -2.807380 | -0.368159 | -2.487205 |
| H | 1.547340 | -0.147547 | -5.281358 | H | -2.807380 | -0.368159 | 2.487205 |
| C | 0.399797 | 0.465556 | 3.566200 | H | -0.389859 | 0.922431 | 4.153558 |
| C | 1.494668 | -0.132837 | 4.199320 | H | 3.272902 | -1.137991 | 1.476922 |
| C | 2.520148 | -0.694520 | 3.452231 | H | 3.272902 | -1.137991 | -1.476922 |

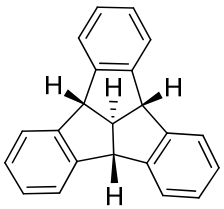

**26**

M06-2X/6-311G(d,p)
point group: $C_{3v}$
total energy: -847.74878 a.u.
ZPE correction: 0.31326 a.u.

| | x | y | z | | x | y | z |
|---|---|---|---|---|---|---|---|
| C | -4.010810 | 1.514794 | -0.675782 | C | 1.403871 | -3.135889 | -0.176073 |
| C | -3.417695 | 0.352157 | -0.176073 | C | 0.717689 | -2.036755 | 0.305877 |
| C | -2.122726 | 0.396840 | 0.305877 | C | -0.717689 | -2.036755 | 0.305877 |
| C | -1.405036 | 1.639914 | 0.305877 | H | -1.231489 | -5.086513 | -1.066495 |
| C | -2.013824 | 2.783732 | -0.176073 | H | 1.231489 | -5.086513 | -1.066495 |
| C | -3.317255 | 2.716066 | -0.675782 | C | -1.272656 | -0.734768 | 0.936076 |
| H | -5.020794 | 1.476756 | -1.066495 | C | 0.000000 | 0.000000 | 0.779503 |
| H | -3.789305 | 3.609757 | -1.066495 | H | 0.000000 | 0.000000 | -0.321969 |
| C | 2.122726 | 0.396840 | 0.305877 | C | 0.000000 | 1.469536 | 0.936076 |

| | | | | | | | |
|---|---|---|---|---|---|---|---|
| C | 3.417695 | 0.352157 | -0.176073 | H | 0.000000 | 1.846115 | 1.966145 |
| C | 4.010810 | 1.514794 | -0.675782 | C | 1.272656 | -0.734768 | 0.936076 |
| C | 3.317255 | 2.716066 | -0.675782 | H | 1.598783 | -0.923058 | 1.966145 |
| C | 2.013824 | 2.783732 | -0.176073 | H | -1.598783 | -0.923058 | 1.966145 |
| C | 1.405036 | 1.639914 | 0.305877 | H | 1.479295 | 3.727298 | -0.174777 |
| H | 5.020794 | 1.476756 | -1.066495 | H | -1.479295 | 3.727298 | -0.174777 |
| H | 3.789305 | 3.609757 | -1.066495 | H | -3.967583 | -0.582542 | -0.174777 |
| C | -1.403871 | -3.135889 | -0.176073 | H | -2.488287 | -3.144756 | -0.174777 |
| C | -0.693554 | -4.230860 | -0.675782 | H | 2.488287 | -3.144756 | -0.174777 |
| C | 0.693554 | -4.230860 | -0.675782 | H | 3.967583 | -0.582542 | -0.174777 |

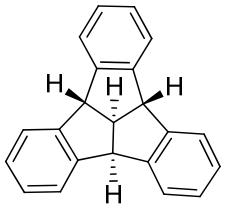


**27**

M06-2X/6-311G(d,p)
point group: $C_s$
total energy: -847.72491 a.u.
ZPE correction: 0.31319 a.u.

| | x | y | z | | x | y | z |
|---|---|---|---|---|---|---|---|
| C | -0.066613 | 4.536247 | 0.692204 | C | -0.075408 | -2.861905 | 2.107566 |
| C | 0.005996 | 3.334283 | 1.410326 | C | -0.138290 | -1.649767 | 1.444829 |
| C | 0.058184 | 2.141165 | 0.723945 | C | 0.010623 | -0.433719 | 2.185053 |
| C | 0.058184 | 2.141165 | -0.723945 | H | 0.393954 | -1.739975 | 5.280017 |
| C | 0.005996 | 3.334283 | -1.410326 | H | 0.180639 | -3.839725 | 4.006900 |
| C | -0.066613 | 4.536247 | -0.692204 | C | 0.199398 | 0.671074 | 1.152381 |
| H | -0.127169 | 5.475275 | 1.229448 | C | -0.592895 | 0.115490 | 0.000000 |
| H | -0.127169 | 5.475275 | -1.229448 | H | -1.597172 | 0.548417 | 0.000000 |
| C | -0.138290 | -1.649767 | -1.444829 | C | 0.199398 | 0.671074 | -1.152381 |
| C | -0.075408 | -2.861905 | -2.107566 | H | 1.259783 | 0.490145 | -0.912411 |
| C | 0.130082 | -2.888708 | -3.490203 | C | -0.627459 | -1.384558 | 0.000000 |
| C | 0.250043 | -1.707080 | -4.206559 | H | -1.661362 | -1.746131 | 0.000000 |
| C | 0.201695 | -0.471925 | -3.553541 | H | 1.259783 | 0.490145 | 0.912411 |
| C | 0.010623 | -0.433719 | -2.185053 | H | 0.327473 | 0.448031 | -4.112571 |
| H | 0.180639 | -3.839725 | -4.006900 | H | 0.005413 | 3.343907 | -2.494032 |
| H | 0.393954 | -1.739975 | -5.280017 | H | 0.005413 | 3.343907 | 2.494032 |
| C | 0.201695 | -0.471925 | 3.553541 | H | 0.327473 | 0.448031 | 4.112571 |
| C | 0.250043 | -1.707080 | 4.206559 | H | -0.204016 | -3.789577 | 1.560242 |
| C | 0.130082 | -2.888708 | 3.490203 | H | -0.204016 | -3.789577 | -1.560242 |

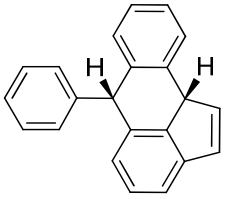

*syn*-**23**

M06-2X/6-311G(d,p)
point group: $C_1$
total energy: -847.81993 a.u.
ZPE correction: 0.31176 a.u.

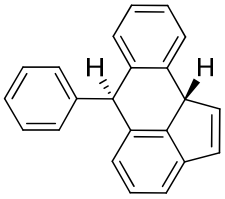

*anti*-**23**

M06-2X/6-311G(d,p)
point group: $C_1$
total energy: -847.81957 a.u.
ZPE correction: 0.31169 a.u.

## 4.2.2 Diketone conformations

**14**-type

M06-2X/6-311G(d,p)
point group: $C_1$
total energy: -998.24219 a.u.
ZPE correction: 0.31784 a.u.

| | x | y | z | | x | y | z |
|---|---|---|---|---|---|---|---|
| C | -0.396277 | -1.090874 | 0.186650 | H | -6.312452 | -0.723332 | 0.319158 |
| C | 0.616188 | -1.881581 | -0.201098 | C | -5.176112 | 0.930956 | -0.453309 |
| H | 0.333525 | -2.823727 | -0.666950 | H | -6.042914 | 1.568507 | -0.581471 |
| C | -1.794458 | -1.643339 | 0.032678 | C | -3.913722 | 1.400322 | -0.798064 |
| C | -0.229458 | 0.216573 | 0.912282 | H | -3.795435 | 2.397897 | -1.203118 |
| C | 2.056606 | -1.622282 | -0.070854 | C | -2.799005 | 0.590192 | -0.620159 |
| C | 2.907184 | -2.015419 | -1.108992 | H | -1.821335 | 0.965335 | -0.902592 |
| H | 2.491272 | -2.528205 | -1.969797 | C | 0.602957 | 1.310934 | 0.312792 |
| C | 4.265687 | -1.735414 | -1.053634 | C | 1.052321 | 1.274777 | -1.007574 |
| H | 4.911699 | -2.031331 | -1.871294 | H | 0.799542 | 0.433068 | -1.641961 |
| C | 4.795400 | -1.083859 | 0.055396 | C | 1.830347 | 2.311739 | -1.505869 |
| H | 5.856350 | -0.869949 | 0.103331 | H | 2.180878 | 2.279329 | -2.530174 |
| C | 3.963931 | -0.724335 | 1.111699 | C | 2.164469 | 3.385534 | -0.687054 |
| H | 4.377442 | -0.239092 | 1.987349 | H | 2.779498 | 4.189295 | -1.074261 |
| C | 2.603669 | -0.991938 | 1.051523 | C | 1.707801 | 3.430930 | 0.627630 |
| H | 1.964444 | -0.732736 | 1.887869 | H | 1.964976 | 4.270516 | 1.262193 |
| C | -2.947131 | -0.699353 | -0.110757 | C | 0.923978 | 2.399893 | 1.124229 |
| C | -4.218880 | -1.173526 | 0.212547 | H | 0.552509 | 2.412019 | 2.141868 |
| H | -4.313006 | -2.185333 | 0.587251 | O | -1.973850 | -2.837996 | -0.005620 |
| C | -5.328281 | -0.357475 | 0.052940 | O | -0.782433 | 0.365873 | 1.977443 |

**30/31/50**-type

M06-2X/6-311G(d,p)
point group: $C_1$
total energy: -998.23881 a.u.
ZPE correction: 0.31767 a.u.

| | x | y | z | | x | y | z |
|---|---|---|---|---|---|---|---|
| C | -0.957978 | 0.870977 | 1.026666 | H | 5.727247 | -1.958444 | -1.446251 |
| C | 0.057571 | -0.199240 | 0.687334 | C | 3.642918 | -1.478079 | -1.632194 |
| C | 1.464702 | 0.186212 | 1.013998 | H | 3.568076 | -1.840368 | -2.650268 |
| C | -0.269570 | -1.447176 | 0.321823 | C | 2.521538 | -0.950271 | -1.001767 |
| H | 0.537110 | -2.173704 | 0.249920 | H | 1.579527 | -0.897718 | -1.534977 |
| C | -0.911486 | 2.142291 | 0.237467 | C | -1.605745 | -1.976744 | 0.013093 |
| C | -0.065742 | 2.297350 | -0.860435 | C | -1.851468 | -3.335979 | 0.230765 |
| C | -0.068058 | 3.486391 | -1.579955 | C | -3.092404 | -3.888019 | -0.056073 |
| H | 0.593070 | 3.605263 | -2.429541 | H | -3.271994 | -4.939765 | 0.131124 |
| C | -0.915730 | 4.521894 | -1.203655 | C | -4.098601 | -3.091207 | -0.590158 |
| H | -0.914310 | 5.450338 | -1.762474 | H | -5.066293 | -3.520099 | -0.821126 |
| C | -1.765420 | 4.369402 | -0.110142 | C | -3.856148 | -1.742894 | -0.837761 |
| H | -2.423851 | 5.178744 | 0.181181 | H | -4.631967 | -1.122174 | -1.269120 |
| C | -1.765307 | 3.182618 | 0.606995 | C | -2.620878 | -1.188020 | -0.539216 |
| H | -2.415389 | 3.036026 | 1.461097 | H | -2.438973 | -0.142057 | -0.757892 |
| C | 2.614573 | -0.468756 | 0.305766 | O | -1.770267 | 0.693897 | 1.898196 |
| C | 3.842722 | -0.509220 | 0.968588 | O | 1.664349 | 1.038222 | 1.850935 |
| C | 4.955222 | -1.053978 | 0.345016 | H | 0.597891 | 1.492680 | -1.158976 |
| H | 5.902521 | -1.095493 | 0.868830 | H | -1.062828 | -3.958416 | 0.639617 |
| C | 4.856154 | -1.539026 | -0.957028 | H | 3.902296 | -0.102926 | 1.971056 |

### 4.2.3 Halogen-halogen interactions

**43** (monomer)

M06-2X/6-311+G(d,p) single point energy at solid state geometry
point group: $C_1$
total energy: -5876.13212 a.u.
ZPE correction: 0.20471 a.u.

**43** (dimer)

M06-2X/6-311+G(d,p) single point energy at solid state geometry
point group: $C_i$
total energy: -11752.26940 a.u.
ZPE correction: 0.41007 a.u.
BSSE: 0.00071 a.u. (counterpoise technique)

| | x | y | z | | x | y | z |
|---|---|---|---|---|---|---|---|
| C | 4.160082 | 7.004582 | 1.884215 | C | -4.160082 | 5.897720 | -1.884215 |
| C | 3.447127 | 8.182266 | 1.826852 | C | -3.447127 | 4.720036 | -1.826852 |
| H | 2.625663 | 8.206832 | 2.149918 | H | -2.625663 | 4.695470 | -2.149918 |
| C | 4.075145 | 9.366504 | 1.352716 | C | -4.075145 | 3.535798 | -1.352716 |
| C | 3.659288 | 5.744247 | 2.486203 | C | -3.659288 | 7.158055 | -2.486203 |
| C | 2.354834 | 5.246076 | 2.375771 | C | -2.354834 | 7.656226 | -2.375771 |
| C | 1.973778 | 4.062961 | 2.993596 | C | -1.973778 | 8.839341 | -2.993596 |
| H | 1.084700 | 3.741126 | 2.901603 | H | -1.084700 | 9.161176 | -2.901603 |
| C | 2.898232 | 3.352637 | 3.746354 | C | -2.898232 | 9.549665 | -3.746354 |
| H | 2.635853 | 2.552514 | 4.186192 | H | -2.635853 | 10.349788 | -4.186192 |
| C | 4.201037 | 3.805779 | 3.858539 | C | -4.201037 | 9.096523 | -3.858539 |
| H | 4.835490 | 3.312124 | 4.364782 | H | -4.835490 | 9.590178 | -4.364782 |
| C | 4.577296 | 4.983450 | 3.229116 | C | -4.577296 | 7.918852 | -3.229116 |
| H | 5.476137 | 5.282177 | 3.302162 | H | -5.476137 | 7.620125 | -3.302162 |
| C | 3.379390 | 10.685390 | 1.417615 | C | -3.379390 | 2.216912 | -1.417615 |
| C | 2.075597 | 10.934817 | 0.985189 | C | -2.075597 | 1.967485 | -0.985189 |
| C | 1.492509 | 12.182818 | 1.146390 | C | -1.492509 | 0.719484 | -1.146390 |
| H | 0.605685 | 12.337981 | 0.843114 | H | -0.605685 | 0.564321 | -0.843114 |
| C | 2.210827 | 13.204280 | 1.753004 | C | -2.210827 | -0.301978 | -1.753004 |
| H | 1.803998 | 14.051523 | 1.891419 | H | -1.803998 | -1.149221 | -1.891419 |
| C | 3.515047 | 12.992954 | 2.156034 | C | -3.515047 | -0.090652 | -2.156034 |
| H | 4.012609 | 13.699922 | 2.549913 | H | -4.012609 | -0.797620 | -2.549913 |
| C | 4.095172 | 11.746643 | 1.983961 | C | -4.095172 | 1.155659 | -1.983961 |
| H | 4.995249 | 11.609801 | 2.255316 | H | -4.995249 | 1.292501 | -2.255316 |
| O | 5.413631 | 6.940922 | 1.481919 | O | -5.413631 | 5.961380 | -1.481919 |
| H | 5.568374 | 7.804744 | 1.200502 | H | -5.568374 | 5.097558 | -1.200502 |
| O | 5.281117 | 9.367652 | 0.954296 | O | -5.281117 | 3.534650 | -0.954296 |
| Br | 1.042032 | 6.071604 | 1.284288 | Br | -1.042032 | 6.830698 | -1.284288 |
| Br | 1.062277 | 9.628059 | 0.046213 | Br | -1.062277 | 3.274243 | -0.046213 |

## 4.2.4 Rotational isomerism in a dihydroindenoindene byproduct

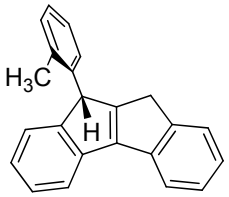


**68**

M06-2X/6-311G(d,p)
point group: $C_1$
total energy: -887.12717 a.u.
ZPE correction: 0.33881 a.u.
free enthalpy (348.15 K): -886.84569 a.u.

| | x | y | z | | x | y | z |
|---|---|---|---|---|---|---|---|
| C | 3.732759 | -2.232330 | -0.344290 | C | 1.185396 | -1.802311 | -0.804377 |
| C | 4.938767 | -1.663157 | 0.069351 | H | 1.142756 | -2.168456 | -1.835763 |
| H | 5.833255 | -2.273103 | 0.112290 | H | 0.762051 | -2.586715 | -0.166623 |
| C | 5.003577 | -0.319363 | 0.425216 | C | 2.601233 | -1.439044 | -0.394991 |
| H | 5.948587 | 0.104295 | 0.744101 | C | -1.998541 | -0.736577 | -0.056238 |
| C | 3.867960 | 0.487420 | 0.377068 | C | -3.269617 | -0.944023 | -0.611174 |
| H | 3.925659 | 1.532900 | 0.655460 | C | -4.229572 | -1.612662 | 0.150458 |
| C | 2.667122 | -0.076943 | -0.034217 | H | -5.214278 | -1.777227 | -0.274490 |
| C | 1.317405 | 0.470520 | -0.191044 | C | -3.950949 | -2.067809 | 1.432364 |
| C | 0.580726 | 1.724136 | -0.004718 | H | -4.714978 | -2.584544 | 2.000906 |
| C | 0.963927 | 2.984697 | 0.434312 | C | -2.691159 | -1.854318 | 1.979201 |
| C | -0.006554 | 3.980591 | 0.535990 | H | -2.461525 | -2.199169 | 2.980204 |
| H | 0.275593 | 4.969040 | 0.878551 | C | -1.725823 | -1.191306 | 1.234046 |
| C | -1.334661 | 3.718552 | 0.213648 | H | -0.740907 | -1.011720 | 1.654836 |
| H | -2.075991 | 4.502116 | 0.314993 | C | -3.615658 | -0.474627 | -2.004081 |
| C | -1.721753 | 2.452275 | -0.230601 | H | -3.412074 | 0.590291 | -2.139219 |
| H | -2.761656 | 2.242932 | -0.459474 | H | -4.672661 | -0.642783 | -2.210970 |
| C | -0.760839 | 1.466391 | -0.349613 | H | -3.038766 | -1.014770 | -2.760379 |
| C | -0.920941 | 0.019056 | -0.813375 | H | 1.993808 | 3.193374 | 0.698501 |
| H | -1.160613 | 0.019331 | -1.882851 | H | 3.688120 | -3.280272 | -0.620888 |
| C | 0.481133 | -0.491754 | -0.627801 | | | | |

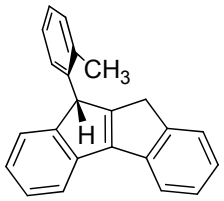


**69**

M06-2X/6-311G(d,p)
point group: $C_1$
total energy: -887.12730 a.u.
ZPE correction: 0.33821 a.u.
free enthalpy (348.15 K): -886.84689 a.u.

| | x | y | z | | x | y | z |
|---|---|---|---|---|---|---|---|
| C | 3.359936 | -2.486226 | -0.007236 | C | 0.902872 | -1.823871 | -0.647668 |
| C | 4.602440 | -2.017134 | 0.424303 | H | 0.874814 | -2.282978 | -1.642254 |
| H | 5.417036 | -2.715575 | 0.573534 | H | 0.358220 | -2.487781 | 0.033806 |
| C | 4.803271 | -0.661141 | 0.665219 | C | 2.330046 | -1.581999 | -0.190270 |
| H | 5.774044 | -0.315363 | 1.000129 | C | -2.093796 | -0.435151 | -0.044608 |

| | | | | | | | |
|---|---|---|---|---|---|---|---|
| C | 3.771065 | 0.257086 | 0.481529 | C | -2.858305 | -1.490871 | -0.563460 |
| H | 3.935363 | 1.311155 | 0.670536 | C | -3.816145 | -2.091164 | 0.254182 |
| C | 2.534238 | -0.207674 | 0.052437 | H | -4.412816 | -2.904073 | -0.146121 |
| C | 1.265580 | 0.467977 | -0.229191 | C | -4.016678 | -1.670789 | 1.562869 |
| C | 0.664259 | 1.803742 | -0.176166 | H | -4.767213 | -2.153137 | 2.177645 |
| C | 1.172296 | 3.051989 | 0.160424 | C | -3.248296 | -0.633395 | 2.075562 |
| C | 0.318227 | 4.153173 | 0.122110 | H | -3.390012 | -0.298157 | 3.095947 |
| H | 0.697335 | 5.133727 | 0.384548 | C | -2.293804 | -0.022806 | 1.272412 |
| C | -1.016754 | 4.009079 | -0.244640 | H | -1.692425 | 0.788860 | 1.667288 |
| H | -1.664510 | 4.877401 | -0.262480 | C | -2.662896 | -1.982638 | -1.976828 |
| C | -1.528303 | 2.755590 | -0.586507 | H | -2.937228 | -1.216208 | -2.707650 |
| H | -2.571462 | 2.640618 | -0.861235 | H | -3.281083 | -2.860049 | -2.166997 |
| C | -0.685446 | 1.660347 | -0.552104 | H | -1.622021 | -2.256319 | -2.168373 |
| C | -0.996666 | 0.206838 | -0.880482 | H | 2.209373 | 3.172353 | 0.449365 |
| H | -1.261766 | 0.136784 | -1.941725 | H | 3.208048 | -3.544075 | -0.192686 |
| C | 0.347244 | -0.432160 | -0.632433 | | | | |

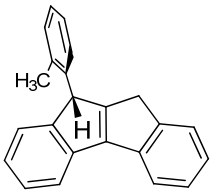


**70**

M06-2X/6-311G(d,p)
point group: $C_1$
total energy: -887.12906 a.u.
ZPE correction: 0.33859 a.u.
free enthalpy (348.15 K): -886.84728 a.u.

| | x | y | z | | x | y | z |
|---|---|---|---|---|---|---|---|
| C | 3.530648 | -2.335027 | -0.253134 | C | 1.034213 | -1.814328 | -0.870747 |
| C | 4.737394 | -1.802212 | 0.204394 | H | 1.027257 | -2.223827 | -1.886497 |
| H | 5.597631 | -2.449481 | 0.325842 | H | 0.541485 | -2.551501 | -0.225360 |
| C | 4.845420 | -0.447801 | 0.505944 | C | 2.441760 | -1.495431 | -0.400797 |
| H | 5.790252 | -0.052985 | 0.860579 | C | -2.151769 | -0.668556 | -0.395374 |
| C | 3.753856 | 0.405815 | 0.358303 | C | -2.212709 | -0.934736 | 0.985471 |
| H | 3.845677 | 1.459232 | 0.594073 | C | -3.314933 | -1.632526 | 1.477429 |
| C | 2.551710 | -0.122115 | -0.096441 | H | -3.367043 | -1.837557 | 2.541475 |
| C | 1.238215 | 0.476135 | -0.345857 | C | -4.342265 | -2.065380 | 0.646487 |
| C | 0.535357 | 1.752711 | -0.197129 | H | -5.185261 | -2.603543 | 1.063295 |
| C | 0.938407 | 3.005194 | 0.247952 | C | -4.279907 | -1.799704 | -0.713221 |
| C | -0.011076 | 4.023554 | 0.326689 | H | -5.071464 | -2.127108 | -1.376388 |
| H | 0.286601 | 5.005141 | 0.675949 | C | -3.187470 | -1.105749 | -1.220687 |
| C | -1.336863 | 3.794707 | -0.029802 | H | -3.134303 | -0.896597 | -2.284164 |
| H | -2.059495 | 4.597989 | 0.049511 | C | -1.135382 | -0.489635 | 1.942327 |
| C | -1.744538 | 2.537354 | -0.482163 | H | -0.191565 | -1.010109 | 1.758902 |
| H | -2.779814 | 2.350603 | -0.747901 | H | -1.437845 | -0.693359 | 2.969867 |
| C | -0.806580 | 1.526830 | -0.565367 | H | -0.935104 | 0.580276 | 1.850791 |
| C | -0.994683 | 0.084716 | -1.026132 | H | 1.966514 | 3.190695 | 0.535213 |
| H | -1.173231 | 0.106035 | -2.109533 | H | 3.451661 | -3.391459 | -0.485968 |
| C | 0.382536 | -0.469225 | -0.783090 | | | | |

**TS 1**

M06-2X/6-311G(d,p)
point group: $C_1$
total energy: -887.12697 a.u.
ZPE correction: 0.33873 a.u.
free enthalpy (348.15 K): -886.84313 a.u.

| | x | y | z | | x | y | z |
|---|---|---|---|---|---|---|---|
| C | 3.503207 | -2.421858 | -0.168048 | C | 1.003852 | -1.833311 | -0.709435 |
| C | 4.740439 | -1.920199 | 0.241013 | H | 0.949657 | -2.268088 | -1.713445 |
| H | 5.584144 | -2.592000 | 0.343738 | H | 0.511013 | -2.533682 | -0.025329 |
| C | 4.899556 | -0.565606 | 0.518194 | C | 2.436135 | -1.551393 | -0.293023 |
| H | 5.867097 | -0.194824 | 0.835213 | C | -2.048515 | -0.544682 | -0.017546 |
| C | 3.829666 | 0.318773 | 0.394222 | C | -3.116670 | -1.233449 | -0.606349 |
| H | 3.961231 | 1.371994 | 0.611416 | C | -4.056973 | -1.844800 | 0.227161 |
| C | 2.597840 | -0.178436 | -0.012147 | H | -4.888406 | -2.376496 | -0.223529 |
| C | 1.296786 | 0.457582 | -0.231970 | C | -3.948777 | -1.785482 | 1.609234 |
| C | 0.647779 | 1.767592 | -0.121470 | H | -4.692335 | -2.268671 | 2.231785 |
| C | 1.113601 | 3.022269 | 0.250375 | C | -2.882960 | -1.104042 | 2.187598 |
| C | 0.214485 | 4.087345 | 0.277541 | H | -2.785749 | -1.050309 | 3.265284 |
| H | 0.560772 | 5.072013 | 0.568330 | C | -1.943469 | -0.490022 | 1.373377 |
| C | -1.123953 | 3.901610 | -0.056309 | H | -1.108141 | 0.047526 | 1.812585 |
| H | -1.807179 | 4.741561 | -0.019745 | C | -3.273397 | -1.331168 | -2.104893 |
| C | -1.593847 | 2.641662 | -0.432724 | H | -3.389050 | -0.344667 | -2.562155 |
| H | -2.639608 | 2.491391 | -0.679793 | H | -4.154900 | -1.920404 | -2.358167 |
| C | -0.705183 | 1.584231 | -0.468630 | H | -2.407078 | -1.809221 | -2.569851 |
| C | -0.967224 | 0.129945 | -0.846011 | H | 2.152358 | 3.174845 | 0.517537 |
| H | -1.232398 | 0.086367 | -1.907360 | H | 3.384193 | -3.478600 | -0.381627 |
| C | 0.400019 | -0.464685 | -0.634306 | | | | |

**TS 2**

M06-2X/6-311G(d,p)
point group: $C_1$
total energy: -887.10324 a.u.
ZPE correction: 0.33967 a.u.
free enthalpy (348.15 K): -886.81729 a.u.

| | x | y | z | | x | y | z |
|---|---|---|---|---|---|---|---|
| C | -3.868708 | -1.916132 | 0.521212 | C | -1.337146 | -1.608981 | 1.124443 |
| C | -4.960079 | -1.372456 | -0.157709 | H | -1.412962 | -1.507132 | 2.215185 |
| H | -5.917432 | -1.878764 | -0.127750 | H | -1.064724 | -2.642440 | 0.922826 |
| C | -4.830573 | -0.184960 | -0.872995 | C | -2.656329 | -1.251421 | 0.473799 |
| H | -5.689239 | 0.221506 | -1.393992 | C | 2.216177 | -0.614111 | 0.261811 |
| C | -3.610410 | 0.485127 | -0.929427 | C | 2.315111 | -1.941539 | -0.199261 |
| H | -3.517554 | 1.403435 | -1.496181 | C | 3.515849 | -2.380365 | -0.767136 |
| C | -2.522971 | -0.056821 | -0.254604 | H | 3.568515 | -3.403048 | -1.124241 |
| C | -1.134738 | 0.378339 | -0.096686 | C | 4.628519 | -1.564678 | -0.884184 |
| C | -0.411807 | 1.645125 | -0.187967 | H | 5.541142 | -1.941475 | -1.330032 |
| C | -0.801050 | 2.880429 | -0.685569 | C | 4.545462 | -0.265000 | -0.413136 |

| | | | | | | | |
|---|---|---|---|---|---|---|---|
| C | -0.008085 | 3.993371 | -0.412645 | H | 5.393653 | 0.405735 | -0.479527 |
| H | -0.298858 | 4.967907 | -0.785962 | C | 3.357985 | 0.186583 | 0.144068 |
| C | 1.126247 | 3.865609 | 0.378029 | H | 3.332875 | 1.208277 | 0.482585 |
| H | 1.705295 | 4.744251 | 0.636049 | C | 1.209790 | -2.959392 | -0.107504 |
| C | 1.521769 | 2.616622 | 0.865115 | H | 1.560615 | -3.920344 | -0.484063 |
| H | 2.379402 | 2.559298 | 1.524381 | H | 0.338406 | -2.664637 | -0.693755 |
| C | 0.780042 | 1.490802 | 0.544648 | H | 0.898940 | -3.105696 | 0.928163 |
| C | 0.966387 | 0.013934 | 0.947895 | H | -1.720861 | 2.986430 | -1.247436 |
| H | 1.126391 | -0.055318 | 2.031838 | H | -3.974371 | -2.840262 | 1.079173 |
| C | -0.416315 | -0.529705 | 0.598262 | | | | |

**TS 3**

M06-2X/6-311G(d,p)
point group: $C_1$
total energy: -887.10198 a.u.
ZPE correction: 0.33946 a.u.
free enthalpy (348.15 K): -886.81663 a.u.

| | x | y | z | | x | y | z |
|---|---|---|---|---|---|---|---|
| C | -3.869244 | -2.011876 | 0.496091 | C | -1.330554 | -1.690639 | 1.060162 |
| C | -4.980621 | -1.464128 | -0.146337 | H | -1.382769 | -1.758529 | 2.153204 |
| H | -5.927573 | -1.989877 | -0.122843 | H | -1.021105 | -2.672340 | 0.695333 |
| C | -4.883246 | -0.248733 | -0.818132 | C | -2.671292 | -1.321352 | 0.459810 |
| H | -5.756208 | 0.159859 | -1.313008 | C | 2.046271 | -0.870235 | 0.255189 |
| C | -3.677606 | 0.448239 | -0.862683 | C | 3.325856 | -0.442327 | -0.160394 |
| H | -3.610866 | 1.389373 | -1.394441 | C | 4.194074 | -1.372952 | -0.743627 |
| C | -2.571494 | -0.094241 | -0.219294 | H | 5.166554 | -1.023803 | -1.072748 |
| C | -1.193750 | 0.369003 | -0.051711 | C | 3.869649 | -2.709188 | -0.905323 |
| C | -0.460537 | 1.622506 | -0.194665 | H | 4.574060 | -3.394082 | -1.361782 |
| C | -0.874598 | 2.856293 | -0.677492 | C | 2.636538 | -3.145733 | -0.452127 |
| C | -0.077763 | 3.972159 | -0.436201 | H | 2.348595 | -4.186882 | -0.534660 |
| H | -0.385471 | 4.945573 | -0.798960 | C | 1.758215 | -2.232582 | 0.112123 |
| C | 1.078329 | 3.848344 | 0.323717 | H | 0.815462 | -2.611016 | 0.465866 |
| H | 1.658619 | 4.729202 | 0.571282 | C | 3.881954 | 0.949082 | 0.005527 |
| C | 1.493764 | 2.600564 | 0.795264 | H | 4.922527 | 0.964594 | -0.318745 |
| H | 2.370185 | 2.548469 | 1.425291 | H | 3.865521 | 1.255402 | 1.052677 |
| C | 0.768318 | 1.463675 | 0.477184 | H | 3.335575 | 1.689698 | -0.576002 |
| C | 0.943140 | -0.001911 | 0.929817 | H | -1.820911 | 2.958227 | -1.194155 |
| H | 1.134086 | -0.012380 | 2.011374 | H | -3.948956 | -2.959907 | 1.017124 |
| C | -0.461621 | -0.529229 | 0.635634 | | | | |

## 4.2.5 Intramolecular cyclizations


M06-2X/6-311G(d,p) [with ultrafine grid for two-electron integrals]
point group: $D_{\infty h}$
total energy: -1.16830 a.u. [-1.16840 a.u.]
ZPE correction: 0.01018 a.u. [0.01019 a.u.]

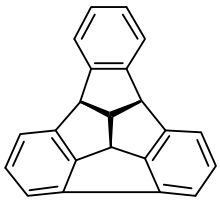

M06-2X/6-311G(d,p)
point group: $C_s$
total energy: -846.55442 a.u.
ZPE correction: 0.29075 a.u.

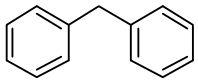


M06-2X/6-311G(d,p)
point group: $C_2$
total energy: -502.51227 a.u.
ZPE correction: 0.21190 a.u.

| | x | y | z | | x | y | z |
|---|---|---|---|---|---|---|---|
| C | 0.000000 | 0.000000 | 1.484424 | H | -0.043772 | 4.500782 | -1.496507 |
| H | -0.877592 | -0.003508 | 2.138076 | C | 0.000000 | -1.263644 | 0.650121 |
| H | 0.877592 | 0.003508 | 2.138076 | C | 0.984466 | -1.461006 | -0.321026 |
| C | 0.000000 | 1.263644 | 0.650121 | C | -0.968732 | -2.247735 | 0.829636 |
| C | 0.968732 | 2.247735 | 0.829636 | C | 1.003739 | -2.619005 | -1.085626 |
| C | -0.984466 | 1.461006 | -0.321026 | H | 1.732809 | -0.690813 | -0.480139 |
| C | 0.955198 | 3.409575 | 0.061695 | C | -0.955198 | -3.409575 | 0.061695 |
| H | 1.741416 | 2.104612 | 1.578119 | H | -1.741416 | -2.104612 | 1.578119 |
| C | -1.003739 | 2.619005 | -1.085626 | C | 0.031664 | -3.598572 | -0.896684 |
| H | -1.732809 | 0.690813 | -0.480139 | H | 1.774924 | -2.758029 | -1.834350 |
| C | -0.031664 | 3.598572 | -0.896684 | H | -1.717928 | -4.164571 | 0.212839 |
| H | 1.717928 | 4.164571 | 0.212839 | H | 0.043772 | -4.500782 | -1.496507 |
| H | -1.774924 | 2.758029 | -1.834350 | | | | |

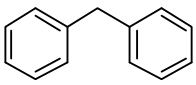

2nd conformer

M06-2X/6-311G(d,p)
point group: $C_1$
total energy: -502.51175 a.u.
ZPE correction: 0.21109 a.u.

| | x | y | z | | x | y | z |
|---|---|---|---|---|---|---|---|
| C | -0.055944 | -1.443079 | -0.100302 | H | -4.506254 | 1.626995 | 0.015899 |
| H | -0.091097 | -2.029926 | -1.023840 | C | 1.258683 | -0.709264 | -0.027127 |
| H | -0.118884 | -2.160805 | 0.723448 | C | 1.756563 | -0.274108 | 1.201945 |
| C | -1.284928 | -0.547642 | -0.051546 | C | 1.978188 | -0.412499 | -1.183020 |
| C | -1.210281 | 0.835296 | -0.199962 | C | 2.948545 | 0.435886 | 1.274441 |
| C | -2.540731 | -1.134103 | 0.124435 | H | 1.198697 | -0.493268 | 2.106909 |
| C | -2.365484 | 1.613249 | -0.175976 | C | 3.171952 | 0.299446 | -1.115778 |
| H | -0.244892 | 1.310639 | -0.331137 | H | 1.597974 | -0.741824 | -2.144699 |
| C | -3.693285 | -0.361147 | 0.147853 | C | 3.660222 | 0.724940 | 0.113797 |
| H | -2.610702 | -2.211017 | 0.244663 | H | 3.323513 | 0.764280 | 2.236737 |
| C | -3.608812 | 1.020232 | -0.003414 | H | 3.720221 | 0.520576 | -2.023993 |
| H | -2.288795 | 2.688173 | -0.291669 | H | 4.590165 | 1.278078 | 0.168789 |
| H | -4.658079 | -0.835134 | 0.286826 | | | | |

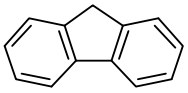

M06-2X/6-311G(d,p)
point group: $C_{2v}$
total energy: -501.32274 a.u.
ZPE correction: 0.18910 a.u.

M06-2X/6-311G(d,p)
point group: $D_{6h}$
total energy: -232.19613 a.u.
ZPE correction: 0.10111 a.u.

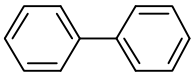

M06-2X/6-311G(d,p)
point group: $D_2$
total energy: -463.21146 a.u.
ZPE correction: 0.18232 a.u.

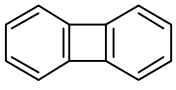

M06-2X/6-311G(d,p)
point group: $D_{2h}$
total energy: -461.93855 a.u.
ZPE correction: 0.15908 a.u.

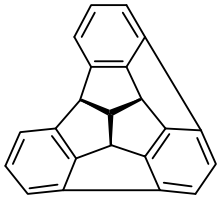

M06-2X/6-311G(d,p)
point group: $C_s$
total energy: -845.26180 a.u.
ZPE correction: 0.26793 a.u.

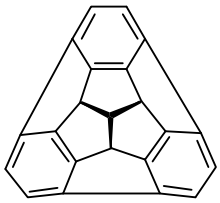

M06-2X/6-311G(d,p)
point group: $C_{3v}$
total energy: -843.96361 a.u.
ZPE correction: 0.24550 a.u.

**74**

| | x | y | z | | x | y | z |
|---|---|---|---|---|---|---|---|
| C | 1.560489 | 1.677377 | -1.624183 | C | -0.681422 | 1.954281 | -0.468815 |
| C | 0.681422 | 1.954281 | -0.468815 | C | -1.560489 | 1.677377 | -1.624183 |
| C | 1.121125 | 1.421446 | 0.841712 | C | -2.232895 | 0.512735 | -1.624183 |
| C | 1.791571 | 0.260200 | 0.841712 | C | -2.033168 | -0.387012 | -0.468815 |
| C | 2.033168 | -0.387012 | -0.468815 | C | -1.791571 | 0.260200 | 0.841712 |
| C | 2.232895 | 0.512735 | -1.624183 | C | -1.121125 | 1.421446 | 0.841712 |
| H | 1.605650 | 2.353835 | -2.469726 | H | -1.605650 | 2.353835 | -2.469726 |
| H | 2.841306 | 0.213616 | -2.469726 | H | -2.841306 | 0.213616 | -2.469726 |
| C | -0.670446 | -1.681646 | 0.841712 | C | 0.000000 | 1.437482 | 1.866630 |
| C | -1.351746 | -1.567269 | -0.468815 | C | 0.000000 | 0.000000 | 2.495331 |
| C | -0.672406 | -2.190112 | -1.624183 | H | 0.000000 | 0.000000 | 3.584158 |
| C | 0.672406 | -2.190112 | -1.624183 | C | 1.244896 | -0.718741 | 1.866630 |
| C | 1.351746 | -1.567269 | -0.468815 | H | 1.968759 | -1.136664 | 2.569716 |
| C | 0.670446 | -1.681646 | 0.841712 | C | -1.244896 | -0.718741 | 1.866630 |
| H | -1.235656 | -2.567451 | -2.469726 | H | -1.968759 | -1.136664 | 2.569716 |
| H | 1.235656 | -2.567451 | -2.469726 | H | 0.000000 | 2.273328 | 2.569716 |

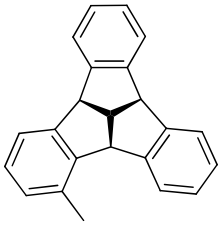

M06-2X/6-311G(d,p) with ultrafine grid for two-electron integrals
point group: $C_1$
total energy: -887.15380 a.u.
ZPE correction: 0.34208 a.u.

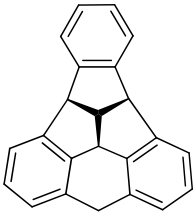

M06-2X/6-311G(d,p) with ultrafine grid for two-electron integrals
point group: $C_s$
total energy: -885.94171 a.u.
ZPE correction: 0.32115 a.u.

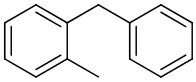

M06-2X/6-311G(d,p) with ultrafine grid for two-electron integrals
point group: $C_1$
total energy: -541.82029 a.u.
ZPE correction: 0.23909 a.u.

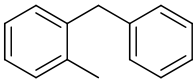

M06-2X/6-311G(d,p) with ultrafine grid for two-electron integrals
point group: $C_s$
total energy: -541.81877 a.u.
ZPE correction: 0.23894 a.u.

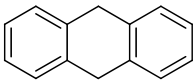

M06-2X/6-311G(d,p) with ultrafine grid for two-electron integrals
point group: $C_{2v}$
total energy: -540.62845 a.u.
ZPE correction: 0.21848 a.u.

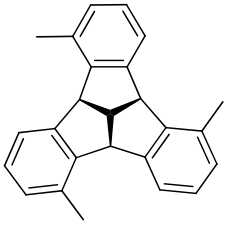

M06-2X/6-311G(d,p) with ultrafine grid for two-electron integrals
point group: $C_3$
total energy: -965.76374 a.u.
ZPE correction: 0.39859 a.u.

Comment: The use of an ultrafine grid for the computation of two-electron integrals and their derivatives was necessary to maintain the $C_3$-symmetry of 1,5,9-trimethyltribenzotriquinacene in the calculations.

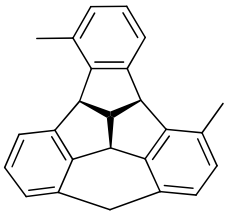

M06-2X/6-311G(d,p) with ultrafine grid for two-electron integrals
point group: $C_1$
total energy: -964.55350 a.u.
ZPE correction: 0.37726 a.u.

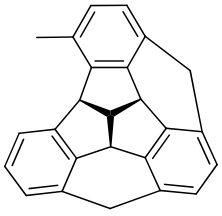

M06-2X/6-311G(d,p) with ultrafine grid for two-electron integrals
point group: $C_1$
total energy: -963.34018 a.u.
ZPE correction: 0.35622 a.u.

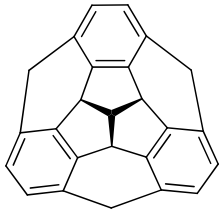

**75**

M06-2X/6-311G(d,p) with ultrafine grid for two-electron integrals
point group: $C_{3v}$
total energy: -962.12674 a.u.
ZPE correction: 0.33569 a.u.

| | x | y | z | | x | y | z |
|---|---|---|---|---|---|---|---|
| C | 2.102285 | 2.023137 | -1.337804 | C | -1.180933 | 1.479977 | 0.786747 |
| C | 1.207832 | 2.333821 | -0.313530 | H | -2.157977 | 2.659926 | -2.214834 |
| C | 1.180933 | 1.479977 | 0.786747 | H | -3.382552 | 0.538900 | -2.214834 |
| C | 1.872164 | 0.282729 | 0.786747 | C | 0.000000 | 1.441436 | 1.731359 |
| C | 2.625064 | -0.120897 | -0.313530 | C | 0.000000 | 0.000000 | 2.332914 |
| C | 2.803231 | 0.809064 | -1.337804 | H | 0.000000 | 0.000000 | 3.420857 |
| H | 2.157977 | 2.659926 | -2.214834 | C | 1.248320 | -0.720718 | 1.731359 |
| H | 3.382552 | 0.538900 | -2.214834 | C | -1.248320 | -0.720718 | 1.731359 |
| C | -0.691231 | -1.762706 | 0.786747 | C | 0.000000 | 3.260354 | -0.459799 |
| C | -1.417232 | -2.212924 | -0.313530 | H | 0.000000 | 3.761603 | -1.428706 |
| C | -0.700946 | -2.832201 | -1.337804 | C | 2.823549 | -1.630177 | -0.459799 |
| C | 0.700946 | -2.832201 | -1.337804 | H | 3.257644 | -1.880802 | -1.428706 |
| C | 1.417232 | -2.212924 | -0.313530 | C | -2.823549 | -1.630177 | -0.459799 |
| C | 0.691231 | -1.762706 | 0.786747 | H | -3.257644 | -1.880801 | -1.428706 |
| H | -1.224575 | -3.198826 | -2.214834 | H | 1.942638 | -1.121583 | 2.475292 |
| H | 1.224575 | -3.198826 | -2.214834 | H | 0.000000 | 2.243165 | 2.475292 |
| C | -1.207832 | 2.333821 | -0.313530 | H | -1.942638 | -1.121583 | 2.475292 |
| C | -2.102285 | 2.023137 | -1.337804 | H | -3.486737 | -2.013069 | 0.322648 |
| C | -2.803231 | 0.809064 | -1.337804 | H | 0.000000 | 4.026137 | 0.322648 |
| C | -2.625064 | -0.120897 | -0.313530 | H | 3.486737 | -2.013069 | 0.322648 |
| C | -1.872164 | 0.282729 | 0.786747 | | | | |

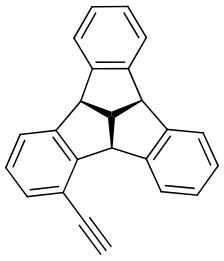

M06-2X/6-311G(d,p)
point group: $C_1$
total energy: -923.98764 a.u.
ZPE correction: 0.32310 a.u.

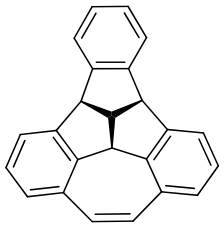

M06-2X/6-311G(d,p)
point group: $C_s$
total energy: -924.04910 a.u.
ZPE correction: 0.32692 a.u.

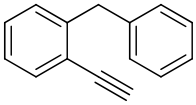

M06-2X/6-311G(d,p)
point group: $C_s$
total energy: -578.65192 a.u.
ZPE correction: 0.22036 a.u.

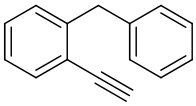

M06-2X/6-311G(d,p)
point group: $C_1$ (1st conformer)
total energy: -578.65152 a.u.
ZPE correction: 0.22068 a.u.

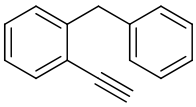

M06-2X/6-311G(d,p)
point group: $C_1$ (2nd conformer)
total energy: -578.65148 a.u.
ZPE correction: 0.22010 a.u.

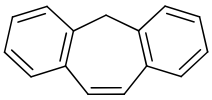

M06-2X/6-311G(d,p)
point group: $C_s$
total energy: -578.71359 a.u.
ZPE correction: 0.22458 a.u.

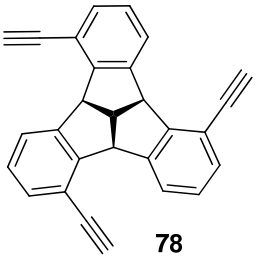

**78**

M06-2X/6-311G(d,p)
point group: $C_3$
total energy: -1076.26593 a.u.
ZPE correction: 0.34178 a.u.

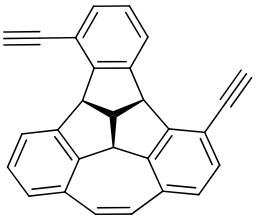

**79**

M06-2X/6-311G(d,p)
point group: $C_1$
total energy: -1076.32842 a.u.
ZPE correction: 0.34553 a.u.

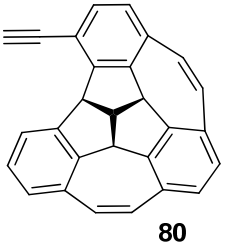

**80**

M06-2X/6-311G(d,p)
point group: $C_1$
total energy: -1076.38811 a.u.
ZPE correction: 0.34928 a.u.

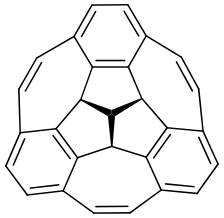

**76**

M06-2X/6-311G(d,p)
point group: $C_{3v}$
total energy: -1076.44570 a.u.
ZPE correction: 0.35249 a.u.

| | x | y | z | | x | y | z |
|---|---|---|---|---|---|---|---|
| C | -0.693709 | 3.549296 | -0.979425 | H | -4.283387 | -1.057790 | -1.626751 |
| C | -1.427392 | 2.612664 | -0.226043 | H | -3.057767 | -3.180627 | -1.626751 |
| C | -0.693239 | 1.795465 | 0.627635 | C | -1.250174 | 0.721789 | 1.519896 |
| C | 0.693239 | 1.795465 | 0.627635 | C | 0.000000 | 0.000000 | 2.112040 |
| C | 1.427392 | 2.612664 | -0.226043 | H | 0.000000 | 0.000000 | 3.199834 |
| C | 0.693709 | 3.549296 | -0.979425 | C | 1.250174 | 0.721789 | 1.519896 |
| H | -1.225620 | 4.238417 | -1.626751 | H | 1.942290 | 1.121381 | 2.266943 |
| H | 1.225620 | 4.238417 | -1.626751 | C | 0.000000 | -1.443577 | 1.519896 |
| C | 1.208299 | -1.498095 | 0.627635 | H | 0.000000 | -2.242763 | 2.266943 |
| C | 1.548937 | -2.542489 | -0.226043 | H | -1.942290 | 1.121381 | 2.266943 |
| C | 2.726926 | -2.375418 | -0.979425 | C | -3.547979 | 1.268768 | -0.421589 |
| C | 3.420635 | -1.173878 | -0.979425 | H | -4.593891 | 1.299774 | -0.715226 |
| C | 2.976329 | -0.070175 | -0.226043 | C | -2.872775 | 2.438256 | -0.421589 |
| C | 1.901538 | -0.297370 | 0.627635 | H | -3.422583 | 3.328539 | -0.715226 |
| H | 3.057767 | -3.180627 | -1.626751 | C | 3.547979 | 1.268768 | -0.421589 |
| H | 4.283387 | -1.057790 | -1.626751 | H | 4.593891 | 1.299774 | -0.715226 |
| C | -2.976329 | -0.070175 | -0.226043 | C | 2.872775 | 2.438256 | -0.421589 |
| C | -3.420635 | -1.173878 | -0.979425 | C | 0.675204 | -3.707024 | -0.421589 |
| C | -2.726926 | -2.375418 | -0.979425 | C | -0.675204 | -3.707024 | -0.421589 |
| C | -1.548937 | -2.542489 | -0.226043 | H | -1.171308 | -4.628313 | -0.715226 |
| C | -1.208299 | -1.498095 | 0.627635 | H | 3.422583 | 3.328539 | -0.715226 |
| C | -1.901538 | -0.297370 | 0.627635 | H | 1.171308 | -4.628313 | -0.715226 |

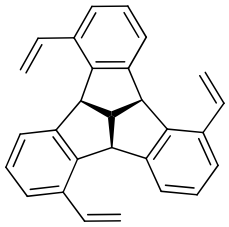

M06-2X/6-311G(d,p)
point group: $C_3$
total energy: -1079.99480 a.u.
ZPE correction: 0.41317 a.u.

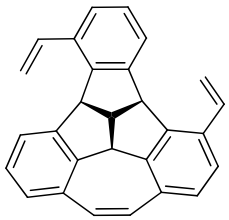

M06-2X/6-311G(d,p)
point group: $C_1$
total energy: -1078.81470 a.u.
ZPE correction: 0.39281 a.u.

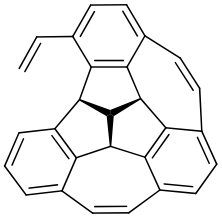

M06-2X/6-311G(d,p)
point group: $C_1$
total energy: -1077.63144 a.u.
ZPE correction: 0.37316 a.u.

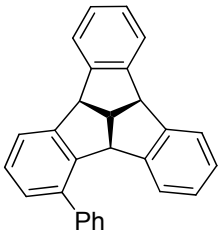


M06-2X/6-311G(d,p)
point group: $C_1$
total energy: -1078.86412 a.u.
ZPE correction: 0.39534 a.u.

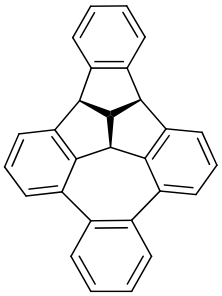

M06-2X/6-311G(d,p)
point group: $C_s$
total energy: -1077.67798 a.u.
ZPE correction: 0.37453 a.u.

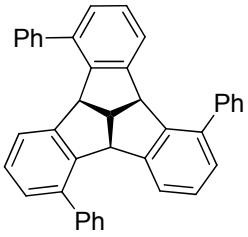


M06-2X/6-311G(d,p)
point group: $C_3$
total energy: -1540.89434 a.u.
ZPE correction: 0.55873 a.u.

| | x | y | z | | x | y | z |
|---|---|---|---|---|---|---|---|
| C | 0.370944 | -3.955512 | -0.850598 | H | -0.997942 | 3.701743 | -0.173296 |
| C | 1.172292 | -3.034767 | -0.171719 | C | 1.500685 | 3.916056 | -0.133371 |
| C | 0.552493 | -1.950958 | 0.464426 | C | 1.246841 | 4.554054 | 1.082689 |
| C | -0.837588 | -1.828565 | 0.447264 | C | 1.239763 | 4.602811 | -1.320962 |
| C | -1.627322 | -2.777185 | -0.196734 | C | 0.709480 | 5.835423 | 1.111270 |
| C | -1.012222 | -3.831924 | -0.859820 | H | 1.483020 | 4.043590 | 2.009526 |
| H | 0.845732 | -4.798789 | -1.340542 | C | 0.701586 | 5.884407 | -1.293913 |
| H | -1.617056 | -4.575331 | -1.365575 | H | 1.428943 | 4.108536 | -2.267452 |
| C | -1.164789 | 1.639655 | 0.447264 | C | 0.425380 | 6.500474 | -0.077538 |
| C | -1.591452 | 2.797895 | -0.196734 | H | 0.516120 | 6.317464 | 2.062343 |
| C | -2.812433 | 2.792572 | -0.859820 | H | 0.488943 | 6.398645 | -2.223810 |

| | | | |
|---|---|---|---|
| C | -3.611046 | 1.656509 | -0.850598 |
| C | -3.214331 | 0.502149 | -0.171719 |
| C | -1.965826 | 0.497006 | 0.464426 |
| H | -3.153824 | 3.688077 | -1.365575 |
| H | -4.578739 | 1.666969 | -1.340542 |
| C | 3.218774 | -0.020710 | -0.196734 |
| C | 3.824654 | 1.039352 | -0.859820 |
| C | 3.240102 | 2.299003 | -0.850598 |
| C | 2.042040 | 2.532618 | -0.171719 |
| C | 1.413333 | 1.453952 | 0.464426 |
| C | 2.002378 | 0.188910 | 0.447264 |
| H | 4.770881 | 0.887253 | -1.365575 |
| H | 3.733007 | 3.131820 | -1.340542 |
| C | 1.198940 | -0.819129 | 1.250713 |
| C | 0.000000 | 0.000000 | 1.811649 |
| H | 0.000000 | 0.000000 | 2.900466 |
| C | -1.308856 | -0.628748 | 1.250713 |
| H | -1.965414 | -0.970461 | 2.054171 |
| C | 0.109916 | 1.447877 | 1.250713 |
| H | 0.142263 | 2.187328 | 2.054171 |
| H | 1.823150 | -1.216868 | 2.054171 |
| H | -2.706832 | -2.715115 | -0.173296 |
| H | 3.704775 | -0.986628 | -0.173296 |
| H | 0.000000 | 7.496595 | -0.055733 |
| C | -4.141746 | -0.658397 | -0.133371 |
| C | -4.567347 | -1.197231 | 1.082689 |
| C | -4.606033 | -1.227739 | -1.320962 |
| C | -5.408364 | -2.303284 | 1.111270 |
| H | -4.243362 | -0.737461 | 2.009526 |
| C | -5.446839 | -2.334613 | -1.293913 |
| H | -4.272568 | -0.816767 | -2.267452 |
| C | -5.842266 | -2.881847 | -0.077538 |
| H | -5.729144 | -2.711759 | 2.062343 |
| H | -5.785861 | -2.775886 | -2.223810 |
| H | -6.492242 | -3.748298 | -0.055733 |
| C | 2.641061 | -3.257659 | -0.133371 |
| C | 3.320506 | -3.356823 | 1.082689 |
| C | 3.366270 | -3.375072 | -1.320962 |
| C | 4.698885 | -3.532139 | 1.111270 |
| H | 2.760341 | -3.306128 | 2.009526 |
| C | 4.745253 | -3.549795 | -1.293913 |
| H | 2.843625 | -3.291769 | -2.267452 |
| C | 5.416885 | -3.618627 | -0.077538 |
| H | 5.213024 | -3.605704 | 2.062343 |
| H | 5.296918 | -3.622759 | -2.223810 |
| H | 6.492242 | -3.748298 | -0.055733 |

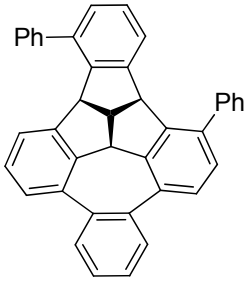


M06-2X/6-311G(d,p)
point group: $C_1$
total energy: -1539.70987 a.u.
ZPE correction: 0.53717 a.u.

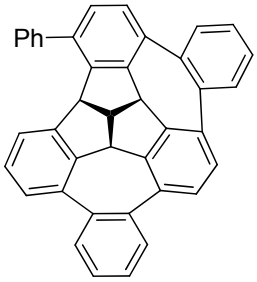


M06-2X/6-311G(d,p)
point group: $C_1$
total energy: -1538.52358 a.u.
ZPE correction: 0.51611 a.u.

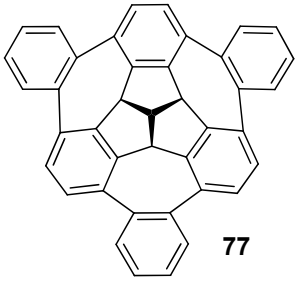

**77**

M06-2X/6-311G(d,p)
point group: $C_{3v}$
total energy: -1537.33606 a.u.
ZPE correction: 0.49468 a.u.

| | x | y | z | | x | y | z |
|---|---|---|---|---|---|---|---|
| C | -0.695364 | 3.421504 | -0.949512 | H | -1.939092 | 1.119535 | 2.433040 |
| C | -1.427367 | 2.579422 | -0.100288 | C | -0.707922 | -3.769588 | -0.167544 |
| C | -0.693144 | 1.793041 | 0.781743 | C | 0.707922 | -3.769588 | -0.167544 |
| C | 0.693144 | 1.793041 | 0.781743 | C | -1.378840 | -4.992524 | -0.284753 |
| C | 1.427367 | 2.579422 | -0.100288 | C | 1.378840 | -4.992524 | -0.284753 |
| C | 0.695364 | 3.421504 | -0.949512 | C | -0.695118 | -6.193394 | -0.393992 |
| H | -1.224099 | 4.037763 | -1.668159 | H | -2.462985 | -4.990790 | -0.270520 |
| H | 1.224099 | 4.037763 | -1.668159 | C | 0.695118 | -6.193394 | -0.393992 |
| C | 1.206247 | -1.496801 | 0.781743 | H | 2.462985 | -4.990790 | -0.270520 |
| C | 1.520162 | -2.525847 | -0.100288 | H | -1.244107 | -7.124267 | -0.469432 |
| C | 2.615427 | -2.312955 | -0.949512 | H | 1.244107 | -7.124267 | -0.469432 |
| C | 3.310791 | -1.108549 | -0.949512 | C | 3.618520 | 1.271716 | -0.167544 |
| C | 2.947529 | -0.053575 | -0.100288 | C | 2.910598 | 2.497872 | -0.167544 |
| C | 1.899391 | -0.296240 | 0.781743 | C | 5.013073 | 1.302151 | -0.284753 |
| H | 2.884756 | -3.078982 | -1.668159 | C | 3.634233 | 3.690372 | -0.284753 |
| H | 4.108855 | -0.958781 | -1.668159 | C | 5.711195 | 2.494707 | -0.393992 |
| C | -2.947529 | -0.053575 | -0.100288 | H | 5.553643 | 0.362387 | -0.270520 |
| C | -3.310791 | -1.108549 | -0.949512 | C | 5.016077 | 3.698687 | -0.393992 |
| C | -2.615427 | -2.312955 | -0.949512 | H | 3.090658 | 4.628403 | -0.270520 |
| C | -1.520162 | -2.525847 | -0.100288 | H | 6.791850 | 2.484705 | -0.469432 |
| C | -1.206247 | -1.496801 | 0.781743 | H | 5.547743 | 4.639562 | -0.469432 |
| C | -1.899391 | -0.296240 | 0.781743 | C | -2.910598 | 2.497872 | -0.167544 |
| H | -4.108855 | -0.958781 | -1.668159 | C | -3.618520 | 1.271716 | -0.167544 |
| H | -2.884756 | -3.078982 | -1.668159 | C | -3.634233 | 3.690372 | -0.284753 |
| C | -1.250680 | 0.722080 | 1.681716 | C | -5.013073 | 1.302151 | -0.284753 |
| C | 0.000000 | 0.000000 | 2.272474 | C | -5.016077 | 3.698687 | -0.393992 |
| H | 0.000000 | 0.000000 | 3.360297 | H | -3.090658 | 4.628403 | -0.270520 |
| C | 1.250680 | 0.722080 | 1.681716 | C | -5.711195 | 2.494707 | -0.393992 |
| H | 1.939092 | 1.119535 | 2.433040 | H | -5.553643 | 0.362387 | -0.270520 |
| C | 0.000000 | -1.444161 | 1.681716 | H | -5.547743 | 4.639562 | -0.469432 |
| H | 0.000000 | -2.239070 | 2.433040 | H | -6.791850 | 2.484705 | -0.469432 |

## 4.2.6 Rearrangement of hydrocarbon 98

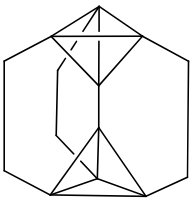

**98**

B3LYP/6-31G(d)
point group: $D_3$
total energy: -540.05882 a.u.
ZPE correction: 0.20645 a.u.
enthalpy (298.15 K): -539.83993 a.u.

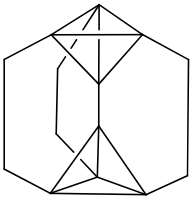

**98**

MP2/cc-pVDZ
point group: $D_3$
total energy: -538.38566 a.u.
SCS-total energy: -538.31762 a.u.
ZPE correction: 0.20560 a.u.
enthalpy (298.15 K): -538.16767 a.u.
SCS-enthalpy (298.15 K): -538.09963 a.u.

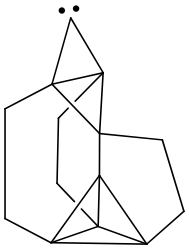

**99**

B3LYP/6-31G(d), singlet
point group: $C_s$
total energy: -540.23101 a.u.
ZPE correction: 0.21090 a.u.
enthalpy (298.15 K): -540.00838 a.u.

| | x | y | z |
|---|---|---|---|
| C | -0.589352 | 1.979422 | 0.000000 |
| C | -1.359192 | 0.815679 | 0.796577 |
| C | -1.359192 | 0.815679 | -0.796577 |
| C | -0.231712 | 0.579414 | 0.000000 |
| C | 1.013795 | -0.067997 | 0.000000 |
| C | 0.815166 | -1.314661 | -0.830822 |
| C | 0.815166 | -1.314661 | 0.830822 |
| C | 1.263776 | -2.404122 | 0.000000 |
| C | -0.365614 | -1.383682 | -1.827981 |
| H | 0.026221 | -1.705576 | -2.801666 |
| H | -1.027550 | -2.191238 | -1.498302 |
| C | 1.960895 | 1.181484 | 0.000000 |
| H | 2.609789 | 1.197054 | -0.881905 |
| H | 2.609789 | 1.197054 | 0.881905 |
| C | -0.365614 | -1.383682 | 1.827981 |
| H | 0.026221 | -1.705576 | 2.801666 |
| H | -1.027550 | -2.191238 | 1.498302 |
| C | -1.229481 | -0.065313 | -2.040261 |
| H | -0.728317 | 0.570579 | -2.781431 |
| H | -2.192070 | -0.345900 | -2.480958 |
| C | -1.229481 | -0.065313 | 2.040261 |
| H | -2.192070 | -0.345900 | 2.480958 |
| H | -0.728317 | 0.570579 | 2.781431 |
| C | 0.931442 | 2.431447 | 0.000000 |
| H | 1.100122 | 3.064002 | -0.876731 |
| H | 1.100122 | 3.064002 | 0.876731 |

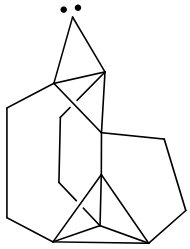

**99**

MP2/cc-pVDZ, singlet
point group: $C_1$ *
total energy: -538.55568 a.u.
SCS-total energy: -538.49702 a.u.
ZPE correction: 0.21032 a.u.
enthalpy (298.15 K): -538.33363 a.u.
SCS-enthalpy (298.15 K): -538.27498 a.u.
* The $C_s$ geometry was a transition state at this level of theory.

| | x | y | z | | x | y | z |
|---|---|---|---|---|---|---|---|
| C | -1.999488 | -0.033184 | -0.596864 | H | -1.187428 | -1.237329 | 2.351406 |
| C | -0.825165 | -0.806737 | -1.377036 | C | 1.443824 | -1.701791 | -0.481795 |
| C | -0.848234 | 0.801195 | -1.354212 | H | 1.950979 | -2.646105 | -0.211149 |
| C | -0.565887 | -0.010302 | -0.223647 | H | 2.116131 | -1.191573 | -1.195627 |
| C | 0.071004 | -0.039228 | 1.027645 | C | -0.009476 | 2.070257 | -1.144081 |
| C | 1.286924 | 0.855968 | 0.857650 | H | -0.672483 | 2.728010 | -0.549162 |
| C | 1.355310 | -0.821530 | 0.785506 | H | 0.222826 | 2.612865 | -2.076425 |
| C | 2.434896 | 0.038280 | 1.251502 | C | 0.091665 | -2.026615 | -1.222447 |
| C | 1.330308 | 1.829733 | -0.345003 | H | 0.317182 | -2.538114 | -2.173846 |
| H | 1.715924 | 2.801797 | 0.014513 | H | -0.500829 | -2.733757 | -0.609681 |
| H | 2.091870 | 1.445698 | -1.047263 | C | -2.398718 | 0.031215 | 0.944847 |
| C | -1.173005 | -0.207760 | 1.953202 | H | -2.792683 | 1.054591 | 1.079843 |
| H | -1.193246 | 0.487093 | 2.810284 | H | -3.231994 | -0.660187 | 1.155506 |

**TS (98 ⟶ 99)**

B3LYP/6-31G(d)
point group: $C_1$
total energy: -540.04689 a.u.
ZPE correction: 0.20555 a.u.
enthalpy (298.15 K): -539.82920 a.u.

| | x | y | z | | x | y | z |
|---|---|---|---|---|---|---|---|
| C | -0.741449 | 0.915499 | 1.431649 | H | -0.951922 | 2.765474 | -1.621099 |
| C | 0.472294 | 0.081059 | 2.149882 | C | 2.402145 | 0.132327 | -0.437644 |
| C | -0.845010 | -0.666759 | 1.496003 | H | 2.683577 | 1.187447 | -0.529241 |
| C | 0.040845 | 0.035297 | 0.685278 | H | 3.300100 | -0.453496 | -0.667064 |
| C | 0.215633 | -0.041097 | -0.623230 | C | -1.474603 | -1.786151 | 0.636386 |
| C | -0.135064 | -0.935283 | -1.649440 | H | -2.528411 | -1.514641 | 0.506303 |
| C | 1.281870 | -0.062362 | -1.542649 | H | -1.472781 | -2.746115 | 1.162390 |
| C | -0.189522 | 0.697387 | -1.744142 | C | 2.045555 | -0.163103 | 1.138626 |
| C | -0.837462 | -2.078995 | -0.862399 | H | 2.176300 | -1.224658 | 1.359042 |
| H | -1.633686 | -2.543851 | -1.452486 | H | 2.741173 | 0.414182 | 1.750156 |
| H | -0.059899 | -2.843207 | -0.741986 | C | -1.087879 | 2.087101 | 0.491565 |
| C | -1.107133 | 1.797994 | -1.133586 | H | -2.050589 | 2.548884 | 0.733715 |
| H | -2.122499 | 1.483230 | -1.402577 | H | -0.322689 | 2.849265 | 0.685056 |

**TS (98 → 99)**

MP2/cc-pVDZ
point group: $C_1$

| | |
|---|---|
| total energy: | -538.37796 a.u. |
| SCS-total energy: | -538.30940 a.u. |
| ZPE correction: | 0.20445 a.u. |
| enthalpy (298.15 K): | -538.16141 a.u. |
| SCS-enthalpy (298.15 K): | -538.09285 a.u. |

| | x | y | z | | x | y | z |
|---|---|---|---|---|---|---|---|
| C | 0.953149 | -0.799388 | 1.415203 | H | 1.715823 | -2.282238 | -1.774146 |
| C | -0.447592 | -0.288298 | 2.157932 | C | -2.250271 | -0.720206 | -0.439943 |
| C | 0.694447 | 0.768959 | 1.551628 | H | -2.157895 | -1.818213 | -0.540340 |
| C | -0.036812 | -0.086423 | 0.689046 | H | -3.303477 | -0.460635 | -0.657590 |
| C | -0.216438 | 0.019077 | -0.611778 | C | 1.041318 | 2.009700 | 0.688444 |
| C | -0.127343 | 1.027761 | -1.623205 | H | 2.117212 | 1.897995 | 0.455422 |
| C | -1.264877 | -0.179273 | -1.578311 | H | 0.942947 | 2.949482 | 1.259268 |
| C | 0.347307 | -0.527080 | -1.799638 | C | -1.995602 | -0.329667 | 1.123212 |
| C | 0.240332 | 2.245798 | -0.716002 | H | -2.308805 | 0.713165 | 1.310085 |
| H | 0.806735 | 3.015973 | -1.268416 | H | -2.617836 | -1.007342 | 1.732861 |
| H | -0.744649 | 2.688754 | -0.471132 | C | 1.501643 | -1.805688 | 0.375829 |
| C | 1.523732 | -1.361732 | -1.195927 | H | 2.526761 | -2.141907 | 0.610730 |
| H | 2.401656 | -0.705246 | -1.349788 | H | 0.843552 | -2.691027 | 0.474099 |

## 4.3 Compliance constants of three-membered rings by various DFT methods

Calculations with 6-311G(d,p) basis set:

| | bond length [Å] / relaxed force constant [N cm$^{-1}$] (% of ethane) | | |
|---|---|---|---|
| | $H_3C-CH_3$ |  |  |
| CCSD(T) | 1.530 / 4.19 | 1.511 / 4.03 (96) | 1.485 / 3.90 (93) |
| QCISD | 1.531 / 4.20 | 1.511 / 4.03 (96) | 1.485 / 3.91 (93) |
| B3LYP | 1.531 / 4.05 | 1.508 / 4.03 (100) | 1.479 / 4.12 (102) |
| M06-2X | 1.527 / 4.29 | 1.502 / 4.39 (102) | 1.471 / 4.62 (108) |
| B97-D | 1.538 / 3.73 | 1.514 / 3.83 (103) | 1.481 / 4.16 (112) |
| B1B95 | 1.520 / 4.31 | 1.498 / 4.37 (101) | 1.471 / 4.50 (104) |
| B3PW91 | 1.525 / 4.20 | 1.504 / 4.20 (100) | 1.476 / 4.30 (102) |
| PW91PW91 | 1.531 / 3.97 | 1.511 / 3.94 (99) | 1.485 / 3.95 (99) |
| mPW1PW91 | 1.522 / 4.30 | 1.502 / 4.28 (100) | 1.474 / 4.40 (102) |
| PBEPBE | 1.531 / 3.98 | 1.511 / 3.97 (100) | 1.486 / 3.98 (100) |

**Table 22.** Performance of DFT methods on three-membered rings (basis set: 6-311G(d,p); CCSD(T)/aug-cc-pVTZ and QCISD/6-311+G(2d,p) as references)

With this basis set, no functional gives a qualitatively correct result for the relaxed force constant of tetrahedrane. The modern functionals M06-2X and B97-D show surprisingly large deviations.

Calculations with 6-311+G(2d,p) basis set:

| | bond length [Å] / relaxed force constant [N cm$^{-1}$] (% of ethane) | | |
|---|---|---|---|
| | $H_3C-CH_3$ |  |  |
| CCSD(T) | 1.530 / 4.19 | 1.511 / 4.03 (96) | 1.485 / 3.90 (93) |
| QCISD | 1.531 / 4.20 | 1.511 / 4.03 (96) | 1.485 / 3.91 (93) |
| B3LYP | 1.529 / 4.01 | 1.507 / 3.93 (98) | 1.477 / 3.96 (99) |
| M06-2X | 1.525 / 4.25 | 1.501 / 4.28 (101) | 1.471 / 4.44 (104) |
| B97-D | 1.537 / 3.67 | 1.514 / 3.70 (101) | 1.481 / 3.98 (108) |
| B1B95 | 1.518 / 4.28 | 1.497 / 4.26 (100) | 1.469 / 4.34 (101) |
| B3PW91 | 1.523 / 4.16 | 1.502 / 4.11 (99) | 1.474 / 4.15 (100) |
| **PW91PW91** | **1.529 / 3.93** | **1.511 / 3.82 (97)** | **1.484 / 3.78 (96)** |
| mPW1PW91 | 1.521 / 4.26 | 1.500 / 4.19 (98) | 1.472 / 4.24 (100) |
| **PBEPBE** | **1.530 / 3.94** | **1.511 / 3.85 (98)** | **1.485 / 3.81 (97)** |

**Table 23.** Performance of DFT methods on three-membered rings (basis set: 6-311+G(2d,p); CCSD(T)/aug-cc-pVTZ and QCISD/6-311+G(2d,p) as references)

PW91PW91 and PBEPBE are the only functionals that give a qualitatively correct result for the relaxed force constant of tetrahedrane. The modern functionals M06-2X and B97-D show surprisingly large deviations.

## 4.4 Calculated compliance constants

This section contains the B3LYP/6-31G(d) data points of Graph 2 that were not included in the tables or text, as these peripheral bonds were not at the focus of the respective chapter. The presented values have the following meaning:

| bond length in Å / relaxed force constant in N $cm^{-1}$ (% of ethane) |
|---|

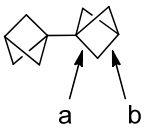


a) 1.565 / 3.27 (78)

b) 1.554 / 3.55 (85)

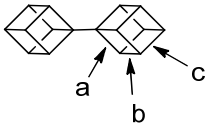


a) 1.581 / 3.37 (80)

b) 1.568 / 3.68 (88)

c) 1.570 / 3.66 (87)

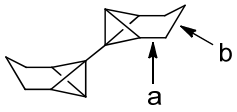


a) 1.530 / 4.02 (96)

b) 1.538 / 3.94 (94)

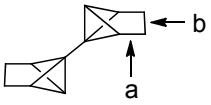


a) 1.534 / 3.84 (92)

b) 1.558 / 3.68 (88)

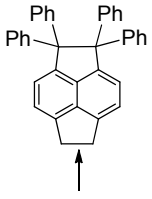


1.583 / 3.33 (79)

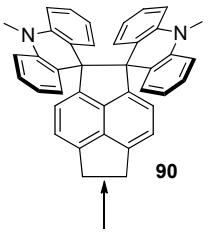


**90**

1.584 / 3.33 (79)

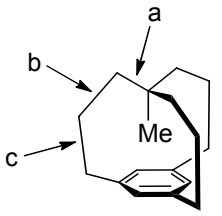


**92**

a) 1.594 / 2.71 (65)

b) 1.629 / 2.21 (53)

c) 1.661 / 1.74 (41)

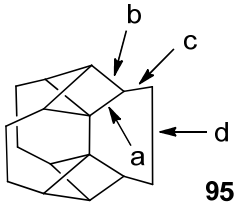


**95**

a) 1.502 / 4.58 (109)

b) 1.636 / 2.03 (48)

c) 1.564 / 3.16 (75)

d) 1.617 / 2.50 (60)

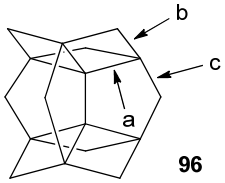


**96**

a) 1.468 / 5.89 (141)

b) 1.621 / 2.48 (59)

c) 1.622 / 2.20 (53)

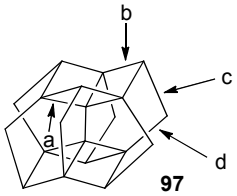


**97**

a) 1.495 / 4.63 (111)

b) 1.648 / 2.02 (48)

c) 1.610 / 2.44 (58)

d) 1.613 / 2.35 (56)

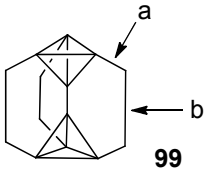


**99**

a) 1.573 / 2.37 (57)

b) 1.661 / 1.60 (38)

# Appendix: Crystallographic Data

*The author thanks Prof. Peter G. Jones for the X-ray analyses and the figures presented herein.*

Data collection and reduction: Crystals were mounted in inert oil on glass fibres and transferred to the cold gas stream of the diffractometer (Oxford Diffraction Xcalibur or Nova). Measurements were performed with monochromated Mo-*K*α radiation (λ = 0.71073 Å) or mirror-focussed Cu-*K*α radiation (λ = 1.54184 Å).

Structure refinement: The structures were refined anisotropically against $F^2$ (program SHELXL-97, [277]). Methyl hydrogens were considered as constituents of idealized rigid groups allowed to rotate but not tip; other hydrogens were included using a riding model starting from calculated positions.

## A1 2-Benzylidene-1,3-diphenylpropane-1,3-dione (14)

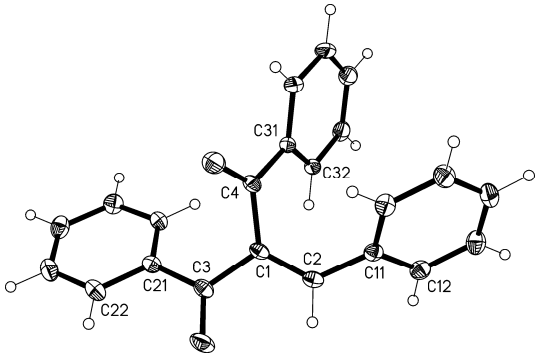


| | | |
|---|---|---|
| Crystal system | Orthorhombic | |
| Space group | $P2_12_12_1$ | |
| Unit cell dim. | a = 10.0980(3) Å | α= 90° |
| | b = 10.6328(3) Å | β= 90° |
| | c = 15.1595(4) Å | γ = 90° |
| Volume (Z = 4) | 1627.67(8) Å$^3$ | |

**Bond lengths in [Å]:**

| | | | |
|---|---|---|---|
| C(1)-C(2) | 1.3406(18) | C(15)-C(16) | 1.384(2) |
| C(1)-C(4) | 1.4971(18) | C(21)-C(26) | 1.3945(17) |
| C(1)-C(3) | 1.4989(17) | C(21)-C(22) | 1.3972(18) |
| C(2)-C(11) | 1.4656(17) | C(22)-C(23) | 1.3875(19) |
| C(3)-O(1) | 1.2255(15) | C(23)-C(24) | 1.388(2) |
| C(3)-C(21) | 1.4956(18) | C(24)-C(25) | 1.386(2) |
| C(4)-O(2) | 1.2231(15) | C(25)-C(26) | 1.3880(19) |
| C(4)-C(31) | 1.4942(18) | C(31)-C(32) | 1.3952(18) |
| C(11)-C(16) | 1.3977(18) | C(31)-C(36) | 1.3957(19) |
| C(11)-C(12) | 1.4009(18) | C(32)-C(33) | 1.3895(18) |
| C(12)-C(13) | 1.386(2) | C(33)-C(34) | 1.384(2) |
| C(13)-C(14) | 1.388(2) | C(34)-C(35) | 1.384(2) |
| C(14)-C(15) | 1.387(2) | C(35)-C(36) | 1.392(2) |

**Bond angles in [°]:**

| | | | |
|---|---|---|---|
| C(2)-C(1)-C(4) | 123.92(11) | C(15)-C(16)-C(11) | 120.49(12) |
| C(2)-C(1)-C(3) | 117.77(11) | C(26)-C(21)-C(22) | 119.38(12) |
| C(4)-C(1)-C(3) | 118.23(11) | C(26)-C(21)-C(3) | 122.14(12) |
| C(1)-C(2)-C(11) | 126.79(12) | C(22)-C(21)-C(3) | 118.40(12) |
| O(1)-C(3)-C(21) | 119.58(12) | C(23)-C(22)-C(21) | 120.14(13) |
| O(1)-C(3)-C(1) | 119.52(12) | C(22)-C(23)-C(24) | 120.06(13) |
| C(21)-C(3)-C(1) | 120.89(11) | C(25)-C(24)-C(23) | 120.09(13) |
| O(2)-C(4)-C(31) | 121.19(11) | C(24)-C(25)-C(26) | 120.13(13) |
| O(2)-C(4)-C(1) | 119.05(12) | C(25)-C(26)-C(21) | 120.17(12) |
| C(31)-C(4)-C(1) | 119.74(11) | C(32)-C(31)-C(36) | 120.16(13) |
| C(16)-C(11)-C(12) | 118.81(12) | C(32)-C(31)-C(4) | 121.50(11) |
| C(16)-C(11)-C(2) | 121.40(12) | C(36)-C(31)-C(4) | 118.34(12) |
| C(12)-C(11)-C(2) | 119.78(11) | C(33)-C(32)-C(31) | 119.58(13) |
| C(13)-C(12)-C(11) | 120.30(12) | C(34)-C(33)-C(32) | 120.26(13) |
| C(12)-C(13)-C(14) | 120.26(13) | C(35)-C(34)-C(33) | 120.27(13) |
| C(15)-C(14)-C(13) | 119.82(13) | C(34)-C(35)-C(36) | 120.26(14) |
| C(16)-C(15)-C(14) | 120.24(13) | C(35)-C(36)-C(31) | 119.46(14) |

## A2 2-(2-Bromobenzylidene)-1,3-diphenylpropane-1,3-dione (30)

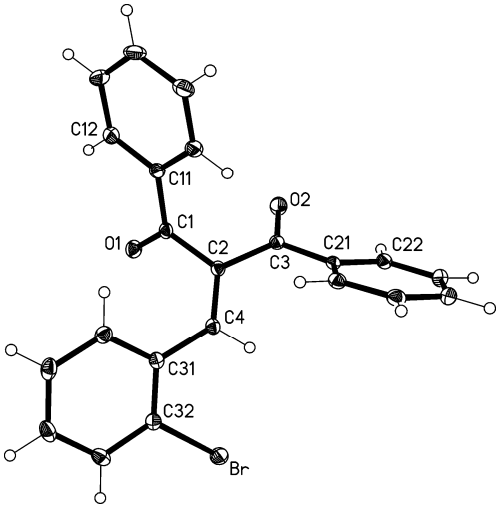


| | | |
|---|---|---|
| Crystal system | Monoclinic | |
| Space group | $P2_1/c$ | |
| Unit cell dim. | a = 7.9385(3) Å | α= 90° |
| | b = 6.9922(3) Å | β= 97.521(4)° |
| | c = 30.7407(12) Å | γ = 90° |
| Volume (Z = 4) | 1691.64(12) Å$^3$ | |

**Bond lengths in [Å]:**

| | | | |
|---|---|---|---|
| C(1)-O(1) | 1.2197(19) | C(12)-C(13) | 1.385(2) |
| C(1)-C(11) | 1.491(2) | C(13)-C(14) | 1.394(3) |
| C(1)-C(2) | 1.517(2) | C(14)-C(15) | 1.389(3) |
| C(2)-C(4) | 1.346(2) | C(15)-C(16) | 1.392(2) |
| C(2)-C(3) | 1.495(2) | C(21)-C(22) | 1.399(2) |
| C(3)-O(2) | 1.2236(19) | C(21)-C(26) | 1.399(2) |
| C(3)-C(21) | 1.493(2) | C(22)-C(23) | 1.388(2) |
| C(4)-C(31) | 1.468(2) | C(23)-C(24) | 1.391(2) |
| C(11)-C(16) | 1.397(2) | C(24)-C(25) | 1.392(2) |
| C(11)-C(12) | 1.401(2) | C(25)-C(26) | 1.391(2) |

| | | | |
|---|---|---|---|
| C(31)-C(32) | 1.400(2) | C(33)-C(34) | 1.389(2) |
| C(31)-C(36) | 1.402(2) | C(34)-C(35) | 1.395(2) |
| C(32)-C(33) | 1.390(2) | C(35)-C(36) | 1.385(2) |
| C(32)-Br | 1.8998(15) | | |

**Bond angles in [°]:**

| | | | |
|---|---|---|---|
| O(1)-C(1)-C(11) | 122.16(14) | C(22)-C(21)-C(26) | 119.67(14) |
| O(1)-C(1)-C(2) | 120.04(14) | C(22)-C(21)-C(3) | 117.87(13) |
| C(11)-C(1)-C(2) | 117.79(13) | C(26)-C(21)-C(3) | 122.32(13) |
| C(4)-C(2)-C(3) | 120.98(13) | C(23)-C(22)-C(21) | 119.93(15) |
| C(4)-C(2)-C(1) | 123.55(13) | C(22)-C(23)-C(24) | 120.31(15) |
| C(3)-C(2)-C(1) | 114.56(12) | C(23)-C(24)-C(25) | 120.00(15) |
| O(2)-C(3)-C(21) | 120.71(14) | C(26)-C(25)-C(24) | 120.09(15) |
| O(2)-C(3)-C(2) | 118.69(14) | C(25)-C(26)-C(21) | 119.97(14) |
| C(21)-C(3)-C(2) | 120.57(13) | C(32)-C(31)-C(36) | 117.11(14) |
| C(2)-C(4)-C(31) | 127.48(14) | C(32)-C(31)-C(4) | 120.81(13) |
| C(16)-C(11)-C(12) | 119.39(14) | C(36)-C(31)-C(4) | 122.01(14) |
| C(16)-C(11)-C(1) | 121.94(14) | C(33)-C(32)-C(31) | 122.38(14) |
| C(12)-C(11)-C(1) | 118.65(14) | C(33)-C(32)-Br | 118.03(12) |
| C(13)-C(12)-C(11) | 120.21(16) | C(31)-C(32)-Br | 119.53(11) |
| C(12)-C(13)-C(14) | 120.11(16) | C(34)-C(33)-C(32) | 118.93(15) |
| C(15)-C(14)-C(13) | 120.08(15) | C(33)-C(34)-C(35) | 120.21(15) |
| C(14)-C(15)-C(16) | 119.96(17) | C(36)-C(35)-C(34) | 119.89(15) |
| C(15)-C(16)-C(11) | 120.24(15) | C(35)-C(36)-C(31) | 121.47(15) |

## A3 2-(2-Methoxybenzylidene)-1,3-diphenylpropane-1,3-dione (31)

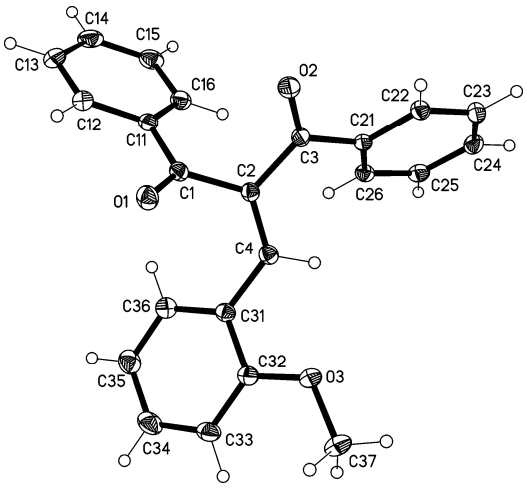


| | |
|---|---|
| Crystal system | Monoclinic |
| Space group | $P2_1/c$ |
| Unit cell dim. | a = 7.8666(3) Å α= 90° |
| | b = 7.0452(3) Å β= 90.205(4)° |
| | c = 31.3099(11) Å γ = 90° |
| Volume (Z = 4) | 1735.24(12) Å$^3$ |

**Bond lengths in [Å]:**

| | | | |
|---|---|---|---|
| C(1)-O(1) | 1.2222(15) | C(21)-C(26) | 1.3961(17) |
| C(1)-C(11) | 1.4895(17) | C(21)-C(22) | 1.4020(16) |
| C(1)-C(2) | 1.5132(17) | C(22)-C(23) | 1.3881(18) |
| C(2)-C(4) | 1.3485(16) | C(23)-C(24) | 1.3914(19) |
| C(2)-C(3) | 1.4924(16) | C(24)-C(25) | 1.3913(18) |
| C(3)-O(2) | 1.2251(15) | C(25)-C(26) | 1.3904(18) |
| C(3)-C(21) | 1.4924(17) | C(31)-C(36) | 1.3978(17) |
| C(4)-C(31) | 1.4674(16) | C(31)-C(32) | 1.4087(16) |
| C(11)-C(16) | 1.3949(18) | C(32)-O(3) | 1.3600(15) |
| C(11)-C(12) | 1.3998(18) | C(32)-C(33) | 1.3959(17) |
| C(12)-C(13) | 1.3911(19) | C(33)-C(34) | 1.384(2) |
| C(13)-C(14) | 1.391(2) | C(34)-C(35) | 1.390(2) |
| C(14)-C(15) | 1.385(2) | C(35)-C(36) | 1.3903(18) |
| C(15)-C(16) | 1.3913(17) | C(37)-O(3) | 1.4327(15) |

**Bond angles in [°]:**

| | | | |
|---|---|---|---|
| O(1)-C(1)-C(11) | 122.13(11) | C(15)-C(16)-C(11) | 120.14(13) |
| O(1)-C(1)-C(2) | 119.80(11) | C(26)-C(21)-C(22) | 119.46(11) |
| C(11)-C(1)-C(2) | 118.07(11) | C(26)-C(21)-C(3) | 122.76(11) |
| C(4)-C(2)-C(3) | 121.41(11) | C(22)-C(21)-C(3) | 117.67(11) |
| C(4)-C(2)-C(1) | 123.14(11) | C(23)-C(22)-C(21) | 119.93(12) |
| C(3)-C(2)-C(1) | 114.61(10) | C(22)-C(23)-C(24) | 120.33(12) |
| O(2)-C(3)-C(2) | 118.75(11) | C(25)-C(24)-C(23) | 119.94(12) |
| O(2)-C(3)-C(21) | 120.74(11) | C(26)-C(25)-C(24) | 120.03(12) |
| C(2)-C(3)-C(21) | 120.51(10) | C(25)-C(26)-C(21) | 120.27(11) |
| C(2)-C(4)-C(31) | 127.18(11) | C(36)-C(31)-C(32) | 118.47(11) |
| C(16)-C(11)-C(12) | 119.60(12) | C(36)-C(31)-C(4) | 122.79(11) |
| C(16)-C(11)-C(1) | 121.84(11) | C(32)-C(31)-C(4) | 118.62(11) |
| C(12)-C(11)-C(1) | 118.55(12) | O(3)-C(32)-C(33) | 124.29(11) |
| C(13)-C(12)-C(11) | 119.94(13) | O(3)-C(32)-C(31) | 115.45(10) |
| C(14)-C(13)-C(12) | 120.00(13) | C(33)-C(32)-C(31) | 120.26(12) |
| C(15)-C(14)-C(13) | 120.27(12) | C(34)-C(33)-C(32) | 119.75(12) |
| C(14)-C(15)-C(16) | 120.05(14) | C(33)-C(34)-C(35) | 121.04(12) |

| | | | |
|---|---|---|---|
| C(36)-C(35)-C(34) | 119.02(13) | C(32)-O(3)-C(37) | 117.21(10) |
| C(35)-C(36)-C(31) | 121.40(12) | | |

## A4 1,3-Bis-(2-bromophenyl)-propane-1,3-dione (43)

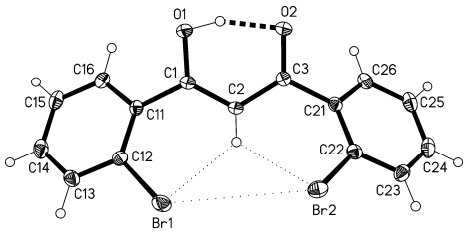


Crystal system Monoclinic

| | | |
|---|---|---|
| Space group | $P2_1/c$ | |
| Unit cell dim. | a = 13.3478(4) Å | $\alpha$= 90° |
| | b = 12.9023(4) Å | $\beta$= 103.064(4)° |
| | c = 7.9266(3) Å | $\gamma$ = 90° |
| Volume (Z = 4) | 1329.77(8) Å$^3$ | |

**Bond lengths in [Å]:**

| | | | |
|---|---|---|---|
| C(1)-O(1) | 1.3181(17) | C(13)-C(14) | 1.388(2) |
| C(1)-C(2) | 1.378(2) | C(14)-C(15) | 1.384(2) |
| C(1)-C(11) | 1.484(2) | C(15)-C(16) | 1.387(2) |
| C(2)-C(3) | 1.422(2) | C(21)-C(22) | 1.396(2) |
| C(3)-O(2) | 1.2701(18) | C(21)-C(26) | 1.400(2) |
| C(3)-C(21) | 1.493(2) | C(22)-C(23) | 1.387(2) |
| C(11)-C(12) | 1.401(2) | C(22)-Br(2) | 1.9016(15) |
| C(11)-C(16) | 1.405(2) | C(23)-C(24) | 1.388(2) |
| C(12)-C(13) | 1.388(2) | C(24)-C(25) | 1.381(2) |
| C(12)-Br(1) | 1.8964(14) | C(25)-C(26) | 1.385(2) |

**Bond angles in [°]:**

| | | | |
|---|---|---|---|
| O(1)-C(1)-C(2) | 121.38(13) | C(15)-C(14)-C(13) | 120.23(15) |
| O(1)-C(1)-C(11) | 113.82(12) | C(14)-C(15)-C(16) | 119.77(15) |
| C(2)-C(1)-C(11) | 124.63(13) | C(15)-C(16)-C(11) | 121.50(14) |
| C(1)-C(2)-C(3) | 119.82(13) | C(22)-C(21)-C(26) | 117.87(14) |
| O(2)-C(3)-C(2) | 121.65(13) | C(22)-C(21)-C(3) | 125.43(13) |
| O(2)-C(3)-C(21) | 117.09(13) | C(26)-C(21)-C(3) | 116.69(13) |
| C(2)-C(3)-C(21) | 121.04(13) | C(23)-C(22)-C(21) | 121.16(14) |
| C(12)-C(11)-C(16) | 117.24(13) | C(23)-C(22)-Br(2) | 116.85(11) |
| C(12)-C(11)-C(1) | 125.76(13) | C(21)-C(22)-Br(2) | 121.86(11) |
| C(16)-C(11)-C(1) | 117.00(13) | C(22)-C(23)-C(24) | 119.69(15) |
| C(13)-C(12)-C(11) | 121.58(14) | C(25)-C(24)-C(23) | 120.23(15) |
| C(13)-C(12)-Br(1) | 115.92(11) | C(24)-C(25)-C(26) | 119.78(15) |
| C(11)-C(12)-Br(1) | 122.36(11) | C(25)-C(26)-C(21) | 121.21(15) |
| C(14)-C(13)-C(12) | 119.66(15) | | |

## A5 2-(2-Methoxybenzylidene)-1,3-bis(2-methoxyphenyl)propane-1,3-dione (50)

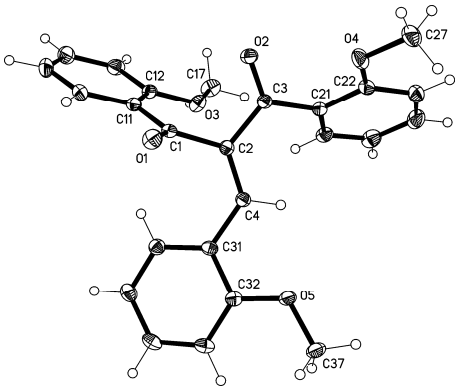


| | | |
|---|---|---|
| Crystal system | Monoclinic | |
| Space group | $P2_1/c$ | |
| Unit cell dim. | a = 13.3307(3) Å | $\alpha$= 90° |
| | b = 11.9411(2) Å | $\beta$= 91.300(2)° |
| | c = 12.4521(3) Å | $\gamma$ = 90° |
| Volume (Z = 4) | 1981.65(7) Å$^3$ | |

**Bond lengths in [Å]:**

| | | | |
|---|---|---|---|
| C(1)-O(1) | 1.2187(12) | C(21)-C(26) | 1.3979(15) |
| C(1)-C(11) | 1.4975(14) | C(21)-C(22) | 1.4107(14) |
| C(1)-C(2) | 1.5094(13) | C(22)-O(4) | 1.3559(13) |
| C(2)-C(4) | 1.3480(13) | C(22)-C(23) | 1.3973(15) |
| C(2)-C(3) | 1.4812(13) | C(23)-C(24) | 1.3875(18) |
| C(3)-O(2) | 1.2263(12) | C(24)-C(25) | 1.3877(18) |
| C(3)-C(21) | 1.4988(14) | C(25)-C(26) | 1.3888(16) |
| C(4)-C(31) | 1.4631(13) | C(27)-O(4) | 1.4309(13) |
| C(11)-C(16) | 1.4026(14) | C(31)-C(36) | 1.3993(14) |
| C(11)-C(12) | 1.4084(15) | C(31)-C(32) | 1.4151(14) |
| C(12)-O(3) | 1.3617(12) | C(32)-O(5) | 1.3606(12) |
| C(12)-C(13) | 1.3991(14) | C(32)-C(33) | 1.3931(14) |
| C(13)-C(14) | 1.3836(16) | C(33)-C(34) | 1.3870(16) |
| C(14)-C(15) | 1.3895(18) | C(34)-C(35) | 1.3890(16) |
| C(15)-C(16) | 1.3848(16) | C(35)-C(36) | 1.3889(15) |
| C(17)-O(3) | 1.4311(13) | C(37)-O(5) | 1.4355(12) |

**Bond angles in [°]:**

| | | | |
|---|---|---|---|
| O(1)-C(1)-C(11) | 120.12(9) | O(3)-C(12)-C(11) | 117.84(9) |
| O(1)-C(1)-C(2) | 117.91(9) | C(13)-C(12)-C(11) | 119.90(10) |
| C(11)-C(1)-C(2) | 121.94(9) | C(14)-C(13)-C(12) | 120.06(11) |
| C(4)-C(2)-C(3) | 123.09(9) | C(13)-C(14)-C(15) | 120.97(10) |
| C(4)-C(2)-C(1) | 123.96(9) | C(16)-C(15)-C(14) | 118.98(11) |
| C(3)-C(2)-C(1) | 112.17(8) | C(15)-C(16)-C(11) | 121.65(11) |
| O(2)-C(3)-C(2) | 118.89(9) | C(26)-C(21)-C(22) | 119.30(10) |
| O(2)-C(3)-C(21) | 121.24(9) | C(26)-C(21)-C(3) | 120.40(9) |
| C(2)-C(3)-C(21) | 119.86(8) | C(22)-C(21)-C(3) | 120.22(9) |
| C(2)-C(4)-C(31) | 127.76(9) | O(4)-C(22)-C(23) | 124.15(10) |
| C(16)-C(11)-C(12) | 118.39(9) | O(4)-C(22)-C(21) | 116.29(9) |
| C(16)-C(11)-C(1) | 116.22(9) | C(23)-C(22)-C(21) | 119.56(10) |
| C(12)-C(11)-C(1) | 125.39(9) | C(24)-C(23)-C(22) | 119.72(11) |
| O(3)-C(12)-C(13) | 122.26(10) | C(23)-C(24)-C(25) | 121.40(11) |

| | | | |
|---|---|---|---|
| C(24)-C(25)-C(26) | 119.00(11) | C(34)-C(33)-C(32) | 119.62(10) |
| C(25)-C(26)-C(21) | 120.97(10) | C(33)-C(34)-C(35) | 120.99(10) |
| C(36)-C(31)-C(32) | 118.05(9) | C(36)-C(35)-C(34) | 119.27(10) |
| C(36)-C(31)-C(4) | 123.00(9) | C(35)-C(36)-C(31) | 121.48(10) |
| C(32)-C(31)-C(4) | 118.68(9) | C(12)-O(3)-C(17) | 116.80(8) |
| O(5)-C(32)-C(33) | 123.85(9) | C(22)-O(4)-C(27) | 118.32(9) |
| O(5)-C(32)-C(31) | 115.55(9) | C(32)-O(5)-C(37) | 117.80(8) |
| C(33)-C(32)-C(31) | 120.59(9) | | |

## A6 2-Benzylidene-1,3-diphenylpropane-*cis*-1,3-diol (*syn*-12)

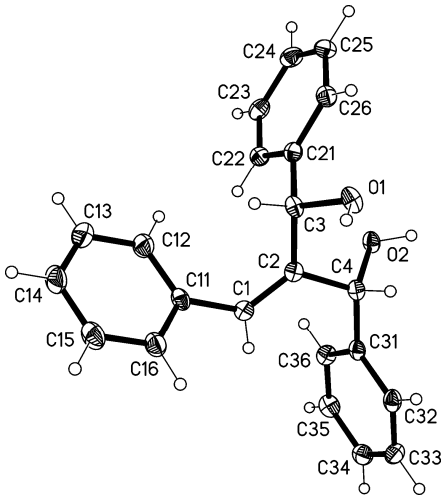


| | | |
|---|---|---|
| Crystal system | Monoclinic | |
| Space group | $P2_1/n$ | |
| Unit cell dim. | a = 14.6795(4) Å | α= 90° |
| | b = 5.57750(12) Å | β= 100.477(4)° |
| | c = 20.8683(6) Å | γ = 90° |
| Volume (Z = 4) | 1680.10(8) Å$^3$ | |

**Bond lengths in [Å]:**

| | | | |
|---|---|---|---|
| C(1)-C(2) | 1.3343(13) | C(15)-C(16) | 1.3855(15) |
| C(1)-C(11) | 1.4854(13) | C(21)-C(26) | 1.3911(13) |
| C(2)-C(3) | 1.5221(13) | C(21)-C(22) | 1.3951(13) |
| C(2)-C(4) | 1.5229(13) | C(22)-C(23) | 1.3851(13) |
| C(3)-O(1) | 1.4321(11) | C(23)-C(24) | 1.3858(14) |
| C(3)-C(21) | 1.5220(13) | C(24)-C(25) | 1.3833(15) |
| C(4)-O(2) | 1.4398(11) | C(25)-C(26) | 1.3896(14) |
| C(4)-C(31) | 1.5105(13) | C(31)-C(32) | 1.3905(13) |
| C(11)-C(12) | 1.3919(14) | C(31)-C(36) | 1.3954(13) |
| C(11)-C(16) | 1.3954(14) | C(32)-C(33) | 1.3939(14) |
| C(12)-C(13) | 1.3879(15) | C(33)-C(34) | 1.3828(15) |
| C(13)-C(14) | 1.3805(15) | C(34)-C(35) | 1.3880(14) |
| C(14)-C(15) | 1.3852(15) | C(35)-C(36) | 1.3819(13) |

**Bond angles in [°]:**

| | | | |
|---|---|---|---|
| C(2)-C(1)-C(11) | 126.69(9) | O(1)-C(3)-C(21) | 108.09(7) |
| C(1)-C(2)-C(3) | 122.10(8) | O(1)-C(3)-C(2) | 109.89(7) |
| C(1)-C(2)-C(4) | 123.11(8) | C(21)-C(3)-C(2) | 115.03(7) |
| C(3)-C(2)-C(4) | 114.41(8) | O(2)-C(4)-C(31) | 109.82(7) |

| | | | |
|---|---|---|---|
| O(2)-C(4)-C(2) | 107.15(7) | C(23)-C(22)-C(21) | 120.83(9) |
| C(31)-C(4)-C(2) | 116.22(8) | C(22)-C(23)-C(24) | 120.24(9) |
| C(12)-C(11)-C(16) | 117.77(9) | C(25)-C(24)-C(23) | 119.45(9) |
| C(12)-C(11)-C(1) | 123.19(9) | C(24)-C(25)-C(26) | 120.40(9) |
| C(16)-C(11)-C(1) | 119.03(9) | C(25)-C(26)-C(21) | 120.61(9) |
| C(13)-C(12)-C(11) | 121.13(10) | C(32)-C(31)-C(36) | 118.42(9) |
| C(14)-C(13)-C(12) | 120.33(11) | C(32)-C(31)-C(4) | 121.12(8) |
| C(13)-C(14)-C(15) | 119.38(10) | C(36)-C(31)-C(4) | 120.38(8) |
| C(14)-C(15)-C(16) | 120.23(10) | C(31)-C(32)-C(33) | 120.77(9) |
| C(15)-C(16)-C(11) | 121.13(10) | C(34)-C(33)-C(32) | 119.98(9) |
| C(26)-C(21)-C(22) | 118.45(8) | C(33)-C(34)-C(35) | 119.74(9) |
| C(26)-C(21)-C(3) | 120.24(8) | C(36)-C(35)-C(34) | 120.14(10) |
| C(22)-C(21)-C(3) | 121.30(8) | C(35)-C(36)-C(31) | 120.94(9) |

## A7 2-Benzylidene-1,3-diphenylpropane-*anti*-1,3-diol (*anti*-12)

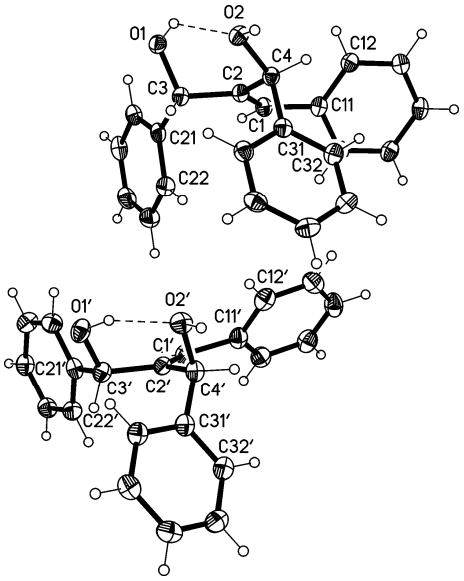


| | | |
|---|---|---|
| Crystal system | Monoclinic | |
| Space group | *C*2/*c* | |
| Unit cell dim. | a = 49.918(3) Å | α= 90° |
| | b = 13.6397(5) Å | β= 93.913(4)° |
| | c = 9.8699(4) Å | γ = 90° |
| Volume (Z = 16) | 6704.4(5) Å$^3$ | |

**Bond lengths in [Å]:**

| | | | |
|---|---|---|---|
| C(1)-C(2) | 1.337(2) | C(15)-C(16) | 1.390(2) |
| C(1)-C(11) | 1.4816(19) | C(21)-C(26) | 1.386(2) |
| C(2)-C(4) | 1.5229(18) | C(21)-C(22) | 1.398(2) |
| C(2)-C(3) | 1.5290(18) | C(22)-C(23) | 1.386(2) |
| C(3)-O(1) | 1.4415(16) | C(23)-C(24) | 1.385(2) |
| C(3)-C(21) | 1.5110(19) | C(24)-C(25) | 1.382(2) |
| C(4)-O(2) | 1.4334(16) | C(25)-C(26) | 1.397(2) |
| C(4)-C(31) | 1.5182(19) | C(31)-C(32) | 1.393(2) |
| C(11)-C(12) | 1.395(2) | C(31)-C(36) | 1.395(2) |
| C(11)-C(16) | 1.400(2) | C(32)-C(33) | 1.385(2) |
| C(12)-C(13) | 1.390(2) | C(33)-C(34) | 1.388(2) |
| C(13)-C(14) | 1.387(2) | C(34)-C(35) | 1.385(2) |
| C(14)-C(15) | 1.389(2) | C(35)-C(36) | 1.387(2) |

| | | | |
|---|---|---|---|
| C(1')-C(2') | 1.341(2) | C(15')-C(16') | 1.383(2) |
| C(1')-C(11') | 1.482(2) | C(21')-C(26') | 1.381(2) |
| C(2')-C(4') | 1.5224(19) | C(21')-C(22') | 1.400(2) |
| C(2')-C(3') | 1.5292(19) | C(22')-C(23') | 1.390(2) |
| C(3')-O(1') | 1.4433(17) | C(23')-C(24') | 1.384(2) |
| C(3')-C(21') | 1.516(2) | C(24')-C(25') | 1.385(2) |
| C(4')-O(2') | 1.4440(17) | C(25')-C(26') | 1.385(2) |
| C(4')-C(31') | 1.523(2) | C(31')-C(32') | 1.392(2) |
| C(11')-C(16') | 1.392(2) | C(31')-C(36') | 1.394(2) |
| C(11')-C(12') | 1.403(2) | C(32')-C(33') | 1.388(2) |
| C(12')-C(13') | 1.393(2) | C(33')-C(34') | 1.387(2) |
| C(13')-C(14') | 1.384(2) | C(34')-C(35') | 1.384(2) |
| C(14')-C(15') | 1.383(2) | C(35')-C(36') | 1.392(2) |

**Bond angles in [°]:**

| | | | |
|---|---|---|---|
| C(2)-C(1)-C(11) | 128.10(13) | C(2')-C(1')-C(11') | 128.72(14) |
| C(1)-C(2)-C(4) | 123.41(12) | C(1')-C(2')-C(4') | 122.71(13) |
| C(1)-C(2)-C(3) | 121.04(12) | C(1')-C(2')-C(3') | 121.09(13) |
| C(4)-C(2)-C(3) | 115.36(11) | C(4')-C(2')-C(3') | 116.13(12) |
| O(1)-C(3)-C(21) | 109.43(11) | O(1')-C(3')-C(21') | 108.70(11) |
| O(1)-C(3)-C(2) | 109.81(11) | O(1')-C(3')-C(2') | 108.35(11) |
| C(21)-C(3)-C(2) | 112.52(11) | C(21')-C(3')-C(2') | 115.06(12) |
| O(2)-C(4)-C(31) | 112.58(11) | O(2')-C(4')-C(2') | 106.47(11) |
| O(2)-C(4)-C(2) | 108.02(10) | O(2')-C(4')-C(31') | 111.10(11) |
| C(31)-C(4)-C(2) | 109.30(11) | C(2')-C(4')-C(31') | 114.20(12) |
| C(12)-C(11)-C(16) | 118.56(13) | C(16')-C(11')-C(12') | 118.52(14) |
| C(12)-C(11)-C(1) | 122.59(13) | C(16')-C(11')-C(1') | 119.18(14) |
| C(16)-C(11)-C(1) | 118.79(13) | C(12')-C(11')-C(1') | 122.01(14) |
| C(13)-C(12)-C(11) | 120.47(13) | C(13')-C(12')-C(11') | 120.33(15) |
| C(14)-C(13)-C(12) | 120.52(14) | C(14')-C(13')-C(12') | 120.02(15) |
| C(13)-C(14)-C(15) | 119.58(13) | C(15')-C(14')-C(13') | 119.99(15) |
| C(14)-C(15)-C(16) | 120.04(14) | C(16')-C(15')-C(14') | 120.23(15) |
| C(15)-C(16)-C(11) | 120.79(14) | C(15')-C(16')-C(11') | 120.87(15) |
| C(26)-C(21)-C(22) | 118.86(13) | C(26')-C(21')-C(22') | 118.70(13) |
| C(26)-C(21)-C(3) | 122.82(13) | C(26')-C(21')-C(3') | 121.41(13) |
| C(22)-C(21)-C(3) | 118.24(13) | C(22')-C(21')-C(3') | 119.89(13) |
| C(23)-C(22)-C(21) | 120.75(15) | C(23')-C(22')-C(21') | 120.93(14) |
| C(24)-C(23)-C(22) | 119.96(15) | C(24')-C(23')-C(22') | 119.56(14) |
| C(25)-C(24)-C(23) | 119.86(15) | C(23')-C(24')-C(25') | 119.63(14) |
| C(24)-C(25)-C(26) | 120.25(15) | C(26')-C(25')-C(24') | 120.78(15) |
| C(21)-C(26)-C(25) | 120.30(14) | C(21')-C(26')-C(25') | 120.38(14) |
| C(32)-C(31)-C(36) | 119.05(13) | C(32')-C(31')-C(36') | 118.61(14) |
| C(32)-C(31)-C(4) | 118.99(12) | C(32')-C(31')-C(4') | 119.27(13) |
| C(36)-C(31)-C(4) | 121.95(12) | C(36')-C(31')-C(4') | 122.09(13) |
| C(33)-C(32)-C(31) | 120.68(14) | C(33')-C(32')-C(31') | 120.82(14) |
| C(32)-C(33)-C(34) | 119.96(14) | C(34')-C(33')-C(32') | 120.20(14) |
| C(35)-C(34)-C(33) | 119.76(14) | C(35')-C(34')-C(33') | 119.49(14) |
| C(34)-C(35)-C(36) | 120.47(14) | C(34')-C(35')-C(36') | 120.38(15) |
| C(35)-C(36)-C(31) | 120.08(14) | C(35')-C(36')-C(31') | 120.50(14) |

## A8 2-(2-Bromobenzylidene)-1,3-diphenylpropane-*anti*-1,3-diol (*anti*-32)

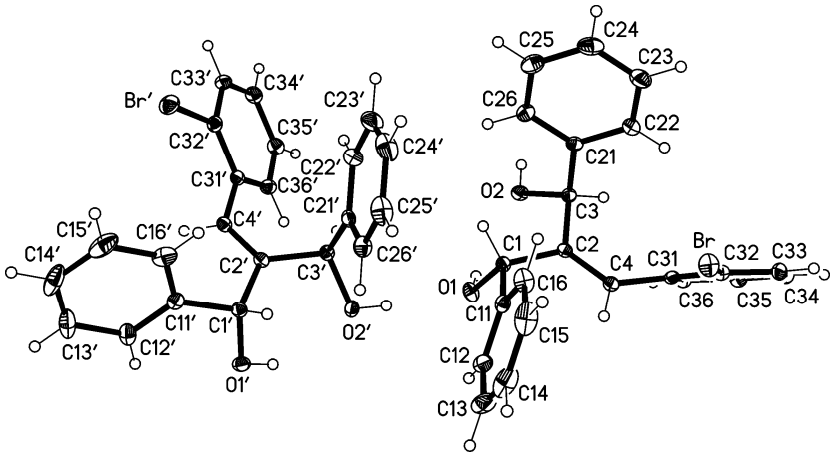


| | | |
|---|---|---|
| Crystal system | Triclinic | |
| Space group | *P*(-1) | |
| Unit cell dim. | a = 9.7718(3) Å | α= 115.426(4)° |
| | b = 14.0566(5) Å | β= 93.788(3)° |
| | c = 14.6957(6) Å | γ = 92.797(3)° |
| Volume (Z = 4) | 1812.38(11) Å$^3$ | |

**Bond lengths in [Å]:**

| | | | |
|---|---|---|---|
| C(1)-O(1) | 1.4420(13) | C(32)-Br | 1.8994(11) |
| C(1)-C(11) | 1.5112(15) | C(33)-C(34) | 1.3854(17) |
| C(1)-C(2) | 1.5262(15) | C(34)-C(35) | 1.3931(16) |
| C(2)-C(4) | 1.3365(15) | C(35)-C(36) | 1.3900(16) |
| C(2)-C(3) | 1.5177(15) | C(1')-O(1') | 1.4445(13) |
| C(3)-O(2) | 1.4298(13) | C(1')-C(11') | 1.5089(15) |
| C(3)-C(21) | 1.5233(15) | C(1')-C(2') | 1.5242(15) |
| C(4)-C(31) | 1.4795(15) | C(2')-C(4') | 1.3376(15) |
| C(11)-C(12) | 1.3885(16) | C(2')-C(3') | 1.5180(15) |
| C(11)-C(16) | 1.3927(16) | C(3')-O(2') | 1.4323(13) |
| C(12)-C(13) | 1.3964(18) | C(3')-C(21') | 1.5217(15) |
| C(13)-C(14) | 1.381(2) | C(4')-C(31') | 1.4799(15) |
| C(14)-C(15) | 1.385(2) | C(11')-C(12') | 1.3883(16) |
| C(15)-C(16) | 1.3903(19) | C(11')-C(16') | 1.3956(16) |
| C(21)-C(26) | 1.3931(16) | C(12')-C(13') | 1.3980(17) |
| C(21)-C(22) | 1.3974(16) | C(13')-C(14') | 1.379(2) |
| C(22)-C(23) | 1.3876(17) | C(14')-C(15') | 1.388(3) |
| C(23)-C(24) | 1.386(2) | C(15')-C(16') | 1.3893(19) |
| C(24)-C(25) | 1.3893(19) | C(21')-C(26') | 1.3912(17) |
| C(25)-C(26) | 1.3948(16) | C(21')-C(22') | 1.3950(16) |
| C(31)-C(32) | 1.3991(15) | C(22')-C(23') | 1.3893(19) |
| C(31)-C(36) | 1.4035(15) | C(23')-C(24') | 1.384(2) |
| C(32)-C(33) | 1.3896(16) | C(24')-C(25') | 1.383(2) |

| | | | |
|---|---|---|---|
| C(25')-C(26') | 1.3942(17) | C(32')-Br' | 1.9010(12) |
| C(31')-C(32') | 1.3994(15) | C(33')-C(34') | 1.3872(18) |
| C(31')-C(36') | 1.4018(16) | C(34')-C(35') | 1.3909(17) |
| C(32')-C(33') | 1.3903(16) | C(35')-C(36') | 1.3893(16) |

**Bond angles in [°]:**

| | | | |
|---|---|---|---|
| O(1)-C(1)-C(11) | 108.40(9) | O(1')-C(1')-C(11') | 108.89(9) |
| O(1)-C(1)-C(2) | 109.97(9) | O(1')-C(1')-C(2') | 109.88(9) |
| C(11)-C(1)-C(2) | 113.20(9) | C(11')-C(1')-C(2') | 113.48(9) |
| C(4)-C(2)-C(3) | 123.81(10) | C(4')-C(2')-C(3') | 124.16(10) |
| C(4)-C(2)-C(1) | 121.08(10) | C(4')-C(2')-C(1') | 121.01(10) |
| C(3)-C(2)-C(1) | 114.94(9) | C(3')-C(2')-C(1') | 114.64(9) |
| O(2)-C(3)-C(2) | 107.38(8) | O(2')-C(3')-C(2') | 107.57(9) |
| O(2)-C(3)-C(21) | 113.40(9) | O(2')-C(3')-C(21') | 112.45(9) |
| C(2)-C(3)-C(21) | 108.25(9) | C(2')-C(3')-C(21') | 108.81(9) |
| C(2)-C(4)-C(31) | 128.05(10) | C(2')-C(4')-C(31') | 128.40(10) |
| C(12)-C(11)-C(16) | 119.05(11) | C(12')-C(11')-C(16') | 119.25(11) |
| C(12)-C(11)-C(1) | 122.32(10) | C(12')-C(11')-C(1') | 122.46(10) |
| C(16)-C(11)-C(1) | 118.62(11) | C(16')-C(11')-C(1') | 118.28(11) |
| C(11)-C(12)-C(13) | 120.19(12) | C(11')-C(12')-C(13') | 120.02(12) |
| C(14)-C(13)-C(12) | 120.39(14) | C(14')-C(13')-C(12') | 120.42(14) |
| C(13)-C(14)-C(15) | 119.68(13) | C(13')-C(14')-C(15') | 119.83(12) |
| C(14)-C(15)-C(16) | 120.14(13) | C(14')-C(15')-C(16') | 120.04(14) |
| C(15)-C(16)-C(11) | 120.54(13) | C(15')-C(16')-C(11') | 120.41(13) |
| C(26)-C(21)-C(22) | 119.00(11) | C(26')-C(21')-C(22') | 119.27(11) |
| C(26)-C(21)-C(3) | 122.60(10) | C(26')-C(21')-C(3') | 122.11(10) |
| C(22)-C(21)-C(3) | 118.33(10) | C(22')-C(21')-C(3') | 118.58(11) |
| C(23)-C(22)-C(21) | 120.79(12) | C(23')-C(22')-C(21') | 120.49(13) |
| C(24)-C(23)-C(22) | 120.01(12) | C(24')-C(23')-C(22') | 120.02(13) |
| C(23)-C(24)-C(25) | 119.73(12) | C(25')-C(24')-C(23') | 119.83(12) |
| C(24)-C(25)-C(26) | 120.43(12) | C(24')-C(25')-C(26') | 120.56(13) |
| C(21)-C(26)-C(25) | 120.04(11) | C(21')-C(26')-C(25') | 119.82(12) |
| C(32)-C(31)-C(36) | 116.94(10) | C(32')-C(31')-C(36') | 116.97(10) |
| C(32)-C(31)-C(4) | 121.01(10) | C(32')-C(31')-C(4') | 120.63(10) |
| C(36)-C(31)-C(4) | 121.88(10) | C(36')-C(31')-C(4') | 122.25(10) |
| C(33)-C(32)-C(31) | 122.66(10) | C(33')-C(32')-C(31') | 122.39(11) |
| C(33)-C(32)-Br | 118.49(8) | C(33')-C(32')-Br' | 117.97(9) |
| C(31)-C(32)-Br | 118.84(8) | C(31')-C(32')-Br' | 119.64(9) |
| C(34)-C(33)-C(32) | 119.01(10) | C(34')-C(33')-C(32') | 119.24(11) |
| C(33)-C(34)-C(35) | 120.04(11) | C(33')-C(34')-C(35') | 119.88(11) |
| C(36)-C(35)-C(34) | 120.21(11) | C(36')-C(35')-C(34') | 120.20(11) |
| C(35)-C(36)-C(31) | 121.14(10) | C(35')-C(36')-C(31') | 121.32(11) |

## A9 2-(2-Methoxybenzylidene)-1,3-diphenylpropane-*syn*-1,3-diol (*syn*-33)

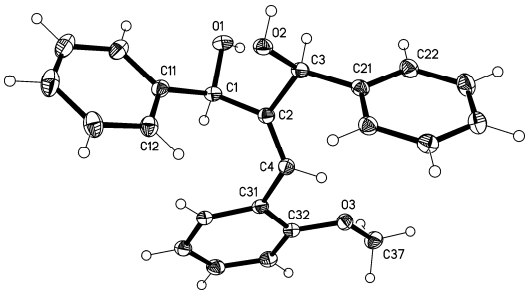


| | | |
|---|---|---|
| Crystal system | Orthorhombic | |
| Space group | $P2_12_12_1$ | |
| Unit cell dim. | a = 5.4825(3) Å | α= 90° |
| | b = 16.3497(8) Å | β= 90° |
| | c = 20.2820(13) Å | γ = 90° |
| Volume (Z = 4) | 1818.03(18) Å$^3$ | |

**Bond lengths in [Å]:**

| | | | |
|---|---|---|---|
| C(1)-O(1) | 1.4260(18) | C(21)-C(26) | 1.390(2) |
| C(1)-C(2) | 1.522(2) | C(21)-C(22) | 1.395(2) |
| C(1)-C(11) | 1.524(2) | C(22)-C(23) | 1.388(3) |
| C(2)-C(4) | 1.344(2) | C(23)-C(24) | 1.383(3) |
| C(2)-C(3) | 1.523(2) | C(24)-C(25) | 1.390(3) |
| C(3)-O(2) | 1.4415(19) | C(25)-C(26) | 1.388(2) |
| C(3)-C(21) | 1.513(2) | C(31)-C(36) | 1.396(2) |
| C(4)-C(31) | 1.480(2) | C(31)-C(32) | 1.416(2) |
| C(11)-C(12) | 1.388(2) | C(32)-O(3) | 1.368(2) |
| C(11)-C(16) | 1.397(2) | C(32)-C(33) | 1.389(2) |
| C(12)-C(13) | 1.394(3) | C(33)-C(34) | 1.390(3) |
| C(13)-C(14) | 1.381(3) | C(34)-C(35) | 1.384(3) |
| C(14)-C(15) | 1.384(3) | C(35)-C(36) | 1.389(2) |
| C(15)-C(16) | 1.389(3) | C(37)-O(3) | 1.431(2) |

**Bond angles in [°]:**

| | | | |
|---|---|---|---|
| O(1)-C(1)-C(2) | 110.50(13) | C(26)-C(21)-C(3) | 121.30(15) |
| O(1)-C(1)-C(11) | 108.62(13) | C(22)-C(21)-C(3) | 119.63(15) |
| C(2)-C(1)-C(11) | 115.89(14) | C(23)-C(22)-C(21) | 120.16(17) |
| C(4)-C(2)-C(1) | 122.61(15) | C(24)-C(23)-C(22) | 120.37(17) |
| C(4)-C(2)-C(3) | 123.04(15) | C(23)-C(24)-C(25) | 119.87(17) |
| C(1)-C(2)-C(3) | 113.88(13) | C(26)-C(25)-C(24) | 119.76(17) |
| O(2)-C(3)-C(21) | 110.92(14) | C(25)-C(26)-C(21) | 120.74(16) |
| O(2)-C(3)-C(2) | 107.60(13) | C(36)-C(31)-C(32) | 117.28(15) |
| C(21)-C(3)-C(2) | 116.24(12) | C(36)-C(31)-C(4) | 123.31(15) |
| C(2)-C(4)-C(31) | 125.68(15) | C(32)-C(31)-C(4) | 119.36(14) |
| C(12)-C(11)-C(16) | 118.79(16) | O(3)-C(32)-C(33) | 123.68(16) |
| C(12)-C(11)-C(1) | 121.62(14) | O(3)-C(32)-C(31) | 115.58(15) |
| C(16)-C(11)-C(1) | 119.43(16) | C(33)-C(32)-C(31) | 120.74(16) |
| C(11)-C(12)-C(13) | 120.57(17) | C(32)-C(33)-C(34) | 119.95(17) |
| C(14)-C(13)-C(12) | 120.44(19) | C(35)-C(34)-C(33) | 120.48(17) |
| C(13)-C(14)-C(15) | 119.29(18) | C(34)-C(35)-C(36) | 119.22(16) |
| C(14)-C(15)-C(16) | 120.74(18) | C(35)-C(36)-C(31) | 122.09(16) |
| C(15)-C(16)-C(11) | 120.17(19) | C(32)-O(3)-C(37) | 117.14(14) |
| C(26)-C(21)-C(22) | 119.06(16) | | |

## A10 2-(2-Bromobenzylidene)-1,3-bis(2-bromophenyl)propane-*anti*-1,3-diol (*anti*-52)

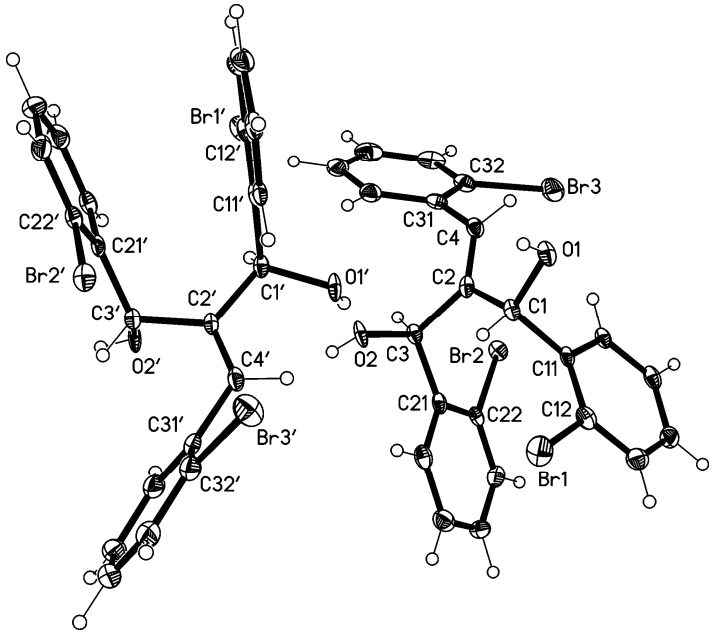


| | | |
|---|---|---|
| Crystal system | Orthorhombic | |
| Space group | *Pbca* | |
| Unit cell dim. | a = 20.3810(5) Å | α= 90° |
| | b = 13.7291(3) Å | β= 90° |
| | c = 28.6591(5) Å | γ = 90° |
| Volume (Z = 16) | 8019.2(3) Å$^3$ | |

**Bond lengths in [Å]:**

| | | | |
|---|---|---|---|
| C(1)-O(1) | 1.440(3) | C(23)-C(24) | 1.386(4) |
| C(1)-C(11) | 1.516(3) | C(24)-C(25) | 1.385(4) |
| C(1)-C(2) | 1.520(3) | C(25)-C(26) | 1.389(4) |
| C(2)-C(4) | 1.328(4) | C(31)-C(32) | 1.396(4) |
| C(2)-C(3) | 1.527(3) | C(31)-C(36) | 1.397(4) |
| C(3)-O(2) | 1.438(3) | C(32)-C(33) | 1.387(4) |
| C(3)-C(21) | 1.524(3) | C(32)-Br(3) | 1.906(3) |
| C(4)-C(31) | 1.481(4) | C(33)-C(34) | 1.385(4) |
| C(11)-C(12) | 1.391(4) | C(34)-C(35) | 1.383(4) |
| C(11)-C(16) | 1.400(4) | C(35)-C(36) | 1.388(4) |
| C(12)-C(13) | 1.384(4) | C(1')-O(1') | 1.437(3) |
| C(12)-Br(1) | 1.907(3) | C(1')-C(11') | 1.518(3) |
| C(13)-C(14) | 1.391(4) | C(1')-C(2') | 1.520(3) |
| C(14)-C(15) | 1.382(4) | C(2')-C(4') | 1.331(4) |
| C(15)-C(16) | 1.384(4) | C(2')-C(3') | 1.528(3) |
| C(21)-C(26) | 1.393(4) | C(3')-O(2') | 1.433(3) |
| C(21)-C(22) | 1.397(3) | C(3')-C(21') | 1.518(3) |
| C(22)-C(23) | 1.380(4) | C(4')-C(31') | 1.481(4) |
| C(22)-Br(2) | 1.903(3) | C(11')-C(12') | 1.392(4) |

| | | | |
|---|---|---|---|
| C(11')-C(16') | 1.399(3) | C(23')-C(24') | 1.385(4) |
| C(12')-C(13') | 1.381(4) | C(24')-C(25') | 1.386(4) |
| C(12')-Br(1') | 1.908(3) | C(25')-C(26') | 1.387(4) |
| C(13')-C(14') | 1.387(4) | C(31')-C(32') | 1.391(4) |
| C(14')-C(15') | 1.378(4) | C(31')-C(36') | 1.398(4) |
| C(15')-C(16') | 1.383(3) | C(32')-C(33') | 1.387(4) |
| C(21')-C(26') | 1.394(4) | C(32')-Br(3') | 1.903(3) |
| C(21')-C(22') | 1.399(3) | C(33')-C(34') | 1.382(4) |
| C(22')-C(23') | 1.384(4) | C(34')-C(35') | 1.386(4) |
| C(22')-Br(2') | 1.903(3) | C(35')-C(36') | 1.385(4) |

**Bond angles in [°]:**

| | | | |
|---|---|---|---|
| O(1)-C(1)-C(11) | 105.83(19) | O(1')-C(1')-C(11') | 106.25(19) |
| O(1)-C(1)-C(2) | 112.1(2) | O(1')-C(1')-C(2') | 111.4(2) |
| C(11)-C(1)-C(2) | 112.9(2) | C(11')-C(1')-C(2') | 112.70(19) |
| C(4)-C(2)-C(1) | 120.9(2) | C(4')-C(2')-C(1') | 120.9(2) |
| C(4)-C(2)-C(3) | 122.6(2) | C(4')-C(2')-C(3') | 121.8(2) |
| C(1)-C(2)-C(3) | 116.5(2) | C(1')-C(2')-C(3') | 117.3(2) |
| O(2)-C(3)-C(21) | 110.9(2) | O(2')-C(3')-C(21') | 111.4(2) |
| O(2)-C(3)-C(2) | 106.48(18) | O(2')-C(3')-C(2') | 105.53(18) |
| C(21)-C(3)-C(2) | 114.5(2) | C(21')-C(3')-C(2') | 114.3(2) |
| C(2)-C(4)-C(31) | 126.4(2) | C(2')-C(4')-C(31') | 126.6(2) |
| C(12)-C(11)-C(16) | 117.2(2) | C(12')-C(11')-C(16') | 117.2(2) |
| C(12)-C(11)-C(1) | 123.4(2) | C(12')-C(11')-C(1') | 123.8(2) |
| C(16)-C(11)-C(1) | 119.3(2) | C(16')-C(11')-C(1') | 119.0(2) |
| C(13)-C(12)-C(11) | 122.4(2) | C(13')-C(12')-C(11') | 122.1(2) |
| C(13)-C(12)-Br(1) | 116.9(2) | C(13')-C(12')-Br(1') | 117.2(2) |
| C(11)-C(12)-Br(1) | 120.7(2) | C(11')-C(12')-Br(1') | 120.76(19) |
| C(12)-C(13)-C(14) | 118.9(3) | C(12')-C(13')-C(14') | 119.3(3) |
| C(15)-C(14)-C(13) | 120.1(3) | C(15')-C(14')-C(13') | 120.1(3) |
| C(14)-C(15)-C(16) | 120.1(3) | C(14')-C(15')-C(16') | 120.1(3) |
| C(15)-C(16)-C(11) | 121.2(3) | C(15')-C(16')-C(11') | 121.2(3) |
| C(26)-C(21)-C(22) | 116.9(2) | C(26')-C(21')-C(22') | 116.9(2) |
| C(26)-C(21)-C(3) | 121.4(2) | C(26')-C(21')-C(3') | 121.2(2) |
| C(22)-C(21)-C(3) | 121.6(2) | C(22')-C(21')-C(3') | 121.9(2) |
| C(23)-C(22)-C(21) | 122.6(2) | C(23')-C(22')-C(21') | 122.2(3) |
| C(23)-C(22)-Br(2) | 117.46(19) | C(23')-C(22')-Br(2') | 117.9(2) |
| C(21)-C(22)-Br(2) | 119.97(19) | C(21')-C(22')-Br(2') | 119.86(19) |
| C(22)-C(23)-C(24) | 119.2(2) | C(22')-C(23')-C(24') | 119.4(3) |
| C(25)-C(24)-C(23) | 119.8(3) | C(23')-C(24')-C(25') | 119.8(3) |
| C(24)-C(25)-C(26) | 120.1(3) | C(24')-C(25')-C(26') | 120.1(3) |
| C(25)-C(26)-C(21) | 121.4(2) | C(25')-C(26')-C(21') | 121.5(3) |
| C(32)-C(31)-C(36) | 116.5(3) | C(32')-C(31')-C(36') | 117.0(3) |
| C(32)-C(31)-C(4) | 122.3(2) | C(32')-C(31')-C(4') | 121.5(2) |
| C(36)-C(31)-C(4) | 121.1(2) | C(36')-C(31')-C(4') | 121.5(3) |
| C(33)-C(32)-C(31) | 122.8(3) | C(33')-C(32')-C(31') | 122.5(3) |
| C(33)-C(32)-Br(3) | 117.9(2) | C(33')-C(32')-Br(3') | 118.4(2) |
| C(31)-C(32)-Br(3) | 119.3(2) | C(31')-C(32')-Br(3') | 119.1(2) |
| C(34)-C(33)-C(32) | 119.1(3) | C(34')-C(33')-C(32') | 119.1(3) |
| C(35)-C(34)-C(33) | 119.7(3) | C(33')-C(34')-C(35') | 119.9(3) |
| C(34)-C(35)-C(36) | 120.4(3) | C(36')-C(35')-C(34') | 120.2(3) |
| C(35)-C(36)-C(31) | 121.5(3) | C(35')-C(36')-C(31') | 121.2(3) |

## A11 2-(2-Methylbenzylidene)-1,3-di-*o*-tolylpropane-*syn*-1,3-diol (*syn*-54)

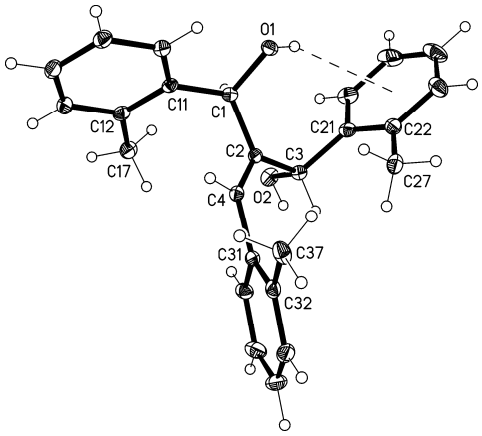


| | | |
|---|---|---|
| Crystal system | Monoclinic | |
| Space group | $P2_1/n$ | |
| Unit cell dim. | a = 12.8122(4) Å | α= 90° |
| | b = 11.8453(4) Å | β= 103.824(3)° |
| | c = 13.5310(5) Å | γ = 90° |
| Volume (Z = 4) | 1994.04(12) Å$^3$ | |

**Bond lengths in [Å]:**

| | | | |
|---|---|---|---|
| C(1)-O(1) | 1.4512(14) | C(21)-C(26) | 1.3962(18) |
| C(1)-C(11) | 1.5124(17) | C(21)-C(22) | 1.4076(19) |
| C(1)-C(2) | 1.5258(16) | C(22)-C(23) | 1.3965(19) |
| C(2)-C(4) | 1.3332(16) | C(22)-C(27) | 1.5044(19) |
| C(2)-C(3) | 1.5227(16) | C(23)-C(24) | 1.386(2) |
| C(3)-O(2) | 1.4293(15) | C(24)-C(25) | 1.375(3) |
| C(3)-C(21) | 1.5269(17) | C(25)-C(26) | 1.390(2) |
| C(4)-C(31) | 1.4850(16) | C(31)-C(36) | 1.4021(18) |
| C(11)-C(16) | 1.3929(17) | C(31)-C(32) | 1.4037(18) |
| C(11)-C(12) | 1.4072(17) | C(32)-C(33) | 1.4017(19) |
| C(12)-C(13) | 1.3943(18) | C(32)-C(37) | 1.496(2) |
| C(12)-C(17) | 1.5060(18) | C(33)-C(34) | 1.382(2) |
| C(13)-C(14) | 1.3873(19) | C(34)-C(35) | 1.379(2) |
| C(14)-C(15) | 1.3827(19) | C(35)-C(36) | 1.3835(19) |
| C(15)-C(16) | 1.3904(18) | | |

**Bond angles in [°]:**

| | | | |
|---|---|---|---|
| O(1)-C(1)-C(11) | 108.53(9) | C(13)-C(12)-C(17) | 119.49(12) |
| O(1)-C(1)-C(2) | 111.10(9) | C(11)-C(12)-C(17) | 122.28(11) |
| C(11)-C(1)-C(2) | 113.40(9) | C(14)-C(13)-C(12) | 121.84(12) |
| C(4)-C(2)-C(3) | 122.64(11) | C(15)-C(14)-C(13) | 119.72(12) |
| C(4)-C(2)-C(1) | 121.88(11) | C(14)-C(15)-C(16) | 119.42(12) |
| C(3)-C(2)-C(1) | 115.41(10) | C(15)-C(16)-C(11) | 121.25(12) |
| O(2)-C(3)-C(2) | 107.07(10) | C(26)-C(21)-C(22) | 119.68(12) |
| O(2)-C(3)-C(21) | 111.24(10) | C(26)-C(21)-C(3) | 119.55(12) |
| C(2)-C(3)-C(21) | 112.76(10) | C(22)-C(21)-C(3) | 120.77(11) |
| C(2)-C(4)-C(31) | 125.57(11) | C(23)-C(22)-C(21) | 118.44(13) |
| C(16)-C(11)-C(12) | 119.55(11) | C(23)-C(22)-C(27) | 119.71(13) |
| C(16)-C(11)-C(1) | 120.59(11) | C(21)-C(22)-C(27) | 121.84(11) |
| C(12)-C(11)-C(1) | 119.85(11) | C(24)-C(23)-C(22) | 121.40(16) |
| C(13)-C(12)-C(11) | 118.22(12) | C(25)-C(24)-C(23) | 119.78(15) |

| | | | |
|---|---|---|---|
| C(24)-C(25)-C(26) | 120.28(15) | C(33)-C(32)-C(37) | 121.18(13) |
| C(25)-C(26)-C(21) | 120.38(16) | C(31)-C(32)-C(37) | 120.59(12) |
| C(36)-C(31)-C(32) | 119.64(12) | C(34)-C(33)-C(32) | 121.38(14) |
| C(36)-C(31)-C(4) | 118.80(11) | C(35)-C(34)-C(33) | 120.20(13) |
| C(32)-C(31)-C(4) | 121.45(11) | C(34)-C(35)-C(36) | 119.71(14) |
| C(33)-C(32)-C(31) | 118.22(13) | C(35)-C(36)-C(31) | 120.84(13) |

## A12 Tribenzotriquinacene (3)

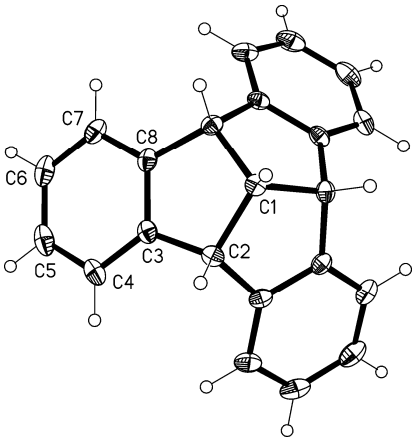


| | | |
|---|---|---|
| Crystal system | Rhombohedral | |
| Space group | *R*3*c* | |
| Unit cell dim. | a = 15.8850(6) Å | α= 90° |
| | b = 15.8850(6) Å | β= 90° |
| | c = 9.4953(4) Å | γ = 120° |
| Volume (Z = 6) | 2074.98(14) Å$^3$ | |

**Bond lengths in [Å]:**

| | | | |
|---|---|---|---|
| C(1)-C(2) | 1.5593(15) | C(4)-C(5) | 1.392(2) |
| C(2)-C(8)#2 | 1.5140(16) | C(5)-C(6) | 1.391(2) |
| C(2)-C(3) | 1.5172(16) | C(6)-C(7) | 1.3908(19) |
| C(3)-C(8) | 1.3949(19) | C(7)-C(8) | 1.3958(18) |
| C(3)-C(4) | 1.3956(17) | | |

Symmetry transformations used to generate equivalent atoms:

#1 -x+y+1,-x+1,z

#2 -y+1,x-y,z

**Bond angles in [°]:**

| | | | |
|---|---|---|---|
| C(2)-C(1)-C(2)#1 | 107.30(9) | C(5)-C(4)-C(3) | 119.11(12) |
| C(8)#2-C(2)-C(3) | 113.47(10) | C(6)-C(5)-C(4) | 120.74(12) |
| C(8)#2-C(2)-C(1) | 104.72(9) | C(5)-C(6)-C(7) | 120.29(12) |
| C(3)-C(2)-C(1) | 104.70(9) | C(6)-C(7)-C(8) | 119.19(12) |
| C(8)-C(3)-C(4) | 120.16(11) | C(3)-C(8)-C(7) | 120.50(11) |
| C(8)-C(3)-C(2) | 111.52(10) | C(3)-C(8)-C(2)#1 | 111.72(10) |
| C(4)-C(3)-C(2) | 128.30(12) | C(7)-C(8)-C(2)#1 | 127.76(12) |

## A13 1,5,9-Trimethyltribenzotriquinacene (57)[a]

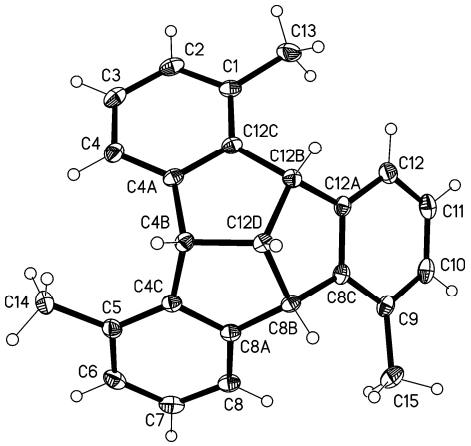


| | | |
|---|---|---|
| Crystal system | Triclinic | |
| Space group | *P*(-1) | |
| Unit cell dim. | a = 8.2455(8) Å | α= 117.577(10)° |
| | b = 10.6895(11) Å | β= 98.993(8)° |
| | c = 10.9922(10) Å | γ = 99.431(8)° |
| Volume (Z = 2) | 816.76(14) Å$^3$ | |

**Bond lengths in [Å]:**

| | | | |
|---|---|---|---|
| C(1)-C(2) | 1.3944(17) | C(7)-C(8) | 1.3887(17) |
| C(1)-C(12C) | 1.4052(16) | C(8)-C(8A) | 1.3929(15) |
| C(1)-C(13) | 1.5002(17) | C(8A)-C(8B) | 1.5184(16) |
| C(2)-C(3) | 1.3897(18) | C(8B)-C(8C) | 1.5130(15) |
| C(3)-C(4) | 1.3874(17) | C(8B)-C(12D) | 1.5576(15) |
| C(4)-C(4A) | 1.3937(16) | C(8C)-C(12A) | 1.3985(16) |
| C(4A)-C(12C) | 1.3962(16) | C(8C)-C(9) | 1.4032(15) |
| C(4A)-C(4B) | 1.5202(15) | C(9)-C(10) | 1.3988(17) |
| C(4B)-C(4C) | 1.5216(15) | C(9)-C(15) | 1.5073(17) |
| C(4B)-C(12D) | 1.5543(15) | C(10)-C(11) | 1.3856(18) |
| C(4C)-C(8A) | 1.4006(15) | C(11)-C(12) | 1.3928(17) |
| C(4C)-C(5) | 1.4007(16) | C(12)-C(12A) | 1.3912(16) |
| C(5)-C(6) | 1.3979(17) | C(12A)-C(12B) | 1.5229(15) |
| C(5)-C(14) | 1.5098(17) | C(12B)-C(12C) | 1.5215(16) |
| C(6)-C(7) | 1.3912(18) | C(12B)-C(12D) | 1.5602(15) |

[a] Structure **57** was deposited at The Cambridge Crystallographic Data Centre (CCDC 904630). The data can be obtained free of charge via www.ccdc.cam.ac.uk/data_request/cif.

**Bond angles in [°]:**

| | | | |
|---|---|---|---|
| C(2)-C(1)-C(12C) | 118.35(11) | C(8C)-C(8B)-C(12D) | 104.56(9) |
| C(2)-C(1)-C(13) | 119.22(11) | C(8A)-C(8B)-C(12D) | 104.51(9) |
| C(12C)-C(1)-C(13) | 122.42(11) | C(12A)-C(8C)-C(9) | 120.89(10) |
| C(3)-C(2)-C(1) | 121.42(11) | C(12A)-C(8C)-C(8B) | 111.54(9) |
| C(4)-C(3)-C(2) | 120.00(11) | C(9)-C(8C)-C(8B) | 127.19(10) |
| C(3)-C(4)-C(4A) | 119.52(11) | C(10)-C(9)-C(8C) | 117.78(11) |
| C(4)-C(4A)-C(12C) | 120.53(10) | C(10)-C(9)-C(15) | 119.54(10) |
| C(4)-C(4A)-C(4B) | 127.45(10) | C(8C)-C(9)-C(15) | 122.55(11) |
| C(12C)-C(4A)-C(4B) | 112.02(10) | C(11)-C(10)-C(9) | 121.35(11) |
| C(4A)-C(4B)-C(4C) | 113.72(9) | C(10)-C(11)-C(12) | 120.27(11) |
| C(4A)-C(4B)-C(12D) | 104.11(9) | C(12A)-C(12)-C(11) | 119.38(11) |
| C(4C)-C(4B)-C(12D) | 104.60(9) | C(12)-C(12A)-C(8C) | 120.05(10) |
| C(8A)-C(4C)-C(5) | 120.58(10) | C(12)-C(12A)-C(12B) | 128.19(10) |
| C(8A)-C(4C)-C(4B) | 111.15(10) | C(8C)-C(12A)-C(12B) | 111.42(9) |
| C(5)-C(4C)-C(4B) | 128.27(10) | C(12C)-C(12B)-C(12A) | 118.94(9) |
| C(6)-C(5)-C(4C) | 117.94(11) | C(12C)-C(12B)-C(12D) | 104.26(9) |
| C(6)-C(5)-C(14) | 119.03(11) | C(12A)-C(12B)-C(12D) | 104.13(9) |
| C(4C)-C(5)-C(14) | 123.01(11) | C(4A)-C(12C)-C(1) | 120.16(10) |
| C(7)-C(6)-C(5) | 121.45(11) | C(4A)-C(12C)-C(12B) | 111.38(10) |
| C(8)-C(7)-C(6) | 120.21(11) | C(1)-C(12C)-C(12B) | 128.28(10) |
| C(7)-C(8)-C(8A) | 119.25(11) | C(4B)-C(12D)-C(8B) | 107.73(9) |
| C(8)-C(8A)-C(4C) | 120.40(11) | C(4B)-C(12D)-C(12B) | 108.14(9) |
| C(8)-C(8A)-C(8B) | 127.99(10) | C(8B)-C(12D)-C(12B) | 107.25(8) |
| C(4C)-C(8A)-C(8B) | 111.47(9) | | |
| C(8C)-C(8B)-C(8A) | 118.26(9) | | |

## A14 9-Phenyl-9,10-dihydroindeno[1,2-a]indene (16)[b]

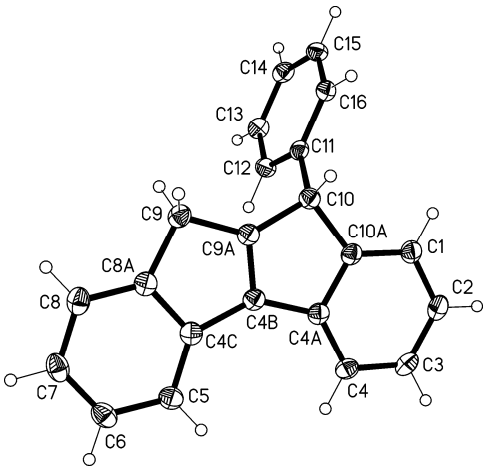


| | | |
|---|---|---|
| Crystal system | Monoclinic | |
| Space group | $P2_1/n$ | |
| Unit cell dim. | a = 9.3986(5) Å | α= 90° |
| | b = 5.4182(3) Å | β= 95.325(5)° |
| | c = 29.0041(16) Å | γ = 90° |
| Volume (Z = 4) | 1470.60(14) Å$^3$ | |

[b] Structure **16** was deposited at The Cambridge Crystallographic Data Centre (CCDC 904629). The data can be obtained free of charge via www.ccdc.cam.ac.uk/data_request/cif.

**Bond lengths in [Å]:**

| | | | |
|---|---|---|---|
| C(1)-C(10A) | 1.3826(14) | C(7)-C(8) | 1.3955(16) |
| C(1)-C(2) | 1.3990(15) | C(8)-C(8A) | 1.3844(14) |
| C(2)-C(3) | 1.3898(16) | C(8A)-C(9) | 1.5148(14) |
| C(3)-C(4) | 1.3996(15) | C(9)-C(9A) | 1.4993(13) |
| C(4)-C(4A) | 1.3911(14) | C(9A)-C(10) | 1.5068(13) |
| C(4A)-C(10A) | 1.4117(14) | C(10)-C(11) | 1.5213(13) |
| C(4A)-C(4B) | 1.4652(14) | C(10)-C(10A) | 1.5281(14) |
| C(4B)-C(9A) | 1.3469(15) | C(11)-C(16) | 1.3895(14) |
| C(4B)-C(4C) | 1.4667(13) | C(11)-C(12) | 1.3962(14) |
| C(4C)-C(5) | 1.3924(15) | C(12)-C(13) | 1.3885(14) |
| C(4C)-C(8A) | 1.4137(14) | C(13)-C(14) | 1.3915(15) |
| C(5)-C(6) | 1.3970(15) | C(14)-C(15) | 1.3859(16) |
| C(6)-C(7) | 1.3910(16) | C(15)-C(16) | 1.3971(14) |

**Bond angles in [°]:**

| | | | |
|---|---|---|---|
| C(10A)-C(1)-C(2) | 118.84(10) | C(4C)-C(8A)-C(9) | 110.45(8) |
| C(3)-C(2)-C(1) | 120.53(9) | C(9A)-C(9)-C(8A) | 101.29(8) |
| C(2)-C(3)-C(4) | 121.05(10) | C(4B)-C(9A)-C(9) | 111.76(9) |
| C(4A)-C(4)-C(3) | 118.45(10) | C(4B)-C(9A)-C(10) | 112.31(9) |
| C(4)-C(4A)-C(10A) | 120.38(9) | C(9)-C(9A)-C(10) | 135.86(9) |
| C(4)-C(4A)-C(4B) | 132.96(9) | C(9A)-C(10)-C(11) | 114.36(8) |
| C(10A)-C(4A)-C(4B) | 106.64(9) | C(9A)-C(10)-C(10A) | 100.37(8) |
| C(9A)-C(4B)-C(4A) | 109.97(9) | C(11)-C(10)-C(10A) | 112.44(8) |
| C(9A)-C(4B)-C(4C) | 110.07(9) | C(1)-C(10A)-C(4A) | 120.76(9) |
| C(4A)-C(4B)-C(4C) | 139.90(10) | C(1)-C(10A)-C(10) | 128.52(9) |
| C(5)-C(4C)-C(8A) | 120.79(9) | C(4A)-C(10A)-C(10) | 110.70(8) |
| C(5)-C(4C)-C(4B) | 132.77(10) | C(16)-C(11)-C(12) | 118.87(9) |
| C(8A)-C(4C)-C(4B) | 106.42(9) | C(16)-C(11)-C(10) | 121.02(9) |
| C(4C)-C(5)-C(6) | 118.44(10) | C(12)-C(11)-C(10) | 120.09(9) |
| C(7)-C(6)-C(5) | 120.77(10) | C(13)-C(12)-C(11) | 120.72(9) |
| C(6)-C(7)-C(8) | 120.77(10) | C(12)-C(13)-C(14) | 120.04(10) |
| C(8A)-C(8)-C(7) | 119.15(10) | C(15)-C(14)-C(13) | 119.74(9) |
| C(8)-C(8A)-C(4C) | 120.05(10) | C(14)-C(15)-C(16) | 120.08(9) |
| C(8)-C(8A)-C(9) | 129.49(10) | C(11)-C(16)-C(15) | 120.55(10) |

## A15 1,5-Dibromo-9-(2-bromophenyl)-9,10-dihydroindeno[1,2-a]indene (58)[c]

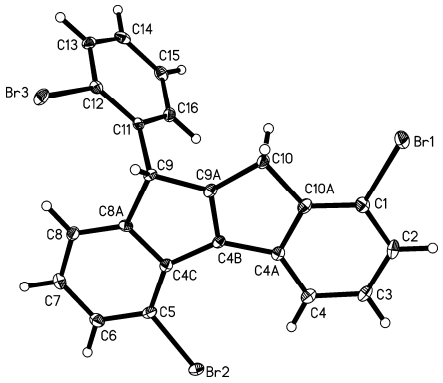


| | | |
|---|---|---|
| Crystal system | Orthorhombic | |
| Space group | *Pbca* | |
| Unit cell dim. | a = 6.7577(2) Å | α= 90° |
| | b = 22.2066(6) Å | β= 90° |
| | c = 23.6241(6) Å | γ = 90° |
| Volume (Z = 8) | 3545.15(17) Å$^3$ | |

**Bond lengths in [Å]:**

| | | | |
|---|---|---|---|
| C(1)-C(10A) | 1.380(3) | C(7)-C(8) | 1.391(3) |
| C(1)-C(2) | 1.394(3) | C(8)-C(8A) | 1.379(3) |
| C(1)-Br(1) | 1.904(2) | C(8A)-C(9) | 1.523(3) |
| C(2)-C(3) | 1.386(3) | C(9)-C(9A) | 1.500(3) |
| C(3)-C(4) | 1.394(3) | C(9)-C(11) | 1.517(3) |
| C(4)-C(4A) | 1.392(3) | C(9A)-C(10) | 1.491(3) |
| C(4A)-C(10A) | 1.416(3) | C(10)-C(10A) | 1.510(3) |
| C(4A)-C(4B) | 1.482(3) | C(11)-C(16) | 1.394(3) |
| C(4B)-C(9A) | 1.358(3) | C(11)-C(12) | 1.395(3) |
| C(4B)-C(4C) | 1.477(3) | C(12)-C(13) | 1.393(3) |
| C(4C)-C(5) | 1.392(3) | C(12)-Br(3) | 1.904(2) |
| C(4C)-C(8A) | 1.419(3) | C(13)-C(14) | 1.385(3) |
| C(5)-C(6) | 1.394(3) | C(14)-C(15) | 1.390(3) |
| C(5)-Br(2) | 1.901(2) | C(15)-C(16) | 1.386(3) |
| C(6)-C(7) | 1.385(3) | | |

**Bond angles in [°]:**

| | | | |
|---|---|---|---|
| C(10A)-C(1)-C(2) | 121.2(2) | C(8)-C(8A)-C(9) | 127.16(19) |
| C(10A)-C(1)-Br(1) | 119.81(17) | C(4C)-C(8A)-C(9) | 110.41(18) |
| C(2)-C(1)-Br(1) | 119.01(17) | C(9A)-C(9)-C(11) | 114.87(18) |
| C(3)-C(2)-C(1) | 118.7(2) | C(9A)-C(9)-C(8A) | 100.84(17) |
| C(2)-C(3)-C(4) | 121.8(2) | C(11)-C(9)-C(8A) | 113.68(17) |
| C(4A)-C(4)-C(3) | 119.0(2) | C(4B)-C(9A)-C(10) | 112.93(19) |
| C(4)-C(4A)-C(10A) | 119.8(2) | C(4B)-C(9A)-C(9) | 112.92(19) |
| C(4)-C(4A)-C(4B) | 134.0(2) | C(10)-C(9A)-C(9) | 134.15(19) |
| C(10A)-C(4A)-C(4B) | 106.11(18) | C(9A)-C(10)-C(10A) | 100.90(17) |
| C(9A)-C(4B)-C(4C) | 108.73(18) | C(1)-C(10A)-C(4A) | 119.5(2) |
| C(9A)-C(4B)-C(4A) | 108.78(19) | C(1)-C(10A)-C(10) | 129.2(2) |
| C(4C)-C(4B)-C(4A) | 142.48(19) | C(4A)-C(10A)-C(10) | 111.28(18) |
| C(5)-C(4C)-C(8A) | 116.80(19) | C(16)-C(11)-C(12) | 117.12(19) |
| C(5)-C(4C)-C(4B) | 136.2(2) | C(16)-C(11)-C(9) | 119.08(19) |

[c] Structure **58** was deposited at The Cambridge Crystallographic Data Centre (CCDC 904631). The data can be obtained free of charge via www.ccdc.cam.ac.uk/data_request/cif.

| | | | |
|---|---|---|---|
| C(8A)-C(4C)-C(4B) | 107.02(18) | C(12)-C(11)-C(9) | 123.79(19) |
| C(4C)-C(5)-C(6) | 121.2(2) | C(13)-C(12)-C(11) | 121.8(2) |
| C(4C)-C(5)-Br(2) | 122.48(17) | C(13)-C(12)-Br(3) | 117.44(16) |
| C(6)-C(5)-Br(2) | 116.28(16) | C(11)-C(12)-Br(3) | 120.73(16) |
| C(7)-C(6)-C(5) | 120.3(2) | C(14)-C(13)-C(12) | 119.5(2) |
| C(6)-C(7)-C(8) | 120.2(2) | C(13)-C(14)-C(15) | 119.9(2) |
| C(8A)-C(8)-C(7) | 119.0(2) | C(16)-C(15)-C(14) | 119.6(2) |
| C(8)-C(8A)-C(4C) | 122.4(2) | C(15)-C(16)-C(11) | 122.0(2) |

## A16 1,5-Dimethoxy-9-(2-methoxyphenyl)-9,10-dihydroindeno[1,2-a]indene (59)[d]

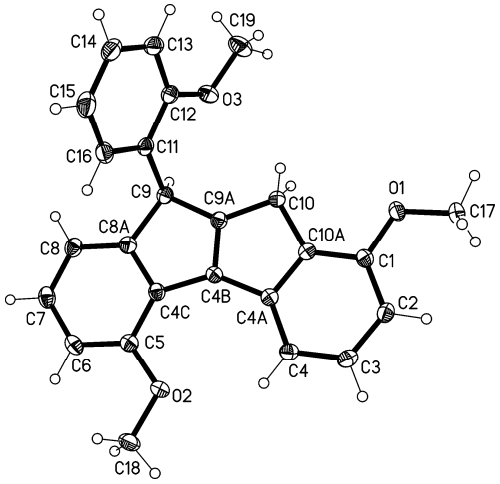


| | | |
|---|---|---|
| Crystal system | Monoclinic | |
| Space group | $P2_1/c$ | |
| Unit cell dim. | a = 12.4262(3) Å | α= 90° |
| | b = 19.7838(5) Å | β= 94.332(3)° |
| | c = 7.4806(2) Å | γ = 90° |
| Volume (Z = 4) | 1833.76(8) Å$^3$ | |

**Bond lengths in [Å]:**

| | | | |
|---|---|---|---|
| C(1)-O(1) | 1.3652(12) | C(8)-C(8A) | 1.3886(14) |
| C(1)-C(10A) | 1.3886(14) | C(8A)-C(9) | 1.5190(14) |
| C(1)-C(2) | 1.3976(14) | C(9)-C(9A) | 1.5058(13) |
| C(2)-C(3) | 1.3953(15) | C(9)-C(11) | 1.5245(14) |
| C(3)-C(4) | 1.3936(14) | C(9A)-C(10) | 1.4934(14) |
| C(4)-C(4A) | 1.3990(14) | C(10)-C(10A) | 1.5095(13) |
| C(4A)-C(10A) | 1.4086(14) | C(11)-C(16) | 1.3908(15) |
| C(4A)-C(4B) | 1.4708(14) | C(11)-C(12) | 1.4005(14) |
| C(4B)-C(9A) | 1.3515(14) | C(12)-O(3) | 1.3704(13) |
| C(4B)-C(4C) | 1.4731(14) | C(12)-C(13) | 1.3937(15) |
| C(4C)-C(5) | 1.3986(14) | C(13)-C(14) | 1.3915(17) |
| C(4C)-C(8A) | 1.4074(14) | C(14)-C(15) | 1.3824(18) |
| C(5)-O(2) | 1.3736(13) | C(15)-C(16) | 1.3958(16) |
| C(5)-C(6) | 1.3950(15) | C(17)-O(1) | 1.4264(12) |
| C(6)-C(7) | 1.3926(16) | C(18)-O(2) | 1.4305(12) |
| C(7)-C(8) | 1.3923(15) | C(19)-O(3) | 1.4231(13) |

[d] Structure **59** was deposited at The Cambridge Crystallographic Data Centre (CCDC 904632). The data can be obtained free of charge via www.ccdc.cam.ac.uk/data_request/cif.

**Bond angles in [°]:**

| | | | |
|---|---|---|---|
| O(1)-C(1)-C(10A) | 115.73(9) | C(9A)-C(9)-C(8A) | 101.20(8) |
| O(1)-C(1)-C(2) | 125.33(9) | C(9A)-C(9)-C(11) | 112.33(8) |
| C(10A)-C(1)-C(2) | 118.95(9) | C(8A)-C(9)-C(11) | 114.65(8) |
| C(3)-C(2)-C(1) | 119.81(9) | C(4B)-C(9A)-C(10) | 112.61(9) |
| C(4)-C(3)-C(2) | 122.08(9) | C(4B)-C(9A)-C(9) | 111.99(9) |
| C(3)-C(4)-C(4A) | 117.82(9) | C(10)-C(9A)-C(9) | 135.39(9) |
| C(4)-C(4A)-C(10A) | 120.45(9) | C(9A)-C(10)-C(10A) | 100.62(8) |
| C(4)-C(4A)-C(4B) | 133.29(9) | C(1)-C(10A)-C(4A) | 120.88(9) |
| C(10A)-C(4A)-C(4B) | 106.25(8) | C(1)-C(10A)-C(10) | 127.82(9) |
| C(9A)-C(4B)-C(4A) | 109.21(9) | C(4A)-C(10A)-C(10) | 111.29(8) |
| C(9A)-C(4B)-C(4C) | 109.26(9) | C(16)-C(11)-C(12) | 118.30(10) |
| C(4A)-C(4B)-C(4C) | 141.53(9) | C(16)-C(11)-C(9) | 122.49(9) |
| C(5)-C(4C)-C(8A) | 119.32(9) | C(12)-C(11)-C(9) | 119.14(9) |
| C(5)-C(4C)-C(4B) | 133.43(9) | O(3)-C(12)-C(13) | 124.03(10) |
| C(8A)-C(4C)-C(4B) | 107.26(9) | O(3)-C(12)-C(11) | 114.92(9) |
| O(2)-C(5)-C(6) | 124.13(9) | C(13)-C(12)-C(11) | 121.05(10) |
| O(2)-C(5)-C(4C) | 116.78(9) | C(14)-C(13)-C(12) | 119.21(10) |
| C(6)-C(5)-C(4C) | 119.09(9) | C(15)-C(14)-C(13) | 120.78(10) |
| C(7)-C(6)-C(5) | 120.78(10) | C(14)-C(15)-C(16) | 119.37(11) |
| C(8)-C(7)-C(6) | 120.84(10) | C(11)-C(16)-C(15) | 121.24(11) |
| C(8A)-C(8)-C(7) | 118.36(10) | C(1)-O(1)-C(17) | 117.77(8) |
| C(8)-C(8A)-C(4C) | 121.61(10) | C(5)-O(2)-C(18) | 116.41(8) |
| C(8)-C(8A)-C(9) | 128.13(9) | C(12)-O(3)-C(19) | 117.49(9) |
| C(4C)-C(8A)-C(9) | 110.25(9) | | |

## A17 1,5-Dimethyl-9-(*o*-tolyl)-9,10-dihydroindeno[1,2-a]indene (60)[e]

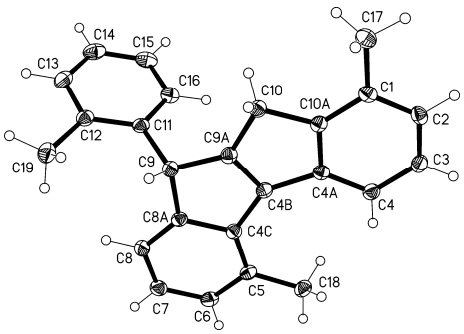


| | | |
|---|---|---|
| Crystal system | Monoclinic | |
| Space group | $P2_1/n$ | |
| Unit cell dim. | a = 9.5254(6) Å | α= 90° |
| | b = 5.8234(4) Å | β= 91.016(6)° |
| | c = 30.799(2) Å | γ = 90° |
| Volume (Z = 4) | 1708.17(19) Å$^3$ | |

**Bond lengths in [Å]:**

| | | | |
|---|---|---|---|
| C(1)-C(10A) | 1.3894(19) | C(7)-C(8) | 1.397(2) |
| C(1)-C(2) | 1.401(2) | C(8)-C(8A) | 1.3816(19) |
| C(1)-C(17) | 1.509(2) | C(8A)-C(9) | 1.5308(19) |
| C(2)-C(3) | 1.390(2) | C(9)-C(9A) | 1.5016(19) |
| C(3)-C(4) | 1.394(2) | C(9)-C(11) | 1.5329(19) |
| C(4)-C(4A) | 1.3947(19) | C(9A)-C(10) | 1.4942(19) |

[e] Structure **60** was deposited at The Cambridge Crystallographic Data Centre (CCDC 904633). The data can be obtained free of charge via www.ccdc.cam.ac.uk/data_request/cif.

| | | | |
|---|---|---|---|
| C(4A)-C(10A) | 1.4155(19) | C(10)-C(10A) | 1.5125(19) |
| C(4A)-C(4B) | 1.4847(19) | C(11)-C(12) | 1.401(2) |
| C(4B)-C(9A) | 1.356(2) | C(11)-C(16) | 1.403(2) |
| C(4B)-C(4C) | 1.4798(19) | C(12)-C(13) | 1.408(2) |
| C(4C)-C(5) | 1.4014(19) | C(12)-C(19) | 1.500(2) |
| C(4C)-C(8A) | 1.4194(19) | C(13)-C(14) | 1.383(2) |
| C(5)-C(6) | 1.401(2) | C(14)-C(15) | 1.384(2) |
| C(5)-C(18) | 1.509(2) | C(15)-C(16) | 1.390(2) |
| C(6)-C(7) | 1.389(2) | | |

**Bond angles in [°]:**

| | | | |
|---|---|---|---|
| C(10A)-C(1)-C(2) | 117.28(13) | C(8)-C(8A)-C(9) | 127.61(13) |
| C(10A)-C(1)-C(17) | 121.18(13) | C(4C)-C(8A)-C(9) | 110.86(12) |
| C(2)-C(1)-C(17) | 121.53(13) | C(9A)-C(9)-C(8A) | 100.37(11) |
| C(3)-C(2)-C(1) | 121.15(13) | C(9A)-C(9)-C(11) | 114.78(11) |
| C(2)-C(3)-C(4) | 121.41(13) | C(8A)-C(9)-C(11) | 113.12(11) |
| C(3)-C(4)-C(4A) | 118.54(13) | C(4B)-C(9A)-C(10) | 112.46(12) |
| C(4)-C(4A)-C(10A) | 119.50(13) | C(4B)-C(9A)-C(9) | 113.10(12) |
| C(4)-C(4A)-C(4B) | 134.05(13) | C(10)-C(9A)-C(9) | 134.43(12) |
| C(10A)-C(4A)-C(4B) | 106.46(12) | C(9A)-C(10)-C(10A) | 101.44(11) |
| C(9A)-C(4B)-C(4C) | 109.14(12) | C(1)-C(10A)-C(4A) | 122.10(13) |
| C(9A)-C(4B)-C(4A) | 108.96(12) | C(1)-C(10A)-C(10) | 127.22(13) |
| C(4C)-C(4B)-C(4A) | 141.89(13) | C(4A)-C(10A)-C(10) | 110.68(12) |
| C(5)-C(4C)-C(8A) | 119.74(13) | C(12)-C(11)-C(16) | 119.14(13) |
| C(5)-C(4C)-C(4B) | 133.74(13) | C(12)-C(11)-C(9) | 122.15(13) |
| C(8A)-C(4C)-C(4B) | 106.52(12) | C(16)-C(11)-C(9) | 118.68(13) |
| C(6)-C(5)-C(4C) | 117.63(13) | C(11)-C(12)-C(13) | 118.56(14) |
| C(6)-C(5)-C(18) | 119.22(13) | C(11)-C(12)-C(19) | 122.50(13) |
| C(4C)-C(5)-C(18) | 123.14(13) | C(13)-C(12)-C(19) | 118.92(13) |
| C(7)-C(6)-C(5) | 122.41(14) | C(14)-C(13)-C(12) | 121.47(14) |
| C(6)-C(7)-C(8) | 119.94(13) | C(13)-C(14)-C(15) | 119.98(14) |
| C(8A)-C(8)-C(7) | 118.76(13) | C(14)-C(15)-C(16) | 119.40(15) |
| C(8)-C(8A)-C(4C) | 121.51(13) | C(15)-C(16)-C(11) | 121.41(14) |

## A18 4b,8b,12b-Tribromotribenzotriquinacene (28)

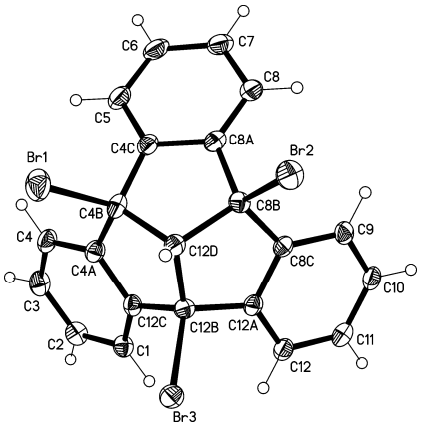


| | | |
|---|---|---|
| Crystal system | Monoclinic | |
| Space group | $P2_1/c$ | |
| Unit cell dim. | a = 8.3353(3) Å | $\alpha$= 90° |
| | b = 12.3269(4) Å | $\beta$= 95.673(4)° |
| | c = 17.6085(6) Å | $\gamma$ = 90° |
| Volume (Z = 4) | 1800.38(11) Å$^3$ | |

**Bond lengths in [Å]:**

| | | | |
|---|---|---|---|
| C(1)-C(2) | 1.390(4) | C(8)-C(8A) | 1.385(5) |
| C(1)-C(12C) | 1.391(4) | C(8A)-C(8B) | 1.508(4) |
| C(2)-C(3) | 1.390(5) | C(8B)-C(8C) | 1.500(4) |
| C(3)-C(4) | 1.383(5) | C(8B)-C(12D) | 1.551(4) |
| C(4)-C(4A) | 1.404(4) | C(8B)-Br(2) | 1.986(3) |
| C(4A)-C(12C) | 1.389(4) | C(8C)-C(12A) | 1.393(4) |
| C(4A)-C(4B) | 1.502(4) | C(8C)-C(9) | 1.396(4) |
| C(4B)-C(4C) | 1.495(5) | C(9)-C(10) | 1.385(5) |
| C(4B)-C(12D) | 1.551(4) | C(10)-C(11) | 1.391(5) |
| C(4B)-Br(1) | 1.983(3) | C(11)-C(12) | 1.390(5) |
| C(4C)-C(5) | 1.390(5) | C(12)-C(12A) | 1.395(4) |
| C(4C)-C(8A) | 1.399(4) | C(12A)-C(12B) | 1.501(4) |
| C(5)-C(6) | 1.385(5) | C(12B)-C(12C) | 1.505(4) |
| C(6)-C(7) | 1.395(5) | C(12B)-C(12D) | 1.553(4) |
| C(7)-C(8) | 1.393(5) | C(12B)-Br(3) | 2.003(3) |

**Bond angles in [°]:**

| | | | |
|---|---|---|---|
| C(2)-C(1)-C(12C) | 118.3(3) | C(8C)-C(8B)-Br(2) | 109.1(2) |
| C(1)-C(2)-C(3) | 120.8(3) | C(8A)-C(8B)-Br(2) | 109.3(2) |
| C(4)-C(3)-C(2) | 121.0(3) | C(12D)-C(8B)-Br(2) | 111.4(2) |
| C(3)-C(4)-C(4A) | 118.5(3) | C(12A)-C(8C)-C(9) | 120.1(3) |
| C(12C)-C(4A)-C(4) | 120.2(3) | C(12A)-C(8C)-C(8B) | 111.5(3) |
| C(12C)-C(4A)-C(4B) | 111.9(3) | C(9)-C(8C)-C(8B) | 128.4(3) |
| C(4)-C(4A)-C(4B) | 127.9(3) | C(10)-C(9)-C(8C) | 118.6(3) |
| C(4C)-C(4B)-C(4A) | 115.0(3) | C(9)-C(10)-C(11) | 121.4(3) |
| C(4C)-C(4B)-C(12D) | 105.1(3) | C(12)-C(11)-C(10) | 120.3(3) |
| C(4A)-C(4B)-C(12D) | 105.1(2) | C(11)-C(12)-C(12A) | 118.5(3) |
| C(4C)-C(4B)-Br(1) | 110.5(2) | C(8C)-C(12A)-C(12) | 121.1(3) |
| C(4A)-C(4B)-Br(1) | 109.5(2) | C(8C)-C(12A)-C(12B) | 111.0(3) |
| C(12D)-C(4B)-Br(1) | 111.4(2) | C(12)-C(12A)-C(12B) | 127.9(3) |
| C(5)-C(4C)-C(8A) | 119.9(3) | C(12A)-C(12B)-C(12C) | 116.8(2) |
| C(5)-C(4C)-C(4B) | 128.4(3) | C(12A)-C(12B)-C(12D) | 105.5(2) |
| C(8A)-C(4C)-C(4B) | 111.7(3) | C(12C)-C(12B)-C(12D) | 105.6(2) |
| C(6)-C(5)-C(4C) | 119.1(3) | C(12A)-C(12B)-Br(3) | 109.57(19) |
| C(5)-C(6)-C(7) | 121.0(3) | C(12C)-C(12B)-Br(3) | 108.7(2) |
| C(8)-C(7)-C(6) | 120.2(3) | C(12D)-C(12B)-Br(3) | 110.5(2) |
| C(8A)-C(8)-C(7) | 118.6(3) | C(4A)-C(12C)-C(1) | 121.2(3) |
| C(8)-C(8A)-C(4C) | 121.2(3) | C(4A)-C(12C)-C(12B) | 110.8(3) |
| C(8)-C(8A)-C(8B) | 127.7(3) | C(1)-C(12C)-C(12B) | 128.0(3) |
| C(4C)-C(8A)-C(8B) | 111.0(3) | C(8B)-C(12D)-C(4B) | 107.0(2) |
| C(8C)-C(8B)-C(8A) | 116.5(3) | C(8B)-C(12D)-C(12B) | 106.1(2) |
| C(8C)-C(8B)-C(12D) | 105.4(2) | C(4B)-C(12D)-C(12B) | 106.3(2) |
| C(8A)-C(8B)-C(12D) | 105.0(2) | | |

# Abbreviations

| | |
|---|---|
| 6-31G(d) | split-valence double-zeta basis set with additional polarization functions on heavy atoms [277] |
| 6-311G(d,p) | split-valence triple-zeta basis set with additional polarization functions on all atoms (additional "+" denotes inclusion of diffuse functions on the heavy atoms) [278] |
| a.u. | atomic units (for energy: 1 hartree = 627.5095 kcal/mol) |
| cat. | catalytic amounts |
| B3LYP | Becke's three-parameter hybrid functional [197] |
| B97-D | Grimme's GGA functional with long-range dispersion correction [200] |
| BSSE | basis set superposition error |
| calcd | calculated |
| cc-pVDZ | Dunning's correlation consistent polarized valence double-zeta basis set [279] |
| cc-pVTZ | Dunning's correlation consistent polarized valence triple-zeta basis set (additional "aug" denotes inclusion of diffuse functions) [279] |
| CID | collision-induced dissociation |
| CCSD(T) | coupled cluster calculation including triple excitations non-iteratively [196,280] |
| decomp | decomposition |
| dim. | dimension(s) |
| DFT | density functional theory [281,282] |
| DSC | differential scanning calorimetry |
| EA | elemental analysis |
| EI | electron impact ionization |

| | |
|---|---|
| ESI | electrospray ionization |
| GGA | general gradient approximation |
| IR | infrared |
| M06-2X | hybrid meta functional by Zhao and Truhlar [198,199] |
| MP2 | 2$^{nd}$ order Møller-Plesset perturbation theory [283] |
| MS | mass spectrometry |
| MsOH | methanesulfonic acid |
| NMR | nuclear magnetic spectroscopy |
| PPA | polyphosphoric acid |
| QCISD | quadratic configuration interaction calculation [196] |
| $R_f$ | retention factor |
| r.m.s. | root mean square |
| r.t. | room temperature |
| TFA | trifluoroacetic acid |
| $TfO_2$ | triflic anhydride |
| TfOH | triflic acid |
| TLC | thin layer chromatography |
| TS | transition state |
| TsOH | *p*-toluenesulfonic acid |
| UV | ultraviolet |
| ZPE | zero-point energy |

# References


1. P. W. Rabideau, A. Sygula, *Acc. Chem. Res.* **1996**, *29*, 235–242.
2. V. M. Tsefrikas, L. T. Scott, *Chem. Rev.* **2006**, *106*, 4868–4884.
3. W. E. Barth, R. G. Lawton, *J. Am. Chem. Soc.* **1966**, *88*, 380–381.
4. R. G. Lawton, W. E. Barth, *J. Am. Chem. Soc.* **1971**, *93*, 1730–1745.
5. L. T. Scott, M. M. Hashemi, D. T. Meyer, H. B. Warren, *J. Am. Chem. Soc.* **1991**, *113*, 7082–7084.
6. A. Borchardt, A. Fuchicello, K. V. Kilway, K. K. Baldridge, J. S. Siegel, *J. Am. Chem. Soc.* **1992**, *114*, 1921–1923.
7. L. T. Scott, P.-C. Cheng, M. M. Hashemi, M. S. Bratcher, D. T. Meyer, H. B. Warren, *J. Am. Chem. Soc.* **1997**, *119*, 10963–10968.
8. A. Sygula, P. W. Rabideau, *J. Am. Chem. Soc.* **2000**, *122*, 6323–6324.
9. A. M. Butterfield, B. Gilomen, J. S. Siegel, *Org. Process Res. Dev.* **2012**, *16*, 664–676.
10. H. Sakurai, T. Daiko, T. Hirao, *Science* **2003**, *301*, 1878.
11. H. Sakurai, T. Daiko, H. Sakane, T. Amaya, T. Hirao, *J. Am. Chem. Soc.* **2005**, *127*, 11580–11581.
12. T. Amaya, T. Nakata, T. Hirao, *J. Am. Chem. Soc.* **2009**, *131*, 10810–10811.
13. T. Amaya, T. Hirao, *Chem. Commun.* **2011**, *47*, 10524–10535.
14. L. T. Scott, M. M. Hashemi, M. S. Bratcher, *J. Am. Chem. Soc.* **1992**, *114*, 1920–1921.
15. T. J. Seiders, K. K. Baldridge, G. H. Grube, J. S. Siegel, *J. Am. Chem. Soc.* **2001**, *123*, 517–525.
16. D. Eisenberg, A. S. Filatov, E. A. Jackson, M. Rabinovitz, M. A. Petrukhina, L. T. Scott, R. Shenhar, *J. Org. Chem.* **2008**, *73*, 6073–6078.
17. T. Amaya, H. Sakane, T. Muneishi, T. Hirao, *Chem. Commun.* **2008**, 765–767.
18. S. Higashibayashi, H. Sakurai, *J. Am. Chem. Soc.* **2008**, *130*, 8592–8593.
19. T. Amaya, W.-Z. Wang, H. Sakane, T. Moriuchi, T. Hirao, *Angew. Chem. Int. Ed.* **2010**, *49*, 403–406.
20. T. Amaya, T. Hirao, *Pure Appl. Chem.* **2012**, *84*, 1089–1100.
21. R. B. Woodward, T. Fukunaga, R. C. Kelly, *J. Am. Chem. Soc.* **1964**, *86*, 3162–3164.
22. D. Kuck, *Angew. Chem. Int. Ed. Engl.* **1984**, *23*, 508–509.
23. D. Kuck, A. Schuster, B. Ohlhorst, V. Sinnwell, A. de Meijere, *Angew. Chem. Int. Ed. Engl.* **1989**, *28*, 595–597.

24. W. Baker, J. F. W. McOmie, S. D. Pareitt, D. A. M. Watkins, *J. Chem. Soc.* **1957**, 4026–4037.
25. D. Kuck, T. Lindenthal, A. Schuster, *Chem. Ber.* **1992**, *125*, 1449–1460.
26. D. Kuck, E. Neumann, A. Schuster, *Chem. Ber.* **1994**, *127*, 151–164.
27. A. Ceccon, A. Gambaro, F. Manoli, A. Venzo, D. Kuck, T. E. Bitterwolf, P. Ganis, G. Valle, *J. Chem. Soc., Perkin Trans. 2* **1991**, 233–241.
28. C. A. Dullaghan, G. B. Carpenter, D. A. Sweigart, D. Kuck, C. Fusco, R. Curci, *Organometallics* **2000**, *19*, 2233–2236.
29. W.-X. Niu, T. Wang, Q.-Q. Hou, Z.-Y. Li, X.-P. Cao, D. Kuck, *J. Org. Chem.* **2010**, *75*, 6704–6707.
30. T. Wang, Q.-Q. Hou, Q.-F. Teng, X.-J. Yao, W.-X. Niu, X.-P. Cao, D. Kuck, *Chem. Eur. J.* **2010**, *16*, 12412–12424.
31. J. Tellenbröker, D. Kuck, *Angew. Chem. Int. Ed.* **1999**, *38*, 919–922.
32. W.-X. Niu, E.-Q. Yang, Z.-F. Shi, X.-P. Cao, D. Kuck, *J. Org. Chem.* **2012**, *77*, 1422–1434.
33. P. E. Georghiou, L. N. Dawe, H.-A. Tran, J. Strübe, B. Neumann, H.-G. Stammler, D. Kuck, *J. Org. Chem.* **2008**, *73*, 9040–9047.
34. T. Wang, Z.-Y. Li, A.-L. Xie, X.-J. Yao, X.-P. Cao, D. Kuck, *J. Org. Chem.* **2011**, *76*, 3231–3238.
35. B. Bredenkötter, S. Henne, D. Volkmer, *Chem. Eur. J.* **2007**, *13*, 9931–9938.
36. H. Langhals, M. Rauscher, J. Strube, D. Kuck, *J. Org. Chem.* **2008**, *73*, 1113–1116.
37. D. Kuck, A. Schuster, B. Paisdor, D. Gestmann, *J. Chem. Soc., Perkin Trans. 1* **1995**, 721–732.
38. D. Kuck, *Synlett* **1996**, *10*, 949–965.
39. D. Kuck, in: *Carbon Rich Compounds I, Topics in Current Chemistry Vol. 196* (Ed.: A. de Meijere), Springer: Berlin Heidelberg, **1998**, pp. 167-220.
40. D. Kuck, *Chem. Rev.* **2006**, *106*, 4885–4925.
41. D. Kuck, *Pure Appl. Chem.* **2006**, *78*, 749–775.
42. A. Schuster, D. Kuck, *Angew. Chem. Int. Ed. Engl.* **1991**, *30*, 1699–1702.
43. D. Kuck, A. Schuster, R. A. Krause, J. Tellenbröker, C. P. Exner, M. Penk, H. Bögge, A. Müller, *Tetrahedron* **2001**, *57*, 3587–3613.
44. E. U. Mughal, D. Kuck, *Org. Biomol. Chem.* **2010**, *8*, 5383–5389.
45. R. Haag, B. Ohlhorst, M. Noltemeyer, A. Schuster, D. Kuck, A. de Meijere, *J. Chem. Soc., Chem. Commun.* **1993**, 1727–1729.
46. R. Haag, D. Kuck, X.-Y. Fu, J. M. Cook, A. de Meijere, *Synlett* **1994**, 340-342.

47. R. Haag, B. Ohlhorst, M. Noltemeyer, R. Fleischer, D. Stalke, A. Schuster, D. Kuck, A. de Meijere, *J. Am. Chem. Soc.* **1995***, 117*, 10474–10485.
48. J. Tellenbroker, D. Barth, B. Neumann, H.-G. Stammler, D. Kuck, *Org. Biomol. Chem.* **2005***, 3*, 570–571.
49. Y. Kirchwehm, A. Damme, T. Kupfer, H. Braunschweig, A. Krueger, *Chem. Commun.* **2012***, 48*, 1502–1504.
50. D. Kuck, T. Hackfort, B. Neumann, H.-G. Stammler, *Polish J. Chem.* **2007***, 81*, 875–892.
51. E. U. Mughal, D. Kuck, *Chem. Commun.* **2012***, 48*, 8880–8882.
52. L. Zhou, T.-X. Zhang, B.-R. Li, X.-P. Cao, D. Kuck, *J. Org. Chem.* **2007***, 72*, 6382–6389.
53. J. Strübe, B. Neumann, H.-G. Stammler, D. Kuck, *Chem. Eur. J.* **2009***, 15*, 2256–2260.
54. J. Tellenbröker, D. Kuck, *Beilstein J. Org. Chem.* **2011***, 7*, 329–337.
55. M. Harig, B. Neumann, H.-G. Stammler, D. Kuck, *Eur. J. Org. Chem.* **2004**, 2381–2397.
56. J. Vile, M. Carta, C. G. Bezzu, N. B. McKeown, *Polym. Chem.* **2011***, 2*, 2257–2260.
57. M. Harig, D. Kuck, *Eur. J. Org. Chem.* **2006***,* 1647–1655.
58. N. J. Head, G. A. Olah, G. K. S. Prakash, *J. Am. Chem. Soc.* **1995***, 117*, 11205–11210.
59. D. Kuck, B. Paisdor, D. Gestmann, *Angew. Chem. Int. Ed. Engl.* **1994***, 33*, 1251–1253.
60. K. Prantz, J. Mulzer, *Chem. Rev.* **2010***, 110*, 3741–3766.
61. D. Kuck, *personal communication*.
62. R. Tanikaga, N. Konya, K. Hamamura, A. Kaji, *Bull. Chem. Soc. Jpn.* **1988***, 61*, 3211–3216.
63. T.-T. Kao, S.-e. Syu, Y.-W. Jhang, W. Lin, *Org. Lett.* **2010***, 12*, 3066–3069.
64. S. E. Gibson, M. P. Castaldi, *Chem. Commun.* **2006**, 3045–3062.
65. M. Mikulás, N. Rück-Braun, in: *Organic Synthesis Highlights IV* (Ed.: H.-G. Schmalz), Wiley-VCH: Weinheim, **2000**, pp. 187–193.
66. C. Moberg, *Angew. Chem. Int. Ed.* **1998***, 37*, 248–268.
67. L. H. Gade, S. Bellemin-Laponnaz, *Chem. Eur. J.* **2008***, 14*, 4142–4152.
68. C. Moberg, *Angew. Chem. Int. Ed.* **2006***, 45*, 4721–4723.
69. S. E. Gibson, M. P. Castaldi, *Angew. Chem. Int. Ed.* **2006***, 45*, 4718–4720.
70. M. J. Hardie, *Chem. Soc. Rev.* **2010***, 39*, 516–527.
71. A. R. A. Palmans, E. W. Meijer, *Angew. Chem. Int. Ed.* **2007***, 46*, 8948–8968.

72. M. L. Bushey, T.-Q. Nguyen, W. Zhang, D. Horoszewski, C. Nuckolls, *Angew. Chem. Int. Ed.* **2004**, *43*, 5446–5453.
73. N. V. Dubrovina, V. I. Tararov, A. Monsees, R. Kadyrov, C. Fischer, A. Börner, *Tetrahedron: Asymmetry* **2003**, *14*, 2739–2745.
74. A. Hu, W. Lin, *Org. Lett.* **2005**, *7*, 455–458.
75. R. Bunce, V. Taylor, H. Reeves, *Org. Prep. Proc. Int.* **1989**, *21*, 337–339.
76. E. P. Kohler, H. M. Chadwell, *Organic Syntheses, Coll. Vol. 1* **1941**, 78.
77. G. E. Southard, G. M. Murray, *J. Org. Chem.* **2005**, *70*, 9036–9039.
78. A. H. More, C. S. Ramaa, *Indian J. Chem.* **2010**, *49B*, 364–367.
79. J. H. Gross, *Mass Spectrometry: A Textbook*, Springer: Berlin Heidelberg, **2004**.
80. J. Barluenga, J. G. Resa, B. Olano, S. Fustero, *J. Org. Chem.* **1987**, *52*, 1425–1428.
81. M. Rueping, B. J. Nachtsheim, A. Kuenkel, *Org. Lett.* **2007**, *9*, 825–828.
82. P. Metrangolo, H. Neukirch, T. Pilati, G. Resnati, *Acc. Chem. Res.* **2005**, *38*, 386–395.
83. P. Metrangolo, T. Pilati, G. Resnati, *CrystEngComm* **2006**, *8*, 946–947.
84. P. Metrangolo, F. Meyer, T. Pilati, G. Resnati, G. Terraneo, *Angew. Chem. Int. Ed.* **2008**, *47*, 6114–6127.
85. K. Rissanen, *CrystEngComm* **2008**, *10*, 1107–1113.
86. A. Anthony, G. R. Desiraju, R. K. R. Jetti, S. S. Kuduva, N. N. L. Madhavi, A. Nangia, R. Thaimattam, V. R. Thalladi, *Cryst. Eng.* **1998**, *1*, 1–18.
87. B. K. Saha, R. K. R. Jetti, L. S. Reddy, S. Aitipamula, A. Nangia, *Cryst. Growth Des.* **2005**, *5*, 887–899.
88. Y. Lu, J. Zou, H. Wang, Q. Yu, H. Zhang, Y. Jiang, *J. Phys. Chem. A* **2005**, *109*, 11956–11961.
89. T. T. T. Bui, S. Dahaoui, C. Lecomte, G. R. Desiraju, E. Espinosa, *Angew. Chem. Int. Ed.* **2009**, *48*, 3838–3841.
90. S. F. Boys, F. Bernardi, *Mol. Phys.* **1970**, *19*, 553–566.
91. S. Simon, M. Duran, J. J. Dannenberg, *J. Chem. Phys.* **1996**, *105*, 11024–11031.
92. D. Kuck, M. K. Cyranski, *unpublished results*.
93. A. T. Wright, Z. Zhong, E. V. Anslyn, *Angew. Chem. Int. Ed.* **2005**, *44*, 5679–5682.
94. G. Hennrich, V. M. Lynch, E. V. Anslyn, *Chem. Eur. J.* **2002**, *8*, 2274–2278.
95. A. Frontera, C. Garau, D. Quiñonero, P. Ballester, A. Costa, P. M. Deyà, *Org. Lett.* **2003**, *5*, 1135–1138.
96. P. Ballester, M. Capó, A. Costa, P. M. Deyà, R. Gomila, A. Decken, G. Deslongchamps, *J. Org. Chem.* **2002**, *67*, 8832–8841.

97. P. Ballester, M. Capó, A. Costa, P. M. Deyà, R. Gomila, A. Decken, G. Deslongchamps, *Org. Lett.* **2000***, 3*, 267–270.
98. P. Ballester, A. Costa, P. M. Deya, G. Deslongchamps, D. Mink, A. Decken, R. Prohens, S. Tomas, M. Vega, *Chem. Commun.* **1997**, 357–358.
99. S. Kubik, R. Goddard, *Eur. J. Org. Chem.* **2001**, 311–322.
100. J. Bitta, S. Kubik, *Org. Lett.* **2001***, 3*, 2637–2640.
101. S. Kubik, R. Goddard, *Chem. Commun.* **2000**, 633–634.
102. S. Kubik, R. Goddard, *J. Org. Chem.* **1999***, 64*, 9475–9486.
103. A. Ardá, F. J. Cañada, C. Nativi, O. Francesconi, G. Gabrielli, A. Ienco, J. Jiménez-Barbero, S. Roelens, *Chem. Eur. J.* **2011***, 17*, 4821–4829.
104. A. L. Cresswell, M.-O. M. Piepenbrock, J. W. Steed, *Chem. Commun.* **2010***, 46*, 2787–2789.
105. M. Mazik, A. Hartmann, P. G. Jones, *Chem. Eur. J.* **2009***, 15*, 9147–9159.
106. M. Mazik, A. Hartmann, *J. Org. Chem.* **2008***, 73*, 7444–7450.
107. M. Mazik, A. C. Buthe, *J. Org. Chem.* **2007***, 72*, 8319–8326.
108. C. Nativi, M. Cacciarini, O. Francesconi, A. Vacca, G. Moneti, A. Ienco, S. Roelens, *J. Am. Chem. Soc.* **2007***, 129*, 4377–4385.
109. M. Mazik, H. Cavga, *J. Org. Chem.* **2007***, 72*, 831–838.
110. D. R. Turner, M. J. Paterson, J. W. Steed, *J. Org. Chem.* **2006***, 71*, 1598–1608.
111. W. J. Belcher, M. Fabre, T. Farhan, J. W. Steed, *Org. Biomol. Chem.* **2006***, 4*, 781–786.
112. M. Mazik, W. Radunz, R. Boese, *J. Org. Chem.* **2004***, 69*, 7448–7462.
113. K. J. Wallace, W. J. Belcher, D. R. Turner, K. F. Syed, J. W. Steed, *J. Am. Chem. Soc.* **2003***, 125*, 9699–9715.
114. S.-G. Kim, K.-H. Kim, J. Jung, S. K. Shin, K. H. Ahn, *J. Am. Chem. Soc.* **2002***, 124*, 591–596.
115. J. Chin, J. Oh, S. Y. Jon, S. H. Park, C. Walsdorff, B. Stranix, A. Ghoussoub, S. J. Lee, H. J. Chung, S.-M. Park, K. Kim, *J. Am. Chem. Soc.* **2002***, 124*, 5374–5379.
116. T. K. Ronson, C. Carruthers, J. Fisher, T. Brotin, L. P. Harding, P. J. Rizkallah, M. J. Hardie, *Inorg. Chem.* **2010***, 49*, 675–685.
117. C. Carruthers, T. K. Ronson, C. J. Sumby, A. Westcott, L. P. Harding, T. J. Prior, P. Rizkallah, M. J. Hardie, *Chem. Eur. J.* **2008***, 14*, 10286–10296.
118. T. K. Ronson, M. J. Hardie, *CrystEngComm* **2008***, 10*, 1731–1734.
119. C. J. Sumby, M. J. Hardie, *Cryst. Growth Des.* **2005***, 5*, 1321–1324.
120. M. J. Hardie, R. M. Mills, C. J. Sumby, *Org. Biomol. Chem.* **2004***, 2*, 2958–2964.
121. M. J. Hardie, C. J. Sumby, *Inorg. Chem.* **2004***, 43*, 6872–6874.

122. M. Schnopp, G. Haberhauer, *Eur. J. Org. Chem.* **2009**, 4458–4467.
123. G. Haberhauer, T. Oeser, F. Rominger, *Chem. Commun.* **2005**, 2799–2801.
124. G. Haberhauer, T. Oeser, F. Rominger, *Chem. Eur. J.* **2005***, 11*, 6718–6726.
125. G. Haberhauer, T. Oeser, F. Rominger, *Chem. Commun.* **2004**, 2044–2045.
126. N. M. Boshta, M. Bomkamp, G. Schnakenburg, S. R. Waldvogel, *Chem. Eur. J.* **2010***, 16*, 3459–3466.
127. M. Bomkamp, C. Siering, K. Landrock, H. Stephan, R. Fröhlich, S. R. Waldvogel, *Chem. Eur. J.* **2007***, 13*, 3724–3732.
128. M. Bomkamp, A. Artiukhov, O. Kataeva, S. R. Waldvogel, *Synthesis* **2007**, 1107–1114.
129. M. C. Schopohl, A. Faust, D. Mirk, R. Fröhlich, O. Kataeva, S. R. Waldvogel, *Eur. J. Org. Chem.* **2005**, 2987–2999.
130. M. C. Schopohl, C. Siering, O. Kataeva, S. R. Waldvogel, *Angew. Chem. Int. Ed.* **2003***, 42*, 2620–2623.
131. S. R. Waldvogel, R. Fröhlich, C. A. Schalley, *Angew. Chem. Int. Ed.* **2000***, 39*, 2472–2475.
132. S. R. Waldvogel, A. R. Wartini, P. H. Rasmussen, J. Rebek Jr., *Tetrahedron Lett.* **1999***, 40*, 3515–3518.
133. A. Jaeschke, H. Muensch, H. G. Schmid, H. Friebolin, A. Mannschreck, *J. Mol. Spec.* **1969***, 31*, 14–31.
134. T. H. Siddall, W. E. Stewart, *J. Org. Chem.* **1969***, 34*, 233–237.
135. D. Kuck, M. Seifert, *Chem. Ber.* **1992***, 125*, 1461–1469.
136. K. Damodaran, S. D. Nielsen, S. J. Geib, W. Zhang, Y. Lu, D. P. Curran, *J. Org. Chem.* **2009***, 74*, 5481–5485.
137. A. Chuvilin, J. C. Meyer, G. Algara-Siller, U. Kaiser, *New J. Phys.* **2009***, 11*, 83019.
138. M. Chen, *Huaxue Tongbao* **1993**, 58–63.
139. B. Hong, Y.-F. Chang, L.-L. Sun, X.-M. Pan, R.-S. Wang, *J. Clust. Sci.* **2011***, 22*, 1-10.
140. B. Hong, Y. Chang, A. F. Jalbout, Z. Su, R. Wang, *Mol. Phys.* **2007***, 105*, 95–99.
141. M. Lin, Y.-N. Chiu, S.-T. Lai, J. Xiao, M.-Z. Fu, *Fullerene Sci. Techn.* **1997***, 5*, 111–126.
142. M. Lin, M. Chen, Q. Zhang, Y.-N. Chiu, S.-T. Lai, *Electron. J. Theor. Chem.* **1997***, 2*, 109–117.
143. C.-R. Wang, Z.-Q. Shi, L.-J. Wan, X. Lu, L. Dunsch, C.-Y. Shu, Y.-L. Tang, H. Shinohara, *J. Am. Chem. Soc.* **2006***, 128*, 6605–6610.

144. X. Han, S.-J. Zhou, Y.-Z. Tan, X. Wu, F. Gao, Z.-J. Liao, R.-B. Huang, Y.-Q. Feng, X. Lu, S.-Y. Xie, L.-S. Zheng, *Angew. Chem. Int. Ed.* **2008**, *47*, 5340–5343.
145. H. W. Kroto, *Nature* **1987**, *329*, 529-521.
146. Q.-B. Yan, Q.-R. Zheng, G. Su, *J. Phys. Chem. C* **2007**, *111*, 549–554.
147. L. Xu, X. Shao, W. Cai, *J. Phys. Chem. A* **2009**, *113*, 10839–10844.
148. C. Tang, W. Zhu, K. Deng, *J. Mol. Struct. (THEOCHEM)* **2009**, *909*, 43–48.
149. Y. Nicolas, P. Blanchard, E. Levillain, M. Allain, N. Mercier, J. Roncali, *Org. Lett.* **2004**, *6*, 273–276.
150. T. Taerum, O. Lukoyanova, R. G. Wylie, D. F. Perepichka, *Org. Lett.* **2009**, *11*, 3230–3233.
151. T. Kashiki, M. Kohara, I. Osaka, E. Miyazaki, K. Takimiya, *J. Org. Chem.* **2011**, *76*, 4061–4070.
152. T. Nakae, S. Mizobuchi, M. Yano, T. Ukai, H. Sato, T. Shinmei, T. Inoue, T. Irifune, H. Sakaguchi, *Chem. Lett.* **2012**, *41*, 140–141.
153. D. P. Riley, *Nature* **1944**, *153*, 587–588.
154. K. Lonsdale, *Phil. Trans. R. Soc. Lond. A* **1947**, *240*, 219–250.
155. W. M. Haynes (ed.), *CRC Handbook of Chemistry and Physics (91st edition)*, Taylor & Francis: Boca Raton, **2010**.
156. Q. Song, D. M. Ho, R. A. Pascal, *J. Am. Chem. Soc.* **2005**, *127*, 11246–11247.
157. H. Kawai, T. Takeda, K. Fujiwara, T. Inabe, T. Suzuki, *Cryst. Growth Des.* **2005**, *5*, 2256–2260.
158. H. Kawai, T. Takeda, K. Fujiwara, M. Wakeshima, Y. Hinatsu, T. Suzuki, *Chem. Eur. J.* **2008**, *14*, 5780–5793.
159. T. Takeda, H. Kawai, R. Herges, E. Mucke, Y. Sawai, K. Murakoshi, K. Fujiwara, T. Suzuki, *Tetrahedron Lett.* **2009**, *50*, 3693–3697.
160. G. Fritz, S. Wartanessian, E. Matern, W. Hönle, H. G. von Schnering, *Z. Anorg. Allg. Chem.* **1981**, *475*, 87–108.
161. H. Irngartinger, A. Goldmann, *Angew. Chem. Int. Ed. Engl.* **1982**, *21*, 775–776.
162. R. Gleiter, R. Haider, P. Bischof, N. S. Zefirov, A. M. Boganov, *J. Org. Chem.* **1984**, *49*, 375–377.
163. D. R. Huntley, G. Markopoulos, P. M. Donovan, L. T. Scott, R. Hoffmann, *Angew. Chem. Int. Ed.* **2005**, *44*, 7549–7553.
164. G. Martínez-Guajardo, K. J. Donald, B. K. Wittmaack, M. A. Vazquez, G. Merino, *Org. Lett.* **2010**, *12*, 4058–4061.
165. M. L. Huggins, *J. Am. Chem. Soc.* **1953**, *75*, 4126–4133.
166. A. A. Zavitsas, *J. Phys. Chem. A* **2003**, *107*, 897–898.

167. J. Grunenberg, N. Goldberg, *J. Am. Chem. Soc.* **2000***, 122*, 6045–6047.
168. M. Kaupp, B. Metz, H. Stoll, *Angew. Chem. Int. Ed.* **2000***, 39*, 4607–4609.
169. M. Kaupp, S. Riedel, *Inorg. Chim. Acta* **2004***, 357*, 1865–1872.
170. A. Greenberg, J. F. Liebman, *Strained organic molecules*, Academic Press: New York, **1978**.
171. D. Cremer, A. Wu, A. Larsson, E. Kraka, *J. Mol. Model.* **2000***, 6*, 396–412.
172. K. Brandhorst, J. Grunenberg, *ChemPhysChem* **2007***, 8*, 1151–1156.
173. K. Exner, P. v. R. Schleyer, *J. Phys. Chem. A* **2001***, 105*, 3407–3416.
174. E. A. Carter, W. A. Goddard, *J. Phys. Chem.* **1986***, 90*, 998–1001.
175. R. F. W. Bader, T. H. Tang, Y. Tal, F. W. Biegler-Koenig, *J. Am. Chem. Soc.* **1982***, 104*, 946–952.
176. S. Grimme, *J. Am. Chem. Soc.* **1996***, 118*, 1529–1534.
177. F. Jensen, *Introduction to Computational Chemistry (2nd edition)*, Wiley & Sons: Chichester, **2007**.
178. J. Grunenberg, *J. Chem. Phys.* **2001***, 115*, 6360–6364.
179. J. Grunenberg, *Angew. Chem. Int. Ed.* **2001***, 40*, 4027–4029.
180. J. Grunenberg, R. Streubel, G. von Frantzius, W. Marten, *J. Chem. Phys.* **2003***, 119*, 165–169.
181. J. C. Decius, *J. Chem. Phys.* **1953***, 21*, 1121–1122.
182. J. C. Decius, *J. Chem. Phys.* **1963***, 38*, 241–248.
183. K. Brandhorst, J. Grunenberg, *Chem. Soc. Rev.* **2008***, 37*, 1558–1567.
184. K. Brandhorst, J. Grunenberg, *J. Chem. Phys.* **2010***, 132*, 184101.
185. L. H. Jones, B. I. Swanson, *Acc. Chem. Res.* **1976***, 9*, 128–134.
186. Z. Konkoli, D. Cremer, *Int. J. Quantum Chem.* **1998***, 67*, 1–9.
187. Z. Konkoli, J. A. Larsson, D. Cremer, *Int. J. Quantum Chem.* **1998***, 67*, 11–27.
188. Z. Konkoli, D. Cremer, *Int. J. Quantum Chem.* **1998***, 67*, 29–40.
189. Z. Konkoli, J. A. Larsson, D. Cremer, *Int. J. Quantum Chem.* **1998***, 67*, 41–55.
190. W. Zou, R. Kalescky, E. Kraka, D. Cremer, *J. Chem. Phys.* **2012***, 137*, 84114.
191. J. A. Larsson, D. Cremer, *J. Mol. Struct.* **1999***, 485–486*, 385–407.
192. E. Kraka, D. Cremer, *ChemPhysChem* **2009***, 10*, 686–698.
193. *Gaussian 09*, Revision A.02, M. J. Frisch, G. W. Trucks, H. B. Schlegel, G. E. Scuseria, M. A. Robb, J. R. Cheeseman, G. Scalmani, V. Barone, B. Mennucci, G. A. Petersson, H. Nakatsuji, M. Caricato, X. Li, H. P. Hratchian, A. F. Izmaylov, J. Bloino, G. Zheng, J. L. Sonnenberg, M. Hada, M. Ehara, K. Toyota, R. Fukuda, J. Hasegawa, M. Ishida, T. Nakajima, Y. Honda, O. Kitao, H. Nakai, T. Vreven, J. J. A. Montgomery, J. E. Peralta, F. Ogliaro, M. Bearpark, J. J. Heyd, E. Brothers, K. N. Kudin, V. N. Staroverov, R. Kobayashi, J. Normand, K.

Raghavachari, A. Rendell, J. C. Burant, S. S. Iyengar, J. Tomasi, M. Cossi, N. Rega, J. M. Millam, M. Klene, J. E. Knox, J. B. Cross, V. Bakken, C. Adamo, J. Jaramillo, R. Gomperts, R. E. Stratmann, O. Yazyev, A. J. Austin, R. Cammi, C. Pomelli, J. W. Ochterski, R. L. Martin, K. Morokuma, V. G. Zakrzewski, G. A. Voth, P. Salvador, J. J. Dannenberg, S. Dapprich, A. D. Daniels, Ö. Farkas, J. B. Foresman, J. V. Ortiz, J. Cioslowski, D. J. Fox. Gaussian, Inc., Wallingford CT, **2009**.

194. *Compliance*, Version 2.0, K. Brandhorst. Braunschweig, **2009**. (http://www.oc.tu-bs.de/Grunenberg/index.html).
195. C. J. Cramer, *Essentials of Computational Chemistry*, John Wiley & Sons: Chichester, **2004**.
196. J. A. Pople, M. Head-Gordon, K. Raghavachari, *J. Chem. Phys.* **1987***, 87*, 5968–5975.
197. A. D. Becke, *J. Chem. Phys.* **1993***, 98*, 5648–5652.
198. Y. Zhao, D. Truhlar, *Theor. Chem. Acc.* **2008***, 120*, 215–241.
199. Y. Zhao, D. G. Truhlar, *Acc. Chem. Res.* **2008***, 41*, 157–167.
200. S. Grimme, *J. Comput. Chem.* **2006***, 27*, 1787–1799.
201. S. Grimme, *Angew. Chem. Int. Ed.* **2006***, 45*, 4460–4464.
202. W. Wu, B. Ma, J. I-Chia Wu, P. v. R. Schleyer, Y. Mo, *Chem. Eur. J.* **2009***, 15*, 9730–9736.
203. P. R. Schreiner, A. A. Fokin, R. A. Pascal, A. de Meijere, *Org. Lett.* **2006***, 8*, 3635–3638.
204. M. D. Wodrich, C. Corminboeuf, P. R. Schreiner, A. A. Fokin, P. v. R. Schleyer, *Org. Lett.* **2007***, 9*, 1851–1854.
205. H. M. Sulzbach, D. Graham, J. C. Stephens, H. F. Schaefer III, *Acta Chem. Scand.* **1997***, 51*, 547–555.
206. A. Baeyer, *Ber. Dtsch. Chem. Ges* **1885***, 18*, 2269–2281.
207. K. B. Wiberg, *Angew. Chem. Int. Ed. Engl.* **1986***, 25*, 312–322.
208. D. Cremer, J. Gauss, *J. Am. Chem. Soc.* **1986***, 108*, 7467–7477.
209. P. R. Khoury, J. D. Goddard, W. Tam, *Tetrahedron* **2004***, 60*, 8103–8112.
210. K. B. Wiberg, in: *The Chemistry of Cyclobutanes* (Eds.: Z. Rappoport, J. F. Liebman), John Wiley & Sons: Chichester, **2005**, pp. 1–15.
211. M. D. Wodrich, C. S. Wannere, Y. Mo, P. D. Jarowski, K. N. Houk, P. v. R. Schleyer, *Chem. Eur. J.* **2007***, 13*, 7731–7744.
212. S. Gronert, *Chem. Eur. J.* **2009***, 15*, 5372–5382.
213. M. J. S. Dewar, *J. Am. Chem. Soc.* **1984***, 106*, 669–682.
214. D. Moran, M. Manoharan, T. Heine, P. v. R. Schleyer, *Org. Lett.* **2003***, 5*, 23–26.

215. P. v. R. Schleyer, J. E. Williams, Blanchard K. R., *J. Am. Chem. Soc.* **1970***, 92*, 2377–2386.
216. A. Nemirowski, H. P. Reisenauer, P. R. Schreiner, *Chem. Eur. J.* **2006***, 12*, 7411–7420.
217. J. P. Amoureux, M. Foulon, *Acta Cryst.* **1987***, B43*, 470–479.
218. M. Bertau, F. Wahl, A. Weiler, K. Scheumann, J. Wörth, M. Keller, H. Prinzbach, *Tetrahedron* **1997***, 53*, 10029–10040.
219. E. B. Fleischer, *J. Am. Chem. Soc.* **1964***, 86*, 3889–3890.
220. A. S. Pine, A. G. Maki, A. G. Robiette, B. J. Krohn, J. K. G. Watson, T. Urbanek, *J. Am. Chem. Soc.* **1984***, 106*, 891–897.
221. J. F. Chiang, S. H. Bauer, *J. Am. Chem. Soc.* **1970***, 92*, 1614–1617.
222. A. Almenningen, B. Andersen, B. A. Nyhus, *Acta Chem. Scand.* **1971**, 1217–1223.
223. R. R. Karl Jr., Y. C. Wang, S. H. Bauer, *J. Mol. Struct.* **1975***, 25*, 17–34.
224. R. J. Buenker, S. D. Peyerimhoff, *J. Phys. Chem.* **1969***, 73*, 1299–1313.
225. R. Hoffmann, S. Swaminathan, B. G. Odell, R. Gleiter, *J. Am. Chem. Soc.* **1970***, 92*, 7091–7097.
226. J. S. Wright, L. Salem, *J. Am. Chem. Soc.* **1972***, 94*, 322–329.
227. G. A. Segal, *J. Am. Chem. Soc.* **1974***, 96*, 7892–7898.
228. S. Pedersen, J. L. Herek, A. H. Zewail, *Science* **1994***, 266*, 1359–1364.
229. S. de Feyter, E. W.-G. Diau, A. A. Scala, A. H. Zewail, *Chem. Phys. Lett.* **1999***, 303*, 249–260.
230. J. S. Wright, L. Salem, *J. Chem. Soc. D* **1969**, 1370–1371.
231. T. Egawa, T. Fukuyama, S. Yamamoto, F. Takabayashi, H. Kambara, T. Ueda, K. Kuchitsu, *J. Chem. Phys.* **1987***, 86*, 6018–6026.
232. E. D. Glendening, A. M. Halpern, *J. Phys. Chem. A* **2005***, 109*, 635–642.
233. T. A. Blake, S. S. Xantheas, *J. Phys. Chem. A* **2006***, 110*, 10487–10494.
234. D. S. Kummli, H. M. Frey, S. Leutwyler, *J. Phys. Chem. A* **2007***, 111*, 11936–11942.
235. P. E. Eaton, K. Pramod, T. Emrick, R. Gilardi, *J. Am. Chem. Soc.* **1999***, 121*, 4111–4123.
236. O. Ermer, P. Bell, J. Schäfer, G. Szeimies, *Angew. Chem. Int. Ed. Engl.* **1989***, 28*, 473–476.
237. P. Kaszynski, J. Michl, *J. Am. Chem. Soc.* **1988***, 110*, 5225–5226.
238. M. Tanaka, A. Sekiguchi, *Angew. Chem. Int. Ed.* **2005***, 44*, 5821–5823.
239. C. Rüchardt, H.-D. Beckhaus, *Angew. Chem. Int. Ed. Engl.* **1980***, 19*, 429–440.

240. P. R. Schreiner, L. V. Chernish, P. A. Gunchenko, E. Y. Tikhonchuk, H. Hausmann, M. Serafin, S. Schlecht, J. E. P. Dahl, R. M. K. Carlson, A. A. Fokin, *Nature* **2011***, 477*, 308–311.
241. A. A. Fokin, L. V. Chernish, P. A. Gunchenko, E. Y. Tikhonchuk, H. Hausmann, M. Serafin, J. E. P. Dahl, R. M. K. Carlson, P. R. Schreiner, *J. Am. Chem. Soc.* **2012***, 134*, 13641–13650.
242. T. Suzuki, Y. Uchimura, Y. Ishigaki, T. Takeda, R. Katoono, H. Kawai, K. Fujiwara, A. Nagaki, J.-i. Yoshida, *Chem. Lett.* **2012***, 41*, 541–543.
243. A. C. Hazell, R. G. Hazell, L. Norskov-Lauritsen, C. E. Briant, D. W. Jones, *Acta Cryst.* **1986***, C42*, 690–693.
244. R. Boese, D. Bläser, *Angew. Chem. Int. Ed. Engl.* **1988***, 27*, 304–305.
245. S. Kammermeier, R. Herges, P. G. Jones, *Angew. Chem. Int. Ed. Engl.* **1997***, 36*, 1757–1760.
246. K. K. Baldridge, Y. Kasahara, K. Ogawa, J. S. Siegel, K. Tanaka, F. Toda, *J. Am. Chem. Soc.* **1998***, 120*, 6167–6168.
247. H. Wang, F. P. Gabbaï, *Org. Lett.* **2004***, 7*, 283–285.
248. E. Kraka, J. A. Larsson, D. Cremer, in: *Computational Spectroscopy* (Ed.: J. Grunenberg), Wiley-VCH: Weinheim, **2010**, pp. 105–149.
249. R. M. Badger, *J. Chem. Phys.* **1934***, 2*, 128–131.
250. R. M. Badger, *J. Chem. Phys.* **1935***, 3*, 710–714.
251. J. M. Wittbrodt, H. B. Schlegel, *J. Mol. Struct. (THEOCHEM)* **1997***, 398–399*, 55–61.
252. J. Cioslowksi, G. Liu, R. A. Mosquera Castro, *Chem. Phys. Lett.* **2000***, 331*, 497–501.
253. E. Kurita, H. Matsuura, K. Ohno, *Spectrochim. Acta Part A* **2004***, 60*, 3013–3023.
254. N. Graulich, H. Hopf, P. R. Schreiner, *Chem. Soc. Rev.* **2010***, 39*, 1503–1512.
255. N. Igor, *Tetrahedron Lett.* **2011***, 52*, 6982–6984.
256. R. Hoffmann, P. v. R. Schleyer, H. F. Schaefer, *Angew. Chem. Int. Ed.* **2008***, 47*, 7164–7167.
257. A. Y. Rogachev, X.-D. Wen, R. Hoffmann, *J. Am. Chem. Soc.* **2012***, 134*, 8062–8065.
258. D. A. Hrovat, E. C. Brown, R. V. Williams, H. Quast, W. T. Borden, *J. Org. Chem.* **2005***, 70*, 2627–2632.
259. H.-S. Wu, H. Jiao, Z.-X. Wang, P. v. R. Schleyer, *J. Am. Chem. Soc.* **2003***, 125*, 10524–10525.
260. D. J. Tantillo, R. Hoffmann, *Angew. Chem. Int. Ed.* **2002***, 41*, 1033–1036.

261. W. von E. Doering, W. R. Roth, *Tetrahedron* **1963**, *19*, 715–737.
262. G. Schröder, *Angew. Chem.* **1963**, *75*, 722.
263. W. von E. Doering, B. M. Ferrier, E. T. Fossel, J. H. Hartenstein, M. Jones Jr., G. Klumpp, R. M. Rubin, M. Saunders, *Tetrahedron* **1967**, *23*, 3943–3963.
264. H. Günther, J. Ulmen, *Tetrahedron* **1974**, *30*, 3781–3786.
265. R. Poupko, H. Zimmerman, Z. Luz, *J. Am. Chem. Soc.* **1984**, *106*, 5391–5394.
266. H. E. Zimmerman, R. W. Binkley, R. S. Givens, G. L. Grunewald, M. A. Sherwin, *J. Am. Chem. Soc.* **1969**, *91*, 3316–3323.
267. R. Pettit, J. S. McKennis, L. Brener, J. S. Ward, *J. Am. Chem. Soc.* **1971**, *93*, 4957–4958.
268. H. Jiao, R. Nagelkerke, H. A. Kurtz, R. V. Williams, W. T. Borden, P. v. R. Schleyer, *J. Am. Chem. Soc.* **1997**, *119*, 5921–5929.
269. M. D. Wodrich, C. Corminboeuf, P. v. R. Schleyer, *Org. Lett.* **2006**, *8*, 3631–3634.
270. M. J. Kryger, A. M. Munaretto, J. S. Moore, *J. Am. Chem. Soc.* **2011**, *133*, 18992–18998.
271. Z. S. Kean, A. L. Black Ramirez, Y. Yan, S. L. Craig, *J. Am. Chem. Soc.* **2012**, *134*, 12939–12942.
272. E. F. Pratt, E. Werble, *J. Am. Chem. Soc.* **1950**, *72*, 4638–4641.
273. R. Antonioletti, P. Bovicelli, S. Malancona, *Tetrahedron* **2002**, *58*, 589–596.
274. H. D. Becker, L. Hansen, *J. Org. Chem.* **1985**, *50*, 277–279.
275. P. P. J. Mulder, J. O. Boerrigter, B. B. Boere, H. Zuilhof, C. Erkelens, J. Cornelisse, J. Lugtenburg, *Recl. Trav. Chim. Pays-Bas* **1993**, *112*, 287–302.
276. G. Sheldrick, *Acta Cryst.* **2008**, *A64*, 112–122.
277. W. J. Hehre, R. Ditchfield, J. A. Pople, *J. Chem. Phys.* **1972**, *56*, 2257–2261.
278. R. Krishnan, J. S. Binkley, R. Seeger, J. A. Pople, *J. Chem. Phys.* **1980**, *72*, 650–654.
279. T. H. Dunning Jr., *J. Chem. Phys.* **1989**, *90*, 1007–1023.
280. K. Raghavachari, G. W. Trucks, J. A. Pople, M. Head-Gordon, *Chem. Phys. Lett.* **1989**, *157*, 479–483.
281. P. Hohenberg, W. Kohn, *Phys. Rev.* **1964**, *136*, B864.
282. W. Kohn, L. J. Sham, *Phys. Rev.* **1965**, *140*, A1133.
283. C. Møller, M. S. Plesset, *Phys. Rev.* **1934**, *46*, 618–622.

# Lebenslauf

geboren in Thessaloniki (Griechenland)

| | |
|---|---|
| 2000 | Abitur in Ludwigshafen/Rhein |
| 2000-2001 | Zivildienst am Universitätsklinikum Heidelberg |
| 2003 | Vordiplom in Chemie, Universität Heidelberg |
| 2004-2005 | Auslandsstudium an der Cornell University, Ithaca (USA) |
| 2007 | Diplom in Chemie, Universität Heidelberg |
| | Betreuer der Diplomarbeit: Prof. Roald Hoffmann, Cornell University |
| 2008-2012 | Doktorand bei Prof. Henning Hopf, TU Braunschweig |

Stipendien:

Fonds der chemischen Industrie (Grundstudium und Promotion)

Studienstiftung des deutschen Volkes (Studium und Promotion)

Heidelberg-Cornell Austauschstipendium

Veröffentlichungen:

D. R. Huntley, G. Markopoulos, P. M. Donovan, L. T. Scott, R. Hoffmann
”Squeezing C-C bonds“
*Angew. Chem. Int. Ed.* **2005**, *44*, 7549–7553; *Angew. Chem.* **2005**, *117*, 7721–7725.

G. Markopoulos, P. Kroll, R. Hoffmann
”Compressing the most hydrogen-rich inorganic ion”
*J. Am. Chem. Soc.* **2010**, *132*, 748–755

N. A. McGrath, J. R. Binner, G. Markopoulos, M. Brichacek, J. T. Njardarson
“An efficient oxidative dearomatization-radical cyclization approach to symmetrically substituted bicyclic guttiferone natural products”
*Chem. Commun.* **2011**, *47*, 209–211

H. Hopf, G. Markopoulos
“The chemistry of bisallenes” (Übersichtsartikel)
*Beilstein J. Org. Chem.* **2012**, *8*, 1936–1998